

Phenotypic analysis of the *Plp*-deficient mouse

A thesis presented to the Faculty of Veterinary Medicine,
University of Glasgow

for the degree of
Doctor of Philosophy

April 2000

©

Donald Andrew Yool

ProQuest Number: 13818710

All rights reserved

INFORMATION TO ALL USERS

The quality of this reproduction is dependent upon the quality of the copy submitted.

In the unlikely event that the author did not send a complete manuscript and there are missing pages, these will be noted. Also, if material had to be removed, a note will indicate the deletion.



ProQuest 13818710

Published by ProQuest LLC (2018). Copyright of the Dissertation is held by the Author.

All rights reserved.

This work is protected against unauthorized copying under Title 17, United States Code
Microform Edition © ProQuest LLC.

ProQuest LLC.
789 East Eisenhower Parkway
P.O. Box 1346
Ann Arbor, MI 48106 – 1346

GLASGOW
UNIVERSITY
LIBRARY

11864 (copy 1)

Abstract

The myelin *proteolipid protein* (*Plp*) gene encodes the major protein components of compact central nervous system myelin. Mutations of this gene lead to severe dysmyelinating disease and oligodendrocyte death suggesting roles for *Plp* gene products as vital structural components of compact myelin and as oligodendrocyte maturation or survival factors. The *Plp* gene knockout mouse was generated (Klugmann *et al.*, 1997) to study the effects of loss of *Plp* gene function on oligodendrocyte development and myelination in the central nervous system. Surprisingly the *Plp* gene knockout mouse showed no gross evidence of dysmyelination but did develop a late onset phenotype associated with progressive axonal changes. This study characterised the phenotype of these mice and assessed the ability of *Plp* gene isoforms to modify the phenotype of *Plp* gene knockout mice by transgenic complementation.

The *Plp* gene knockout mouse formed large volumes of myelin and maintained oligodendrocyte numbers into adulthood. However, in the central nervous system, myelin was ultrastructurally abnormal and a proportion of small diameter axons failed to acquire myelin sheaths. Axonal changes consisted of swollen and degenerate axons and were confined to myelinated regions of the central nervous system where small diameter fibres appeared to be preferentially affected. Transgenic complementation with constructs expressing all of the components of the *Plp* gene ameliorated the phenotype of the *Plp* gene knockout mouse demonstrating that these changes were the direct result of loss of *Plp* gene function.

These results indicate that, although the *Plp* gene products play roles in initiating myelination and in stabilising myelin lamellae, they are not vital components for oligodendrocyte development or myelin formation. The development of axonal changes appears to depend on the presence of myelin and demonstrates a potential role for the *Plp* gene in axoglial interaction. In addition, the changes in the *Plp* gene knockout mouse highlight the increasingly recognised role of gene dosage in the pathogenesis of *Plp* gene-related disease.

Klugmann,M., Schwab,M.H., Pühlhofer,A., Schneider,A., Zimmermann,F., Griffiths,I.R. and Nave,K.-A. (1997) Assembly of CNS myelin in the absence of proteolipid protein. *Neuron*. **18**, 59-70.



List of Contents

Abstract	i
List of Contents	ii
List of Figures	viii
List of Tables	xi
Declaration	xii
Acknowledgements	xiii
1. INTRODUCTION	1
1.1 Background	1
1.2 CNS structure	1
1.2.1 The axon	2
1.2.2 The oligodendrocyte	3
1.2.3 The astrocyte	7
1.2.4 The microglia	7
1.2.5 Axoglial interactions	8
1.3 The <i>proteolipid protein</i> gene: structure and function	9
1.3.1 The <i>Plp</i> gene locus	9
1.3.2 The <i>DM</i> gene family and phylogenetic evolution of the <i>Plp</i> gene	11
1.3.3 Regulation of <i>Plp</i> gene expression in the CNS	12
1.3.4 Expression of the <i>Plp</i> gene in the PNS	15
1.3.5 Translation and post-translational modification of PLP/DM20 protein	16
1.3.6 Proposed functions of the <i>Plp</i> gene	18
1.3.7 Lower molecular weight proteolipid proteins in the CNS	19
1.4 <i>Plp</i> gene mutations and disease	19
1.4.1 <i>PLP</i> gene-related disorders in man	19
1.4.2 <i>Plp</i> gene mutations in animals	22
1.4.3 <i>Plp</i> transgenic animals	28
1.4.4 Pathogenesis of <i>Plp</i> gene-related disorders	31
1.4.5 Clinically affected female carriers	33
1.4.6 Modifying loci	34
1.5 Experimental strategies for studying the roles of myelin proteins	35

1.5.1	Traditional transgenic technology	35
1.5.2	Targeted gene replacement	35
1.5.3	Targeted gene replacement using recombinase systems	37
1.6	Aims of thesis	37
2.	MATERIALS AND METHODS	39
2.1	Miscellaneous	39
2.2	Mouse Breeding	39
2.2.1	Animal breeding facilities	39
2.2.2	Transgenic lines of mice	39
2.2.3	Maintenance of transgenic lines of mice	41
2.2.4	Crossing of transgenic lines of mice	46
2.3	Isolation and quantification of nucleic acids	46
2.3.1	Tail biopsy and mouse identification	46
2.3.2	Extraction of genomic DNA (gDNA) from mouse tails	46
2.3.3	Extraction of RNA from mouse tissue	47
2.3.4	Quantification and standardisation of nucleic acids	51
2.3.5	Nucleic acid electrophoresis	52
2.4	PCR Genotyping	53
2.4.1	PCR core programme	53
2.4.2	Genomic PCR	53
2.4.3	Primers for PCR genotyping and sexing	53
2.5	Tissue fixation	57
2.5.1	Fixatives	57
2.5.2	Fixation techniques	58
2.6	Tissue processing and sectioning	58
2.6.1	Paraffin wax processing and sectioning	58
2.6.2	Resin processing and sectioning	59
2.6.3	Cryopreservation and sectioning	59
2.6.4	Agar embedding and vibratome sectioning of paraformaldehyde fixed tissue	60
2.7	Staining techniques	60
2.7.1	Light microscopy	60
2.7.2	Electron microscopy	61
2.8	Morphological studies	61

2.8.1	Quantification of corrected glial cell densities	61
2.8.2	Quantification of swollen axons and degenerate fibres	62
2.8.3	Assessment of axonal size and myelination status	62
2.8.4	Presentation of data and statistical analysis	63
2.9	Immunohistochemistry	64
2.9.1	Immunohistochemical markers	64
2.9.2	Peroxidase anti-peroxidase (PAP) immunohistochemistry	64
2.9.3	Immunofluorescence of fresh, cryo-preserved tissue	67
2.9.4	Agar-embedded tissue staining	68
2.9.5	F4/80 Microglial staining	68
2.10	Plasmid DNA (pDNA) preparation	69
2.10.1	Plasmids	69
2.10.2	Preparation of competent cells	69
2.10.3	Transformations	70
2.10.4	Plasmid preparation	70
2.11	Semi-quantitative reverse transcription PCR (RT-PCR)	72
2.11.1	cDNA Synthesis	72
2.11.2	RT-PCR	72
2.12	<i>In Situ</i> Hybridisation	73
2.12.1	Preparation of apparatus and solutions	73
2.12.2	Preparation of digoxigenin-labelled riboprobes	73
2.12.3	Prehybridisation of sections	74
2.12.4	Hybridisation	74
2.12.5	Slide development and mounting	75
2.13	Western Blotting	75
2.13.1	Extraction of Protein from Tissue	75
2.13.2	SDS-Polyacrylamide gel electrophoresis	76
2.13.3	Western Blotting	76
3.	THE PHENOTYPE AND PATHOLOGY OF THE <i>PLP</i> GENE KNOCKOUT MOUSE	78
3.1	Introduction	78
3.2	Aims	79
3.3	Materials and methods	79

3.3.1	Animal breeding	79
3.3.2	Molecular analysis of the knockout animals	79
3.3.3	Histopathology	80
3.3.4	Morphometric analysis	80
3.3.5	Immunostaining	81
3.3.6	<i>In situ</i> hybridisation	81
3.4	Results	82
3.4.1	Analysis of <i>Plp</i> gene activity in the <i>Plp</i> gene knockout mouse	82
3.4.2	Clinical phenotype of the <i>Plp</i> gene knockout mouse	85
3.4.3	Pathological description of the CNS changes in the <i>Plp</i> gene knockout mouse	87
3.4.4	Survey of the PNS of the <i>Plp</i> gene knockout mice	123
3.5	Discussion	125
4.	<i>PLP</i>^{TMKN1} HETEROZYGOUS MICE	132
4.1	Background	132
4.2	Aims	132
4.3	Materials and Methods	133
4.3.1	Animal breeding	133
4.3.2	Histopathology	133
4.3.3	Immunostaining	133
4.3.4	Quantification of axonal changes	133
4.4	Results	133
4.4.1	Clinical phenotype	133
4.4.2	Histopathology	134
4.4.3	Myelin ultrastructure	134
4.4.4	Mosaicism of <i>Plp</i> gene expression in oligodendrocytes	134
4.4.5	Quantification of axonal changes in heterozygous knockout mice	135
4.5	Discussion	141
5.	TRANSGENIC COMPLEMENTATION OF THE <i>PLP</i> GENE KNOCKOUT MOUSE	143
5.1	Background	143
5.2	Aims	143

5.3	Materials and Methods	144
5.3.1	Animal breeding and identification	144
5.3.2	Molecular characterisation of the transgenic complementation models	144
5.3.3	Histopathology	145
5.3.4	Axonal swelling and degeneration quantification	145
5.3.5	Glial cell quantification	145
5.3.6	Immunostaining	145
5.4	Results	146
5.4.1	#66 and #72 transgenic complementation of knockout mice	146
5.4.2	<i>Plp</i> -cDNA and <i>Dm20</i> -cDNA transgenic complementation of knockout mice	158
5.4.3	<i>PLP</i> -LacZ transgenic complementation of knockout mice	163
5.5	Discussion	168
5.5.1	#66 and #72 transgenic complementation of knockout mice	168
5.5.2	<i>Plp</i> -cDNA and <i>Dm20</i> -cDNA transgenic complementation of knockout mice	169
5.5.3	<i>PLP</i> -LacZ fusion transgene expression in knockout mice	171
6.	FINAL DISCUSSION AND FURTHER WORK	172
7.	APPENDIX	177
7.1	APES-coated slides	177
7.2	DEPC-treated water	177
7.3	Fixatives	177
7.3.1	Buffered neutral formaldehyde, 4% (BNF)	177
7.3.2	Karnovsky's modified fixative (paraformaldehyde/ glutaraldehyde 4%/5%)	178
7.3.3	Periodate-lysine-paraformaldehyde	178
7.3.4	4% Paraformaldehyde in PBS	179
7.4	Tissue processing protocols	179
7.4.1	Paraffin wax processing	179
7.4.2	Resin processing	180
7.5	<i>In situ</i> hybridisation solutions and protocols	181
7.5.1	20x SSC (Sodium chloride/sodium citrate)	181
7.5.2	Prehybridisation washes	182
7.5.3	Post-hybridisation washes	183
7.5.4	Alkaline phosphate substrate buffer	183
7.6	Staining protocols	184

7.6.1	Dewaxing and hydration of paraffin sections	184
7.6.2	Dehydration and clearing of sections	184
7.6.3	Haematoxylin and eosin	185
7.6.4	Haematoxylin	186
7.6.5	Staining for electron microscopy	186
7.7	Staining solutions	187
7.7.1	Methylene blue/ azur II	187
7.7.2	Mayers haematoxylin	187
7.7.3	Scots tap water substitute	187
7.8	General Buffers	188
7.8.1	Tris buffered saline	188
7.8.2	Phosphate buffered saline (PBS)	188
7.8.3	0.1M phosphate buffer	188
7.8.4	Tris-EDTA buffer (TE buffer)	189
7.8.5	Tris acetate EDTA buffer x10 (TAE buffer)	189
7.9	Hybaid Recovery™ buffers	189
7.9.1	Resuspension solution (Hybaid) containing RNase	189
7.9.2	Cell lysis solution (Hybaid)	190
7.9.3	Neutralisation solution (Hybaid)	190
7.9.4	Equilibration solution (Hybaid)	190
7.9.5	Wash solution (Hybaid)	190
7.10	Gel loading dye x6 (for TAE conditions)	190
7.11	Bacteriological media	191
7.11.1	Luria-Bertani (LB) medium	191
7.11.2	Ampicillin-LB medium	191
7.11.3	Ampicillin-LB agar plates	191
7.12	Northern blotting	192
7.12.1	RNA electrophoresis and transfer to nylon membranes	192
7.12.2	Random-primed DNA probe production	192
7.12.3	Prehybridisation, hybridisation and washing	193
7.12.4	Autoradiography	193
8.	ABBREVIATIONS	194
9.	REFERENCE LIST	198

List of Figures

Figure 1	The organisation of the <i>Plp</i> gene and its major transcription products ...	10
Figure 2	Proposed membrane topology of the PLP protein isoform.....	17
Figure 3	Graphical representations of point mutations of the <i>PLP/Plp</i> gene.....	23
Figure 4	<i>Plp^{tmkn1}</i> targeting strategy and PCR primer positions	42
Figure 5	#66 and #72 transgene construct and PCR primer positions	43
Figure 6	<i>Plp</i> Tg1 and <i>Dm20</i> Tg2 transgene constructs and PCR primer positions	44
Figure 7	a) ND3a transgene construct and PCR primer positions b) <i>Plp-LacZ</i> fusion protein transgene construct.....	45
Figure 8	Genomic DNA extracted from mouse tail using the QIAmp Tissue Kit.	48
Figure 9	Assessment of quality of gDNA extracted using the QIAmp Tissue Kit (Qiagen).....	49
Figure 10	Assessment of total cellular RNA extraction and cDNA synthesis.....	50
Figure 11	PCR products from transgenic mice genotyping	56
Figure 12	Plasmids used for riboprobe production	71
Figure 13	<i>In situ</i> hybridisation using an anti-sense <i>Plp</i> -riboprobe on spinal cord from wild type and knockout mice at 20 days of age.....	83
Figure 14	Dorsal columns of spinal cord from 120 day-old wild type and knockout mice immunostained for PLP/DM20 and MBP proteins	84
Figure 15	Body weight measurements of male knockout and wild type mice	86
Figure 16	Methylene blue/ azurII stained 1µm resin section of mid optic nerve from a 20 day-old knockout mouse.....	89
Figure 17	Electron micrograph of knockout CNS showing poorly compacted myelin and comparing this to wild type	90
Figure 18	Methylene blue/ azur II stained section of optic nerve from a 360 day-old knockout mouse demonstrating swollen axons and degenerate fibres.....	91
Figure 19	Methylene blue/ azur II stained sections from a 640 day-old knockout mouse demonstrating tract specificity of neurodegeneration.....	92
Figure 20	Progression of neurodegenerative changes in knockout mice	93
Figure 21	Widespread neurodegeneration throughout the white matter and affecting myelinated fibres in the grey matter of an aged knockout mouse.....	94

Figure 22 Splitting and vacuolation of the myelin sheath in aged knockout mice ..	95
Figure 23 Corrected total cell densities in mid optic nerve and spinal cord of knockout and wild type mice.....	96
Figure 24 Corrected oligodendrocyte and microglial densities in mid optic nerve and spinal cord of knockout and wild type.....	97
Figure 25 <i>In situ</i> hybridisation with anti-sense <i>Mog</i> riboprobe to compare oligodendrocyte densities in 20 day-old wild type and knockout mice	100
Figure 26 Carbonic anhydrase II staining of oligodendrocyte cell bodies in cerebellum of 20 day-old wild type and knockout mice	101
Figure 27 F4/80 immunoreactivity in brain and spinal cord from aged knockout and wild type mice	102
Figure 28 GFAP immunoreactivity in spinal cord (C2-3) from aged knockout and wild type mice	103
Figure 29 Electron micrograph showing axonal lesions in the optic nerve of a 360 day-old knockout mouse.....	104
Figure 30 Electron micrographs of a) neurofilamentous and b) dense body axonal swellings in a knockout mouse.....	105
Figure 31 Electron micrograph of degenerate and dystrophic axons in knockout mice.....	106
Figure 32 Section of lamina cribrosa from a knockout mouse showing neurodegeneration restricted to myelinated regions.....	107
Figure 33 Electron micrograph showing three types of myelin periodicity in knockout mice	109
Figure 34 Electron micrograph demonstrating increased proportion of non-myelinated axons in the optic nerve of knockout mice.....	110
Figure 35 Percentage of non-myelinated fibres in the mid optic nerve and spinal cord of wild type and knockout mice	111
Figure 36 Axon diameter frequency distribution (total fibres) from A) optic nerve and B) cervical cord in knockout and wild type mice.....	113
Figure 37 Axon diameter frequency distribution of A) non-myelinated fibres and B) myelinated fibres in optic nerve of knockout and wild type mice	115
Figure 38 Axon diameter frequency distribution of A) non-myelinated fibres and B) myelinated fibres in cervical cord of knockout and wild type mice.....	117

Figure 39A-C Total fibre densities of wild type and knockout optic nerve.....	120
Figure 40 Methylene blue/ azur II stained section of sciatic nerve (TS) from a knockout mouse.....	124
Figure 41 Correlation of phenotypic severity and proportion of PLP/DM20-positive myelin sheaths in 540 day-old heterozygous knockout mice.....	136
Figure 42 Myelin periodicity in heterozygous knockout mice.....	137
Figure 43 Mosaic and diffuse patterns of <i>Plp</i> gene expression in heterozygous knockout mice.....	138
Figure 44 PLP/DM20 and MBP immunoreactivity in serial sections of spinal cord from a heterozygous knockout mouse.....	139
Figure 45 Point count analysis of swollen axon and degenerate fibre volumes in heterozygous knockout mice.....	140
Figure 46 Semi-quantitative RT-PCR analysis of <i>Plp</i> gene isoform expression in knockout and transgene-complemented knockout mice.....	147
Figure 47 Western analysis of knockout and transgene-complemented knockout mice.....	148
Figure 48 Methylene blue/ azur II stained sections of mid optic nerve from knockout mice complemented with the #66 or #72 transgene.....	150
Figure 49 Methylene blue/ azur II stained sections from aged #72 transgene-complemented knockout mice and aged hemizygous #72 transgenic mice...	151
Figure 50 Vibratome sectioned tissue (50µm) demonstrating PLP/DM20 immunoreactivity localising to the myelin sheath (confocal image).....	153
Figure 51 PLP/DM20-positive myelin in 1µm resin sections from #66 and #72 transgene-complemented knockout mice.....	154
Figure 52 Myelin periodicity in #72 transgene-complemented knockout mice.....	155
Figure 53 Point count analysis of swollen axon and degenerate fibre volumes in #72 transgene-complemented knockout mice.....	156
Figure 54 Total corrected glial cell densities from 120 day-old wild type, knockout and #72 transgene-complemented knockout mice.....	157
Figure 55 Methylene blue/ azur II stained sections of optic nerve from mice complemented with <i>Plp</i> Tg1, <i>DM20</i> Tg2 and <i>Plp</i> Tg1/ <i>Dm20</i> Tg2 transgenes..	160
Figure 56 PLP/DM20 immunoreactivity in 120 day-old <i>Plp</i> Tg1 transgene-complemented knockout mice.....	161

Figure 57 Myelin periodicity in <i>Plp</i> Tg1-transgene complemented knockout mice	162
Figure 58 Methylene blue/ azur II section of spinal cord from ND3A transgene-complemented knockout mouse	164
Figure 59 PLP/DM20 immunoreactivity in ND3A transgene-complemented knockout mice	165
Figure 60 Electron micrograph showing myelin ultrastructure in ND3A transgene-complemented knockout mice	166
Figure 61 PLP-LacZ fusion protein expression in sagittal hindbrain from <i>PLP-LacZ</i> transgene-complemented knockout mice	167

List of Tables

Table 1 <i>PLP</i> gene point mutations causing PMD and SPG2	24
Table 2 <i>PLP</i> gene duplications, deletions and polymorphisms.....	25
Table 3 Spontaneous <i>Plp</i> gene mutations in animal models	26
Table 4 Transgenic animals expressing <i>Plp</i> genomic transgenes and <i>Plp</i> -cDNA and <i>Dm20</i> -cDNA transgenes	29
Table 5 PCR primers for genotyping and semi-quantitative RT-PCR.....	55
Table 6 Primary antibodies used for immunohistochemistry with appropriate dilutions (dilutions for western blotting in the text).....	65
Table 7 Link antibodies, PAP complexes and dilutions used for PAP immunostaining (sourced from Sigma).....	66
Table 8 Fluorescent secondary antibody dilutions for immunohistochemistry (sourced from Southern Biotech)	66

Declaration

I, Donald Andrew Yool, do hereby declare that the work carried out in this thesis is original, was carried out by myself or with due acknowledgement, and has not been presented for award or degree at any other university.

Acknowledgements

First, I would like to thank my supervisor, Prof. Ian Griffiths, for guidance and support during this project. I would also like to thank Dr James Anderson for his general help and advice, Drs Paul Montague and Demetrius Vouyiouklis for assistance with molecular techniques and Dr Christine Thompson for establishing the *Plp* gene knockout mouse colony and for providing many of the animals used during this study. I am very grateful for the excellent technical assistance and advice received from Mailis McCulloch, Jennifer Barrie, Douglas Kirkham and Catrina Kivlin.

The generous funding of the Biology and Biotechnology Sciences Research Council enabled me to complete this work.

I would like to thank and acknowledge Dr. Mark MacLauchlin who performed the western blots and supplied the images that have been presented in this thesis (page 148)

Colin Chapmann and other staff of the Glasgow Parasitology Unit provided excellent care of the animals used in this study.

Thanks to Allan May for some of the photography, Susan Cain for image scanning and editing and Prof. Stuart Reid for statistical advice.

Dr Diane Sherman and Dr Steven Tait from Prof. Peter Brophy's laboratory performed the confocal microscopy presented in this thesis (page 153).

I am very grateful to Prof. Klaus-Armin Nave and Dr Matthias Klugmann who generated the *Plp* gene knockout mouse line. In addition, I would like to acknowledge Prof. Carol Readhead for originally donating the #66 and #72 transgenic lines, Prof. Nancy Nadon for originally donating the *PlpTg1* and *Dm20Tg2* transgenic lines, Prof. Fabrizio Mastronardi for donating the ND3A transgenic line and Prof. Wendy Macklin for donating the *PLP-LacZ* transgenic line.

I would also like to thank Dr Pamela Johnston, Dr Julia Edgar, Marie Ward, friends and family for their help and support during this project.

1. Introduction

1.1 Background

Myelin disorders account for a large group of debilitating human diseases and similar disorders in experimental animals have proved useful in studying the mechanisms of these diseases and of myelin formation. Particular interest has centred on the functions and roles of the *proteolipid protein (Plp)* gene, the major myelin gene of the central nervous system (CNS). Although the *Plp* gene products constitute a large proportion of the CNS myelin proteins and disorders of this gene lead to severe disruptions of myelin formation, the functions of the gene remain elusive. In order to clarify some of the roles of the *Plp* gene and the pathogenic mechanisms of *Plp* gene-related disease, a *Plp* gene knockout mouse was generated (Klugmann *et al.*, 1997) that was expected to mirror the severe dysmyelinated phenotypes characteristic of other *Plp* gene-related disorders. However, the *Plp* gene knockout mouse appeared to develop normally and survived into old age before a clinical phenotype became obvious. This study describes the pathological changes that developed in the *Plp* gene knockout mouse and the ability of transgenic complementation to modify these changes. Early in the course of the investigation, it became apparent that *Plp* gene knockout mice develop a progressive axonopathy, a finding that is hard to correlate with the available data on *Plp* gene function. The introduction to this thesis summarises the current knowledge of *Plp* gene function as it relates to myelin formation and disease pathogenesis and summarises the role of axoglial interaction in the mature CNS. This will enable the results from this study to be discussed within the context of myelin formation and the pathogenesis of myelin disease.

1.2 CNS structure

The cellular architecture of the CNS is extremely specialised with complex interactions between neuronal processes and the macroglial supporting cells, the oligodendrocytes and astrocytes. In addition, microglia, a CNS-subpopulation of mononuclear phagocytic cells, and vascular endothelial cells contribute to the CNS structure. This section describes how these cells relate to one another particularly in the context of myelination. It does not expand on the complex organisation of neurones and their processes into functional groups or on the differences between CNS and peripheral nervous system (PNS) structure.

Membranous sheaths of myelin surround many of the axons of the central and peripheral nervous systems and are a feature of most vertebrates. The majority of CNS axons are myelinated by oligodendrocyte processes that form regular sheaths around consecutive sections of axon. Each internode (a single myelin/ axon subunit) is separated from neighbouring internodes by a small gap (0.8 to 0.11 μm), the node of Ranvier. This gap represents a specialised section of the axon (the nodal axon) that is capable of depolarisation to generate an action potential and then repolarisation to return it to a resting state. Myelin appears to have two important roles in nerve conduction (Hildebrand *et al.*, 1993). Firstly, it increases the speed of nerve conduction by enabling saltatory conduction. The lipid-rich structure insulates the axolemma maintaining its electrophysiological stability and enables action potentials to pass between nodes of Ranvier rather than along consecutively depolarising sections of axon. Secondly, as only nodal regions of the axolemma need to depolarise and repolarise to generate action potentials, myelination improves the energy efficiency of conduction.

1.2.1 The axon

Axons are elongated neuronal cell processes that conduct action potentials away from the neuronal soma. Action potentials originate in the axon initial segment and pass down the axon either by depolarisation of consecutive regions of the axolemma or by saltatory conduction along myelinated axons. Most CNS axons greater than 0.2 μm in diameter are myelinated.

The axoplasm is divided into three compartments. The subaxolemmal domain constitutes the axoplasmic cortex, a peripheral layer of microfilaments located just beneath the axolemma that supports the axolemma and anchors the cytoskeleton to it. The neurofilament domain contains the neurofilamentous cytoskeleton and determines the shape and size of the axon. Microtubular domains intersperse through the neurofilament domain and contain fast axonal transport mechanisms that move membrane-bound organelles along the axon. These mechanisms are necessary because the axon lacks transcriptional machinery and cellular products must be produced in the soma and transported along the axon. The fast axonal transport mechanisms have high energy requirements utilising translocators such as kinesin (anterograde) and dynein (retrograde) to transport membrane bound organelles along the microtubular network (reviewed by Hirokawa, 1993). Golgi-derived vesicles are transported anterogradely away from the soma; lysosomal-derived vesicles are transported retrogradely towards the soma; organelles such as mitochondria move bidirectionally along the axon.

1.2.2 The oligodendrocyte

1.2.2.1 Oligodendrocyte development

The mature oligodendrocyte is a highly specialised CNS-specific cell that is responsible for the elaboration and maintenance of myelin from its numerous cell processes (see below). It plays a vital role in maintaining the normal CNS architecture and perturbations of the oligodendrocyte can severely affect neurological function. Evidence of other roles for the oligodendrocyte is emerging. Perineuronal oligodendrocytes may control the microenvironment surrounding the neuronal cell body and roles in influencing axonal development and maintenance have also been proposed (see *1.2.5 Axoglial interaction*, page 8).

The origin and migration of immature oligodendrocytes remains a contentious issue. Most recent evidence points towards oligodendrocyte precursors originating from neuroectodermal cells in the ventral subventricular region of the neural tube (Warf *et al.*, 1991; Noll and Miller, 1993; Timsit *et al.*, 1995; Ono *et al.*, 1995; Dickinson *et al.*, 1996; Hall *et al.*, 1996; Spassky *et al.*, 1998; Chandross *et al.*, 1999). Two separate lineages of oligodendrocyte progenitor can be identified from embryonic day 9.5 in the mouse (Spassky *et al.*, 1998) and appear to migrate to populate all white matter areas (Noll and Miller, 1993; Spassky *et al.*, 1998). However, alternative views are that oligodendrocyte progenitors are capable of developing ubiquitously throughout the white matter (Hardy and Friedrich, Jr., 1996) or originate in both the dorsal and ventral areas of the developing neural tube (Cameron-Curry and Le Douarin, 1995). Whether the progenitors migrate or develop ubiquitously throughout the embryonic CNS, they must proliferate in the future white matter tracts before maturing into myelin-competent oligodendrocytes. A combination of intrinsic and extrinsic factors appears to control these processes (reviewed by McMorris and McKinnon, 1996). One feature of this system is that immature oligodendrocyte numbers far exceed the final requirements for these cells and many of these progenitors, as much as fifty percent, undergo apoptotic cell death (Barres *et al.*, 1992).

1.2.2.1.1 Myelinogenesis

As oligodendrocytes reach maturity, they elaborate numerous cell processes. These contact and start to enwrap neighbouring axons forming multilamellar myelin sheaths (reviewed by Raine, 1984). The oligodendrocyte process closely associates with the axolemmal membrane maintaining a 12 to 14nm gap, the periaxonal space. Successive layers of the oligodendrocyte process become closely apposed at their extracellular surfaces forming paired thin electron-dense structures, the intraperiod lines. Initially the cytoplasmic membrane surfaces remain separated but, as spiral

enwrapment progresses, cytoplasm becomes extruded from the oligodendrocyte process and the cytoplasmic surfaces fuse to form an electron dense layer, the major dense line. In cross section, myelin lamellae repeat through the myelin sheath with a regular interval referred to as the periodicity of myelin (approximately 11nm in the CNS from electron-microscopy images). Cytoplasm is retained at the outer edges of each successive myelin lamellae, which collectively form the lateral cytoplasmic loops, and in the inner and outer tongues of oligodendrocyte process. Each consecutive lateral cytoplasmic loop overlaps the loop below it to attach to the paranodal axolemma by tight junction-like complexes collectively forming the paranodal loops. Each oligodendrocyte is capable of producing up to fifty myelin sheaths however consecutive internodes along a single axon are unlikely to originate from the same cell.

Myelination has a spatio-temporal pattern of development; myelination in the PNS preceding that in the CNS and myelination of different parts of the CNS initiating at different time points. In general, the first CNS area to myelinate is the cervical spinal cord. From here, a wave of myelination spreads caudally along the spinal cord and rostrally through the brain. The optic nerve myelinates later than the spinal cord and hindbrain. Large diameter fibre tracts myelinate in advance of small diameter fibre tracts so that the ventral columns of the spinal cord myelinate before the dorsal tracts, the corticospinal tracts being last (Schwab and Schnell, 1989).

Oligodendrocytes can be divided into subpopulations on the basis of the number and diameter of the axons that they myelinate (reviewed by Hildebrand *et al.*, 1993). Some oligodendrocytes myelinate large numbers of small diameter axons whereas others myelinate smaller numbers of larger diameter axons. At one extreme, some oligodendrocytes in the ventral white matter tracts of the spinal cord form a 1:1 relationship with large axons so that each cell only elaborates one myelin sheath (Remahl and Hildebrand, 1990). Although it is difficult to demonstrate directly, the molecular structure of myelin does appear to vary with axon diameter (reviewed by Norton and Cammer, 1984). For example, myelin from large diameter axons has more myelin basic protein (MBP) and less PLP immunostaining than myelin from small diameter axons (Hartman *et al.*, 1982). This could support the view that oligodendrocytes myelinating small diameter axons are intrinsically different from those myelinating large diameter axons. Alternatively, the stoichiometric relationship between myelin proteins may change depending on the thickness (and total myelin volume) of each internode. Some cell markers such as carbonic anhydrase II (Butt *et al.*, 1995) and transferrin (Espinosa de los Monteros and Vellis, 1990) also vary between oligodendrocytes but a clear molecular basis for dividing oligodendrocytes into functional subpopulations has not been found. In

fact, work from transplantation experiments suggests that all oligodendrocytes are capable of myelinating a full range of axon sizes (Fanarraga *et al.*, 1998). This indicates that an extrinsic factor, possibly axonally derived, may be responsible for oligodendrocyte diversity.

1.2.2.1.2 Myelin biology

The myelin sheath is composed of lipids contributing to the phospholipid bilayer, which are interspersed with the myelin proteins. Although mature oligodendrocytes are post-mitotic, they remain extremely active continually turning over the lipid and protein components of myelin.

1.2.2.1.2.1 Lipid composition

Lipids constitute approximately seventy percent of the dry weight of myelin (Norton and Cammer, 1984). Although none of the lipids is unique to myelin, the high proportions of the galactosphingolipids (galactocerebroside and the sulphatides), cholesterol and plasmalogen are characteristic of myelin (Hildebrand *et al.*, 1993). Galactocerebroside, in particular, is restricted almost exclusively to the oligodendrocyte making it a useful myelin marker (Raff *et al.*, 1978). As well as having structural roles, the sphingolipids have been implicated in signal transduction (Dyer, 1993).

1.2.2.1.2.2 Protein composition

Proteolipid protein

PLP is the major myelin protein and, with its minor isoform, DM20, accounts for fifty percent of the myelin proteins. These proteins may have important structural roles in maintaining myelin compaction. In particular, they may act as adhesive struts supporting the intraperiod line and retaining the close apposition of the extracellular surfaces of adjacent myelin lamellae (see *1.3 The proteolipid protein gene: structure and function*, page 9).

Myelin basic protein

MBP proteins are a group of at least five isoforms of the *Mbp* gene ranging in size from 14 to 21.5kDa (Ferra *et al.*, 1985; Newman *et al.*, 1987; Aruga *et al.*, 1991) that are among the first myelin proteins to be upregulated during active myelination in the CNS (Kanfer *et al.*, 1989). These proteins are present in myelin forming cells and contribute forty percent of central myelin proteins (Lemke, 1988). These small

extrinsic membrane proteins are extremely basic, hydrophilic, charged molecules that localise to the cytoplasmic surface of compacted myelin (McLaurin *et al.*, 1993). In the CNS, the MBP proteins are responsible for maintaining fusion of the cytoplasmic surfaces of myelin lamellae to produce the major dense line (Privat *et al.*, 1979; Readhead *et al.*, 1987).

The *Mbp* gene transcriptional unit is itself contained within a larger gene complex, the *gene-of-oligodendrocyte-lineage* (*Golli-mbp* gene) (Pribyl *et al.*, 1993). The *Golli-mbp* gene utilises additional exons and the *Mbp* gene to express a range of isoforms predominantly in neural tissue. However, the regulation of the *Mbp* gene appears to be separate from that of the *Golli-mbp* gene (Pribyl *et al.*, 1993).

Myelin-associated oligodendrocyte basic protein (MOBP)

The MOBP group of proteins are small, highly charged, basic proteins produced by alternative splicing of the *Mobp* gene (Yamamoto *et al.*, 1994). These proteins localise in compact myelin at the major dense line and with the microtubular cytoskeletal elements (Montague *et al.*, 1998). They may have roles in the initiation of myelin compaction and in the late formation or stabilisation of the major dense line (Yamamoto *et al.*, 1994; Montague *et al.*, 1997). These proteins may also contribute to the formation of the radial component of myelin (Yamamoto *et al.*, 1999).

2', 3'-cyclic nucleotide 3'-phosphodiesterase (CNP)

The *Cnp* gene products catalyse the hydrolysis of several 2', 3'-cyclic nucleoside monophosphates *in vitro* and, in the CNS, are expressed exclusively by oligodendrocytes. Two isoforms of CNP (46 and 48kDa) constitute five percent of the total myelin proteins (Lemke, 1988) and localise to non-compacted regions of the myelin membrane (Trapp *et al.*, 1988). These proteins are expressed in oligodendrocyte progenitors and mature cells localising to the cytoplasmic surface of the plasma membrane where they bind microtubules possibly anchoring cytoskeletal elements to the membrane (Laezza *et al.*, 1997).

Myelin associated glycoprotein (MAG)

MAG proteins are highly glycosylated transmembrane proteins that constitute two differentially regulated isoforms (67 and 72kDa). These are not major components of myelin and account for only one percent of central and peripheral myelin proteins (Quarles *et al.*, 1992). The MAG protein isoforms are not structural components of compact myelin but localises to the non-compacted regions of the central myelin

sheath including the adaxonal cytoplasmic sheath and the paranodal loops (Trapp and Quarles, 1984). Specifically, they localise at points where oligodendrocyte and axonal membranes come into close apposition and are expressed before myelin compaction in ensheathing oligodendrocytes. They have marked similarities to N-CAM, an adhesive membrane protein expressed by neurones, and may have roles in axoglial interaction or in forming and maintaining the periaxonal space (Yoshihara *et al.*, 1991). However, *Mag* gene knockout mice myelinate well and have normal periaxonal spaces (Fruttiger *et al.*, 1995; Fujita *et al.*, 1998).

Minor myelin proteins

Small amounts of other myelin specific proteins have been identified but the functions of many of these remain obscure. These include myelin/ oligodendrocyte protein (MOG) (Linington *et al.*, 1984), oligodendrocyte-myelin glycoprotein (OMpg) (Mikol *et al.*, 1993) and myelin oligodendrocyte specific protein (MOSP) (Dyer *et al.*, 1991). Although these are not major components of myelin, they may have important roles in myelin production and maintenance.

1.2.3 The astrocyte

Astrocytes make up a heterogeneous population of cells that are thought to have roles in neural development and in supporting the architecture of the mature CNS (reviewed by Montgomery, 1994). During development, radial glia, which develop into astrocytes, provide a radial support for neuroblasts to migrate along and may guide axonal migration. In the mature CNS, in addition to supporting neural architecture and forming the glia limitans, astrocytes may support the nodal architecture and may help to maintain the ionic homeostasis of the CNS. During CNS injury, astrocytic hypertrophy supports damaged regions of the CNS and roles in modifying immune and inflammatory responses have also been proposed.

1.2.4 The microglia

The microglia are a resting population of mononuclear phagocytic cells that remove cellular debris produced from normal cell turnover within the CNS (reviewed by Stoll and Jander, 1999). Microglia also respond to CNS injury where they have phagocytic and antigen presenting roles. In the murine CNS microglia rarely become fully activated and marked microglial-induced inflammatory changes are uncommon. Active inflammatory lesions are produced when circulating macrophages migrate into damaged regions of the murine CNS.

1.2.5 Axoglia interactions

As well as supporting CNS architecture, axoglia interactions play important roles in neural development (reviewed by Barres, 1997). Neurones, for example, secrete mitogenic and survival factors that regulate glial maturation. Early in oligodendrocyte development, these factors promote progenitor proliferation and survival but prevent their differentiation and maturation (Barres *et al.*, 1993; Canoll *et al.*, 1996; Canoll *et al.*, 1999). As numbers of immature oligodendrocytes increase above demand, apoptotic pathways are triggered possibly through increasing competition for these survival factors (Barres *et al.*, 1992). These mechanisms control oligodendrocyte numbers ensuring that sufficient precursors populate the CNS to myelinate the white matter tracts. Myelination itself may simply be regulated through permissive signalling that allows oligodendrocytes to survive until they become myelin competent. However, there is mounting evidence that other, non-survival orientated pathways regulate myelination. For example, axons in the corticospinal and other tracts do not acquire myelin sheaths until after they have stopped migrating (Schwab and Schnell, 1989). One explanation is that, until reaching its target, the axon may release inhibitory factors that prevent oligodendrocyte differentiation (Barres, 1997). Other *in vitro* work suggests that soluble factors secreted by astrocytes mediate oligodendrocyte maturation and myelination (Bhat and Pfeiffer, 1986; Rosen *et al.*, 1989).

Increasingly, roles for glial cells in determining neuronal development are being identified. There is some evidence to suggest that glial cells guide migration of neuronal processes and promote the differentiation and survival of neuronal precursors (Barres, 1997). In the differentiated neurone, glial interactions are involved in regulating axonal structure (Colello *et al.*, 1994). Oligodendrocyte ensheathment induces local radial axonal growth. This is independent of myelin formation and may be mediated through a local membrane-bound kinase system that causes neurofilament phosphorylation (Sánchez *et al.*, 1996). Oligodendrocytes also release a soluble factor that induces sodium channel clustering, a vital step in defining the nodal axon. However, the location and spacing of the nodes is an intrinsic axonal feature and is not influenced by oligodendrocyte interaction (Kaplan *et al.*, 1997).

Collectively, these studies show that neurones and glia interact extensively during development through the release of soluble factors and through direct cellular contact. Altered gene regulation in oligodendrocytes following axotomy indicates that regulatory axoglia interactions continue throughout life (McPhilemy *et al.*, 1990). The identification of axonal pathology in increasing numbers of myelin diseases such as *quaking*, *rumpshaker* and *jimpy* mice (see 1.4.2.3 *Axonal changes*,

page 28) and in some chronic, progressive multiple sclerosis lesions may indicate a reciprocal role for oligodendrocytes in maintaining normal axon function (De Stefano *et al.*, 1998). Axoglial interactions are clearly important in neural development and maintenance and increasing evidence suggests that they may also have roles in disease pathogenesis.

1.3 The *proteolipid protein* gene: structure and function

1.3.1 The *Plp* gene locus

The *PLP* gene maps to a single locus on the X-chromosome (at Xq21.33-22 in man) (Willard and Riordan, 1985; Milner *et al.*, 1985; Mattei *et al.*, 1986) and encodes the major integral membrane proteins of compacted CNS myelin. Although the gene is predominantly expressed in oligodendrocytes, the recent identification of an eighth exon located within intron 1 has led to the discovery of splice variants of the *Plp* gene that are expressed in neuronal subpopulations (Bongarzone *et al.*, 1999). The gene is also expressed in premyelinating CNS tissue, Schwann cells, thymocytes, cardiac myocytes and spleen (Campagnoni *et al.*, 1992; Griffiths *et al.*, 1995; Dickinson *et al.*, 1996; Pribyl *et al.*, 1996). The organisation of the *Plp* gene and its transcription products are shown in Figure 1 (page 10).

The *Plp* structural gene covers approximately 17kb and contains eight exons and seven introns (Diehl *et al.*, 1986; Macklin *et al.*, 1987; Bongarzone *et al.*, 1999). The *Plp* gene contains two translation initiation codons (Bongarzone *et al.*, 1999). Exon 1 contains the 5'-UTR and major translation initiation codon with the first nucleotide of codon 2 (glycine) that will become the amino-terminal of the major mature *Plp* gene products (Macklin *et al.*, 1987). Exon 1.1 is located 122 base pairs downstream from exon 1 (Bongarzone *et al.*, 1999). It divides intron 1 in two and contains the second translation initiation codon and eleven additional codons that are spliced in-frame into exon 2 (Bongarzone *et al.*, 1999). The intronic sequence between exons 1.1 and 2 is the largest intron of the *Plp* gene and may have important regulatory functions (Wight and Dobretsova, 1997) (see *1.3.3.1 Transcriptional control*, page 12). The remaining exons are more closely spaced with exon 7 encoding the carboxy-terminus and the entire 3'-UTR (2.3kb) (Macklin *et al.*, 1987). Through alternate splicing of the primary transcript, the *Plp* gene produces two major protein isoforms, PLP (30kDa) and DM20 (26.5kDa) and two minor protein isoforms, srPLP and srDM20 (molecular weights not available) (see *1.3.3.2 Post-transcriptional regulation of Plp*, page 13). The presence of a ninth

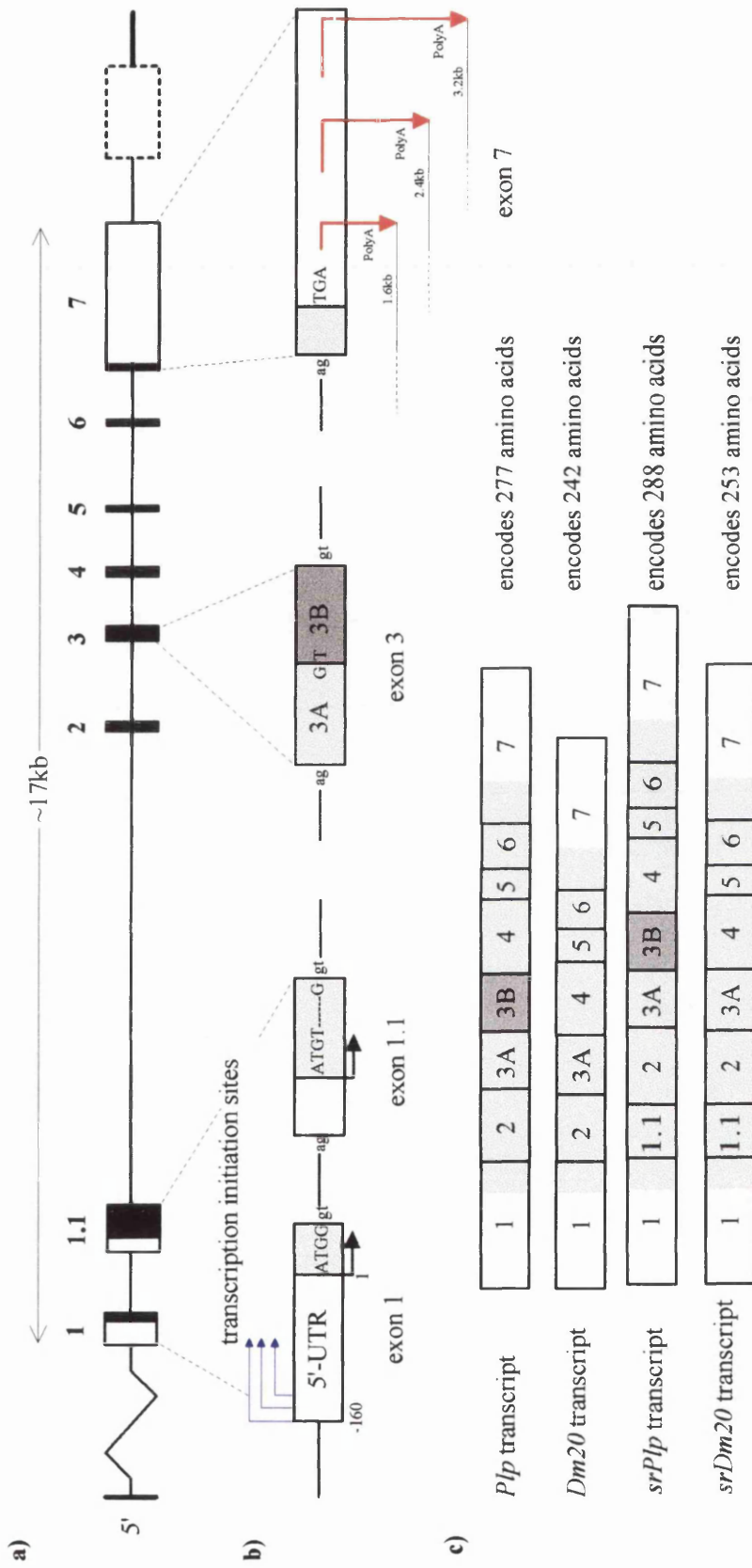


Figure 1 Organisation of the murine *Pip* gene and its major transcription products

a) Chromosomal arrangement of the *Pip* gene - a possible ninth exon in the 3' flanking sequence is shown (hatched box)

b) Regions producing *Pip* gene transcript heterogeneity - three transcription start sites (blue arrows), two translation initiation codons (black arrows), splice site within exon 3 and three polyadenylation signals (red arrows) are represented (sizes of the three populations of transcripts are given)

c) Arrangement of exons in the transcripts encoding the known splice variants of the *Pip* gene (exons are represented by numbered boxes; coding regions are shaded)

exon in the 3' flanking region has been proposed by Kamholz *et al.* (1992) and several lower molecular weight proteolipids may represent rarer splice variants of the *Plp* gene (see 1.3.7 *Lower molecular weight proteolipid proteins in the CNS*, page 19).

Plp gene transcript heterogeneity exists through alternative use of three cap sites in the 5'-UTR (Milner *et al.*, 1985; Macklin *et al.*, 1987) and three polyadenylation signals in the 3'-UTR (Milner *et al.*, 1985; Gardinier *et al.*, 1986; Macklin *et al.*, 1987) (see Figure 1, page 10). Three populations of transcripts, each containing all message isoforms, are produced by alternate use of these polyadenylation signals (Macklin *et al.*, 1987; Bongarzone *et al.*, 1999). Although 5' transcript heterogeneity has been associated with regulation of tissue-specific expression of other genes, no clear functional consequences have been identified for the *Plp* gene. Similarly, differential polyadenylation of the *Plp* gene transcripts appears to have no biological effect.

1.3.2 The *DM* gene family and phylogenetic evolution of the *Plp* gene

1.3.2.1 Conservation of the *Plp* gene

The *Plp* gene shows a remarkable level of sequence conservation between species at both the amino acid and nucleotide levels. When compared to man, amino acid sequence identity reaches 100% in rodents, >99% in the dog and >97% in the cow (Milner *et al.*, 1985; Macklin *et al.*, 1987). Nucleotide changes that occur between species tend to be silent and the exon boundaries are invariant. Even more unusually, high levels of sequence identity extend into the non-coding and non-transcribed regions. Between rat and human there is 93% overall identity of the 5'-UTR and up to 86% identity (overall 76%) of the 3'-UTR (Roth *et al.*, 1986). The proximal region of the 5'-UTR at the cap sites is one of the most highly conserved areas of the gene (100% between rodents and man) (Macklin *et al.*, 1987). Conservation of sequence also extends a considerable distance into the 5' flanking (95% over 1.1kb between rat and mouse; 75% over 0.7kb between rat and man) (Montague and Griffiths, 1997).

This level of conservation is almost unique to the *Plp* gene. Proteins that have specialised functions, particularly if these depend on close interaction with other proteins, can show high levels of conservation of their primary structure (75 to 90%). For example, the actin monomers structurally interact with six other molecules to function and show a comparable level of conservation of their primary structures (reviewed by Hudson and Nadon, 1992). The high level of conservation

within the non-coding and non-transcribed regions of the *Plp* gene is highly unusual and may be of more interest than the conservation of the peptide sequence. This level of conservation may indicate that the *Plp* gene is under tight regulatory control that could be vital for the function of the gene (see 1.3.3.1 *Transcriptional control*, page 12). The extreme conservation of the transcription initiation sites and the immediate 5' flanking sequence of the *Plp* gene strongly supports this hypothesis (Macklin *et al.*, 1987).

1.3.2.2 Phylogenetic evolution of the *Plp* gene and the *DM* gene family

The evolution of the *Plp* gene has been reviewed by Schliess & Stoffel (1993), Yoshida & Colman (1996) and Kurihara *et al.* (1997). The primordial gene encoding the DM20 protein first appeared in cartilaginous fish where myelin protein zero (P0) contributes to myelin compaction in both the peripheral and central nervous systems. The unique region of the PLP protein isoform was acquired after terrestrial vertebrates diverged from bony fish. The subsequent formation of the internal splice site within exon 3 as higher vertebrates diverged from amphibians enabled the expression of both isoforms. The evolution of the *Plp* gene appears to have been permissive with the drop out of P0 from the CNS indicating that *Plp* gene products may also have adhesive properties necessary for maintaining myelin compaction.

The *Plp* gene appears to be part of a large family of related genes with high levels of sequence identity, the *DM* gene family. These locate predominantly to the CNS and include the glycoprotein-encoding genes *Dm- α* , *Dm- β* and *Dm- γ* in bony fish (Kitagawa *et al.*, 1993) and *M6a* and *M6b* in mammals (Yan *et al.*, 1993). Some members of the *DM* gene family are found on epithelial surfaces involved in active ion transport and show significant degrees of sequence identity with the channel-forming regions of the ligand-gated acetylcholine and glutamate receptors (Kitagawa *et al.*, 1993). This adds weight to possible non-structural roles for the *Plp* gene (see 1.3.6.2 *Non-structural roles*, page 18) and may indicate that the *DM* gene family evolved from a duplicated ancestral gene that preceded the development of myelin (Kitagawa *et al.*, 1993).

1.3.3 Regulation of *Plp* gene expression in the CNS

1.3.3.1 Transcriptional control of *Plp* gene expression

Plp gene expression is controlled predominantly at the level of gene transcription. This is a common feature of genes that are expressed in a tissue-specific pattern and have transcripts that account for a large proportion of total cellular mRNA. Nuclear

run-on assays show that *Plp* gene transcripts are moderately stable and protein production closely mirrors transcript levels (Cook *et al.*, 1992). There is no evidence to support transcript instability or regulation of protein translation and degradation as being major points of control of *Plp* gene regulation (Cambi and Kamholz, 1994). The developmental profiles of the *Mbp* and *Plp* gene transcripts closely parallel each other and MBP protein levels mirror transcript production. This suggests that the *Mbp* gene is also transcriptionally controlled and that a single pathway may control the expression of both genes (Cook *et al.*, 1992). Comparison of the 5' flanking regions of the *Plp*, *Mag*, *Mog* and *Mbp* genes has revealed putative *cis*-regulatory elements, including a Sp-1-like binding site, that may coordinate expression of myelin genes through common *trans*-acting factors (Nave and Lemke, 1991; Janz and Stoffel, 1993).

In vitro and *in vivo* studies have been used to identify promoter and enhancer elements in the 5' flanking region and in intron 1 of the *Plp* gene. Wight and Dobretsova (1997) have identified potential *cis*-regulatory elements in intron 1 although the significance of these is unknown. They suggest that the *Plp* gene promoter is promiscuous and that intron 1 controls tissue specific expression by repressing promoter activity in non-glial cells. However, mounting evidence from other studies suggests that relatively short sequences of the *Plp* gene promoter itself control tissue specific expression (Nadon *et al.*, 1989; Nave and Lemke, 1991; Gout *et al.*, 1991; Cook *et al.*, 1992; Janz and Stoffel, 1993; Cambi and Kamholz, 1994; Johnson *et al.*, 1995).

1.3.3.2 Post-transcriptional regulation of *Plp* gene expression

The two major protein isoforms of the *Plp* gene, PLP and DM20, are translated from mRNAs produced by alternate splicing of the same pre-mRNA to give open reading frames of 831 and 726 base pairs respectively (Nave *et al.*, 1987a). The *Dm20*-mRNA differs from the *Plp*-mRNA only by the omission of 115 nucleotide residues that constitute exon 3b (see Figure 1, page 10). This results from alternate use of an internal 5' splice site (5'-CAACG**G**TAACAG-3') within exon 3 instead of the 5' splice site at the exon 3/ intron 3 boundary. This splice site delineates exon 3a from exon 3b and its utilisation causes the in-frame deletion of exon 3b. Although the production of multiple isoforms by alternate splicing to exclude entire exons is well described (for example *Mbp* and *Mag* genes), the utilisation of splice sites within exons is rare in mammalian genes (for example *CD44*: Sreaton *et al.*, 1992; *EAAT2*: Meyer *et al.*, 1998; *Il-15*: Prinzet *et al.*, 1998). The two minor protein isoforms, srPLP and srDM20, show similar alternate use of the internal splice site within exon 3. In addition, the *srPlp* and *srDm20* transcripts retain exon 1.1 that is

spliced in-frame with exon 2 and produces transcripts with open reading frames of 864 and 759 base pairs respectively (Bongarzone *et al.*, 1999).

Plp and *Dm20* message isoforms show different spatio-temporal expression patterns that are determined by splice site selection. There is no difference in the affinity for either 5' splice site in exon 3 so differential splicing patterns are not dependent on the position of the splice sites (Nave *et al.*, 1987a). One possibility is that splice site selection is under tight regulatory control and is regulated in a spatio-temporal manner. However, as the expression of the PLP protein isoform predominates during maximum *Plp* gene expression, splice site selection may be a feature of total transcript level. This would explain the marked change in proportion of the two isoforms that coincides with upregulation of the *Plp* gene. It may also offer an explanation as to why the DM20 protein predominates in the PNS and extra-neural tissues that express the *Plp* gene at low levels (see 1.3.4 *Expression of the Plp gene in the PNS*, page 15).

1.3.3.3 Developmental expression of the *Plp* gene in the CNS

The major cell type expressing the *Plp* gene in the CNS is the mature oligodendrocyte (Hartman *et al.*, 1982). *Plp* isoform transcripts can be detected from 0 to 2 days post-natally in the murine CNS, coinciding with the onset of myelination, and are rapidly followed by the incorporation of protein into myelin. *Plp* gene upregulation follows the developmental pattern of myelination starting in the medulla oblongata and proceeding rostrally in the brain and caudally in the spinal cord (Verity and Campagnoni, 1988). *Plp* isoform expression peaks when myelination is most active (post-natal day 22 in the mouse) (Verity and Campagnoni, 1988) but drops to approximately 60% of this level in the adult (Sorg *et al.*, 1987). In the myelinated CNS, *Plp* isoform transcripts predominate as the major product of the *Plp* gene. *Dm20* isoform expression is also upregulated during myelination but transcript levels never reach more than 50% of *Plp*-mRNA levels (Nave *et al.*, 1987a). Although peak *Plp* gene expression occurs during myelination, *Dm20* transcripts can be identified as early as embryonic day 9.5 in the developing murine CNS (Timsit *et al.*, 1992; Spassky *et al.*, 1998) and DM20 protein is identified from embryonic day 12 (Dickinson *et al.*, 1996). Initially *Dm20* isoform expression localises in the basal plate of the diencephalon and the caudal hypothalamus but later this spreads into the major white matter tracts. Unlike previously described oligodendrocyte progenitors, the *Dm20* transcript-positive cells do not express platelet-derived growth factor α -receptor (PDGFR α) although they do develop into mature oligodendrocytes. *Dm20*⁺, PDGFR α ⁻ cells are thought to represent a distinct lineage of oligodendrocyte precursors indicating that

oligodendrocytes may arise from two distinct populations of progenitor cells (Spassky *et al.*, 1998). The significance of *Dm20* isoform expression in these cells is unclear but its presence may indicate that the DM20 protein has roles early in oligodendrocyte development.

In the developing CNS, *srPlp* and *srDm20* transcripts show similar spatio-temporal expression patterns to *Plp* and *Dm20* transcripts respectively but are also expressed in neurones (Bongarzone *et al.*, 1999). Further analysis of the early *srDm20* transcript patterns in the developing CNS is necessary to establish if the expression of this isoform is confined to the same neural precursor cells as *Dm20* transcripts.

1.3.4 Expression of the *Plp* gene in the PNS

The *Plp* gene is expressed in the myelin-forming and non-myelin-forming Schwann cells of the PNS (Griffiths *et al.*, 1995). Both PLP and DM20 proteins are produced (Kamholz *et al.*, 1992) and appear to undergo similar post-translational modifications as in the CNS (Tetzloff and Bizzozero, 1993). However, the level of gene expression is much lower in Schwann cells and is uncoupled from the expression of other myelin genes suggesting that, in the PNS, the *Plp* gene may be under different transcriptional control than in the CNS.

In contrast to the CNS, the PLP isoform constitutes only a small proportion of the *Plp* gene products of the Schwann cell and appears to be localised to the perinuclear region (Griffiths *et al.*, 1995). DM20 is the major protein isoform produced in the PNS and localises to the non-compacted regions of the Schwann cell cytoplasm including the cell body, the Schmidt-Lanterman incisures, the paranodes and the outer Schwann cell cytoplasm. Although the presence of PLP or DM20 proteins cannot be demonstrated readily in peripheral compacted myelin there is some evidence to suggest that there may be low levels of each isoform present (Agrawal and Agrawal, 1991; Garbern *et al.*, 1997). In particular, Garbern *et al.* (1997) have demonstrated a low level of PLP immunoreactivity in peripheral compact myelin. Garbern *et al.* (1997) also described a family with a point deletion leading to a *PLP* gene-null allele. This family unusually developed a peripheral demyelinating neuropathy suggesting that the *Plp* gene does have roles in forming or maintaining peripheral myelin (see 1.4 *Plp* gene mutations, page 19). These results mean that the role of the *Plp* gene in the PNS may need to be re-evaluated.

The DM20 protein isoform is also expressed in the satellite cells of the peripheral ganglia and the olfactory bulb ensheathing cells (Griffiths *et al.*, 1995).

1.3.5 Translation and post-translational modification of PLP/DM20 protein

1.3.5.1 Translation and post-translational modification

Plp and *Dm20* message isoforms are translated on the rough endoplasmic reticulum and the proteins progress through the secretory pathway to the plasma membrane where they incorporate into myelin (Gow *et al.*, 1994a). Two post-translational events occur, the amino-terminal methionine is lost and the proteins undergo acylation. Some proteins, for example the myelin protein P0, require cleavage of an amino-terminal signalling peptide before the protein can be translocated to the plasma membrane (D'Urso *et al.*, 1990). PLP/DM20 proteins do not have a cleaved targeting sequence (Milner *et al.*, 1985) but the minor isoforms srPLP and srDM20 appear to have a targeting sequence encoded by exon 1.1 (Bongarzone *et al.*, 1999). The twelve peptide sequence shows some homology to known soma-restrictive targeting sequences and may restrict these proteins to the cell body of oligodendrocytes and neurones but does not undergo post-translational cleavage (Bongarzone *et al.*, 1999).

The PLP protein is acylated at six cysteine residues (see Figure 2, page 17) increasing its overall hydrophobicity. The DM20 protein is also acylated but lacks two of the acylation sites that are located in the peptide region unique to the PLP isoform (Weimbs and Stoffel, 1992). The two isoforms are acylated by similar ratios of long chain fatty acids predominantly comprising palmitic, palmitoleic, oleic and stearic acids (Bizzozero and Lees, 1999). The function of these fatty acids is unknown but alterations in their composition do lead to changes in protein conformation. Some evidence exists to suggest that the long-chain fatty acid composition of the proteolipids is linked to gene function. The relative proportions of fatty acids acylating the *Plp* gene products are highly conserved between species despite diversity in the proportions of other cell lipids. This implies that the pattern of acylation is also important for normal protein function (Bizzozero and Lees, 1999). Additionally, aberrant proteolipid acylation has been identified in at least one neurodegenerative disorder, X-linked adrenoleukodystrophy, although its significance in disease pathogenesis is uncertain (Bizzozero and Lees, 1999).

1.3.5.2 PLP and DM20 protein topology

Although several different models of PLP protein membrane topology have been proposed, the one suggested by Popot *et al.* (1991) is the most widely accepted (see Figure 2, page 17). The DM20 protein isoform lacks the hydrophilic, highly

charged, basic region unique to the PLP isoform (Weimbs and Stoffel, 1992) and may adopt a different topology. This may indicate that DM20 and PLP proteins have different roles as protein function can be intimately linked to conformation.

1.3.6 Proposed functions of the *Plp* gene

1.3.6.1 Structural roles

The abundance of the PLP protein in compacted CNS myelin and its proposed transmembrane topology provide strong circumstantial evidence for an important structural role in the formation and maintenance of compact myelin. Further evidence comes from the *Plp* gene mutants that characteristically have CNS hypomyelination with altered myelin periodicity, predominantly showing condensed intraperiod lines (1.4.2 *Plp* gene mutations in animal, page 22). In particular, the *Plp* gene products may act as adhesive struts supporting the intraperiod line and hence contributing to myelin compaction and stability (Duncan *et al.*, 1987a; Sinoway *et al.*, 1994). *In vitro* studies provide evidence that the extracellular domains of the *Plp* gene protein isoforms may have adhesive properties possibly through the formation of homophilic or heterophilic interactions between PLP and DM20 proteins (Sinoway *et al.*, 1994). Sinoway *et al.* (1994) specifically suggest that DM20 may be necessary to allow PLP transport to the cell surface and hence its incorporation into compact myelin although this view is not supported by other work (Thomson *et al.*, 1997).

1.3.6.2 Non-structural roles

The expression of the *Plp* gene before the formation of myelin in the CNS and in non-neural tissues has led to the suggestion that it may have functions other than as a structural component of compact myelin. The presence of *Dm20* transcripts in early embryonic tissues (Timsit *et al.*, 1992) and the reduction in mature oligodendrocyte numbers in most *Plp* mutants (Knapp, 1996) provide some evidence for a role, particularly of the DM20 protein isoform, in oligodendrocyte differentiation and survival. Yamada *et al.* (1999) reported from *in vitro* studies that a secreted *Plp* gene product may act as a mitotic factor increasing astrocyte and oligodendrocyte numbers. They suggested that this product may have autocrine or paracrine roles in the CNS but were unable to demonstrate its presence directly.

As the *Plp* gene products and other members of the *DM* gene family show considerable similarity to channel-forming proteins (see 1.3.2.2 *Phylogenetic evolution of the *Plp* gene and the *DM* gene family*, page 12), a role in regulating the ion permeability of myelin has been proposed. Experimental data from artificial

lipid bilayers provides support for the *Plp* gene protein isoforms acting as ionophores (Diaz *et al.*, 1990).

The isolation of *srDm20* transcripts to developing neural tissue and of srPLP and srDM20 proteins to the soma of oligodendrocytes and subpopulations of neurones suggests potential roles in early neural development and in mature oligodendrocyte and neuronal function (Bongarzone *et al.*, 1999).

1.3.7 Lower molecular weight proteolipid proteins in the CNS

Biochemical fractionation of CNS tissue has shown small amounts of low molecular weight proteolipids that may represent rare protein isoforms of the *Plp* gene. One of these peptides (M_r 20 kDa) has been identified in bovine foetal tissue (Schindler *et al.*, 1990). Two other proteolipids (M_r 14 kDa and 16 kDa) have been isolated from adult bovine brain (Lepage *et al.*, 1986) and embryonic murine tissue (Nussbaum and Mandel, 1973). The presence of these proteins with the DM20 protein isoform in pre-myelinating CNS tissue may indicate a non-structural role for the *Plp* gene. However, to date, no reports of transcripts coding these putative isoforms have been published and they may represent artefacts of biochemical fractionation.

1.4 *Plp* gene mutations and disease

Spontaneous *Plp* gene mutations cause severe dysmyelinating disease in man and in animals. The study of these disorders and the generation of *Plp* transgenic animals have provided valuable insights into the functions of the *Plp* gene and its role in neurological disease.

1.4.1 PLP gene-related disorders in man

Two dysmyelinating diseases have been described in man that have an X-linked recessive mode of inheritance and have been shown to map to the *PLP* gene locus; Pelizaeus-Merzbacher disease (PMD) and X-linked Spastic Paraplegia type 2 (SPG2). Both were originally defined by their clinical features and are now considered allelic disorders of the *PLP* gene.

1.4.1.1 Pelizaeus-Merzbacher Disease

PMD (OMIM 312080) was first described in 1885 by Pelizaeus and in 1910 by Merzbacher. It produces a progressive clinical syndrome of nystagmus, delayed psychomotor development, spasticity, cerebellar ataxia, optic atrophy, laryngeal stridor, seizures and mental deterioration that leads to death in adolescence or early adulthood (Hodes *et al.*, 1993; Seitelberger, 1995). Marked variation in the severity

of disease has been noted both between unrelated families and within related families and three classifications of disease have been proposed (Seitelberger, 1995). These are PMD type I (“classic PMD”, onset within the first 5 years), PMD type II (congenital or “connatal” PMD, onset from birth), and PMD type III (“transitional PMD” with an intermediate phenotype between type I and II). Due to its X-linked mode of inheritance, males are predominantly affected while females, heterozygous for the disease allele, act as asymptomatic carriers. Occasionally, disease is reported in females from affected families (see 1.4.5 *Clinically affected female carriers*, page 33).

Pathologically, PMD is characterised by diffuse, symmetrical CNS hypomyelination that is most marked in late myelinating areas such as the cerebellar and cerebral white matter. Oligodendrocytes are reduced in number with ultrastructural abnormalities and there is a dense fibrillary astrocytosis. Myelin, when present, is poorly compacted and there is some evidence of demyelination. Complete amyelination, which is seen in connatal (Type II) PMD, is reflected clinically by early disease onset and death (Seitelberger, 1995). Although *PLP* gene mutations are not classically considered to affect the PNS, one report describes a demyelinating peripheral neuropathy in a family with a *PLP* gene-null mutation and alludes to possible similar pathology in other PMD families (Garbern *et al.*, 1997) (see also 1.3.4 *Expression of the Plp gene in the PNS*, page 15).

1.4.1.2 X-Linked Spastic Paraplegia Type 2

X-linked spastic paraplegia is a rare disorder that occurs in two clinically distinct forms. The pure spastic form is characterised by spasticity of the lower limbs with normal mental function. Most cases reported take on a more complicated phenotype of spasticity, cerebellar ataxia, mental retardation and, occasionally, congenital malformations. Some cases of complicated SPG with congenital abnormalities result from mutations of the *LICAM* gene at Xq28 locus (SPG 1; OMIM 312920). Other cases of complicated SPG and uncomplicated (pure) SPG map to the *PLP* gene locus and are classified as SPG2 (OMIM 312920). Some of the clinical features of SPG2 are similar to those of PMD including mental retardation, nystagmus and optic atrophy. In most reports, only male patients are clinically affected while females act as asymptomatic carriers (Saugier-Weber *et al.*, 1994). As with PMD, there are occasional reports of clinical disease in females from affected families and there can be marked heterogeneity of disease within families (Bonneau *et al.*, 1993; Sivakumar *et al.*, 1999). Pathologically, most of the CNS white matter is spared but the longitudinal spinal tracts are severely dysmyelinated (Seitelberger, 1995).

1.4.1.3 Genetic basis of *PLP* gene-related disorders in man

Point mutations of the *PLP* gene were first reported by Hudson *et al.* (1989) , Gencic *et al.* (1989) and Trofatter *et al.* (1989) who described three separate mutations leading to PMD. Trofatter *et al.* (1989) noted genetic heterogeneity of PMD as these point mutations could not be identified in six additional affected families and these findings have subsequently been supported by the numerous reports of novel mutations leading to disease. To date, at least 62 point mutations have been described in coding regions of the *PLP* gene leading to PMD or SPG2 (Table 1, page 24) but only two *PLP* gene polymorphisms have been found (Table 2, page 25) (for reviews see OMIM 312080; Garbern, 2000; Hodes *et al.*, 1993). Although some of these mutations are predicted to lead to protein truncation or aberrant splicing (for example G434A, C700T), others lead to conservative amino acid substitutions that are not expected to dramatically alter protein conformation (for example C728T, Ala243Val). The intolerance of even conservative amino acid changes adds weight to the argument that the functions of the *PLP* gene are dependent on the primary peptide sequences indicating a possible role in protein-protein interactions (see 1.3.2.1 *Conservation of the Plp gene*, page 11). Other mutations affecting non-coding regions have been described and some families with linkage to the *PLP* gene locus but no observed mutation are thought to have mutations in non-transcribed regulatory regions (Cambi *et al.*, 1996; Inoue *et al.*, 1997). These findings suggest that altered gene regulation can also lead to disease.

One of the major groups of *PLP* gene mutations leading to disease involve alterations in copy number of the *PLP* gene (Sistermans *et al.*, 1998; Mimault *et al.*, 1999) (Table 2, page 25). Interphase fluorescence *in situ* hybridisation has shown that many, perhaps even the majority, of cases of PMD result from duplication of the *PLP* gene (Osaka *et al.*, 1996; Woodward *et al.*, 1998). In addition, several families, often with milder PMD phenotypes, have been described that have *PLP* gene deletions (Raskind *et al.*, 1991; Osaka *et al.*, 1996) or mutations in exon 1 predicted to cause functional null alleles (Garbern *et al.*, 1997). These findings show that at least one subgroup of PMD results from alterations in *PLP* gene dosage and suggest that null mutations of the *PLP* gene lead to comparatively mild phenotypes.

Heterogeneity of disease within affected families may be the result of modifying genes (see 1.4.6 *Modifying loci*, page 34). Tables 1 and 2 (pages 24 and 25) list the known *PLP* gene mutations that cause PMD and SPG2. Point mutations in the coding regions of the gene are demonstrated graphically in Figure 3 (page 23).

1.4.2 *Plp* gene mutations in animals

Plp gene mutations have been described in the mouse (*Plpip*, *Plpip-4j*, *Plpip-msd*, *Plpip-rsh*), rat (*Plpmd*), dog (*Plpsh*) and rabbit (*Plppt*) (see Table 3, page 26) (for review see Knapp, 1996). The *jimpy* mouse results from a point mutation in intron 4 that disrupts the 3' acceptor splice site (Hudson *et al.*, 1987; Nave *et al.*, 1987b). This leads to the deletion of exon 5 from the *Plp* gene transcripts and is predicted to produce a truncated protein with a novel, cysteine-rich carboxy terminus. The other mutants result from point mutations causing amino acid substitutions (see Table 3, page 26 and Figure 3, page 23) (*Plpmd*: Boison & Stoffel, 1989; *Plpip-msd*: Gencic & Hudson, 1990; *Plpsh*: Nadon *et al.*, 1990; *Plpip-rsh*: Schneider *et al.*, 1992; *Plppt*: Tosic *et al.*, 1994; *Plpip-4j*: Pearsall *et al.*, 1997).

Most of these mutants develop fatal dysmyelinating phenotypes (Knapp, 1996). The CNS is severely hypomyelinated with a paucity of mature oligodendrocytes. Microglia proliferate in response to oligodendrocyte death (Vela *et al.*, 1996) and astrocyte hypertrophy contributes to a general gliosis (Billings-Gagliardi *et al.*, 1995; Duncan, 1995). The animals develop a marked tremor as they start to ambulate (from 10 to 12 days in the mouse) and seizures are common. Affected individuals usually die in the late post-natal period (around 25 to 30 days in the mouse). PLP and DM20 are often absent from the few myelin sheaths that do form and all the myelin proteins are reduced (Sorg *et al.*, 1987; Billings-Gagliardi *et al.*, 1995; Nadon and Duncan, 1996). *Plp* gene expression is reduced in the PNS of at least some of these mutants (Tosic *et al.*, 1996) but this has no effect on Schwann cell function and the peripheral myelin is normal.

Unlike other *Plp* gene mutants, *rumpshaker* mice and *paralytic tremor* rabbits have mild clinical phenotypes that are non-lethal and partially regress with time. Both dysmyelinate but partially recover as they age (Taraszewska, 1988; Fanarraga *et al.*, 1992; Tosic *et al.*, 1996).

1.4.2.1 Dysmyelination

In the CNS of most *Plp* gene mutants, only a minority of axons is myelinated, the proportion reflecting the severity of the phenotype. The sheaths that form are thin and occur as solitary internodes (Ransom *et al.*, 1985; Billings-Gagliardi *et al.*, 1995; Duncan, 1995). What little myelin that is present is loosely compacted and ultrastructurally abnormal (Duncan *et al.*, 1987a; Billings-Gagliardi *et al.*, 1995). Most of the lamellae have abnormal intraperiod lines that condense to a single electron-dense band indistinguishable from the major dense line. This leads to a

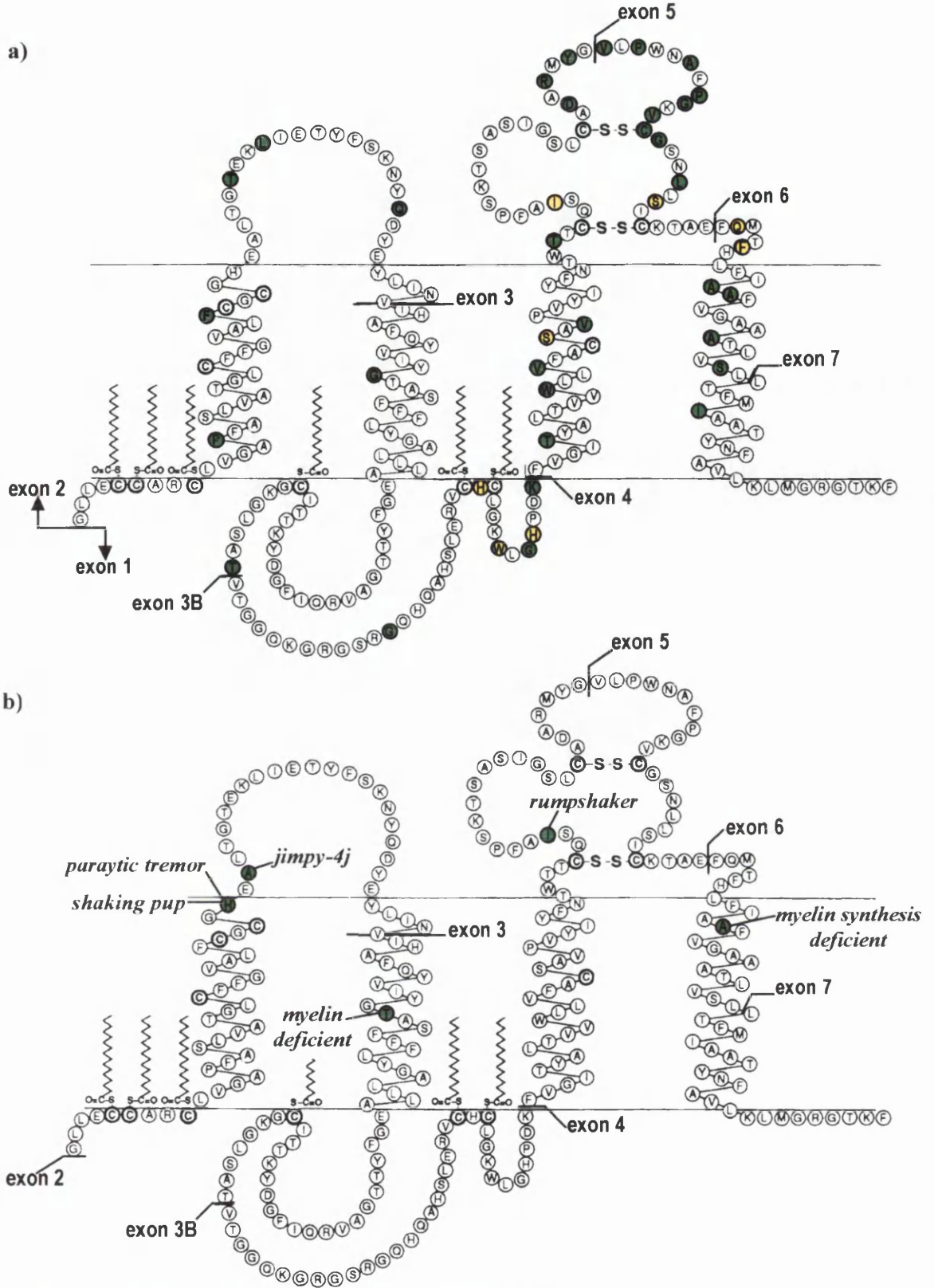


Figure 3 Sites of amino acid substitutions caused by point mutations in coding regions of the *PLP/Plp* gene
a) Sites of amino acid substitution leading to PMD (green) and SPG2 (yellow)
b) Sites of amino acid substitution leading to dysmyelinating disease in animals (green) - phenotypic names are given
For a full description of the protein model used in this diagram see Figure 3, page 10)

**Table 1 *PLP* gene point mutations causing PMD and SPG2
(numbering starts from the methionine translation initiation codon)**

Classification	Region	Nucleotide	Amino acid	Disease
missense	exon 1	G 003 A	Met 001 Ile	PMD-I
	exon 2	C 044 T	Pro 015 Leu	PMD-I
	exon 2	T 094 G	Phe 032 Val	PMD-I PMD-II
	exon 2	C 128 T	Thr 043 Ile	PMD-I
	exon 2	T 137 G	Leu 046 Arg	PMD-I
	exon 2	T 137 C	Leu 046 Pro	PMD-II
	exon 3	G 220 A	Gly 074 Arg	PMD-I
	exon 3	C 337 A	Thr 116 Lys	PMD-I
	exon 3B	C 384 G	Gly 128 Gly	PMD-II
	exon 3B	C 418 T	His 140 Tyr	SPG2
	exon 3B	A 441 T	Gly 147 Gly	PMD-I
	exon 3B	C 442 T	His 148 Tyr	SPG2
	exon 3B	G 453 C	Lys 151 Asn	PMD-I
	exon 3B	G 453 T	Lys 151 Asn	PMD-I
	exon 4	C 467 T	Thr 156 Ile	PMD-I
	exon 4	T 487 C	Trp 163 Arg	PMD-II
	exon 4	T 497 A	Val 166 Glu	PMD-I
	exon 4	T 497 G	Val 166 Gly	PMD-I
	exon 4	T 505 C	Cys 168 Arg	PMD
	exon 4	C 509 T	Ser 170 Phe	SPG2
	exon 4	T 515 C	Val 172 Ala	PMD-II
	exon 4	A 524 G	Tyr 175 Cys	PMD
	exon 4	G 542 A	Trp 181 Ala	PMD
	exon 4	A 544 C	Thr 182 Pro	PMD-II
	exon 4	C 548 A	Thr 183 Asn	PMD
	exon 4	T 560 C	Ile 187 Thr	SPG2 (<i>Plp^{jp-rsh}</i>)
	exon 4	G 607 C	Asp 203 His	PMD-I
	exon 4	A 608 T	Asp 203 Val	PMD-I
	exon 4	A 608 G	Asp 203 Gly	PMD
	exon 4	T 609 A	Asp 203 Glu	PMD
	exon 4	A 613 G	Arg 205 Gly	PMD-I
	exon 4	A 620 G	Tyr 207 Cys	PMD-I
	exon 5	T 626 A	Val 209 Asp	PMD-I
	exon 5	T 629 A	Leu 210 His	PMD
	exon 5	C 632 T	Pro 211 Leu	PMD-I
	exon 5	T 214 C	Trp 212 Arg	PMD
	exon 5	C 641 G	Ala 214 Pro	PMD-I
	exon 5	C 646 T	Pro 216 Ser	PMD-I
	exon 5	G 649 A	Gly 217 Ser	PMD-I
	exon 5	G 655 T	Val 219 Phe	PMD-I
	exon 5	G 659 A	Cys 220 Tyr	PMD-I
	exon 5	G 661 T	Gly 221 Cys	PMD-II
	exon 5	C 670 A	Leu 224 Ile	PMD-II

cont/....

Table 1 continued

Classification	Region	Nucleotide	Amino acid	Disease
missense	exon 5	T 671 C	Leu 224 Pro	PMD-II
	exon 5	T 676 C	Ser 226 Pro	SPG2
	exon 5	T 682 C	Cys 228 Tyr	PMD
	exon 6	A 234 T	Gln 234 Pro	PMD
	exon 6	T 710 C	Phe 237 Ser	SPG2
	exon 6	G 724 C	Ala 242 Pro	PMD-I
	exon 6	C 728 T	Ala 243 Val	PMD-II (<i>PLP^{jp-msd}</i>)
	exon 6	G 737 A	Gly 245 Glu	PMD
	exon 6	C 743 A	Ala 248 Glu	PMD
	exon 6	G 745 C	Ala 249 Pro	PMD-I
exon 6	C 758 T	Ser 253 Phe	PMD-I	
deletion	exon 1	G 003	no translation	PMD-I
nonsense	exon 3B	G 434 A	Trp 145 Stop	SPG2
	exon 6	C 700 T	Gln 234 Stop	SPG2 PMD-I
	exon 7	insert G 775 frameshift	stop 268	PMD-II
splice site	exon 3	C 347 A	Thr 116 Lys	SPG2 PMD-I
substitution	5'-flanking	C -442 G	regulatory	PMD-I
	5'-UTR	C -031 T	regulatory	PMD-I

Table 2 *PLP* gene duplications, deletions and polymorphisms

a) Duplications and deletions of the *PLP* gene locus; b) Partial *PLP* gene deletions; c) *PLP* gene polymorphisms (numbering starts from the methionine translation initiation codon)

a)

Classification	Region	Disease
gene duplication	entire locus	PMD-I
gene deletion	entire locus	PMD-I

b)

Classification	Region	Nucleotide	Amino acid	Disease
deletion	5'flank-intron 1	frame-shift		SPG2
	exon 3B	A352 to T497	Thr 118 to Val 166	PMD-I
	exon 3B to 4	in frame	Val 117 to Leu165	PMD-I PMD-II
deletion/ insertion	intron 5	T 675+2→G	5' splice site	PMD-I

c)

Region	Polymorphism	Amino acid
exon 2	A 168 G	Gln 056 Gln
exon 4	T 609 C	Asp 203 Asp

**Table 3 Spontaneous *Plp* gene mutations in animal models
(numbering starts from the methionine translation initiation codon)**

Species	Mutant	Allele	Region	Classification	Nucleotide	Amino acid
mouse	<i>jimpy</i>	<i>Plp^{jp}</i>	3'splice site of exon 4	missense with frameshift	A621-2→G splice site 4	
	<i>jimpy-4j</i>	<i>Plp^{jp-4j}</i>	exon 2	missense	G 117 T	Ala 039 Ser
	<i>rumpshaker</i>	<i>Plp^{jp-rsh}</i>	exon 4	missense	T 562 C	Ile 187 Thr
	<i>myelin synthesis deficient</i>	<i>Plp^{jp-msd}</i>	exon 6	missense	C 730 T	Ala 243 Val
rabbit	<i>paralytic tremor</i>	<i>Plp^{Pt}</i>	exon 2	missense	T 113 A	His 037 Gln
dog	<i>shaking pup</i>	<i>Plp^{sh-pup}</i>	exon 2	missense	A 112 C	His 037 Pro
rat	<i>myelin deficient</i>	<i>Plp^{md}</i>	exon 3	missense	A 225 C	Thr 075 Pro

reduction of myelin periodicity from 11nm in the wild type to 9nm in the mutants (Duncan *et al.*, 1987a). Myelin lamellae occasionally form with normal intraperiod lines but these are rare and could represent areas of myelin containing very low levels of the abnormal *Plp* gene proteins (Duncan *et al.*, 1987a). Most axons are naked and have no association with oligodendrocyte processes (Thomson *et al.*, 1997).

The *rumpshaker* mouse is hypomyelinated with increased numbers of unmyelinated small axons and thin sheaths surrounding larger axons. The small diameter (late myelinating) axons of the optic nerve have normal-thickness myelin sheaths when present but a large proportion of axons remains unmyelinated. As the animal matures, the clinical phenotype recovers and most of the axons acquire myelin sheaths although these still remain comparatively thin (Fanarraga *et al.*, 1992). Although many sheaths have normal periodicity, others have condensed intraperiod lines (Griffiths *et al.*, 1990). The *paralytic tremor* rabbit has delayed and incomplete central myelination predominantly affecting the small diameter fibres (Taraszewska, 1988; Tomic *et al.*, 1996).

1.4.2.2 Oligodendrocyte abnormalities and death

Mature oligodendrocyte numbers are severely reduced in the *jimpy*, *jimpy-4j* and *myelin synthesis deficient* mice, the *myelin deficient* rat and the *shaking pup* (Billings-Gagliardi *et al.*, 1995; Knapp, 1996). Death of mature oligodendrocytes probably accounts for this in most mutants as immature oligodendrocyte numbers are not reduced (Nadon and Duncan, 1995; Skoff, 1995; Gow *et al.*, 1998; Lipsitz *et al.*, 1998; Grinspan *et al.*, 1998). Oligodendrocytes in the *shaking pup* do not die but remain immature and fail to produce many myelin sheaths (Nadon and Duncan, 1996). Some of the mutants have abnormal oligodendrocyte morphology with distension of the rough endoplasmic reticulum and swollen Golgi vesicles (Billings-Gagliardi *et al.*, 1995; Knapp, 1996). Oligodendrocytes from *myelin synthesis deficient* and *jimpy* mice show PLP/DM20 immunoreactivity in the rough endoplasmic reticulum but no evidence of protein in the Golgi or at the cell surface (Roussel *et al.*, 1987; Gow *et al.*, 1998). These results suggest a disruption of protein trafficking in oligodendrocytes leading to an inability to incorporate abnormal *Plp* gene products into myelin.

The *rumpshaker* mouse and *paralytic tremor* rabbit are notable as they maintain normal oligodendrocyte numbers despite having disrupted protein trafficking pathways. DM20 protein levels are maintained and this isoform is incorporated into the myelin sheath (Griffiths *et al.*, 1990; Karthigasan *et al.*, 1996). Only small amounts of the abnormal PLP isoform are produced and these are retained in the

rough endoplasmic reticulum (Karthigasan *et al.*, 1996).

1.4.2.3 Axonal changes

Axonal pathology is seen in *jimpy* and *rumpshaker* mice (Rosenfeld and Friedrich, Jr., 1983; Fanarraga *et al.*, 1992), the *paralytic tremor* rabbit (Taraszewska, 1988) and the *myelin deficient* rat (Dentinger *et al.*, 1982; Duncan *et al.*, 1995). Axonal swellings are found with accumulations of cytoskeletal elements and membrane bound organelles such as dense bodies. In the longer-lived mutants, degenerate axons can also be identified.

1.4.3 *Plp* transgenic animals

Several lines of transgenic mice have been generated that express *PLP* transgenes. Both genomic transgenic constructs encoding PLP and DM20 proteins and cDNA transgenic constructs expressing one or other of the two isoforms have been used. There is little correlation between the transgene copy number and the transcript and protein levels in the transgenic mice when compared to levels of endogenous *Plp* gene expression. This indicates that some of these transgenes are less efficiently transcribed than the endogenous *Plp* gene (Johnson *et al.*, 1995) and that transcript and protein processing may be altered.

1.4.3.1 Expression of genomic *Plp* transgenes

Three transgenic lines of mice containing two separate transgenes have been produced that express both major splice variants of the *Plp* gene (lines #66 and #72: Readhead *et al.*, 1994; line #4e: Kagawa *et al.*, 1994a). The constructs include fragments encompassing all the known exonic sequence of the murine *Plp* gene covalently linked to 5' and 3' *Plp* gene flanking sequences (see Table 4, page 29). These produce transcripts that undergo normal splicing.

Transgenic mice from these lines develop dysmyelinating and demyelinating phenotypes that are influenced by gene dosage. Homozygous #4e and #66 mice develop severe dysmyelinating phenotypes that cause tremor, seizing and death by 60 days of age (Readhead *et al.*, 1994; Kagawa *et al.*, 1994a; Inoue *et al.*, 1996). Homozygous #72 mice have lower transgene copy numbers than homozygous #66 mice and develop a milder dysmyelinating phenotype that leads to death by 4 months of age (Anderson *et al.*, 1998). Hemizygotes from all three lines myelinate well initially but develop late phenotypes associated with subsequent demyelination (Kagawa *et al.*, 1994a; Inoue *et al.*, 1996; Anderson *et al.*, 1998). Occasional

Table 4 Transgenic animals expressing *Plp* genomic transgenes and *Plp*-cDNA and *Dm20*-cDNA transgenes

Line	Construct details		Structural gene unit	3' sequence	Haploid copy number	Original reference
	Source	5' sequence				
#66	mouse	3.5kb	7 exons/ 6 introns	6.1kb	7	Readhead <i>et al.</i> , 1994
#72					3	
#4e	mouse	20.0kb	7 exons/ 6 introns	3.0kb	2	Kagawa <i>et al.</i> , 1994
<i>Plp</i> Tg1	human	4.2kb	<i>Plp</i> -cDNA	1.5kb	30	Nadon <i>et al.</i> , 1994
<i>Dm20</i> Tg2			<i>Dm20</i> -cDNA		?	
ND3A	human	2.9kb	<i>Dm20</i> -cDNA	SV40	17	Mastronardi <i>et al.</i> , 1993
ND4				polyA signal	70	Johnson <i>et al.</i> 1995

swollen and degenerate axons are seen as late changes in #66 homozygotes and are prominent features of #72 homozygotes, along with some demyelination, prior to death (Anderson *et al.*, 1998). Axonal pathology is also seen in hemizygous mice from these two lines (Anderson *et al.*, 1998). The axonal changes predominantly affect tracts with small diameter fibres such as the optic nerve, corticospinal tract and fasciculus gracilis.

1.4.3.2 Expression of *Plp*-cDNA and *Dm20*-cDNA transgenes

Several lines of *Dm20*-cDNA transgenic mice and one line of *Plp*-cDNA transgenic mice have been generated (see Table 4, page 29) (Nadon *et al.*, 1994; Johnson *et al.*, 1995). The ND4 and ND3A lines of *Dm20*-cDNA transgenic mice generated by Johnson *et al.* (1995) offer further examples of the influence of gene dosage on *Plp* gene-related disease. ND4 hemizygous mice (70 transgenic cassettes) develop central demyelination leading to death at 10 months of age (Mastronardi *et al.*, 1993). ND3A homozygous mice (34 transgenic cassettes) have similar pathological features to the ND4 hemizygous mice but a milder clinical phenotype that develops from 12 to 16 months of age (Mastronardi *et al.*, 1996). ND3A hemizygous mice (17 transgenic cassettes) do not develop CNS pathology at all.

1.4.3.3 Targeted gene replacements of the *Plp* gene

Boison and Stoffel (1994) attempted to generate mice that expressed only the *Dm20*-mRNA isoform by targeted mutation of the endogenous *Plp* gene. The targeting construct removed exon 3B from the *Plp* gene and introduced a selectable marker, the neomycin resistance gene (*neo*), into intron 3. During splicing, because of the presence of the *neo* cassette, the *Plp* gene transcripts retained intron 3 and no proteins were translated. From this targeting strategy, two lines of mice with functional null alleles of the *Plp* gene were generated. Poorly compacted myelin sheaths surround the larger diameter CNS axons of these mice but many of the small diameter axons remain unmyelinated (Boison and Stoffel, 1994; Boison *et al.*, 1995). The myelin that does form shows variable ultrastructural abnormalities. The intraperiod lines are often condensed or the extracellular interface between adjacent myelin lamellae may be disrupted (Rosenbluth *et al.*, 1996).

These mice are notably different from the missense *Plp* gene mutants as they show only subtle clinical phenotypes and produce large amounts of myelin. This is comparable to the milder forms of PMD with deletions and functional null alleles of the *PLP* gene (Raskind *et al.*, 1991; Osaka *et al.*, 1996; Garbern *et al.*, 1997). There are some common features between the *Plp* gene-null mutants and the other *Plp* gene mutants such as ultrastructural abnormalities of myelin. However, some of the

features of missense *Plp* gene mutants must arise through mechanisms other than the loss of functional *Plp* gene products.

1.4.4 Pathogenesis of *Plp* gene-related disorders

Several mechanisms, including gain of function, loss of function and gene dosage effects, could account for the pathogenesis of *Plp* gene-related disease. Several different pathogenic pathways may lead to disease in *Plp* gene mutants as evidence exists supporting each of these mechanisms.

1.4.4.1 Gain of function of mutated gene products

The accumulation of *Plp* gene protein isoforms in the rough endoplasmic reticulum of mutant oligodendrocytes probably results from conformational changes within altered proteins leading to ineffective protein trafficking. It has been suggested that oligodendrocyte death and dysmyelination results from the abnormal trafficking (Gow *et al.*, 1998). Alternatively, an inability of mutant polypeptides to form multimeric complexes may directly prevent their integration into myelin (Gow *et al.*, 1994b). *In vitro* studies demonstrate that the degree of disruption of protein trafficking correlates with phenotypic severity in mutant animals (Gow and Lazzarini, 1996; Thomson *et al.*, 1997). In addition, the inability of transgenic complementation to rescue *jimpy* mice adds weight to the theory that novel gains of function of abnormal *Plp* gene products prove toxic to the oligodendrocyte (Nadon *et al.*, 1994; Kagawa *et al.*, 1994a; Schneider *et al.*, 1995).

However, *jimpy* oligodendrocytes can survive longer and reach mature phenotypes when cultured in normal astrocyte-conditioned medium (Knapp *et al.*, 1996) and their survival is also enhanced by transplantation into normal and *shiverer* CNS tissue (Lachapelle *et al.*, 1991). These findings suggest that *jimpy* oligodendrocytes are intrinsically viable and die only because the local environment is not permissive to their survival. The contradictory findings in these mutants must be clarified before toxic properties can be ascribed to mutated *Plp* gene products.

1.4.4.2 Loss of function of *Plp* gene products

The ultrastructural abnormalities of myelin in *Plp*-null mice (Boison and Stoffel, 1994) and in the spontaneous *Plp* gene mutants that express low levels of potentially non-functional protein provide evidence that PLP and DM20 are structural components of myelin. The condensation of the intraperiod lines and poor maintenance of myelin compaction in these mutants are consistent with PLP and DM20 proteins acting as adhesive struts supporting the extracellular interface between adjacent myelin lamellae. Transgenic complementation of the *jimpy* mouse

can reverse these ultrastructural changes although the rescued mice remain severely hypomyelinated (Schneider *et al.*, 1995). This provides evidence that these ultrastructural abnormalities are the direct result of loss of functional *Plp* gene products. In addition, PMD cases with deletions or effective null alleles of the *PLP* gene show that at least some of the disease features result from loss of normal PLP and DM20 proteins (Raskind *et al.*, 1991; Osaka *et al.*, 1996; Garbern *et al.*, 1997).

The proposals that PLP/DM20 proteins are important for oligodendrocyte survival and maturation will be expanded in relation to the results of this study (page 125).

1.4.4.3 Effect of *Plp* gene dosage

1.4.4.3.1 Stoichiometric relationship to other myelin constituents

Gene dosage as a pathogenic mechanism has been well documented in mutations of the *peripheral myelin protein 22 (PMP22)* gene, a minor component of compacted PNS myelin (Gabriel *et al.*, 1997; Hanemann and Müller, 1998). A severe peripheral neuropathy, Charcot-Marie-Tooth type 1A (CMT1A), results from duplications of the *PMP22* gene. In contrast, deletions of this gene lead to the mild disease, hereditary neuropathy with liability to pressure palsies (HNPP). *PMP22* protein levels in these disease groups correlate well with gene dosage and disease severity (Gabriel *et al.*, 1997). The correlation between *PMP22* protein levels, gene copy number and disease has led to speculation that these peripheral neuropathies are a feature of abnormal *PMP22* protein stoichiometry in peripheral myelin (Gabriel *et al.*, 1997).

A similar phenomenon is seen in *Plp* gene-related disease in which deletions, duplications and transgenic over-expression of the gene can have similar effects to missense mutations (Hodes and Dlouhy, 1996). A strong correlation between gene dosage and severity of disease is particularly well documented in mice harbouring additional copies of the *Plp* gene (see 1.4.3.1 *Expression of genomic Plp transgenes*, page 28). The stoichiometric relationship both between PLP and DM20 proteins and between PLP/DM20 and the other myelin proteins may prove to be important in elaborating and maintaining central myelin (Mastronardi *et al.*, 1993; Johnson *et al.*, 1995; Inoue *et al.*, 1996).

1.4.4.3.2 Abnormal protein processing due to increased *Plp* gene dosage

Homozygous #4e transgenic mice have striking similarities to the spontaneous *Plp* gene mutants with ultrastructural evidence of disrupted protein trafficking and increased oligodendrocyte apoptosis (Kagawa *et al.*, 1994a; Inoue *et al.*, 1996). However, unlike missense *Plp* gene mutants, oligodendrocyte dysfunction cannot

occur through gains of function of mutated gene products. Instead, increased protein turnover in over-expressing cells blocking protein trafficking may disrupt oligodendrocyte function sufficiently to affect myelination (Inoue *et al.*, 1996; Gow *et al.*, 1998).

ND4 transgenic mice that express high levels of *Dm20* transcripts develop demyelination as they mature (Barrese *et al.*, 1998). The *Plp* gene products from the ND4 mice undergo abnormal post-translational modifications. Acylation is increased several-fold, a different population of fatty acids is esterified and the amino-terminal glycine becomes methylated (Barrese *et al.*, 1998). These changes increase the hydrophobicity of the proteins and may affect their cellular processing and integration into myelin. The altered characteristics of PLP and DM20 proteins could be pivotal in the demyelination process making abnormal post-translational modification a potential mechanism for disease pathogenesis in cases of increased *Plp* gene dosage.

1.4.4.4 Pathogenesis of axonal changes

Axonal pathology may reflect a specific response to disrupted *Plp* gene function in the oligodendrocyte or to disrupted gene function in the neuron itself as the srPLP and srDM20 proteins are located in some subpopulations of neurons (Bongarzone *et al.*, 1999). However, the identification of axonal pathology in other myelin mutants such as the *quaking* mouse (Friedrich, Jr. *et al.*, 1980) indicates that axonal changes could be a general response to abnormal oligodendrocyte function.

1.4.5 Clinically affected female carriers

Female carriers of X-linked disease rarely develop severe phenotypes due to the process of X-inactivation. Mice heterozygous for the *jimpy* mutation demonstrate the influence of this process in suppressing the development of clinical disease. In these mice, X-inactivation creates a mosaic pattern of *Plp* gene expression; a proportion of oligodendrocytes expresses the *jimpy* allele, the remainder expresses the wild type *Plp* allele. The majority of oligodendrocytes expressing the *jimpy* allele appear to die during post-natal development (Kagawa *et al.*, 1994b). This leaves predominantly cells that express the wild type allele and that are capable of adequately myelinating the CNS (Skoff and Ghandour, 1995). Pockets of dysmyelination are present presumably created by the small percentage of oligodendrocytes expressing the *jimpy* allele that survive. However, these patches resolve as the animal matures reflecting the ability of oligodendrocytes expressing the wild type *Plp* allele to compensate by myelinating these regions (Bartlett and Skoff, 1986; Skoff and Ghandour, 1995). Both the death of cells expressing the

disease allele and the ability of cells expressing the wild type allele to compensate may suppress the development of clinical disease in female carriers of X-linked disease (reviewed by Belmont, 1996).

Despite these mechanisms, female carriers of X-linked disease can show clinical phenotypes and some reports describe both juvenile-onset (C044T; Hodes *et al.*, 1995; G434A; Hodes *et al.*, 1997) and adult-onset (C037A; Nance *et al.*, 1996) disease in females with *PLP* gene mutations. Extreme skewing of X-inactivation develops normally in 5 to 10% of females. If X-inactivation skews heavily towards the mutated allele remaining active, female carriers are likely to develop clinical disease, a syndrome called “unfortunate Lyonisation” (Willard, 1995). Female animals heterozygous for the *shaking pup* allele demonstrate the link between skewing of X-inactivation and the development of clinical phenotypes. These animals develop a range of phenotypes that varies depending on the degree of myelin mosaicism present (Cuddon *et al.*, 1998). A severe phenotype develops if large numbers of axons remain nonmyelinated. This is assumed to reflect skewing towards expression of the mutated allele by the majority of oligodendrocytes. Conversely, milder phenotypes correlate with a lower percentage of nonmyelinated fibres.

The *myelin deficient* rat demonstrates a further potential cause of disease in females. This line of rats has a high incidence of phenotypically silent X-chromosome monosomy (XO). In female rats that exhibit monosomy in combination with carrying the *Plp^{md}* allele (*Plp^{md}/O*) all somatic cells express the mutant allele and these female rats develop a phenotype that is indistinguishable from affected males (*Plp^{md}/Y*) (Koeppen *et al.*, 1992). To date, there are no reports of disease in human female carriers of *PLP* gene-related disease who have concurrent X-chromosome monosomy (Turners syndrome).

1.4.6 Modifying loci

More severe phenotypes seen with some large intrachromosomal duplications that include the *PLP* gene locus (Isenmann *et al.*, 1997; Inoue *et al.*, 1999) and heterogeneity within families with point mutations of the *PLP* gene (Bonneau *et al.*, 1993; Sivakumar *et al.*, 1999) have highlighted the potential role of modifying loci in affecting disease severity. Both the *myelin deficient* rat (Duncan *et al.*, 1995) and the *rumpshaker* mouse (I.R. Griffiths, personal communication) develop two different phenotypes that can be selected for by breeding and probably result from different modifying alleles.

1.5 Experimental strategies for studying the roles of myelin proteins

1.5.1 Traditional transgenic technology

The evaluation of spontaneous mutants has been the mainstay of myelin research but advances in recombinant DNA technology have enabled more controlled investigations into the roles of myelin genes. Transfection studies allow gene function and disease pathogenesis to be examined *in vitro* (for example Filbin *et al.*, 1990; Filbin and Tennekoon, 1991; Gow *et al.*, 1994b; Thomson *et al.*, 1997) but cannot replicate the complex intercellular interactions and temporal changes seen *in vivo*. Transgenic systems overcome these problems by stably altering the mammalian genome *in vivo*. However, incomplete transgenic regulation and insertional mutagenesis can lead to misleading results. Poor transgenic regulation occurs if the transgenic cassette does not include the necessary regulatory elements or if the transgene inserts into a transcriptionally inactive region of the genome. The level of transgenic expression is also difficult to predict as there is no control over the number of copies of the transgenic cassette that insert into the genome and because of the effects of repeat-induced gene silencing (Garrick *et al.*, 1998). One limitation of these studies is that the endogenous gene remains active largely limiting their use to increased gene dosage studies. However, reporter genes driven by myelin gene promoters can overcome the problems of endogenous gene activity (for example *Plp-LacZ* fusion protein: Wight *et al.*, 1993 and *Mbp*-promoter *LacZ* transgene: Wrabetz *et al.*, 1998) and the use of antisense transgenic technology can prevent translation of endogenous gene products (for example the *Mbp* gene: Katsuki *et al.*, 1988).

1.5.2 Targeted gene replacement

Targeted gene replacement overcomes many of the problems of traditional transgenic systems by avoiding random transgenic integration and by preventing endogenous gene expression (reviewed by Capecchi, 1994). The targeting cassette contains the desired genetic defect flanked by sequences homologous to regions of the endogenous target gene. The cassette integrates into the genome by homologously recombining with these regions on the target gene replacing a section of the target gene with the transgene construct. Disrupting transcriptional or translational control elements of the target gene generates null alleles, so called "gene knockouts". Alternatively, additional genetic information can be introduced into the target locus, "gene knock-ins". The targeting constructs contain positive selectable markers embedded within the homologous regions and negative

selectable markers on non-homologous flanking sequences. After the constructs have been introduced into embryonic stem-cells, isolated homologous integration events can be identified by using these positive and negative selectable markers.

1.5.2.1 Problems of targeted gene replacement systems

One frustrating feature of many knockout models is the high incidence of normal phenotypes produced. Many examples of genetic redundancy have been reported where the roles of the targeted gene are replaced probably by closely related members of the same gene family (Hummler *et al.*, 1994; Gibson and Spring, 1998). Other examples exist where unrelated genes may have convergent functions that lead to genetic redundancy. The *Mbp* gene shows this form of genetic redundancy in the PNS where both MBP and P0 proteins in isolation are capable of supporting the major dense line (Martini *et al.*, 1995). Although genetic redundancy shows that these genes are not vital *per se*, it is difficult to comment on the importance of the roles that the genes fulfil.

Other problems of gene targeting relate to the targeting strategy. Targeted mutations that prove lethal to the embryo may provide little information about gene function. A subtler problem may arise through the retention of selectable markers within the mutated gene that can influence gene regulation. One example of this is the targeted *Plp* gene mutation described by Boison & Stoffel (1994) that was designed to express *Dm20*-mRNA in isolation (see 1.4.3.3 *Targeted gene replacements of the Plp gene*, page 30). The retention of the *neo* gene within the mutated allele led to aberrant transcript splicing and produced a functional null allele.

The limited number of embryonic stem-cell lines available for gene targeting leads to problems of mixed genetic backgrounds in these systems (reviewed by Crawley, 1996; Gerlai, 1996; Lathe, 1996). Embryonic stem cell lines are chosen because they are capable of producing viable embryos, not because they offer a suitable genetic background in which to maintain a transgenic line. For example, the sv129 line is associated with poor fertility, behavioural abnormalities and neuro-anatomical defects. Chimeric animals produced using this line generally are crossed into more robust strains such as C57BL/6 and C3H/101. This produces a mixed genetic background that requires at least twenty generations of back-crossing until a fully inbred strain is produced. Until this is achieved, modifying loci can lead to misleading phenotypic variation even between littermates. In addition, the targeted gene is selected for as part of a locus of up to thirty topographically linked alleles from the embryonic stem-cell line. Even with successive generations crossed into the new background strain, these linked genes separate almost exclusively with the

targeted allele and will not be present in wild type littermate controls.

1.5.2.2 Transgenic complementation of gene knockouts

Many of the problems of mixed genetic strains and the uncertain influence of modifying genes can be overcome by transgenic complementation to replace the functions of the disrupted gene in knockout animals (Gerlai, 1996). If the phenotype of the knockout is reversed by transgenic complementation, it is the direct result of loss-of-function of the targeted gene. Examples of similar complementation experiments within the context of myelination come from *shiverer* (Readhead *et al.*, 1987; Kimura *et al.*, 1998) and *myelin deficient* (Popko *et al.*, 1987) mice. The phenotypes of these spontaneous *Mbp* gene-null mutants can be reversed by complementation with *Mbp* transgenes. Clearly, these systems are limited by the availability of appropriately expressed complementary transgenes.

1.5.3 Targeted gene replacement using recombinase systems

Recent advances in targeted gene replacement technology overcome many of the problems of simple gene targeting strategies. The utilisation of recombinase technology in transgenic systems produces high rates of enzyme-mediated homologous recombination between specific recombination sites. The *Cre-loxP* system derived from P1 phages, for example, drives Cre-recombinase mediated recombination at *loxP* sites (reviewed by Plück, 1996; Kühn and Schwenk, 1998). The *loxP* sites are introduced into target genes allowing easy insertion and deletion of genetic material and making gene targeting much more efficient by exposure to Cre-recombinase during embryonic stem-cell manipulation. *LoxP* sites are also used to flank selectable markers so that these can be excised. More sophisticated systems allow spatio-temporal control of genetic modification by activating Cre-mediated recombination *in vivo* using *Cre-recombinase* transgenes driven by inducible or tissue-specific promoters. Although the targeted allele still shows strong linkage to other genes at that locus, by not exposing it to Cre-recombinase activity an effective wild type allele is retained allowing the influence of linked genes to be evaluated.

1.6 Aims of thesis

This study aims to dissect some of the roles of the *Plp* gene by describing the pathological changes that develop in the *Plp* gene knockout mouse (Klugmann *et al.*, 1997). In addition to a detailed histological description of the changes that developed, morphometric analysis has been used to investigate the ability of PLP/DM20-deficient mice to elaborate and maintain myelin within the CNS. A

survey of the PNS has been undertaken to establish if the *Plp* gene is necessary for maintaining peripheral myelin as suggested by Garbern *et al.* (1997). The axonal changes that develop have been described ultrastructurally and quantified using morphometric analysis and their relationship to PLP/DM20-deficient myelin sheaths has been investigated. The significance of findings from these studies is discussed within the context of myelin disease and oligodendroglial function.

To confirm that the phenotype that develops in *Plp* gene knockout mice is the direct result of loss of *Plp* gene function, these mice have been supplemented with genomic *Plp* transgenes (Readhead *et al.*, 1994). The role of the major *Plp* gene isoforms in oligodendrocyte function and in the formation of myelin has been investigated through transgenic complementation using *Plp*-cDNA and *Dm20*-cDNA transgenes (Mastronardi *et al.*, 1993; Nadon *et al.*, 1994). In the final discussion, the findings from this study are critically appraised and future areas of work that may expand on some of the points raised by this thesis are discussed.

2. Materials and Methods

2.1 Miscellaneous

Inorganic chemicals were of AnalAR[®] or molecular biology grade and were sourced from Sigma or BDH. Solutions were sterilised as appropriate: bulk solutions were autoclaved; small volumes and fluids that could not be autoclaved were filter sterilised using a Flowpore 0.22µm filter (Biomedicals Ltd.). Gloves, eye protection and other protective clothing were worn when appropriate. Fixatives and other volatile liquids and toxic powders were prepared in a fume cupboard.

The Appendix (page 177) gives details of the preparation of fixatives, stains, buffers and bacteriological media and of staining and processing protocols. These are cross-referenced by page number in this section. The production of 3-aminopropyltiethoxy-saline (APES)-coated slides and diethyl pyrocarbonate (DEPC)-treated water are detailed in the Appendix but are not cross-referenced in the text.

2.2 Mouse Breeding

2.2.1 Animal breeding facilities

Mice were bred at the Glasgow Parasitology Unit, University of Glasgow Veterinary School and at the animal breeding facilities, ZMBH, Heidelberg. The breeding facility at Glasgow is known to have evidence of murine hepatitis virus and picorna virus infections both of which have been associated with neurological disease in mice (Lipton *et al.*, 1994; Fujiwara, 1994). During the period of this study, there was no evidence of clinical disease and the phenotypes and pathology identified in transgenic mice were not identified in wild type controls also bred in this facility. Similarly, mice bred at ZMBH, a specific-pathogen free facility, had phenotypes and pathology that were consistent with those seen in the mice bred at Glasgow. This suggests that these viruses did not contribute to the phenotypes and pathology described in this study.

2.2.2 Transgenic lines of mice

2.2.2.1 *Plp* gene knockout mice

Plp gene knockout transgenic mice were generated by Klugman *et al.* (1997) at

ZMBH, Heidelberg (Figure 4, page 42). The endogenous *Plp* gene was disrupted by introducing a targeting vector designed to disrupt the ATG translation start codon in exon 1. The targeting vector is also predicted to disrupt exon 1.1, preventing the transcription of *srPlp* and *srDm20* mRNA (Bongarzone *et al.*, 1999). The targeting vector replaced exons 1 to 3 of the wild type allele by homologous recombination and was introduced into R1 embryonic stem cells by electroporation. The *neo* gene, in reverse orientation to the *Plp* gene and under the control of the herpes simplex virus (HSV) promoter, was used to disrupt the translation start codons. It replaced the 3' end of exon 1 and 2.5kb of intron 1 between the *Bam*H1 site in exon 1 and the *Kpn*1 site in intron 1. A negative selector, the *thymidine kinase (tk)* gene also under the HSV promoter, was used to select against random (non-homologous) vector insertion as it was located immediately upstream of the 5' homology region of the targeting vector. Construct-mediated G418 resistance positively selected for stem cells containing the targeting construct and cells that had random vector insertion were negatively selected against using gancyclovir. Homologous recombination and a single integration event were confirmed by Southern blot analysis. Cells containing the *Plp* gene-null allele (*Plp^{tmkn1}*) were microinjected into blastocysts from C57BL/6J mice to produce chimeras. The chimeras were used to establish founder stock of *Plp* gene knockout mice containing the *Plp^{tmkn1}* allele by back crossing onto C57BL/6J mice (Klugmann *et al.*, 1997).

2.2.2.2 #66 and #72 transgenic mice

#66 and #72 transgenic mice were generated by Readhead *et al.* (1994) (Figure 5, page 43). The murine *Plp* gene was isolated from a cosmid library and used to construct a 26.6kb transgene insert. The transgenic cassette is predicted to include all eight exons of the *Plp* gene, 3.5kb of the 5' regulatory region and a small vector fragment containing the T7 promoter sequence at the 3' end of the transgene. This was introduced into B6D3F2-fertilised ova by pronuclear microinjection and produced two lines of transgenic mice containing the intact *Plp* transgene (#66 and #72). These were assessed by Southern blot analysis and were estimated to respectively contain seven and three copies of the transgene per haploid genome. The transgene copies co-segregated in subsequent generations following an autosomal inheritance pattern suggesting that, in both lines, the transgenes had inserted in tandem at autosomal sites (Readhead *et al.*, 1994).

2.2.2.3 *Plp*Tg1 and *Dm20*Tg2 transgenic mice

*Plp*Tg1 and *Dm20*Tg2 transgenic mice were generated by Nadon *et al.* (1994) (Figure 6, page 44). *Plp*Tg1 mice carried thirty copies of a human *PLP*-cDNA construct. The *PLP*-cDNA construct was flanked on the 5' side by a 4.2kb fragment

of the human *Plp* gene promoter and on the 3' side by a 1.5kb fragment from the 3'-UTR of the human *PLP* gene that provided a polyadenylation signal. *Dm20Tg2* mice carried an unknown number of copies of a *DM20*-cDNA transgene construct. This construct was similar to the *PlpTg1* transgene but a portion of the *PLP*-cDNA clone from the *Bam*H1 site in exon1 to the *Nco*1 site in exon 5 was replaced with a fragment from a rat *Dm20*-cDNA clone. The *PlpTg1* and *Dm20Tg2* transgenic lines were produced by pronuclear microinjection of the transgenes into B6C3F2 fertilised ova (Nadon *et al.*, 1994).

2.2.2.4 #ND3A transgenic mice

#ND3A transgenic mice were generated by Johnson *et al.* (1995) (Figure 7a, page 45). The transgene construct contained a human *DM20*-cDNA covalently linked at the *Bam*H1 site in exon 1 to 2.9kb of the human *PLP* gene promoter. An SV40 polyadenylation signal was inserted at the *Eco*R1 site in exon 7. The transgene was introduced into CD1 fertilised ova by pronuclear microinjection to produce transgenic mice. Of the four stable lines produced, the ND3A line was estimated by Southern analysis to have 17 copies of the transgene inserted in tandem at an autosomal site (Johnson *et al.*, 1995).

2.2.2.5 *Plp*-LacZ fusion protein transgenic mice

Plp-LacZ transgenic mice were generated by Wight *et al.* (1993) (Figure 7b, page 45). The transgene comprised 2.4kb of 5' upstream sequence, exon 1, intron 1 and the first 37bp of exon 2 (to the *Apa*1 site) from the murine *Plp* gene. The *Apa*1 site in *Plp* exon 2 was converted to a *Sph*1 site and fused in frame with a LacZ fusion gene with SV40 polyadenylation signals. The transgene was introduced into B6D3F2 fertilised ova by pronuclear microinjection to produce transgenic mice (Wight *et al.*, 1993).

2.2.3 Maintenance of transgenic lines of mice

The #72, #66, *PlpTg1*, *Dm20Tg2* and #ND3A lines of transgenic mice were maintained by creating harems containing transgene positive and negative animals from the same background. Brother-sister matings were avoided and background strains were not mixed. The *Plp*-LacZ mice were maintained through homozygous mating. The *Plp* gene knockout transgenic line was maintained by creating harems of *Plp^{tmkn1}* hemizygous male and homozygous female mice. In addition, harems containing wild type mice from this line and mice carrying the *Plp^{tmkn1}* allele ensured the production of *Plp^{tmkn1}* heterozygotes and wild type littermate controls.

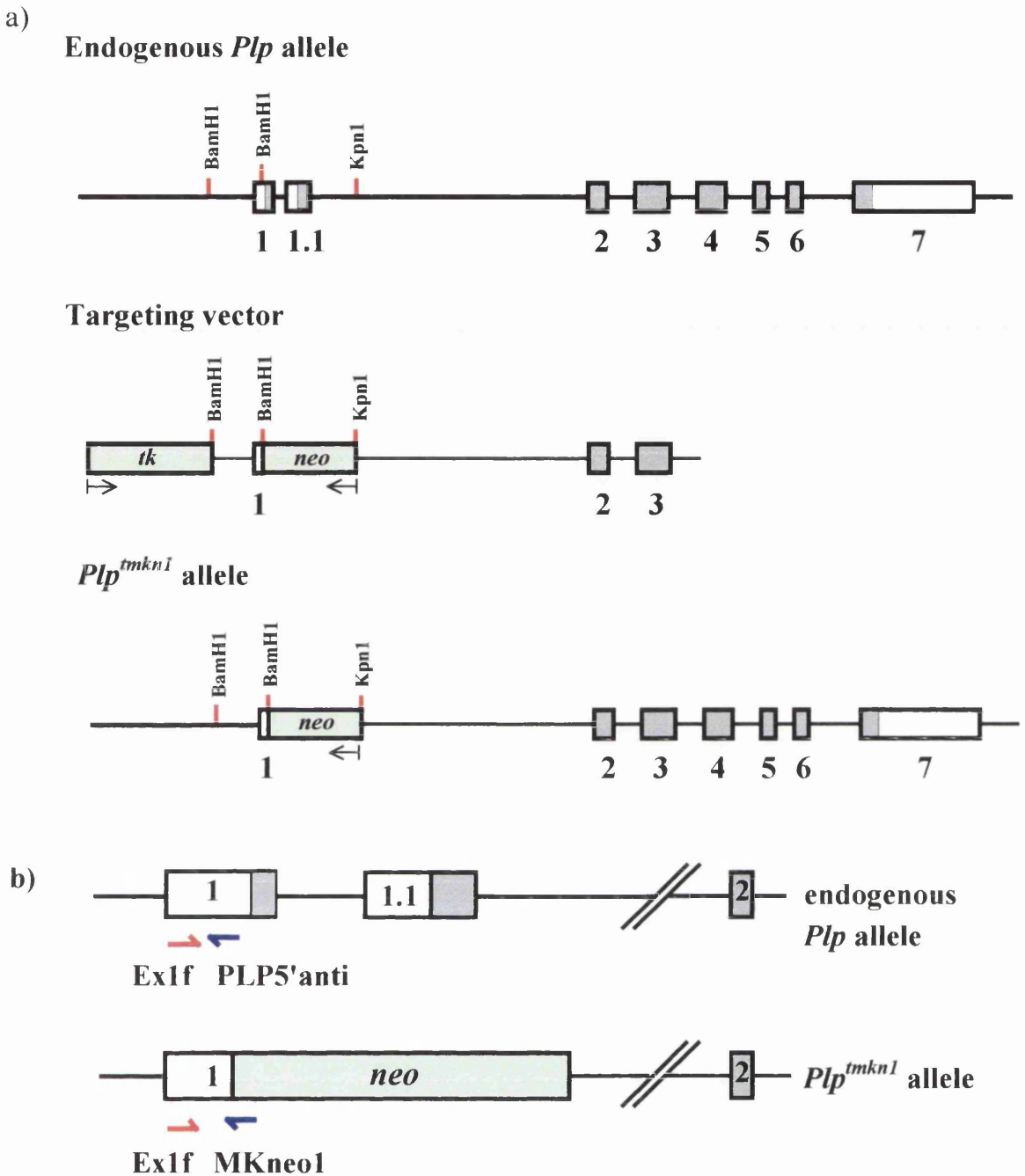
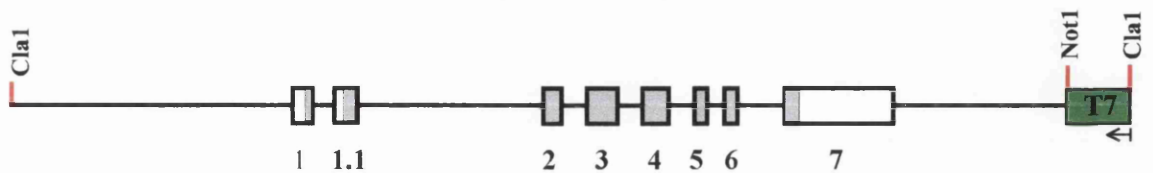


Figure 4 a) Targeting strategy used to create the *Plp^{tmkn1}* allele: the negative selectable marker (*tk* gene) is lost during homologous recombination; the positive selectable marker (*neo* gene) is retained (relevant restriction sites are shown)

b) PCR primer positions for identification of the endogenous and mutated *Plp* gene alleles (positions of forward primer in red and reverse primers in blue)

(exons are represented by numbered boxes, coding regions are shaded grey; selectable markers are denoted by green boxes, black arrows show orientation)

a)



b)

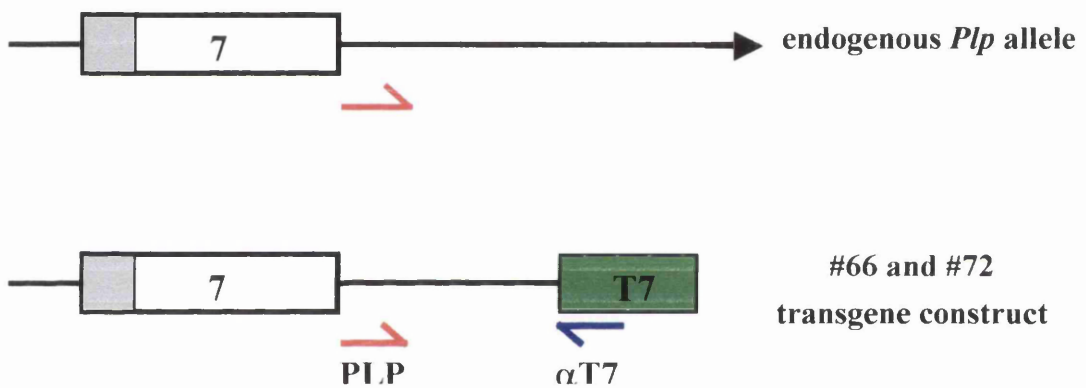


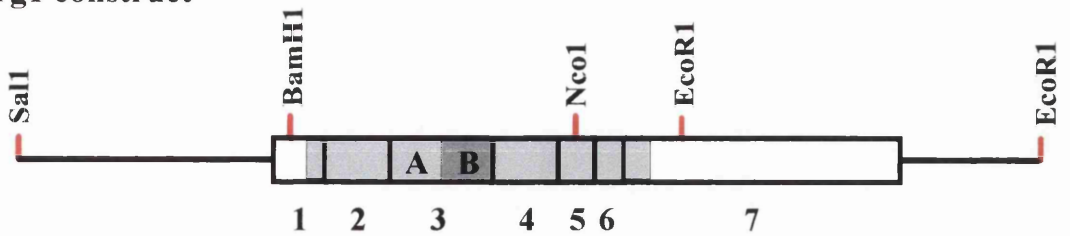
Figure 5 a) Transgene construct from the #66 and #72 lines (relevant restriction sites are shown)

b) PCR positions for identifying the transgene construct from the #66 and #72 lines (positions of forward primer in red and reverse primer in blue)

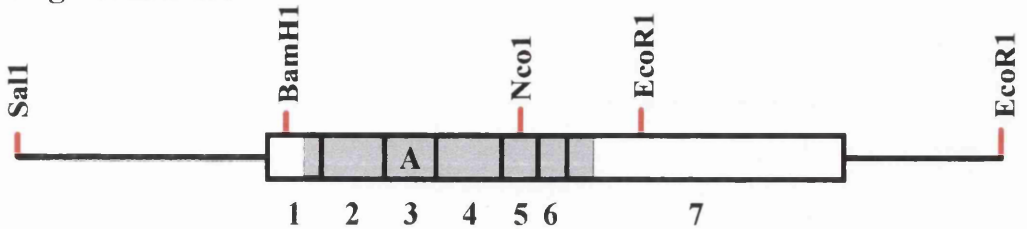
(exons are represented by numbered boxes, coding regions are shaded grey; the transgene-specific T7 promoter sequence is represented by a green box, a black arrow indicates the orientation of this sequence)

a)

PlpTg1 construct



Dm20Tg2 construct



b)

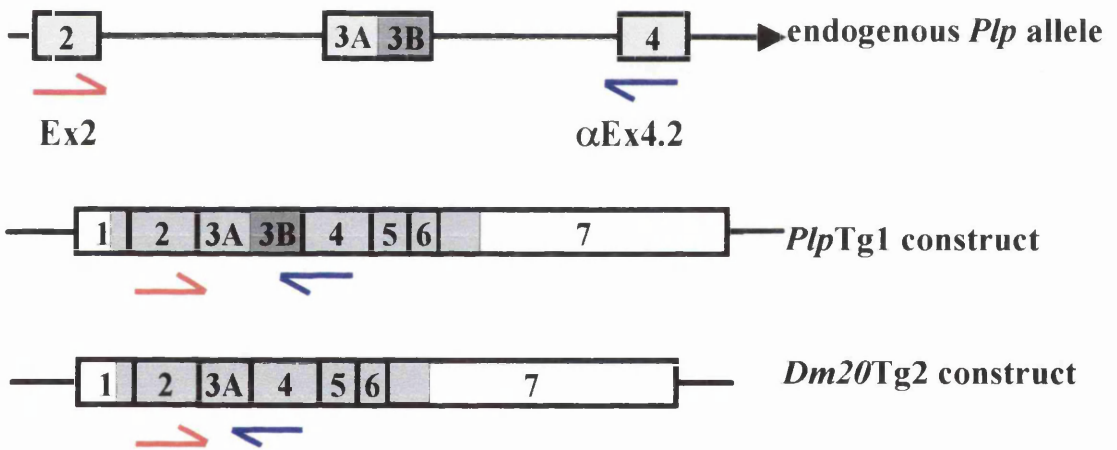


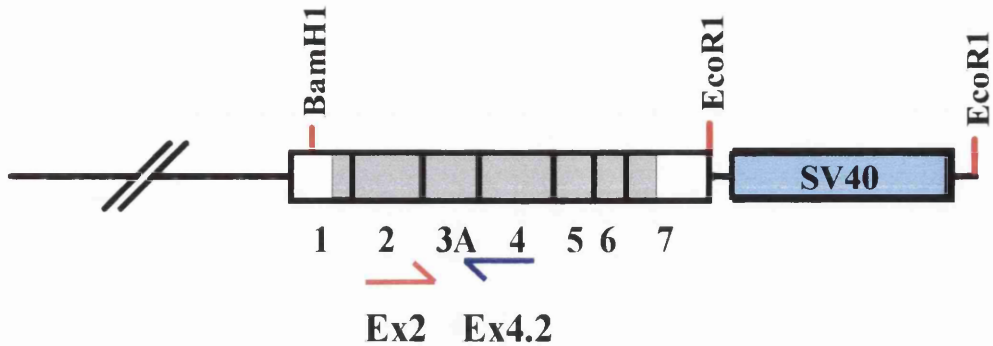
Figure 6 a) *PlpTg1* and *Dm20Tg2* transgene constructs (relevant restriction sites are shown)

b) PCR primer positions for identification of the *PlpTg1* and *Dm20Tg2* transgene constructs: the endogenous *Plp* gene allele produces a ~2168bp PCR product using these primers which can rarely be demonstrated (positions of forward primer in red and reverse primer in blue)

(exons are represented by numbered boxes; coding regions are shaded; exon 3 is shown divided into exon 3A and exon 3B)

a)

ND3A transgene construct



b)

PLP-LacZ fusion protein transgene

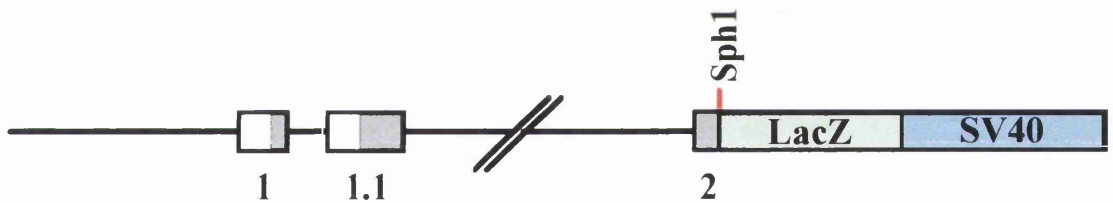


Figure 7 a) ND3A transgene construct: exon 7 is truncated by the addition of a SV40 polyadenylation signal; PCR primer positions are demonstrated (forward primer in red and reverse primer in blue)

b) PLP-LacZ fusion protein transgene construct: the first 14 codons of exon 2 are spliced in-frame with the LacZ gene coding region (shaded green) linked to a SV40 polyadenylation signal

(relevant restriction sites are shown; exons are represented by numbered boxes, coding regions are shaded grey; SV40 polyadenylation signals are shaded blue)

2.2.4 Crossing of transgenic lines of mice

For transgenic complementation of the *Plp* gene knockout mice, hemizygous transgene positive males were bred with *Plp^{tmkn1}* homozygous females. This ensured that all F1 males were *Plp^{tmkn1}* hemizygotes and that a number were also transgenic hemizygotes. Transgene negative littermates from the same breeding programme were used as internal controls.

2.3 Isolation and quantification of nucleic acids

2.3.1 Tail biopsy and mouse identification

Mice were anaesthetised using halothane (Rhone-Poulenc Chemicals Ltd.). 1.2cm of the tip of the tail was removed using aseptic techniques and the wound was cauterised. The tail biopsy was cut into 3mm pieces, placed in a labelled Nunc cryotube (GibcoBRL), rapidly frozen in liquid nitrogen and stored at -20°C.

Mice were marked for future identification using a numeric ear punching system.

2.3.2 Extraction of genomic DNA (gDNA) from mouse tails

gDNA for genotyping was isolated from tail samples collected at biopsy and at *post mortem*. The QIAmp Tissue Kit (Qiagen) was used for all gDNA preparations as it provided a speedy and reliable method of gDNA extraction. The kit also offered the advantages of safety and ease when handling large numbers of samples over traditional phenol extraction methods. The QIAmp Tissue Kit utilises a spin column containing a silica membrane to bind nucleic acids. Residual protein and other cell debris are washed from the column before nucleic acid elution. All buffers used were provided as part of the commercial kit and manufacturers' recommendations were followed.

2.3.2.1 Use of the QIAmp Tissue Kit

Tissue samples were lysed for 3 to 5 hours at 55°C in the manufacturers' sodium dodecyl sulphate (SDS) buffer containing 2mg.ml⁻¹ proteinase K (see 2.3.2.2 *Preparation of Proteinase K*, page 47). SDS caused cell membrane lysis and proteinase K denatured proteins including endogenous and contaminating deoxyribonucleases (DNases). Salt and pH conditions of the cell lysate were altered to ensure preferential binding to the silica membrane of nucleic acids over protein and other cellular debris by the addition of a second buffer. The lysate was loaded onto the QIAmp spin column, centrifuged to remove unbound residues and washed twice to remove remaining contaminants. Nucleic acids were eluted by incubation

at 70°C in elution buffer. To prevent degradation by contaminating DNases during long-term storage, gDNA was stored at -20°C. For short-term storage before polymerase chain reaction (PCR) analysis gDNA was stored at 4°C to prevent physical degradation of samples through repeated thermal insults.

2.3.2.2 Preparation of Proteinase K

Proteinase K was supplied lyophilised with the QIAmp Tissue Kit. This was reconstituted in sterile distilled water (SDW) at 20mg.ml⁻¹ and stored at -20°C in 110µl aliquots until required.

2.3.2.3 Assessment of gDNA quality

Yields in excess of 40µg of gDNA in a final volume of 400µl of elution buffer were attained using the QIAmp Tissue Kit. gDNA up to 50kb in length was eluted but the predominant population was in the range of 20-30kb (Figure 9, page 49). Purified gDNA was initially assessed to ensure that it was free from contaminating DNase activity and capable of enzymatic manipulation. 500ng samples of gDNA were incubated at 37°C for 2 hours in the presence 20U *EcoR*I (BRL) and the appropriate manufacturers' buffer to assess gDNA digestibility. To determine that gDNA degradation was not due to contaminating DNases, a control was performed using gDNA incubated under similar conditions but in the absence of exogenous enzyme. A second control consisting of gDNA in the presence of enzyme and buffer incubated at 4°C for 2 hours was included to demonstrate that degradation did not occur due to other physical or chemical factors. These samples were compared on a 0.7% agarose gel (Figure 9, page 49).

2.3.3 Extraction of RNA from mouse tissue

2.3.3.1 Prevention of ribonuclease (RNase) activity

In order to prevent endogenous RNase activity, freshly dissected tissues were immediately frozen and stored in liquid nitrogen until use. Non-sterile equipment was soaked in DEPC-treated water overnight to remove contaminating RNases. Plastic-ware was guaranteed RNase-free (Anachem) negating the need to pretreat it with DEPC-treated water. All steps were carried out on ice unless otherwise stated.

2.3.3.2 RNA extraction

RNA was extracted using RNazol B (Biotech Laboratories Inc.) solution following the manufacturers' recommendations. This method is a modification of a one step procedure described by Chomczynski & Sacchi (1987). RNazol B contains a

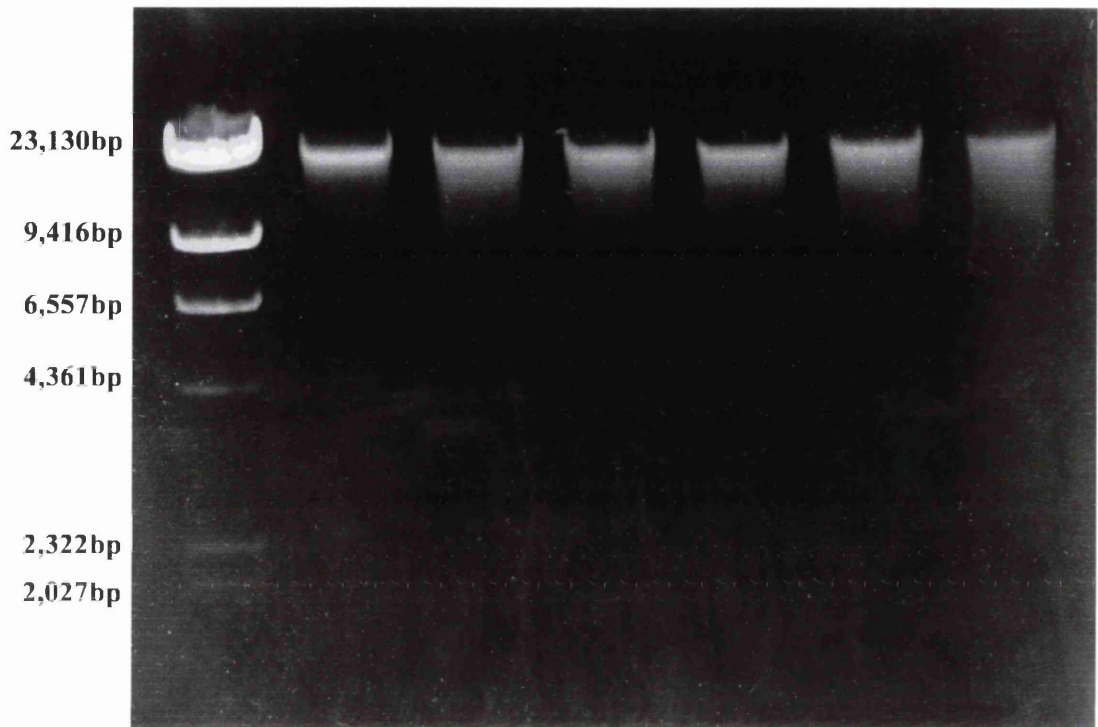


Figure 8 Genomic DNA extracted from mouse tail using the QIAmp Tissue Kit (Qiagen). The predominant population of gDNA species separated with the 23kb marker indicating that gDNA had been extracted with minimal degradation using this protocol (200ng aliquots of gDNA separated on a 0.7% agarose gel; size marker λ -DNA/*Hind*III).

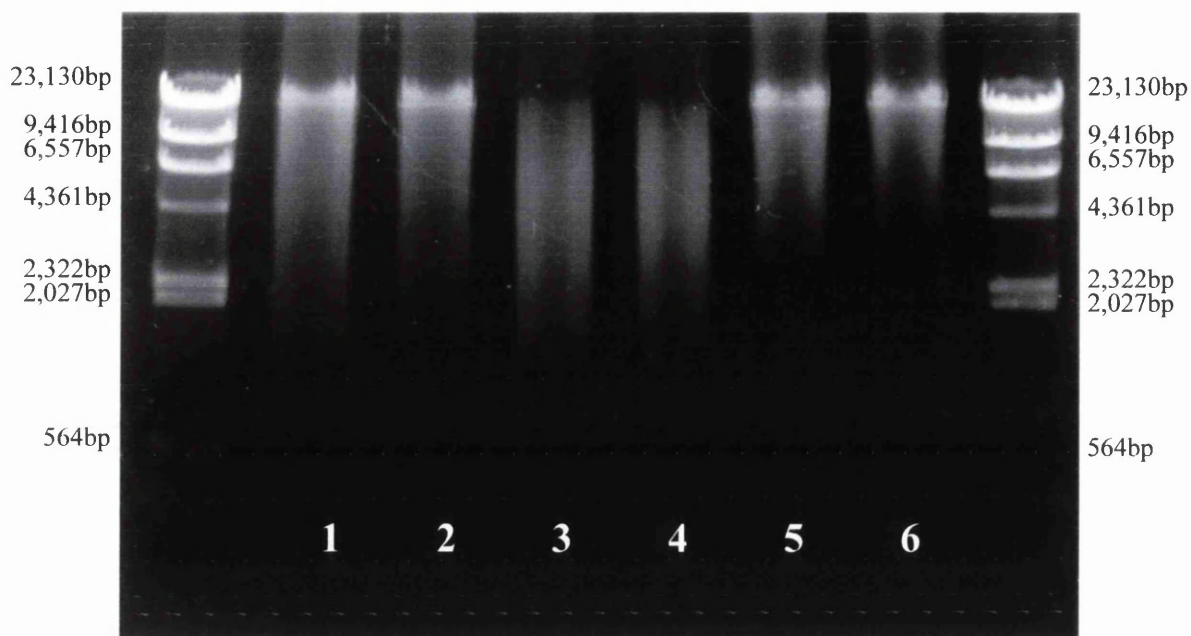


Figure 9 Assessment of quality of gDNA extracted from mouse tail using the QIAmp Tissue Kit (Qiagen)

To assess gDNA quality, 500ng aliquots of gDNA were compared after incubation for 2 hours in an appropriate enzyme buffer (BRL) with or without 20units of *EcoR1* restriction endonuclease (BRL) and at 37°C or 4°C (size marker: λ -DNA/*HindIII*).

Lanes 1 and 2: samples incubated at 37°C without enzyme; the gDNA did not degrade indicating that the samples were not contaminated with DNAses.

Lanes 3 and 4: samples incubated at 37°C in the presence of enzyme; the gDNA was digested indicating that the samples were suitable for enzymatic manipulation.

Lanes 5 and 6: samples incubated at 4°C in the presence of enzyme; the gDNA did not degrade indicating that digestion of DNA in the samples (lanes 3 and 4) did not result through non-enzymatic mechanisms.

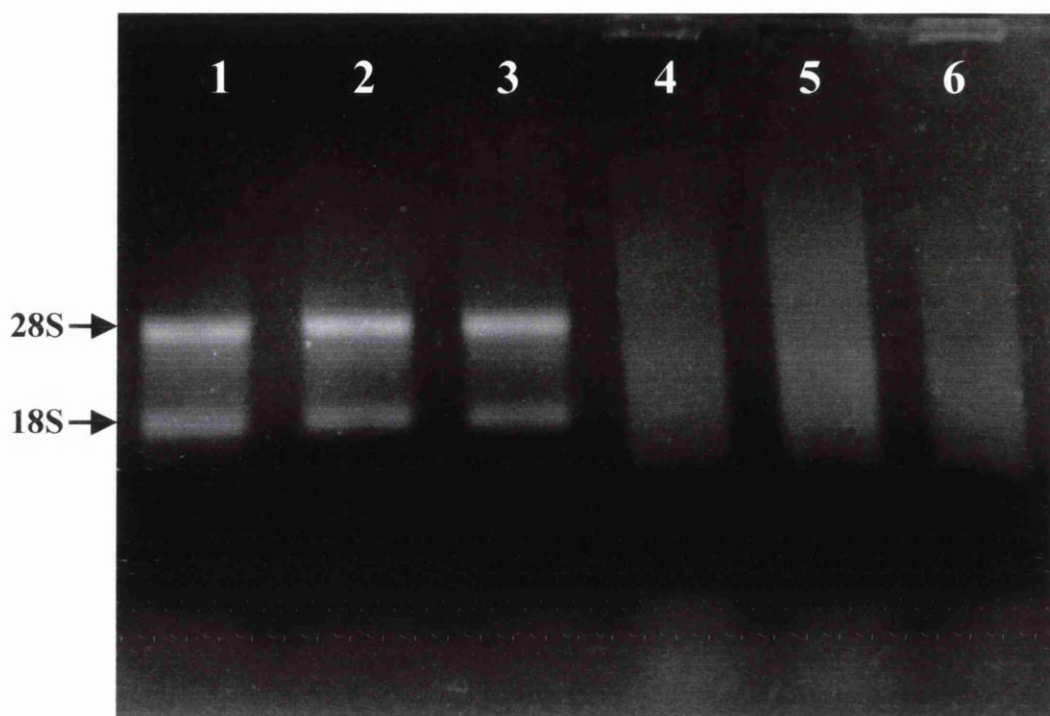


Figure 10 Total cellular RNA and cDNA from 20 day-old mouse brain. Lanes 1 to 3 show 200ng aliquots of total cellular RNA and lanes 4 to 6 show the corresponding aliquots of cDNA populations synthesised from RNA samples (estimated to contain 200ng of cDNA). The 28S and 18S bands of ribosomal RNA are marked, the 5S band could not be identified. The samples were separated on a 1.3% nondenaturing agarose gel.

monophasic solution of guanidium and phenol chloroform. Guanidium rapidly inactivates RNase activity and forms complexes with RNA and water allowing RNA to be retained in the aqueous phase while DNA and proteins separate with the phenol phase.

The sample was broken into fine grit using a liquid nitrogen-cooled pestle and mortar, transferred to an appropriate volume of RNAzol B (2ml RNAzol B.100mg⁻¹ of sample) at 4°C and thoroughly mixed by vortexing. To ensure complete separation of RNA from endogenous RNases and other contaminants, the suspension of tissue was needle homogenised through a series of increasingly fine needles (16 to 23 gauge). A one tenth volume of chloroform was added to remove traces of phenol from the aqueous phase. The solution was emulsified by vortexing, incubated on ice for 5 minutes and centrifuged at 13,000rpm for 15 minutes at 4°C. The aqueous phase was collected and RNA was precipitated by the addition of 500µl of propan-2-ol and incubation on ice for 15 minutes. RNA was pelleted by centrifugation at 13,000rpm for 15 minutes at 4°C, washed in 70% ethanol/ DEPC-treated water, air-dried and resuspended in a small volume of DEPC-treated water. The sample was quantified and adjusted to 2µg.µl⁻¹ before storage at -70°C to minimise RNase activity. Before use, the total cellular RNA samples were assessed to ensure they had not degraded (Figure 10, page 50).

2.3.4 Quantification and standardisation of nucleic acids

2.3.4.1 Quantification of nucleic acids

RNA and gDNA samples were quantified using a GeneQuant RNA/DNA calculator (Pharmacia Biotech) with a 70µl spectrophotometer cell. Small volumes of pDNA extracted from gels were quantified by comparison at gel analysis against a series of dilutions of pDNA of known concentration.

2.3.4.2 Dilution of nucleic acids

Nucleic acids were diluted to working concentrations in SDW or TE Buffer (see *Appendix* page 189). For PCR analysis, gDNA samples were diluted to a concentration of 25ng.µl⁻¹. RNA was diluted to 2µg.µl⁻¹ for cDNA synthesis.

2.3.4.3 Ethanol precipitation and concentration of nucleic acids

Nucleic acid samples were precipitated to enable concentration and purification. Precipitation was performed in the presence of 0.3M sodium acetate (pH 5.2) and two to three times the sample volume of 100% filtered ethanol chilled to -20°C. The sample was stored at -70°C for 2 hours, pelleted by centrifugation at 13,000rpm

for 10 minutes at 4°C and washed in 70% ethanol at room temperature to remove traces of salt. The nucleic acids were repelleted by centrifugation, the supernatant was removed and the pellet was air-dried for 5 to 10 minutes. The pellet was resuspended in an appropriate volume of SDW or TE buffer to give the desired final concentration allowing for an estimated 10% loss of nucleic acid during the precipitation process. The sample was requantified and the concentration was adjusted as necessary.

2.3.5 Nucleic acid electrophoresis

2.3.5.1 Agarose gels

Routine analysis of DNA and RNA was performed on 0.7 to 2% agarose gels in tris acetate ethylene-di-amine-tetra-acetate (TAE) buffer (see *Appendix* page 189). 0.7% agarose was used for the analysis of gDNA; 1% for the analysis of RNA; 1.3% for the separation of digested plasmids; 2% for the analysis of PCR products. Gels were made from ultra pure, electrophoresis grade agarose (GibcoBRL) melted in TAE buffer. Ethidium bromide (from a stock of 1mg.ml⁻¹) was added to the cooled gel to give a final concentration of 0.5µg.ml⁻¹. Samples were loaded with 6x gel loading buffer (see *Appendix* page 190) and TAE was used as the electrophoresis buffer.

2.3.5.2 Gel imaging and photography

Gels were viewed with a “Fotoprep I” ultraviolet (UV) transilluminator (Fotodyne Inc.). Gels were recorded using a Polaroid MP4 land camera (Polaroid) on Polaroid 667 (ASA 3000) film through a Wratten 22A filter (Kodak) or using a Kaiser RA1 CCD camera and a Sony UP-890CE video graphic thermal printer.

2.4 PCR Genotyping

2.4.1 PCR core programme

Amplifications for genotyping were performed on a Perkin Elmer DNA thermal cycler or on a PHC-3 (Techne) thermal cycler.

1) Initial cycle	denaturing temperature	94°C	3 min
	annealing temperature	58°C	1 min
	extension temperature	72°C	2 min
2) Step cycle (35 cycles)	denaturing temperature	93°C	40 sec
	annealing temperature	58°C	1 min
	extension temperature	72°C	30 sec
3) Final cycle	denaturing temperature	93°C	40 sec
	annealing temperature	58°C	1 min
	extension temperature	72°C	2 min

2.4.2 Genomic PCR

25µl PCR reactions were carried out in 0.5ml thin-walled microcentrifuge tubes (Anachem). Reactions contained 50ng target, 0.25mM dNTP Master Mix (Bioline) and forward and reverse primers at 0.2µM. All reactions apart from those using the Ex2/αEx4.2 primer pair were performed with 1.5mM MgCl₂. For Ex2/αEx4.2 primer pair reactions, 3mM MgCl₂ was used. Reactions were performed in the presence of 1 unit of *Taq* DNA polymerase (Bioline) and an ammonium buffer (Bioline) and overlaid with 25µl of molecular biology grade mineral oil (Sigma) to prevent evaporation of the reaction mix. The reaction was stopped by adding 6x gel loading dye (see *Appendix* page 190) and by storing at 4°C before analysis. PCR products were harvested by pipetting beneath the oil layer and analysed on 2% agarose gels.

2.4.3 Primers for PCR genotyping and sexing

Primer sequences and product sizes are listed in Table 5 (page 55) and the PCR products are demonstrated in (Figure 11, page 56). Primer positions are represented graphically in the figures describing the transgenes and are cross-referenced in the

text. Positive and negative controls were included with each set of samples. A control reaction with the sample replaced by SDW was included to ensure that there were no contaminating nucleic acids.

2.4.3.1 *Plp* gene knockout mice

The transgenic status of the *Plp* gene knockout mice was assessed using one forward and two reverse primers (Figure 4, page 42). The Ex1f forward primer recognised a region at the start of exon 1 and was common to both the wild type and mutant alleles. The α MkNeo1 reverse primer recognised a region in the *neo* gene and produced a 429bp product from the *Plp^{tmkn1}* allele. The reverse primer, α PLP5'anti, recognised a region in exon 1 that was deleted in the *Plp^{tmkn1}* allele but produced a 389bp product from the wild type allele (Figure 11, page 56). The reverse primers were taken from a protocol initially described by Klugman *et al.* (1997). The forward primer was designed in house (DA Vouyiouklis, personal communication).

These primers did not distinguish between the endogenous *Plp* gene and the #66 and #72 transgenes. This led to false wild type bands in mice hemizygous for the *Plp^{tmkn1}* allele that had been crossed with the #66 and #72 mice and contained copies of these transgenes. This pattern was indistinguishable from heterozygosity for the *Plp^{tmkn1}* allele. To avoid confusion, only male animals were examined in the study of transgenic complementation of the *Plp* gene knockout mouse.

2.4.3.2 *Plp*Tg1, *Dm20*Tg2 and ND3A transgenic mice

The transgenic status of the *Plp*Tg1, *Dm20*Tg2 and ND3A transgenic mice was assessed using primers that recognised regions in exon 2 (Ex2 forward primer) and exon 4 (α Ex4.2 reverse primer) (Figure 6, page 44) (Griffiths *et al.*, 1995). These primers differentiated the *Plp*Tg1 transgene product (506bp) from the *Dm20*Tg2 and ND3A transgene products (401bp) as exon 3B (105bp) was only present in the *Plp*Tg2 transgene (Figure 11, page 56). The endogenous *Plp* gene product (~2168bp estimated from human *PLP* gene sequence data) was rarely identified as it was too large to be reliably amplified using this protocol.

2.4.3.3 #66 and #72 transgenic mice

A transgene-specific portion of the T7 promoter from the original plasmid was retained at the 3' end of the #66 and #72 transgenic cassette (Figure 5, page 43). The primers used recognised the T7 promoter region and a region at the 3' end of the murine *Plp* gene producing a ~400bp PCR product from the transgene (Figure 5, page 43) (Readhead *et al.*, 1994; Anderson, 1997). This PCR reaction was

Table 5 PCR primers for genotyping and semi-quantitative RT-PCR

Amplify	Primer	Sequence	Size	Reference
<i>Plp^{tmkin1}</i> allele	Ex1f	5' GGA-GGA-TTA-AGA-ACC-CCT-CC 3'	429bp	Klugmann <i>et al.</i> (1997)
	α MKneo1	5' TAC-GGT-ATC-GCC-GCT-CCC-GAT-TCG-CA 3'		
<i>Plp</i> wild type allele	Ex1f	5' GGA-GGA-TTA-AGA-ACC-CCT-CC 3'	389bp	
	α PLP5'anti	5' CTG-TTT-TGC-GGC-TGA-C TT-TG 3'		
<i>Plp</i> Tg1 transgene	Ex2	5' GCT-CTC-ACT-GGT-ACA-GAA 3'	506bp (<i>Plp</i>)	Griffiths <i>et al.</i> (1995)
<i>Dm20Tg2</i> transgene	α Ex4.2	5' TAC-ATT-CTG-GCA-TCA-GCG-CAG-AGA-CTG-C 3'	401bp (<i>Dm20</i>)	
<i>Plp</i> gene transcript cDNAs	PLP	5' CAG-GTG-TTG-AGT-CTG-ATC-TAC-ACA-AG 3'	~400bp	Readhead <i>et al.</i> (1994)
	α T7	5' GCA-TAA-TAC-GAC-TCA-CTA-TAG-GGA-TC 3'		
#66 and #72 transgenes	Sry1a	5' GGG-ACT-GGT-GAC-AAT-TGT-C 3'	347bp	Schneider <i>et al.</i> (1995)
<i>Sry</i> gene (Y-chromosome specific)	α Sry1b	5' CAC-TGC-AGA-AGG-TTG-TAC 3'		
<i>Cyclophylin</i> transcript cDNA	CyclC	5' ACC-CCA-CCG-TGT-TCT-TCG-AC 3'	300bp	Danielson <i>et al.</i> (1988)
	α CyclG	5' CAT-TTG-CCA-TGG-ACA-AGA-TG 3'		

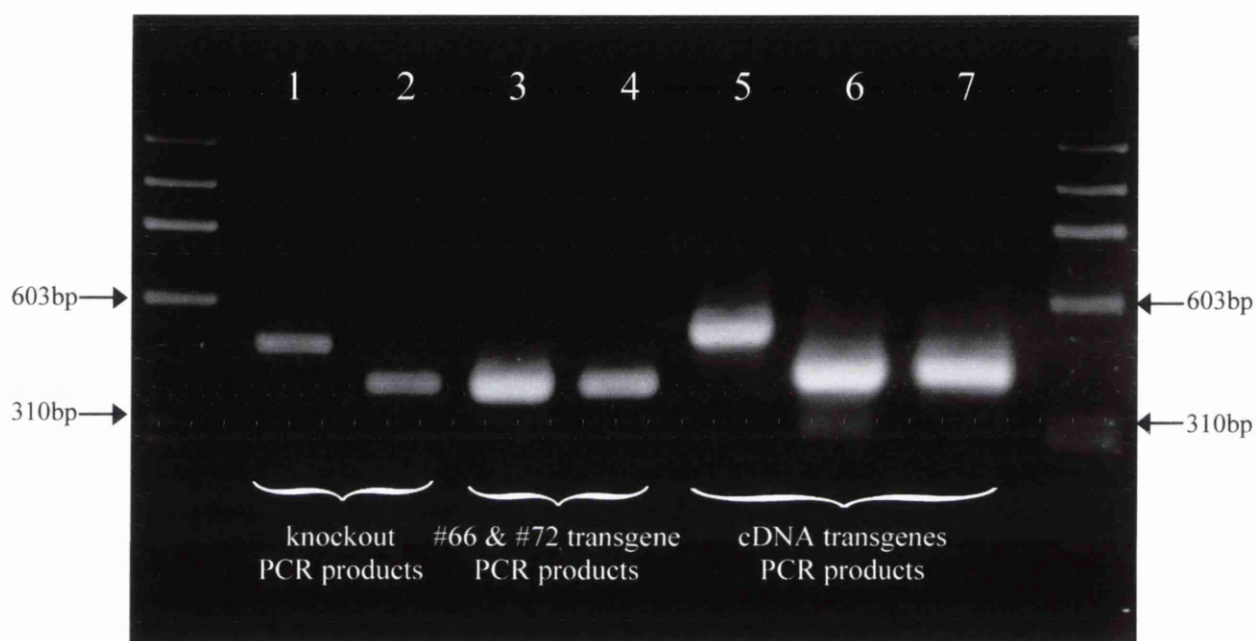


Figure 11 Genotyping transgenic mice by PCR analysis
 (PCR product lengths in brackets; size marker: DNA/HaeIII)

Lanes 1 and 2 show PCR products from the PCR strategy to distinguish *Plp* gene knockout and wild type *Plp* alleles: lane 1 from knockout mouse DNA (429bp) and lane 2 from wild type mouse DNA (389bp) (see page 54)

Lanes 3 and 4 show PCR products from the PCR strategy to identify #66 and #72 transgenes: lane 3 from #66 transgenic line DNA and lane 4 from #72 transgenic line DNA (both ~400bp) (see page 54)

Lanes 5 to 7 show PCR products from the PCR strategy to identify *Plp*Tg1, *Dm20*Tg2 and ND3A transgenes: lane 5 from *Plp*Tg1 transgenic line DNA (506bp); lane 6 from *Dm20*Tg2 transgenic line DNA and lane 7 from ND3A transgenic line DNA (both 401bp) (see page 54)

particularly sensitive to target concentration requiring gDNA to be accurately quantified before PCR.

2.4.3.4 Y-chromosome specific primers

Y-chromosome specific primers were used to confirm the sex of neonatal animals that had been culled for tissue collection. The primers described by Schneider *et al.* (1995) recognised the *sex-determining region of the Y chromosome (Sry)* gene, one of a group of sex determining genes located on the Y-chromosome. They produced a 347bp product by amplifying a region at the start of the open reading frame of the *Sry* gene (bp228 to bp575) that included the high-mobility-group-protein box, a highly conserved DNA binding region.

2.5 Tissue fixation

2.5.1 Fixatives

2.5.1.1 Buffered neutral formaldehyde, 4% (BNF)

BNF (see *Appendix* page 177) was used for the preservation of tissues for paraffin embedding and *in situ* hybridisation, immunohistochemistry and routine haematoxylin and eosin (H & E) staining.

2.5.1.2 Karnovsky's modified fixative (paraformaldehyde/glutaraldehyde 4%/5%)

Karnovsky's modified fixative (see *Appendix* page 178) was used for the preservation of tissues for resin embedding before light and electron microscopy.

2.5.1.3 Periodate-lysine-paraformaldehyde (P-L-P) fixative

P-L-P fixative (see *Appendix* page 178) was used for the preservation of tissues destined for staining with the microglia marker F4/80. After perfusion, tissues were post-fixed and cryoprotected before rapid freezing for cryostat sectioning (see 2.6.3.2 *Cryopreservation of P-L-P fixed material*, page 59).

2.5.1.4 4% Paraformaldehyde in PBS

4% paraformaldehyde in PBS (see *Appendix* page 179) was used for the preservation of tissues destined for immunohistochemistry using vibratome sections of agar-embedded tissue and for post-fixation of cryopreserved and paraffin sections.

2.5.2 Fixation techniques

2.5.2.1 Cardiac perfusion

Mice over 10 days of age were killed in a carbon dioxide chamber. Mice less than 10 days of age were killed in a halothane (Rhone-Poulenc Chemicals Ltd.) chamber. Once death had been confirmed, the thoracic cavity was opened and the right atrium of the heart was incised to allow blood and perfusion fluids to escape. Perfusion was carried out by instilling solutions into the left ventricle through a 21 to 25 gauge 1.5-inch hypodermic needle (depending on body size). 0.85% saline was instilled to flush blood from the circulatory system followed by fixative. 20 to 60ml of fixative were used depending on carcass size and degree of fixation was assessed by carcass rigidity.

2.5.2.2 Tissue Dissection

Tissues were dissected using a low power dissection microscope and microsurgical instruments. Skin and muscle were reflected from the head and dorsum and the calvarium and vertebral arches were removed to reveal the brain and spinal cord. The cord was severed using a razor blade as it entered the brain stem and the brain was removed by incising the cranial nerves and meninges. The optic nerve tracts were incised just caudal to the optic chiasm allowing the optic nerves and globes to be removed separately and intact. The cord was removed by incising the meninges and spinal nerve roots.

2.5.2.3 Tissue storage

Carcasses were stored at 4°C in fixative until tissues were dissected. P-L-P fixed tissue was dissected within 1 hour and post-fixed in fixative for 4 to 6 hours before sucrose protection and freezing. BNF fixed tissue was dissected within 24 hours and processed. Karnovsky's modified fixative tissue was dissected within 7 days and stored in fixative at 4°C until processing. 4% paraformaldehyde/ PBS fixed tissue was dissected within 24 hours and stored for up to 7 days in fixative before being processed.

2.6 Tissue processing and sectioning

2.6.1 Paraffin wax processing and sectioning

Neural tissue and muscle from mice perfused with BNF were wrapped in pieces of filter paper, placed in processing cassettes and loaded in the basket of a Shandon Elliot automatic processor (Histokinette). The tissues were passed through

dehydrating solutions and infiltrated with wax at 60°C (see *Appendix* page 179) before being embedded in wax. 8µm sections were cut using a Biocut 2035 microtome (Leica) and mounted onto APES-coated slides that were baked overnight at 56°C to ensure good adherence of the sections.

2.6.2 Resin processing and sectioning

Neural tissues from mice perfused with Karnovsky's modified fixative were processed for resin embedding using a Lynx microscopy tissue processor (Leica) that automated the dehydration and resin infiltration steps (see *Appendix* page 180). Once processed, the tissues were placed in resin filled rubber moulds for polymerisation at 60°C overnight. Blocks were cut on an Ultracut-E Reichert-Jung ultratome producing 1µm 'thick' sections for light microscopy and 70nm 'ultra-thin' sections for electron microscopy. Thick sections were cut using a glass knife and mounted on plain slides for light microscopy or on APES-coated slides for immunohistochemistry. Ultra-thin sections were cut with a diamond knife and mounted on 200-mesh 3.06mm-diameter copper grids.

2.6.3 Cryopreservation and sectioning

2.6.3.1 Cryopreservation of fresh neural tissue

Tissues required for immunohistochemistry and *in situ* hybridisation were cryopreserved. Nervous tissue was dissected from freshly culled mice, suspended in Tissue-Tek O.C.T compound (Miles Inc) and frozen in 2-methylbutane cooled to at least -80°C in liquid nitrogen. Frozen O.C.T blocks were wrapped twice in NescoFilm (Bando Chemical Ind. Ltd.) to prevent dehydration and stored at -20°C.

2.6.3.2 Cryopreservation of P-L-P fixed material

Cryopreserved, P-L-P fixed tissue was collected for F4/80 immunostaining. Immediately after perfusion, neural tissues were removed and post-fixed in P-L-P fixative for 4 to 6 hours at 4°C. The tissues were then cryoprotected by immersion in 20% sucrose in PBS for 24 to 48 hours at 4°C and frozen in O.C.T as described above.

2.6.3.3 Cryopreservation of fresh muscle

Skeletal muscle samples from freshly culled mice were dissected maintaining tension during and after dissection to limit contraction artefact. They were orientated on strips of 3MM filter paper (Whatman), dusted with talcum powder to reduce ice artefact and snap frozen in liquid nitrogen for sectioning on the day of

collection.

2.6.3.4 Sectioning of cryopreserved tissue

Cryopreserved tissue was cut on an OTF cryostat (Bright Instrument Company) at 15 μ m. The sections were thaw-mounted onto APES-coated slides and stored at -20°C. Sections for *in situ* hybridisation were not allowed to thaw before use (see *Appendix* page 181).

2.6.4 Agar embedding and vibratome sectioning of paraformaldehyde fixed tissue

Neural tissue dissected from mice that had been perfused with 4% paraformaldehyde/ PBS was embedded in 4% low gelling temperature agarose type IV (Sigma) melted in PBS. Sections were cut on a D.S.K Microslicer DTK-1000 vibratome (Polaron) with cutting speed and frequency optimised to reduce artefact. Sections of spinal cord were cut at 50-75 μ m and sagittal hindbrain was cut at 75-100 μ m. These were stored free-floating in fixative at 4°C until required.

2.7 Staining techniques

2.7.1 Light microscopy

2.7.1.1 Haematoxylin and Eosin (H & E)

Paraffin sections and cryopreserved muscle sections were stained with H & E to assess tissue morphology and preservation (see *Appendix* page 185). Once stained, sections were mounted in DPX (BDH).

2.7.1.2 Haematoxylin

Cryosections for *in situ* hybridisation and paraffin sections for immunostaining were counterstained with haematoxylin to show nuclear detail (see *Appendix* page 186)

2.7.1.3 Methylene blue/ azur II

Resin sections for light microscopy were stained with methylene blue/ azur II (see *Appendix* page 187). Sections were heated on a hot plate to 60°C, flooded with stain for 1 minute and washed in running water. These were mounted in DPX after drying overnight.

2.7.2 Electron microscopy

Copper grid-mounted, thin resin sections were stained with uranyl acetate and lead citrate for electron microscopy (see *Appendix* page 186).

2.8 Morphological studies

2.8.1 Quantification of corrected glial cell densities

Quantification of glial cells was performed on 1 μ m resin sections stained with methylene blue/azur II. Sections were cut at 14 μ m intervals to avoid sectioning individual nuclei in multiple sections and thus counting the same cell twice. A 6.3x eyepiece with a 100x oil immersion lens was used to visualise cells within a 100-square graticule (Graticules Ltd.).

Transverse sections of the second to third cervical spinal cord segments (C2-3) and of the mid-optic nerve were counted. On cord sections, glial cell nuclear profiles were counted within an area of the white matter adjacent to the ventromedian fissure. Two fields, one on each side of the fissure, were examined and at least four sections from each animal were counted giving a total of eight hundred graticule squares. On optic nerve sections, one and a half fields could be counted per section and three sections were counted from each animal giving a total of four hundred and fifty graticule squares. Nuclear profiles were selected if they lay within the area of the graticule squares using an inclusion/ exclusion technique; all profiles completely within the boundaries of each square and those profiles crossing the upper and left-hand boundaries of the square were counted. Those profiles crossing the bottom and right-hand boundaries of the square were excluded. Endothelial cell and pyknotic nuclear profiles were excluded.

In both areas, longitudinal sections were taken immediately caudal to the counting area in order to estimate the mean and maximum nuclear lengths. The mean nuclear lengths were used in the calculation of glial cell densities and total glial cell counts (see below). The maximum nuclear lengths were used to determine the interval between sections to prevent sectioning of the same nucleus twice. The white matter area was calculated for each section from Polaroid light microscopy images using Sigma Scan/Image measurement software (Jandel Scientific Software) and a SummaSketch III graphics tablet (Summagraphics). Corrected glial cell densities and corrected total cell glial counts were calculated using Abercrombie's correction factor (Sturrock, 1983). Three to six animals were counted from each group and the results were plotted using Graphpad Prism software (Graphpad Software Inc.).

2.8.2 Quantification of swollen axons and degenerate fibres

Densities of swollen axons and degenerating fibres were measured using an adaptation of a point counting method described by Williams (1977) for calculating myelin density. Measurements were made from electron-micrographs of ultra-thin transverse sections of mid-optic nerve that were taken at 7,500 times magnification and magnified 2 times at printing. Tissue from at least three animals from each group was included and 10 to 12 electron micrographs from each tissue sample were counted.

2.8.2.1 Measurement of swollen axon densities

A ruled transparency with a grid of 1.5cm^2 squares was placed over each electron micrograph. The numbers of swollen and normal axons crossed by the grid intercepts were recorded. The densities of normal and swollen axons were expressed respectively as a ratio of the number of intercepts hit by each group to the total number of possible intercept hits. This gave values of axonal density that had arbitrary units but that were directly comparable with each other.

2.8.2.2 Measurement of degenerate fibre densities

A ruled transparency with a grid of 2cm^2 squares was placed over each electron micrograph. The numbers of degenerate and normal myelinated fibres crossed by the intercepts were recorded and fibre densities were calculated as above.

2.8.3 Assessment of axonal size and myelination status

Measurements were made from electron micrographs of ultra-thin sections of mid-optic nerve and of spinal cord ventral columns (C2-3). Electron micrographs were taken from randomly selected fields of optic nerve and cervical cord. Optic nerve micrograph images were collected at 7,500 times magnification at all ages and cervical cord images were collected at 5,000 times (20 days of age) and 3,000 times (60 and 120 days of age) magnification respectively. To resolve the axon profiles and their associated glial processes, these electron micrographs were printed at 5 times magnification. A diffraction grating with 2160 lines per mm was photographed for calibration. A rectangle was drawn on each electron micrograph to define an area that only contained axons completely included within the field of view of the electron micrograph. Axons for assessment were selected using an inclusion/ exclusion system to include all axons completely contained within the rectangle and those axons that crossed either of two adjacent boundaries of the rectangle. Axons crossing the remaining two boundaries of the rectangle were excluded. All the selected axons were numbered. Two to three hundred axons were

selected from each mouse and four mice were assessed from each group. Swollen axons or those associated with degenerating fibres and cross-sections of nodes and paranodes were excluded.

2.8.3.1 Assessment of axonal diameter

Few axons are truly circular in cross-section at electron microscopy and a direct comparison of axonal diameters, and hence axonal size, is impossible. In this study, a projected axonal diameter was used as the measurement of axonal size. The cross-sectional area of each axon was calculated using Sigma Scan/Image measurement software (Jandel Scientific Software) and a SummaSketch III graphics tablet (Summagraphics). The projected axonal diameter was calculated by assuming that all axons were circular in cross-section and extrapolating a projected axonal diameter from the measurement of axonal area.

2.8.3.2 Assessment of myelination status

The myelination status of each axon was assessed. Axons were classified as myelinated if they were encircled by one or more compacted myelin lamellae. Ensheathed axons were fully encircled at least once by an oligodendrocyte process but no compacted myelin was present. Axons associated with but not ensheathed by oligodendrocytes and those associated with astrocyte processes were classified as unmyelinated. Data from non-myelinated axons encompasses data collected from unmyelinated and ensheathed axons.

2.8.4 Presentation of data and statistical analysis

Data have been presented graphically and, where group sizes permit, the non-parametric two-tailed Mann-Whitney test has been used to compare data sets statistically. Statistical significance has been set at P less than 0.05 throughout this study.

Axon diameter data are presented as mean relative frequency distributions. These are calculated for each time point from the relative frequency distributions of axon diameters for each data set. The bin values are collated from the data sets by plotting the mean values with the standard error of the mean.

Myelinated (or non-myelinated) axon diameter frequency distributions are presented in proportion to the total population of axon diameters. To achieve this, the relative frequency distribution bin values for each data set are adjusted by multiplying by the percentage of myelinated (or non-myelinated) fibres in that data set and the separate

data sets are collated as above.

2.9 Immunohistochemistry

Descriptions of the standard immunohistochemical techniques are followed by modified techniques employed for staining of agar embedded tissue and for microglial staining. Incubation steps were performed in a humidity chamber and control sections with the primary antibodies omitted were included to ensure specificity.

2.9.1 Immunohistochemical markers

The sources and titres of antibody used are described in Table 6 (page 65).

Anti-PLP C-terminal antibody (NP Groome, Oxford, UK) recognises the carboxy terminus (amino acids 271 to 276) of the *Plp* gene protein isoforms (Fanarraga *et al.*, 1993). This antibody was used to identify endogenous and transgenic *Plp* gene products by immunohistochemistry and western blotting. Anti-PLP isoform specific antibody (NP. Groome, Oxford, UK) recognises the 35 amino acid epitope encoded by exon 3B that is unique to the PLP protein isoform. Anti-MBP antibody (NP. Groome, Oxford, UK) was used to identify central compact myelin. Anti-CAII antibody (AM. Butt, London, UK) recognises carbonic anhydrase II, an oligodendrocyte-specific marker in mature CNS white matter defining a subpopulation of cells that myelinate small diameter axons (Butt *et al.*, 1995). It also recognises neurones in grey matter and a wider range of glial cells in immature animals but was used to confirm comparative oligodendrocyte densities in white matter tracts between mature mice in this study. Anti-F4/80 hybridoma supernatant (Serotec) recognises a macrophage-specific epitope (F4/80) (Austyn and Gordon, 1981; Perry *et al.*, 1985) and was used to identify microglia. Anti-gial fibrillary acidic protein (GFAP) antibody (Dako) was used to identify astrocytes (Bignami *et al.*, 1972). Anti-SMI-31 antibody (Affiniti Research Products Ltd.) recognises a phosphorylated neurofilament epitope and was used to identify axons and phosphorylated neurofilaments in neuronal cell bodies. Anti- β -galactosidase antibody (Promega) was used to identify the PLP-LacZ fusion protein.

2.9.2 Peroxidase anti-peroxidase (PAP) immunohistochemistry

2.9.2.1 Preparation of slides

2.9.2.1.1 Resin sections

Resin was removed from the sections by immersion with rotation in sodium

ethoxide (50% ripened sodium ethoxide in 50% absolute alcohol) for 30 minutes. The slides were washed in absolute alcohol (6 changes in 30 minutes) to remove traces of sodium ethoxide and then in running water for 30 minutes. Endogenous peroxidase activity was quenched by immersion in 3% hydrogen peroxide in water for 30 minutes. Sections were washed again in running water for 30 minutes before blocking.

2.9.2.1.2 Paraffin sections

Paraffin sections were dewaxed in xylene and hydrated through alcohols (see *Appendix* page 184). Endogenous peroxidase activity was quenched by immersion in 3% hydrogen peroxide in alcohol for 30 minutes. Sections were washed in running water for 30 minutes before blocking.

Table 6 Primary antibodies used for immunohistochemistry with appropriate dilutions (dilutions for western blotting in the text)

Primary antibody		Dilution	
anti-PLP C-terminal	rabbit polyclonal	IgG	1:600
anti-PLP isoform specific	rabbit polyclonal	IgG	1:600
anti-MBP	rat monoclonal	IgG	1:500
anti-CAII	rabbit polyclonal	IgG	1:1500
anti-F4/80	rat monoclonal	IgG	1:1000
anti-GFAP	rabbit polyclonal	IgG	1:1000
anti-SMI-31	mouse monoclonal	IgG1	1:1500
anti- β -galactosidase	mouse monoclonal	IgM2a	1:1000

Table 7 Link antibodies, PAP complexes and dilutions used for PAP immunostaining (sourced from Sigma)

Link antibody		PAP complex		Source
goat-anti-rabbit	1:10	rabbit	1:40	ICN
goat-anti-mouse	1:10	mouse	1:1250	Sigma

Table 8 Fluorescent secondary antibody dilutions for immunohistochemistry (sourced from Southern Biotech)

Secondary antibody	Dilution
goat-anti-rabbit IgG FITC	1:80
goat-anti-rat IgG FITC	1:50
goat-anti-mouse IgG1 FITC	1:80
goat-anti-mouse IgGM2a FITC	1:25
goat-anti-rat IgG TxR	1:50
goat-anti-mouse IgG1 TxR	1:75

2.9.2.2 PAP staining

Non-specific binding of antibodies was blocked by incubation of the sections with 1% normal goat serum (NGS) in PBS for 2 hours at room temperature. Excess blocking solution was removed and the primary antibody was applied diluted in more blocking solution. The sections were incubated in the primary antibody overnight at 4°C.

Once the sections had warmed to room temperature, they were washed in PBS (6 changes in 30 minutes). The appropriate link antibody (Table 7, page 66) was applied diluted in blocking solution for 1 hour at room temperature and then washed off with PBS (6 changes in 30 minutes). Sections were incubated in PAP complex (Table 7, page 66) for 30 minutes at room temperature and then washed in PBS (6 changes in 30 minutes). The chromogen was developed in filtered PBS containing 0.5 mg.ml⁻¹ 3,4,3',4',-tetraminobiphenyl hydrochloride (DAB) and 0.003% hydrogen peroxide until the required colour change was seen (30 seconds to 5 minutes). DAB was removed by washing in PBS for 2 minutes and running water for 5 minutes.

Paraffin sections were counterstained with haematoxylin (see *Appendix* page 186). Resin sections were immersed in 1% osmium/caccodylate buffer for 2 min before washing. All sections were dehydrated through alcohols, cleared (see *Appendix* page 184) and mounted in DPX.

2.9.3 Immunofluorescence of fresh, cryo-preserved tissue

After thawing, cryostat sections were soaked in PBS for 10 minutes to remove the embedding medium and fixed in 4% paraformaldehyde/ PBS at room temperature for 20 minutes. Depending on the antibody used, sections were permeabilised by immersion in methanol for 10 minutes at -20°C. The sections were washed twice in PBS for 5 minutes and incubated in a humidity chamber with the primary antibody diluted in 1% NGS/ PBS at 4°C overnight. The primary antibody was removed by washing twice in PBS for 5 minutes and the appropriate secondary antibody was applied for 30 minutes at room temperature (Table 7, page 66). The sections were washed and mounted in Citifluor antifade mountant (UCK Chem Lab) under sealed coverslips. Sections were stored in the dark at 4°C to limit fading.

Secondary antibodies were labelled with fluorescein isothiocyanate (FITC) and Texas red (TXR) (Table 7, page 66) and sections were examined by epifluorescence. FITC absorbs light with a wavelength 495nm and emits it at

525nm that can be visualised as green light using a blue filter. TXR absorbs light at 596nm and emits it at 620nm that can be visualised as red light using a green filter.

2.9.4 Agar-embedded tissue staining

Immunofluorescence on agar-embedded, formaldehyde-fixed tissue was performed using a technique modified from Trapp *et al.* (1997). The main factor that determined the efficacy of staining was the primary antibody incubation step. Sections were washed 3 times in PBS for 5 minutes between each step. Except for the primary antibody incubation step, all steps were performed at room temperature. The steps were performed on free-floating sections in microwell plates containing 300µl of reagent.

The sections were washed, permeabilised in 5% Triton X-100/ 3% hydrogen peroxide for 30 minutes, washed again and blocked in 3% NGS in PBS for 30 minutes. Excess blocking solution was removed and the sections were incubated with the primary antibody diluted in 3%NGS in PBS at 4°C. Sections were incubated in anti-SMI-31 or anti-MBP primaries for 3 days; sections were incubated in anti-PLP C-terminal primary for 5 days.

Sections were washed and incubated for 1 hour with the secondary antibody (Table 7, page 66). After further washing, the sections were mounted in Citifluor antifade **mountant under sealed coverslips. If nuclear counterstaining was required, sections** were washed and incubated in 4',6-diamidino-2-phenyl-indole (DAPI) (Sigma) diluted to 1:400 for 30 seconds before washing and mounting. Sections were stored in the dark at 4°C to limit fading. Any remaining agar was removed by gentle traction before mounting.

2.9.5 F4/80 Microglial staining

Immunostaining with the F4/80 hybridoma supernatant was performed on cryostat sections of P-L-P perfusion fixed tissue that had been cryoprotected before freezing (see 2.6.3.2 *Cryopreservation of P-L-P fixed material*, page 59). Sections were washed thoroughly in PBS (6 changes in 20 minutes) between steps and reagents were diluted in PBS. All incubations were performed at room temperature.

Sections were thawed and washed to remove the embedding medium before being blocked in 1% NGS for 30 minutes. Excess blocking medium was removed and the F4/80 antisera was applied at 1:20 for 60 minutes. The sections were washed and biotinylated rabbit anti-rat IgG secondary antibody at a 1:100 dilution was applied for 45 minutes. After further washing, endogenous peroxidase activity was quenched by soaking the slides in 0.3% hydrogen peroxide in ethanol for 20

minutes. The sections were washed in PBS and incubated in avidin-biotin complex (Elite ABC) for 45 minutes. The chromogen was developed in filtered PBS containing 0.5 mg.ml⁻¹ DAB and 0.003% hydrogen peroxide until the required colour change was seen (30 seconds to 5 minutes). After excess chromogen had been removed by washing, the sections were exposed to 0.01% osmium tetroxide for 30 seconds to enhance the chromogen intensity. The sections were washed, counterstained with haematoxylin (see *Appendix* page 186), cleared through alcohols (see *Appendix* page 184) and mounted in DPX.

2.10 Plasmid DNA (pDNA) preparation

2.10.1 Plasmids

Digoxigenin labelled anti-sense and sense *Plp*-riboprobes were generated from an 836bp *Plp*-cDNA that encompassed most of the coding region of the *Plp*-cDNA inserted into a pGEM4 vector (Promega) (Figure 8, page 47) (Milner *et al.*, 1985). This plasmid, pPLP-1, was linearised by *Bam*H1 digestion for anti-sense probe production (T7 promoter) and by *Hind*III digestion for sense probe production (SP6 promoter).

Digoxigenin labelled anti-sense and sense *Mog*-riboprobes were generated from a 780bp *Mog*-cDNA that included all eight exons of the murine *Mog* gene (Daubas *et al.*, 1994). This had been subcloned from the pCL642 plasmid into a pGEM-4Z expression vector (Promega) denoted pG4MOG (Figure 8, page 47) (King, 1998). This was linearised by *Hind*III digestion for anti-sense probe production (T7 promoter) and by *Eco*R1 digestion for sense probe production (SP6 promoter).

2.10.2 Preparation of competent cells

Escherichia Coli Dh5 α {*endA1 hsdR17(r_km⁺_k) supE44 thi-1 recA1 gyrA* (Nal^r) *relA1* Δ (*lacZYA-argF*)_{U169} (ϕ 80*lacZ* Δ M15)} was used for competent cell preparation. A single colony was seeded into 10ml Luria-Bertani (LB) medium (see *Appendix* page 191) and incubated at 37°C with agitation overnight. 2ml of the overnight culture were inoculated into a 1 litre flask containing 200ml LB medium. This was incubated at 37°C with agitation until an OD₆₀₀ of 0.2 to 0.3 was obtained. The cultures were left on ice for 10 minutes before centrifugation at 5,000rpm for 5 minutes at 4°C. The harvested cells were gently resuspended in 50ml of 100mM calcium chloride, incubated on ice for 20 to 60 minutes, centrifuged at 5,000rpm for 5 minutes at 4°C and resuspended in 10ml of 100mM calcium chloride with 15% glycerol. The suspension was aliquoted, placed in liquid

nitrogen and stored at -80°C.

2.10.3 Transformations

In a 40ml polypropylene tube, a 100µl aliquot of ice-thawed competent cells was added to 5ng of pDNA in 100µl of TE buffer. This was incubated on ice for 30 minutes then heat shocked at 42°C for 2 minutes. Following the addition of 800 µl of LB medium, the tubes were incubated at 37°C with gentle agitation. 200µl aliquots were spread onto ampicillin-LB agar plates (see *Appendix* page 191), inverted and incubated at 37°C overnight.

2.10.4 Plasmid preparation

A single colony was seeded into 2ml ampicillin-LB medium (see *Appendix* page 191) and incubated at 37°C with agitation for 6 to 8 hours. 50µl of the starter culture was seeded into 25ml ampicillin-LB medium and incubated overnight at 37°C with gentle agitation. The cells were pelleted by centrifugation at 5,000rpm for 5 minutes at 4°C. pDNA was prepared using the Hybaid Recovery™ Quick Flow Midi Kit (Hybaid) according to manufacturers' instructions and using the manufacturers' buffers (see *Appendix* page 189). Briefly, the pellet was resuspended in 4ml of Cell Resuspension Buffer (Hybaid) containing RNase followed by the addition of 4ml of Cell Lysis Buffer and incubated at room temperature for 5 minutes. Following the addition of 4ml Neutralisation Buffer (Hybaid), the mixture was centrifuged at 18,000rpm for 10 minutes at 22°C. The supernatant was applied to a pre-equilibrated column under gravity flow. The bound material was washed twice in 10 ml Wash Solution (Hybaid) and eluted in 5ml of Elution Buffer. pDNA was precipitated by the addition of a 0.7 volume of propan-2-ol and immediately centrifuged at 18,000 rpm for 10 minutes at 4°C. The pellet was washed in 70% ethanol, collected by centrifugation at 18,000 rpm for 10 minutes at 4°C, air dried for 15 minutes and resuspended in 250µl of TE buffer. Yields in the range of 50 to 100µg of pDNA were obtained.

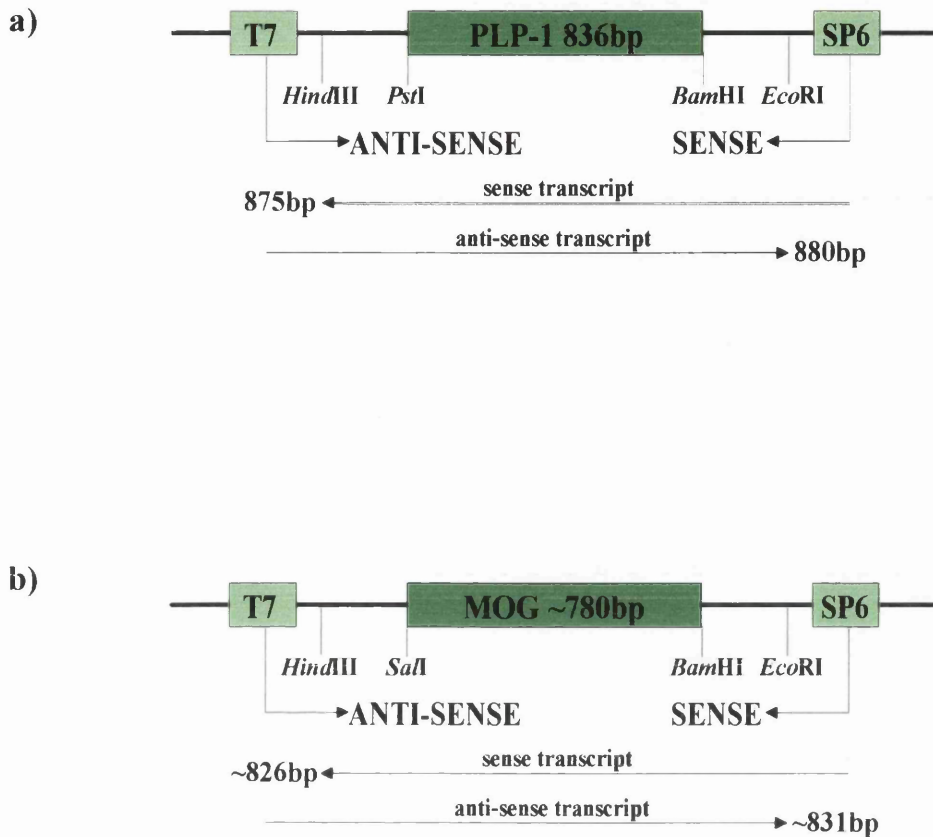


Figure 12 Plasmids used for riboprobe production

a) pPLP-1 plasmid for generation of anti-sense and sense *Plp*-riboprobes

b) pG4MOG plasmid for generation of anti-sense and sense *Mog*-riboprobes

(dark green boxes represent cDNA fragments; light green boxes represent T7 and SP6 vector promoters; restriction sites for cDNA insertion and for plasmid linearisation are shown; arrows denote direction of transcription of anti-sense and sense riboprobes; sizes of cDNA inserts and riboprobes are given)

2.11 Semi-quantitative reverse transcription PCR (RT-PCR)

The semi-quantitative RT-PCR method described has been used extensively in this laboratory to study *Plp* gene transcript ratios and previously established conditions were adopted for this study (Dickinson, 1995).

2.11.1 cDNA Synthesis

2µg of total cellular RNA was heat denatured at 65°C for 5 minutes and quenched on ice. First strand cDNA synthesis was performed from this RNA in a reaction mix containing 3µg random oligo d(N)₆ (GibcoBRL), 0.5mM dNTP, 10mM DDT, 20U RNase inhibitor (RNasin, Promega) and 400U Moloney murine leukaemia virus reverse transcriptase in the manufacturers buffer (GibcoBRL). This was incubated first at 37°C for 30 minutes, then at 42°C for 60 minutes and finally quenched by the addition of EDTA to a concentration of 25mM. Nucleic acids were precipitated at -80°C over 2 hours in the presence of 0.3M sodium acetate (pH5.2) and a 2x volume of ethanol. The nucleic acids were pelleted by centrifugation at 13,000 rpm for 30 minutes at 4°C, washed in 70% ethanol, air dried and reconstituted to 0.5ng/µl cDNA assuming maximal reverse transcription. cDNAs were gel checked to ensure efficient reverse transcription and accurate quantification (Figure 10, page 50).

2.11.2 RT-PCR

2.11.2.1 RT-PCR reaction Mix

RT-PCR was performed on 1ng and 2ng aliquots of cDNA in 50µl reaction volumes. Each reaction contained 0.25mM dNTP Master Mix (Bioline), 3mM MgCl₂, forward and reverse primers at 0.2µM, 2 units of *Taq* DNA polymerase (Bioline) and an ammonium buffer (Bioline). The reactions were overlaid with 50µl of molecular biology grade mineral oil (Sigma) to prevent evaporation. The Ex2 and αEx4.2 primer pair (see 2.4.3.2 *PlpTg1*, *Dm20Tg2* and *ND3A* transgenic mice, page 54) were used to amplify *Plp*-cDNA and *Dm20*-cDNA species. To assess consistency of sample loading and PCR conditions between tubes, primers that amplified cDNAs of transcripts from the ubiquitously expressed housekeeping gene, *cyclophylin*, were included in separate reactions (Table 5, page 55) (Danielson *et al.*, 1988).

2.11.2.2 RT-PCR Programme

To ensure consistency all amplifications were performed on the same thermal cycler (Perkin Elmer) and each experiment was repeated at 25 and 30 cycles of step 2.

1) Initial cycle	denaturing temperature	94°C	3 min
	annealing temperature	58°C	1 min
	extension temperature	72°C	2 min
2) Step cycle (25 and 30 cycles)	denaturing temperature	93°C	40 sec
	annealing temperature	58°C	1 min
	extension temperature	72°C	30 sec
3) Final cycle	denaturing temperature	93°C	40 sec
	annealing temperature	58°C	1 min
	extension temperature	72°C	2 min

2.12 *In Situ* Hybridisation

2.12.1 Preparation of apparatus and solutions

To minimise RNase activity, all solutions were made using DEPC-treated water. Glassware was cleaned by soaking overnight in 6% sulphuric acid/ 6% potassium dichromate, washed in DEPC-treated water and baked at 180°C for 4 hours loosely wrapped in foil. Plastic-ware was guaranteed RNase free (Anachem).

2.12.2 Preparation of digoxigenin-labelled riboprobes

2.12.2.1 Riboprobe production

Digoxigenin-labelled-UTP riboprobes were generated using the DIG RNA Labelling Kit (SP6/T7) (Boehringer Mannheim). Each 20µl reaction contained 0.5µg of linearised pDNA template, NTPs at 1mM, 1mM digoxigenin-labelled UTP, 10U RNase inhibitor and 10U of either SP6 or T7 RNA polymerase in transcription buffer supplied with the kit. The reaction mixture was incubated at 37°C for 1 hour and then quenched on ice. Template was treated with 5U of RNase-free DNase (Boehringer Mannheim) by incubation at 37°C for 10 minutes followed by the addition of 1µl of 0.2M EDTA. RNA was ethanol precipitated in the presence of

0.3M lithium chloride and resuspended in 50 μ l of DEPC-treated water in the presence of 0.5U. μ l⁻¹ RNase inhibitor. The reconstituted riboprobe was stored at -70°C until use.

2.12.2.2 Assessment of riboprobe activity

To assess digoxigenin-labelled riboprobe activity, dot blots of dilutions of the riboprobe were compared to standards supplied by the manufacturers. The test samples of probe were dot blotted onto a Hybond N+ nylon membrane (Hybaid). The membrane was air-dried for 10 minutes, baked at 80°C for a minimum of 2 hours and washed in maleate buffer (0.1M maleic acid, 0.15M NaCl, pH 7.5). A blocking solution of 10% foetal calf serum diluted in maleate buffer was applied to the membrane for 30 minutes. Sheep-derived, alkaline phosphatase-labelled anti-digoxigenin antibody (Anti-Digoxigenin-AP Fab fragments, Boehringer Mannheim) was applied to the membrane for 30 minutes at 1:4500 in 0.1M Tris/ 0.15M NaCl (pH7.5) buffer. After two 15 minute washes in 0.1M Tris the enzymatic reaction was developed by adding the alkaline phosphate substrate buffer (see *Appendix* page 183). Once the reaction had started to develop (taking up to 30 minutes) the filter was washed and the activity of the riboprobe dilutions was compared to standards. Riboprobes were used at dilutions that corresponded to 0.5 to 5ng.ml⁻¹.

2.12.3 Prehybridisation of sections

Paraffin sections were dewaxed by washing in xylene for 10 minutes followed by 5 minute washes in ethanol, methylated spirits, 0.85% saline and PBS. Both paraffin and cryosections then went through a series of washes (see *Appendix* page 182) including two fixation steps in 4% paraformaldehyde, proteinase K treatment to destroy RNase activity and acetylation in triethanolamine/acetic anhydride. The sections were dehydrated through alcohols and left to dry before hybridisation.

2.12.4 Hybridisation

Probe was diluted to final concentration of 0.5 to 5ng.ml⁻¹ in hybridisation buffer containing 50% formamide, 10% dextran sulphate, 1x Denhardt's, 20mM Tris HCl pH8, 0.3M NaCl, 5mM EDTA, 10mM NaPO₄ pH8 and 0.5mg.ml⁻¹ yeast tRNA. The probe were heated to 80°C for 2 minutes to denature secondary RNA structures and cooled on ice before being applied to sections under coverslips. Slides were placed horizontally in a holding box that contained a sponge reservoir of 50% formamide in 5x SSC to maintain humidity. This was sealed and placed in a humidified oven at 50°C for overnight hybridisation.

2.12.5 Slide development and mounting

Slides were passed through a series of increasingly stringent washes and equilibrated with the substrate buffer conditions (see *Appendix* page 183). After blocking, sheep-derived, alkaline phosphatase-labelled anti-digoxigenin antibody (Anti-Digoxigenin-AP Fab fragments, Boehringer Mannheim) was applied at 1:500 in 0.1M Tris/ 0.15M NaCl (pH7.5) buffer for 1 hour at room temperature. Antibody was removed by washing in TBS and the reaction was developed by adding substrate buffer (see *Appendix* page 183) for 5 minutes to 12 hours. Once the reaction had developed, slides were washed in running water for at least 10 minutes, counterstained and mounted in glycerol under sealed coverslips.

2.13 Western Blotting

2.13.1 Extraction of Protein from Tissue

Protein was extracted from whole spinal cords and brain that had been dissected from freshly killed animals and stored in liquid nitrogen. During the extraction process, all steps were performed at 4°C and the protein extracts were stored at -20°C until required

2.13.1.1 Isolation of protein from whole brain and spinal cord

Tissue samples were homogenised in 75µl aliquots of tissue lysis buffer containing 10mM Tris (pH6.0), 150mM NaCl, 1mM EDTA, 1mM ethylene-glycol-bis-(beta-amino-ethylether)-N,N'-tetra-acetic acid, 0.2mM phenylmethylsulfonyl fluoride, 0.5% NP-40, 1% TritonX-100. The homogenate was centrifuged at 13000rpm for 30 minutes to pellet the cell debris and the supernatant was retained. Total protein concentration was measured using the BCA assay (Pierce).

2.13.1.2 Isolation of protein from myelin extracts of brain and spinal cord

Tissue samples were homogenised in buffer containing 0.85M sucrose, 10mM Hepes (pH7.4), 3mM dithiothreitol (DTT), 1mM N α -p-tosyl-l-lysine chloro-methyl ketone (TLCK). Additional buffer was added to give a final volume of 7.4ml (approximately 20x that of the tissue sample). This was overlain with 4.6ml of buffer containing 0.25M sucrose, 10mM Hepes (pH7.4), 3mM DTT, 1mM TLCK and centrifuged at 70,000g for 90 minutes. This produced a biphasic solution with cellular debris left in the lower phase (0.85M sucrose), lipid floating on top of the upper phase (0.25M sucrose) and myelin protein trapped at the interface between the two phases. The protein layer was removed and osmotically challenged to solubilise any remaining cellular organelles. 12ml of SDW was added to the sample and this

was centrifuged at 23,000g for 30 minutes to sediment the protein. The supernatant was discarded and the process was repeated 3 times with the final centrifugation at 17,000g to ensure that only protein sedimented. The protein pellet was washed in a small volume of SDW before being resuspended in 50µl of SDW. Total protein concentration was measured using the BCA assay (Pierce).

2.13.2 SDS-Polyacrylamide gel electrophoresis

2.13.2.1 SDS-Polyacrylamide gel preparation

Proteins were resolved on a 40ml vertical SDS-polyacrylamide gel produced by polymerisation of acrylamide cross-linked with N,N'-methylene bisacrylamide at a ratio of 30:8. The catalyst for the reaction was ammonium persulphate and the accelerator was N,N,N,N',-tetramethylethylenediamine (TEMED). A 5 to 20% gradient gel was poured using a Biorad mode 385 gradient former from 5% and 20% solutions of acrylamide-bisacrylamide containing 0.375M Tris (pH 8.8), 0.1% SDS, 0.05% TEMED, 0.075% ammonium persulphate. Once this had polymerised a stacking gel (2.5% acrylamide-bisacrylamide, 0.125M Tris (pH 6.8) 0.1% SDS, 0.05% TEMED, 0.075% ammonium persulphate) with wells was laid on top.

2.13.2.2 Protein electrophoresis

Aliquots of the protein samples (25µg of myelin extracts and 50µg of whole extracts) were made up to a volume of 25µl in a buffer containing 62.5mM Tris (pH6.8), 40mM DTT, 5% 2-mercaptoethanol, 0.002% bromophenol blue, 2% SDS, 10% glycerol and denatured by boiling for 5 minutes. This allowed the SDS to bind to the denatured polypeptides in a constant weight ratio so that they had similar charges and would separate on the basis of size. The samples were loaded onto the gel with equine myelin and size markers as controls.

The samples were electrophoresed in a discontinuous buffer system using a buffer containing 25mM Tris (pH8.3), 19.2mM glycine, 0.1% SDS at 4°C. The samples were electrophoresed for 45 minutes at 125mA to stack the samples and then at 35mA overnight to resolve the proteins.

2.13.3 Western Blotting

2.13.3.1 Electrophoretic protein transfer

The gel was washed in SDS-transfer buffer (25mM Tris (pH8.3), 150mM glycine, 20% methanol, 0.1% SDS). The proteins were transferred onto Hybond ECL nitrocellulose membrane (Amersham Life Sciences) in a transblot cell (Bio-Rad).

The cell was run for 4 hours at 300mA in the SDS-transfer buffer that was cooled to 4°C. The gel was stained with Comassie blue R250 to check for loading accuracy and efficiency of transfer.

2.13.3.2 Immunostaining

The membrane was blocked overnight at 4°C by soaking in blocking buffer containing 0.2% gelatin, 5% dried milk, 0.1% TritonX-100 in TBS (pH 7.6). Primary antibodies were diluted in blocking buffer and applied for 1 hour at room temperature. The membrane was washed repeatedly in blocking buffer over 2 hours and the link antibody, diluted at 1:2500 in blocking buffer, was applied for 60 minutes. The membrane was washed again in blocking buffer and rinsed in TBS (pH 7.6). The membrane was incubated in equal volumes of luminol enhancer solution and stable peroxide solution (both from Pierce Chemical Co.) for five minutes at room temperature and wrapped in Saran wrap. X-omat imaging film (Kodak) was exposed to the membrane for 30 seconds and the film was developed in an automatic processor (Dupont Cronex CX-130).

Anti-PLP C-terminus antibody was applied at 1:5000 and anti-MBP antibody (rabbit polyclonal supplied by JM. Matthieu, Lausanne, Switzerland) was applied at 1:2000; both were detected with goat anti-rabbit IgG antibody conjugated to peroxidase. Anti-actin antibody was applied at 1:2000 and detected with anti-mouse IgG antibody conjugated to peroxidase.

3. The phenotype and pathology of the *Plp* gene knockout mouse

3.1 Introduction

Much of the evidence supporting roles for the *Plp* gene in oligodendrocyte development and survival comes from studies of spontaneous *Plp* gene mutants. These are characterised by early-onset, dysmyelinating phenotypes with reduced numbers of mature oligodendrocytes and small numbers of thin myelin sheaths (reviewed in introduction to this thesis). Two disease mechanisms have been proposed for the pathogenesis of these phenotypes. The ‘loss-of-function’ hypothesis (page 31) proposes that *Plp* gene products play vital roles in oligodendrocyte development and myelin stability and that, without these, the oligodendrocyte is not viable. This is supported by similar disease in humans with deletions and functional null alleles of the *PLP* gene and by the paucity of gene products in people and animals with missense mutations of the *Plp/PLP* gene. The ‘gain-of-function’ hypothesis (page 31) proposes that mutated *Plp* gene products gain toxic properties disrupting oligodendrocyte function. The inability of transgenic complementation to rescue the phenotypes of some spontaneous *Plp* gene mutants and evidence of abnormal protein trafficking within mutant oligodendrocytes adds weight to this theory.

In order to clarify some of these points and provide a model to examine the effects of gene dosage, a targeted mutation of the *Plp* gene was induced producing mice with null alleles of the *Plp* gene (Klugmann *et al.*, 1997). Surprisingly, despite the complete absence of *Plp* gene products, these mice myelinated well showing no evidence of gross dysmyelination. They remained clinically normal into adulthood and were indistinguishable from unaffected littermate controls. On closer examination however, they did show evidence of neurodegeneration that was characterised by a progressive axonopathy with fibre degeneration. Two further mouse models described by Boison and Stoffel (1994) that had functional *Plp* gene null-alleles also showed few clinical signs but appeared to have selective dysmyelination, small diameter axons remaining unmyelinated (Boison and Stoffel, 1994; Boison *et al.*, 1995). In addition, they reported poor compaction of central myelin with abnormalities of the intraperiod lines (Rosenbluth *et al.*, 1996) and reduced optic nerve conduction velocities (Boison and Stoffel, 1994).

3.2 Aims

One of the major aims of this study was to characterise the *Plp* gene knockout mouse generated by Klugman *et al.* (1997) and thus elucidate the roles of the *Plp* gene. These mice are referred to as *knockout mice* in this text and a description of the targeting strategy is given in *Chapter 2 Materials and Methods (2.2.2.1 Plp gene knockout mice, page 39)*. This section describes the clinical and pathological features of the knockout mice in comparison to age-matched controls from the same breeding programme that lack the targeted mutation (wild type mice). In addition to CNS dysfunction, humans with deletions and functional null-alleles of the *PLP* gene show evidence of demyelinating peripheral neuropathies (Garbern *et al.*, 1997). This suggests that the *PLP* gene plays a role in maintaining peripheral myelin. In order to investigate a similar role for the murine *Plp* gene products, a histopathological survey of the PNS of knockout mice was undertaken.

In this chapter, molecular analysis of the knockout mice is described to show that the targeted mutation prevents endogenous *Plp* gene activity. A summary of the clinical and pathological findings in the knockout mice is given followed by more detailed descriptions of the axonal, glial and myelin changes. Electron microscopy, immunostaining and morphometric analyses are included where relevant to highlight the changes that developed. Results from the survey of the peripheral nervous system are included at the end.

A separate description of female animals heterozygous for the targeted allele (*Plp^{tmkn1}*) is given in *Chapter 4 Plp^{tmkn1} heterozygous animals (page 132)*.

3.3 Materials and methods

3.3.1 Animal breeding

Over 450 animals were bred as described in *2.2 Mouse Breeding (page 39)* during a three year period. Both male and female mice were used for survey histopathology and molecular analyses. Only male mice were used for morphometric analyses and body weight measurements, to control for differences between genders. Genotypes of knockout mice were confirmed by PCR (see *2.4 PCR Genotyping, page 53*).

3.3.2 Molecular analysis of the knockout animals

Mice were compared by RT-PCR and western analysis at the peak of normal *Plp* gene expression (20 days of age).

3.3.2.1 Tissue collection

Total cellular RNA was extracted from whole brain homogenates as described in 2.3.3 *Extraction of RNA from mouse tissue* (page 47). Protein was extracted from whole brain homogenates and from the myelin fraction of brain as described in 2.13.1 *Extraction of Protein from Tissue* (page 75).

3.3.2.2 Semi-quantitative RT-PCR

Semi-quantitative RT-PCR was performed as described in 2.11 *Semi-quantitative reverse transcription PCR (RT-PCR)* (page 72) to assess the level of *Plp* gene transcription.

3.3.2.3 Western analysis

Western analysis of protein samples from whole tissue and myelin extracts of brain and spinal cord were compared using the anti-PLP C-terminal antibody as described in 2.13 *Western Blotting* (page 75).

3.3.3 Histopathology

A histological survey of CNS tissue was performed from 1µm resin sections stained with methylene blue/ azur II (see 2.6.2 *Resin processing and sectioning*, page 59). Tissues were collected from 20, 60, 120, 240, 360 and 540 day-old wild type and knockout mice. Occasional knockout mice surviving for more than 540 days of age without developing severe neurological dysfunction and wild type mice up to 2 years of age were included. Tissue from 98 knockout mice (of which 39 were 360 days of age or older) and 62 wild type mice (of which 19 were 360 days of age or older) was examined.

A survey of the peripheral neuromuscular system of aged knockout mice was performed. Resin sections from a range of peripheral nervous tissues (sciatic, peroneal, tibial, vagus and trigeminal nerves, lumbar nerve roots and brachial plexus) were examined from six knockout mice aged 600 days or older. Cryosections of skeletal muscles (biceps brachii, triceps brachii, quadratus femoris, cranial tibialis, gluteals) and neuromuscular junctions from a 540 day old knockout mouse were compared to an age-matched control.

3.3.4 Morphometric analysis

To study neural development and maturation, glial cell quantification and myelin morphometry were performed on the ventral columns of spinal cord (C2-3) and on mid optic nerve. Analysis at 20 days allowed glial cell development and

myelination to be compared at the peak of myelination but before secondary neurodegenerative changes had developed. By 120 days, the axonal changes and fibre degeneration were well established enabling the axonal changes to be quantified and the glial cell responses to be recorded. 60 days of age was chosen as an intermediary stage when neural development was complete but degenerative changes had not become prominent.

3.3.4.1 Axon diameters and myelination status

Axon diameters and myelination status were calculated as described in 2.8.3 *Assessment of axonal size and myelination status* (page 62).

3.3.4.2 Glial cell quantification

Glial cell densities and numbers were calculated as described in 2.8.1 *Quantification of corrected glial cell densities* (page 61). *In situ* hybridisation and immunocytochemical markers were used to confirm these findings because of the inaccuracy of glial cell identification based on nuclear morphology and the inadequacies of Abercrombie's correction factor (Sturrock, 1983b; reviewed by Coggeshall, 1992; Clarke, 1992; Hedreen, 1998; Sturrock, 1983b).

3.3.5 Immunostaining

Immunohistochemistry was performed as described in 2.9 *Immunohistochemistry* (page 64). Anti-F4/80 hybridoma supernatant and anti-GFAP antisera were used to demonstrate microglial densities and astrocytic bulk respectively. Anti-CAII antiserum was used to estimate oligodendrocyte densities.

3.3.6 *In situ* hybridisation

In situ hybridisation was performed as described in 2.12 *In Situ Hybridisation* (page 73). 15µm cryosections were probed using digoxigenin-labelled riboprobes that recognised transcripts from *Plp* and *Mog* genes (page 69). Oligodendrocyte densities were confirmed by *in situ* hybridisation using antisense *Mog* digoxigenin labelled riboprobes (Salvati *et al.*, 1996; Solly *et al.*, 1996).

3.4 Results

3.4.1 Analysis of *Plp* gene activity in the *Plp* gene knockout mouse

3.4.1.1 *Plp* gene expression

3.4.1.1.1 Semi-quantitative RT-PCR

Transcript analysis by RT-PCR of knockout and control animals are demonstrated in Figure 46 (page 147, *Chapter 5*) where these results are compared to results obtained from knockout animals complemented with various transgenes. Transcripts from the *Plp* gene were identified only at very low levels in knockout mice by RT-PCR.

3.4.1.1.2 *In situ* hybridisation

In situ hybridisation at 20 days of age using an anti-sense *Plp*-riboprobe demonstrated high levels of *Plp* gene activity predominantly in the white matter of wild type mice but failed to detect any transcripts in knockout mice (Figure 13, page 83)

3.4.1.2 PLP and DM20 protein levels

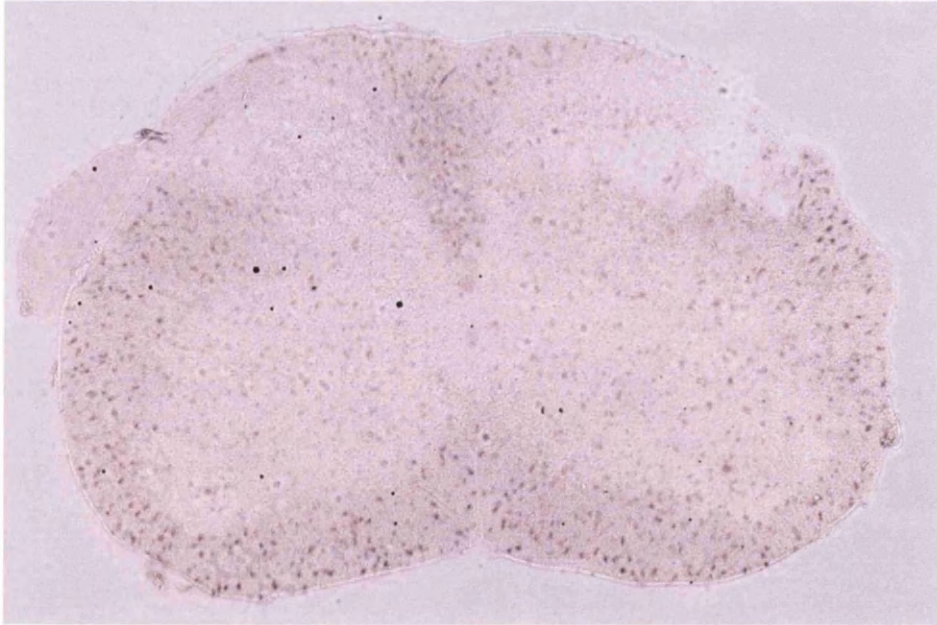
3.4.1.2.1 Western blotting

Protein analysis by western blotting of knockout and control animals are demonstrated in Figure 47 (page 148, *Chapter 5*) where these results are compared to results obtained from knockout animals complemented with various transgenes. Neither PLP nor DM20 protein isoforms could be detected in knockout mice at 20 days of age.

3.4.1.2.2 Immunostaining

No PLP/DM20 immunoreactivity could be identified in knockout mice at 20 days of age although the myelin of knockout mice did immunostain for other myelin specific proteins such as MBP (Figure 14, page 84).

a)



b)

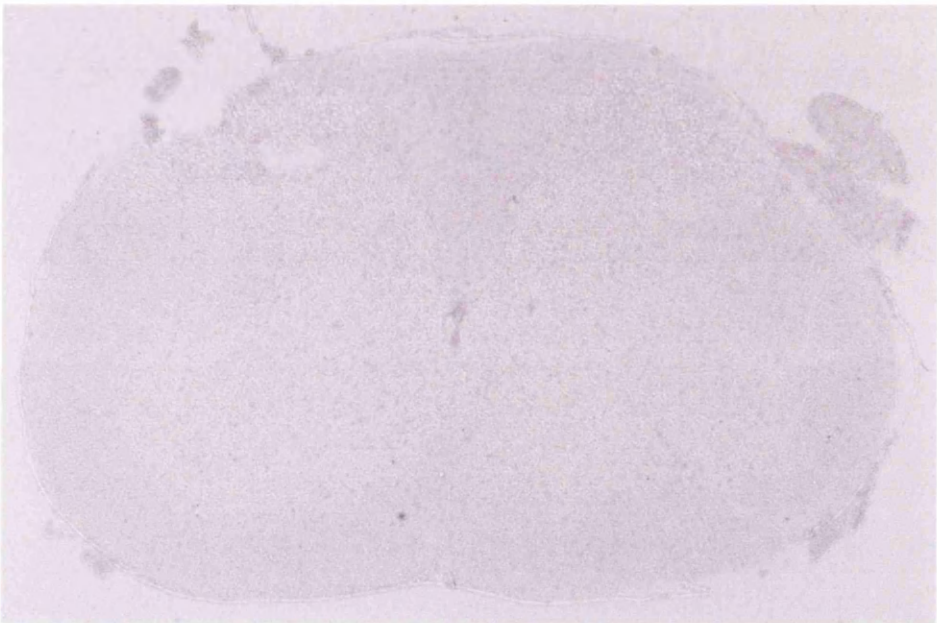


Figure 13 *In situ* hybridisation using a digoxigenin labelled antisense-*Plp* riboprobe on 15 μ m sections of spinal cord (C2-3) from a) wild type and b) knockout mice at 20 days of age. Strong hybridisation signal was detected predominantly throughout the white matter regions of the spinal cord of the wild type mouse. In contrast, no hybridisation signal was detected in the spinal cord section from the knockout mouse indicating that the *Plp* gene was transcriptionally inactive. (50x magnification)

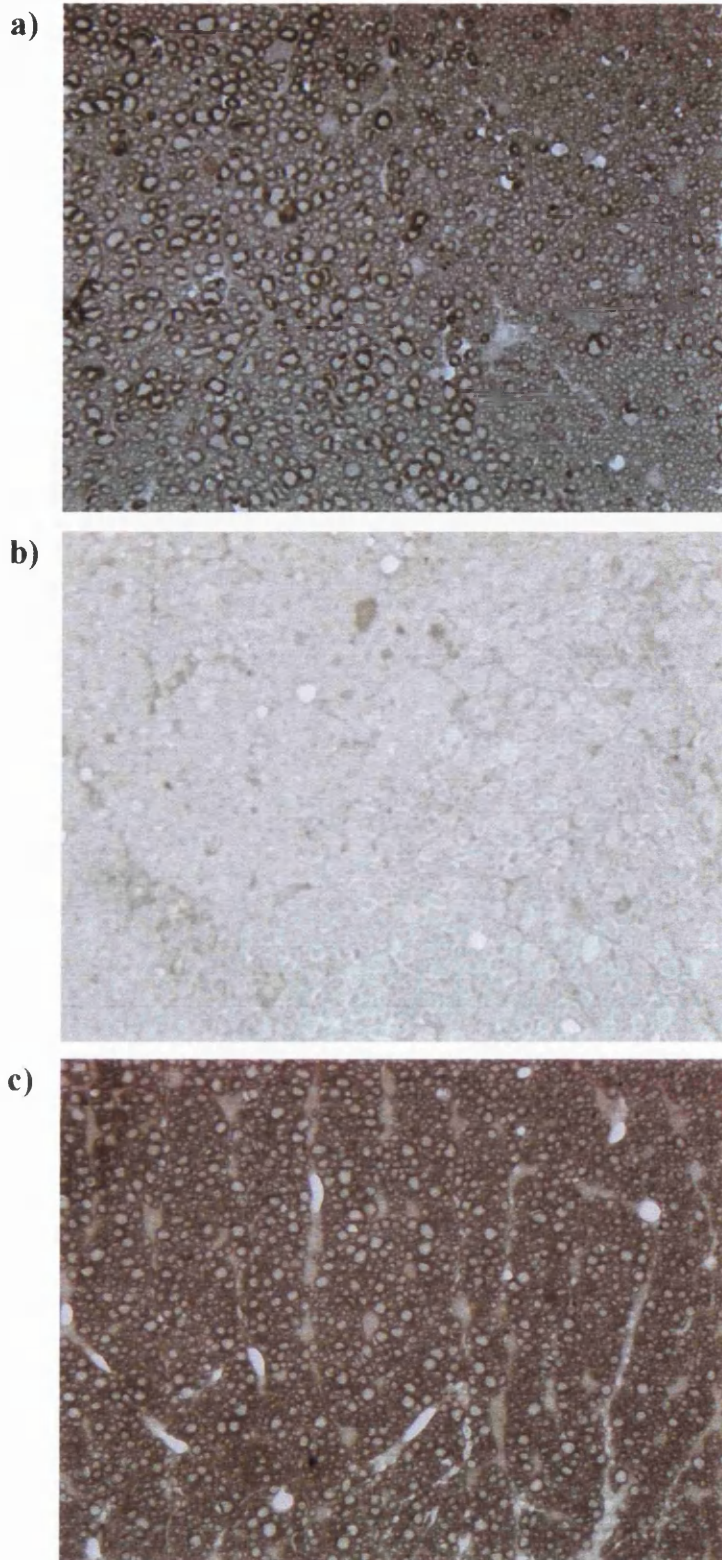
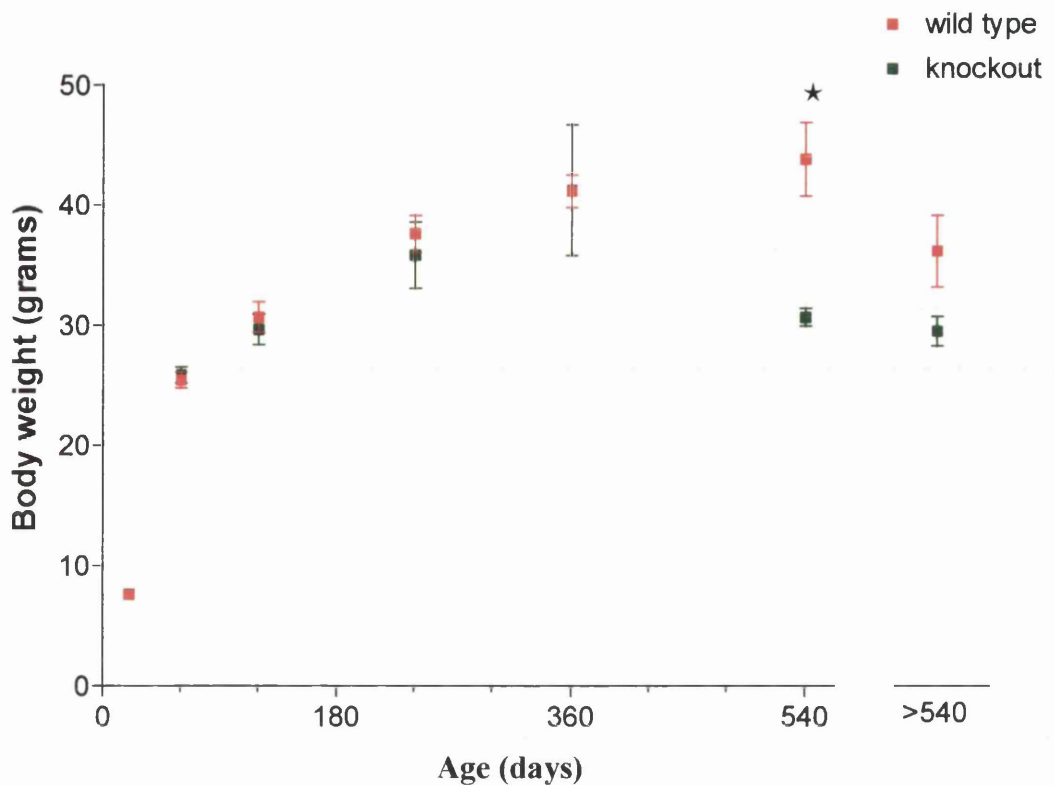


Figure 14 Dorsal columns of spinal cord (C2-3) from 120 day-old wild type and knockout mice immunostained for (a and b) PLP/DM20 and (c) MBP
 a) Wild type mice demonstrated PLP/DM20 immunoreactivity localised to myelin sheaths throughout the section. b) PLP/DM20 immunoreactivity could not be detected in knockout mice although large volumes of myelin formed and immunostained for myelin markers such as MBP (c) (412x magnification)

3.4.2 Clinical phenotype of the *Plp* gene knockout mouse

The knockout mice appeared to develop normally maintaining their body weights (Figure 15, page 86) and reaching reproductive ages without showing evidence of neurological dysfunction. However, aged mice developed a progressive clinical phenotype characterised by paresis, urinary incontinence, poor grip and weight loss. Most knockout mice remained clinically indistinguishable from controls until 15 to 18 months of age. However, some mice showed signs of disease from as early as 12 months of age while a small number did not develop a phenotype until they were over 20 months of age. The oldest knockout mouse recorded reached 670 days before being culled because of neurological dysfunction. No difference in age of onset or progression of signs was noted between male and female mice.

The first signs of neurological dysfunction were perineal urine staining and poor grip. Male mice quickly developed priapism but otherwise both sexes remained stable for 3 to 6 weeks. Subsequently, the mice showed rapid progression of other signs and deteriorated over a further 4 to 5 week period before euthanasia was necessary. They developed progressive paresis, muscle atrophy and weight loss. Although the changes were widespread, muscle wastage and paresis were most obvious affecting the hindlimbs. When encouraged to walk along a narrow ledge, affected mice developed a marked shake and generally fell off. Control animals were capable of walking along the ledge and showed only mild instability. Affected mice made no attempt to grasp the cage bars with their hindlimbs and could not retain their forelimb grip when gentle traction was applied. Wild type mice maintained strong forelimb and hindlimb grips even when the surface that they were holding onto was inverted. Severely affected mice made little attempt to walk tending to move backwards or to turn on their rumps in a tight circle when trying to move. Some of the more advanced cases showed evidence of faecal incontinence with large amounts of impacted faeces in the anus and externally caking the perineum. Weight loss and general debility progressed until euthanasia was necessary. The mice did not develop seizures or gross tremors, both common features of other *Plp* gene mutants.



Age	Wild type			Knockout		
	mean	SEM	n	mean	SEM	n
20	7.6	0.133	7	7.6	0.113	7
60	25.5	0.675	16	25.9	0.681	8
120	31.6	1.191	9	29.7	0.972	8
240	39.5	1.206	5	35.8	2.745	7
360	41.2	1.358	13	41.2	5.456	5
540	43.9	3.053	8	30.7	0.761	15
>540	36.2	2.987	7	29.5	1.232	14

Figure 15 Grouped data from body weight measurements of male knockout and wild type mice taken at culling (mean body weight plotted with SEM)

Knockout mice maintained normal body weights to 360 days of age. By 540 days of age, the knockout mice had significantly reduced body weights (* equals $P=0.0003$ at 540 days of age). From grouped data of mice greater than 540 days of age (range 550 to 720 days), the body weights of wild type mice fell and the difference between wild type and knockout mice became less dramatic ($P=0.0524$)

3.4.3 Pathological description of the CNS changes in the *Plp* gene knockout mouse

3.4.3.1 Gross pathology findings

The most severely affected knockout mice had little muscle bulk and no subcutaneous fat reserves at *post mortem*. The urinary bladder was distended suggesting that perineal urine staining resulted from defective bladder emptying with urinary overflow. Knockout animals culled before developing neurological dysfunction were grossly normal at *post mortem*.

3.4.3.2 Overview of histopathological findings

The knockout mice developed well myelinated central white matter tracts by 20 days of age (Figure 16, page 89). Myelin sheaths were of an appropriate thickness for the size of axon, glial cell densities appeared normal and there was no evidence of demyelination. However, the myelin sheaths of the knockout mice were more irregular than in control animals and electron microscopy confirmed that they were poorly compacted (Figure 17, page 90).

As the animals aged, evidence of axonal pathology developed (see 3.4.3.4 *Axonal changes and fibre degeneration*, page 99). Occasional swollen axons and degenerate fibres were established by 60 days of age and these changes became progressively more prominent (Figure 18, page 91 and Figure 20, page 93). Initially, the lesions showed tract specificity predominantly developing in the small diameter (late myelinating) areas such as the optic nerve, the corticospinal tracts and the fasciculus gracilis (Figure 19, page 92). Changes were prominent in these areas at 120 days of age but steadily progressed to affect all white matter regions. Swollen and degenerate fibres began to appear in the ventral and lateral columns and swollen axons could occasionally be found in the myelinated fibres of the grey matter (Figure 21, page 94). The majority of swollen axons and all identified degenerate axons were surrounded by myelin membranes. Sheaths associated with larger swellings were often attenuated but could be visualised on electron microscopy (Figure 30, page 105). Occasional swellings were identified that had no associated myelin sheath but swollen axons were not identified in non-myelinated areas of the CNS (see 3.4.3.4.2 *The lamina cribrosa*, page 99).

A generalised progressive gliosis developed throughout the white matter tracts from 120 days of age. Increased cell densities were most obvious in areas that showed prominent axonal changes and microglia appeared to be the predominant cell type (Figure 19, page 92). Although the axonal and glial cell changes became extensive

as the animals aged, no evidence of demyelination was seen. Some aged mice (greater than 540 days) developed vacuolation and splitting of the myelin sheaths (Figure 22, page 95).

Dorsal root ganglion and retinal ganglion neurones project axons into the fasciculus gracilis and optic nerve respectively, the areas most severely affected by the knockout axonopathy. These neurones and other neurones throughout the CNS were examined to establish if they were affected by neurodegenerative changes. Although no attempt was made to quantify the neurones, no evidence of neuronal degeneration or death was found.

Wild type animals remained essentially normal throughout their life-span (greater than 2 years of age). They did develop some CNS changes characteristic of ageing, most notably occasional 'dystrophic' axonal swellings. These swellings contained excessive volumes of axoplasmic reticulum and were easily distinguished from the knockout-associated axonal changes because of their homogeneous appearance, ultrastructural features and low numbers.

3.4.3.3 Glial cell changes

Corrected total and differential glial cell densities and counts were calculated from nuclear profiles. Immunostaining and *in situ* hybridisation were used to confirm these findings.

3.4.3.3.1 Corrected total glial cell densities and numbers

Total corrected glial cell densities were calculated from sections of mid optic nerve and ventral columns of spinal cord (C2-3). At 20 and 60 days of age, no difference between knockout and control animals was seen. By 120 days of age, a significant gliosis ($P=0.022$) had developed in both areas confirming the subjective identification of increased glial cell numbers on light microscopy (Figure 23, page 96). The spinal cord and optic nerve areas were equivalent between knockout and wild type mice at each age and the total corrected glial cell counts reflected similar findings.

3.4.3.3.2 Corrected differential glial cell densities

Corrected differential cell densities revealed that normal oligodendrocyte densities were maintained in the knockout mice at least until 120 days of age (Figure 24A, page 97). Microglial cells accounted for the increasing cell densities ($P=0.0095$ at 120 days) (Figure 24B, page 98). The temporal and spatial association between increasing cell density and developing axonal pathology suggested that the two processes were linked.

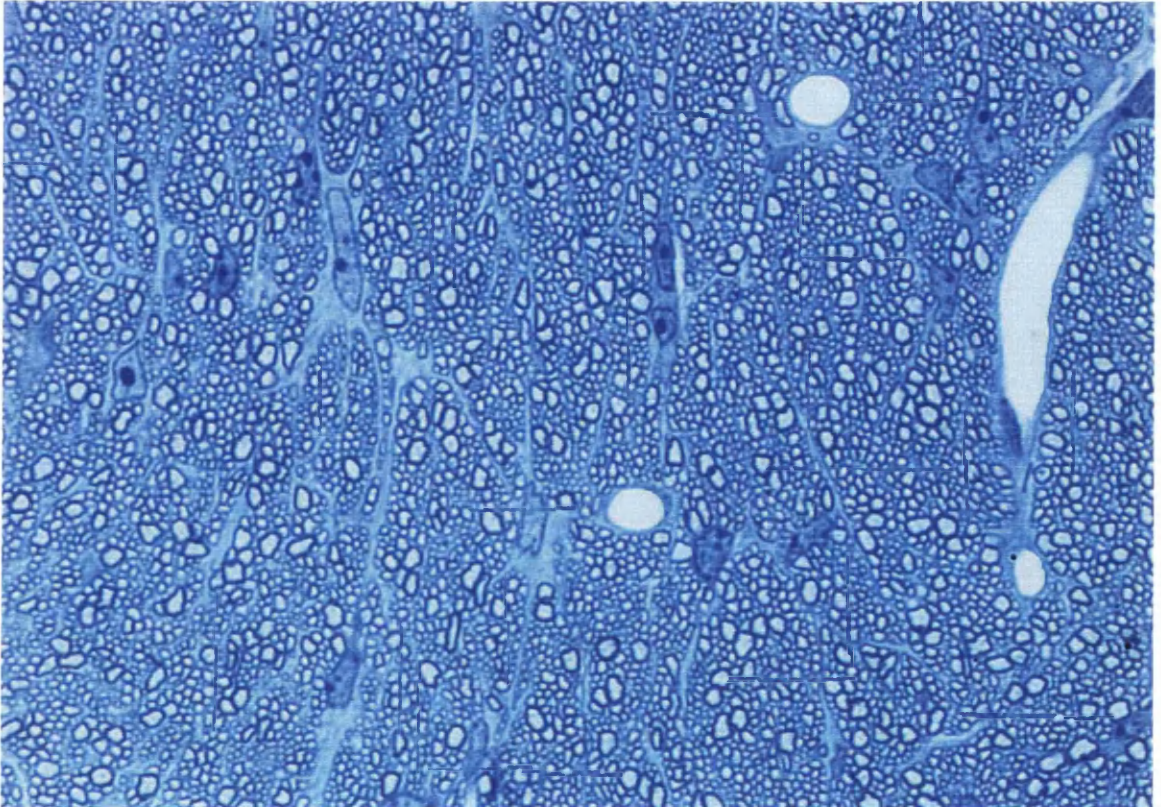


Figure 16 Methylene blue/ azur II stained 1µm resin section of mid optic nerve from a 20 day-old knockout mouse. The optic nerve was well myelinated with no gross evidence of myelin or glial abnormalities. (1300x magnification)

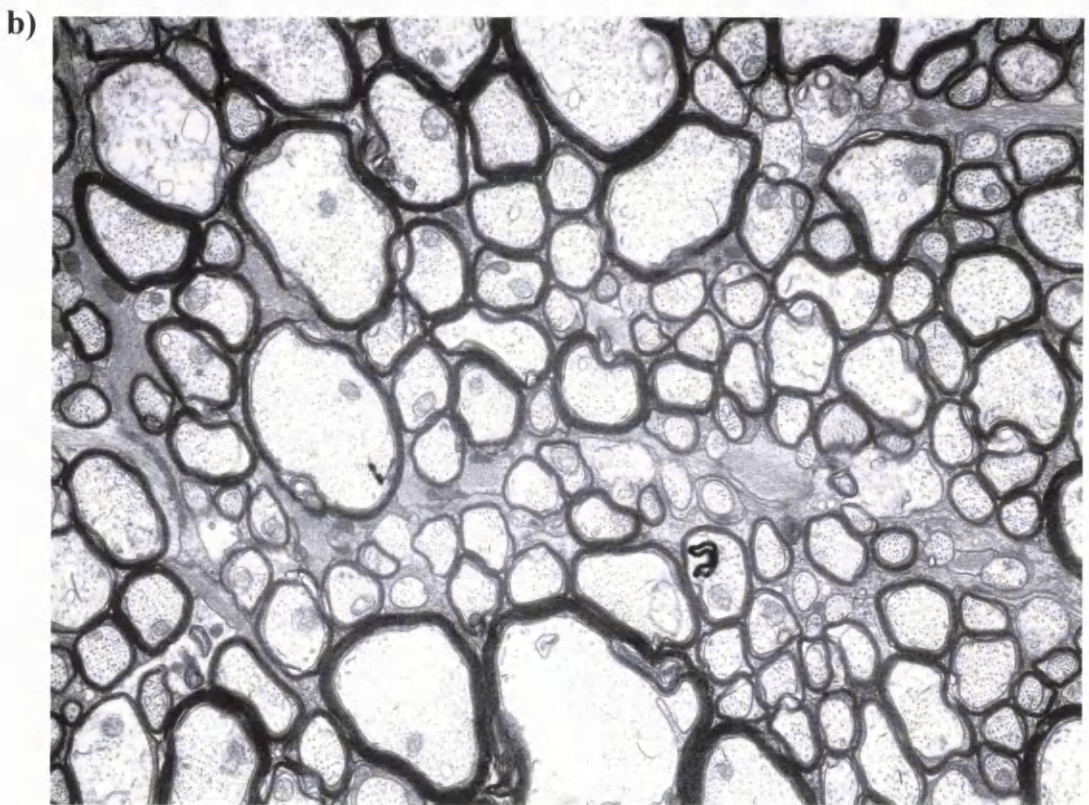
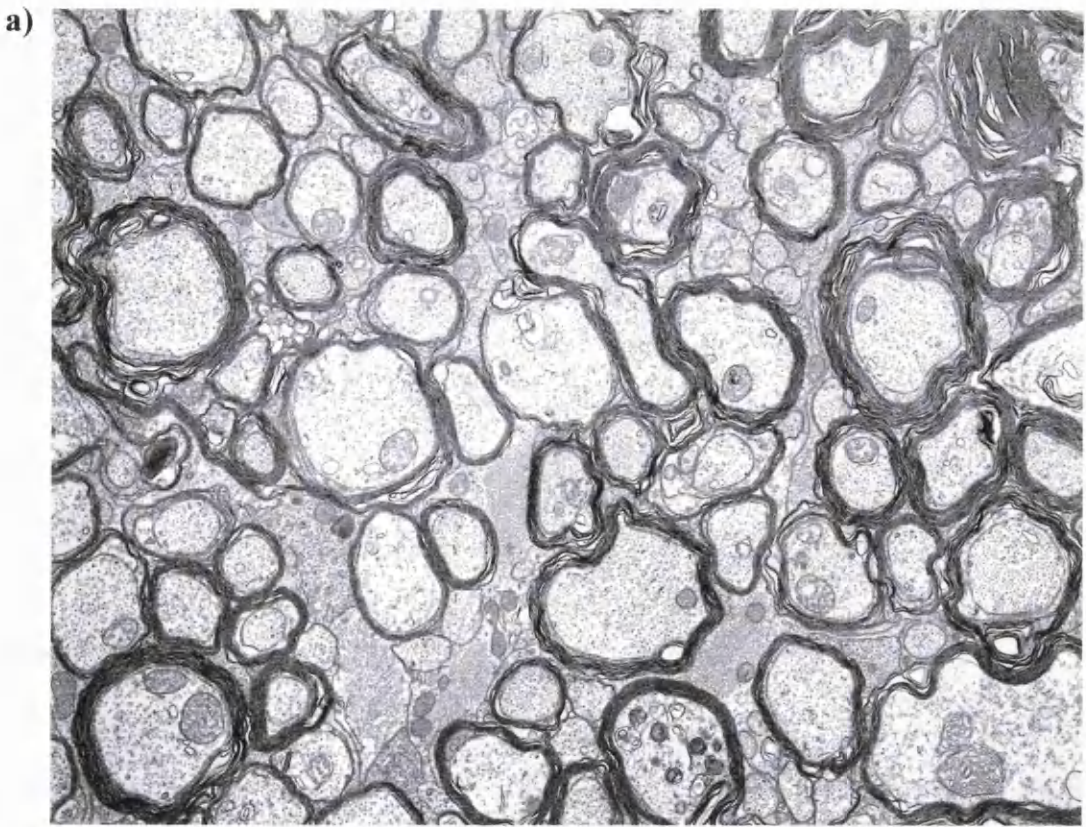


Figure 17 Myelinated fibres in the optic nerve of a) knockout and b) wild type mice at 120 days of age. The level of myelin compaction varied greatly between individual fibres in the knockout mouse. However, in general, myelin sheaths in the knockout mouse were poorly compacted on comparison with controls.

(10,000x magnification)

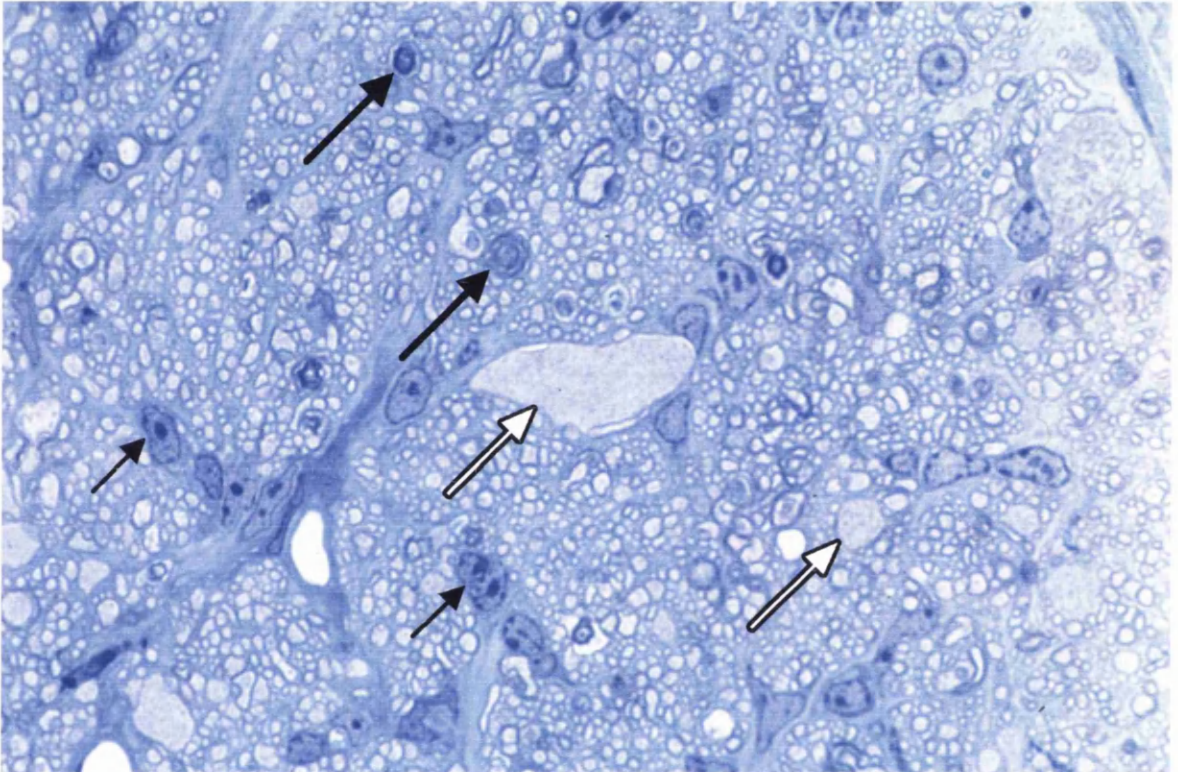
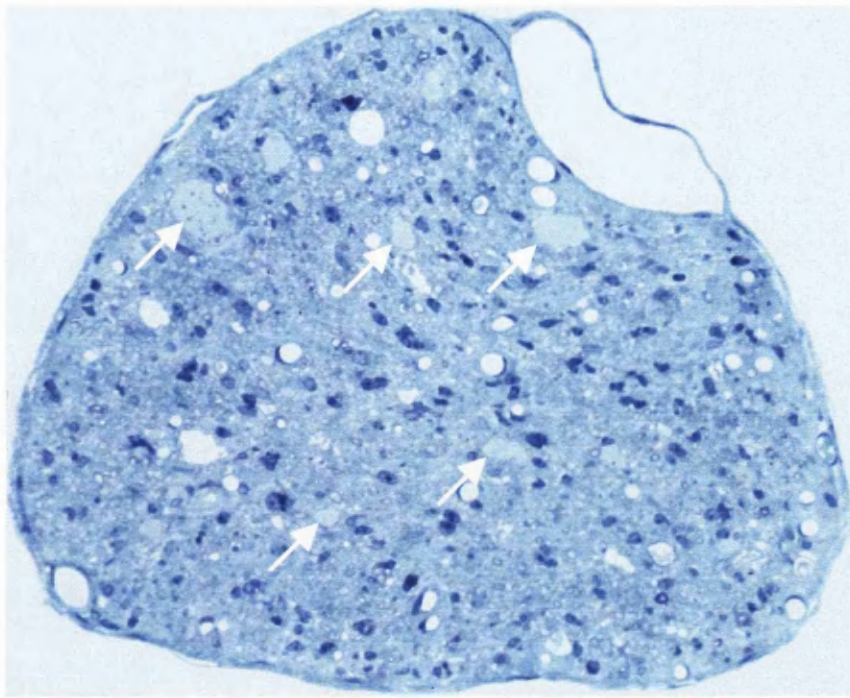


Figure 18 Methylene blue/ azur II stained 1µm resin section from mid optic nerve of a 360 day-old knockout mouse demonstrated swollen axons (open arrows) and degenerate fibres (closed large arrows). Numerous microglia (closed small arrows) were identified as darkly stained nuclei with condensed chromatin patterns (1000 magnification)

a)



b)

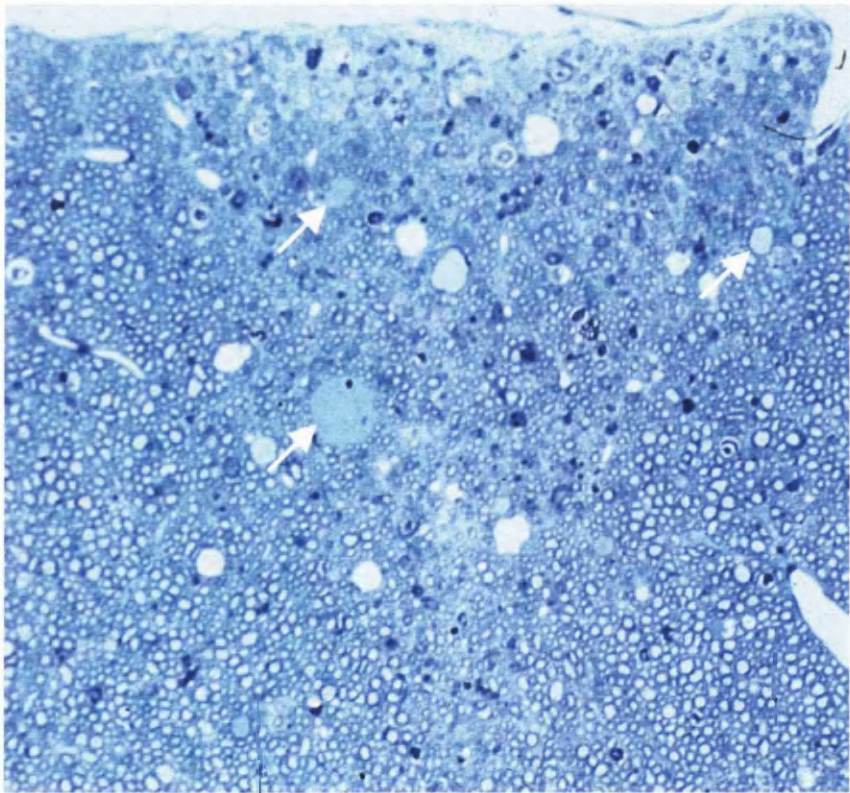
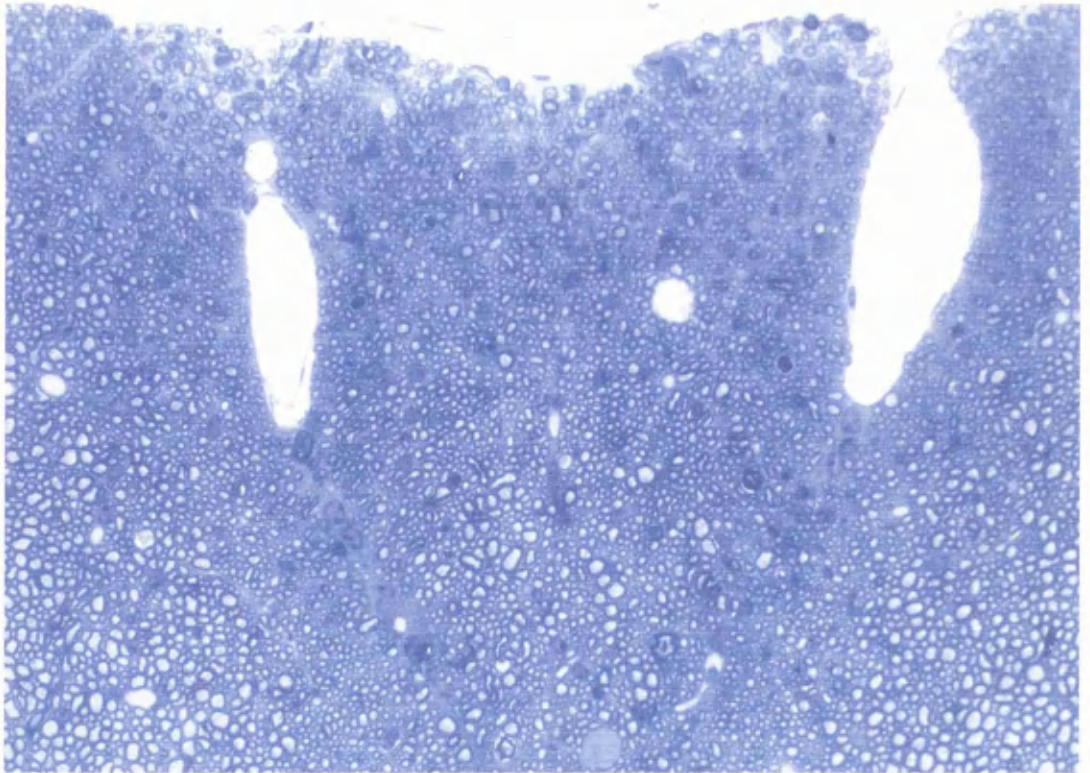


Figure 19 Methylene blue/ azur II stained $1\mu\text{m}$ resin sections from a 640 day old knockout mouse: a) mid optic nerve with numerous large axonal swellings (arrows), b) dorsal columns of cervical spinal cord (C2-3) showing axonal swelling, predominantly in the fasciculus gracilis (arrows) (360x magnification)

a)



b)

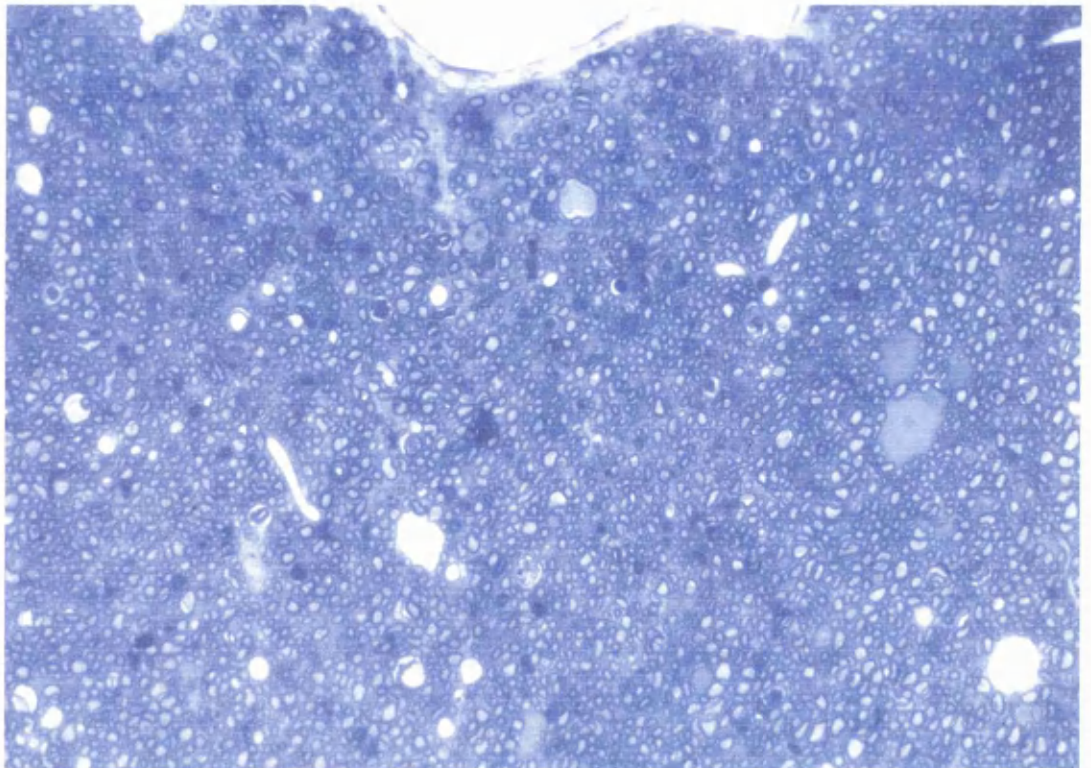


Figure 20 Methylene blue/ azur II stained 1 μ m resin sections of spinal cord (C2-3) showing progression of neurodegenerative changes in the fasciculus gracilis of knockout mice between a) 360 days of age and b) 670 days of age (375x magnification)

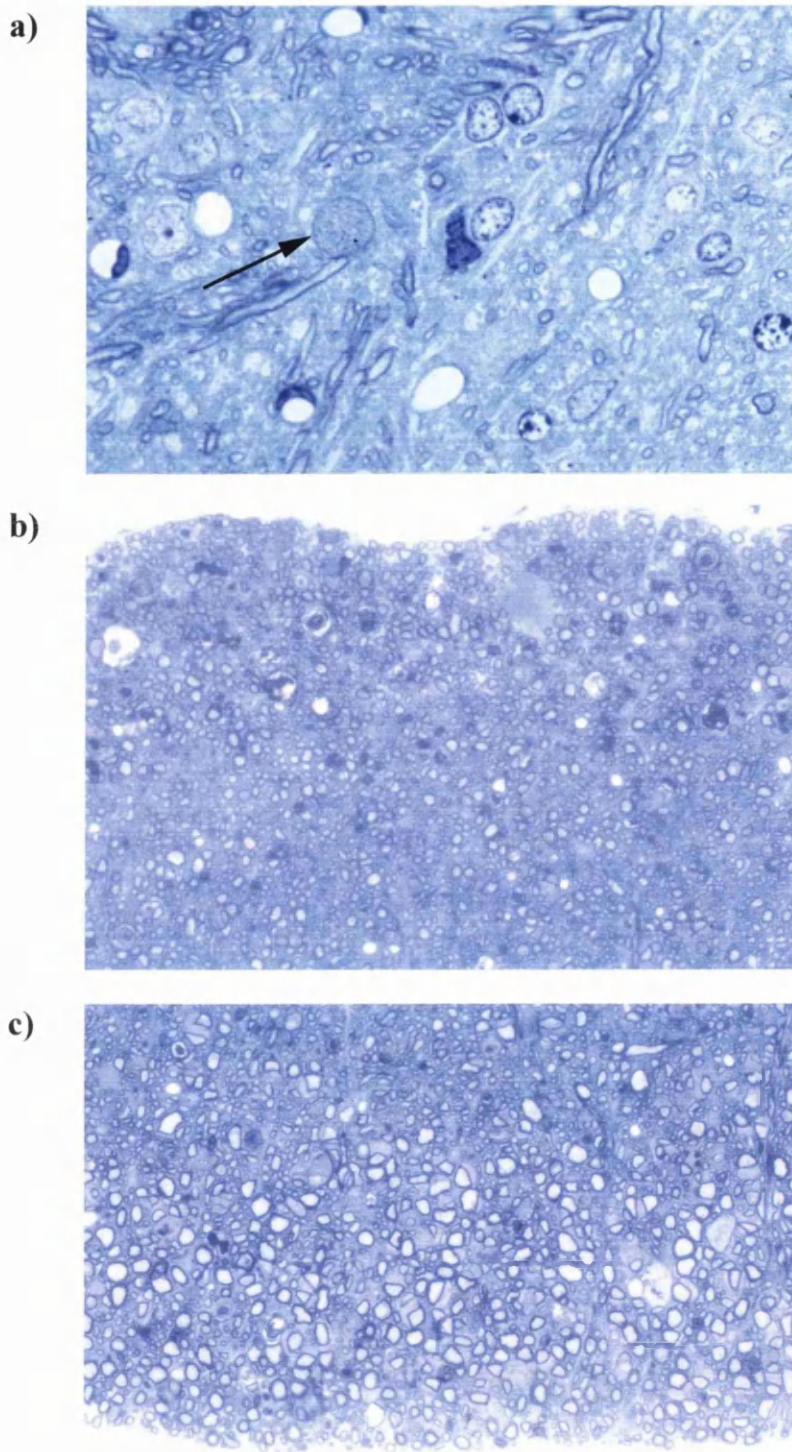


Figure 21 Methylene blue/ azur II stained 1 μ m resin sections from an aged knockout mouse demonstrating widespread neurodegenerative changes in spinal cord (C2-3): a) swollen axon of a myelinated fibre (arrow) in the gray matter (750x magnification); b) neurodegeneration affecting the lateral columns (300x magnification); c) neurodegeneration affecting the ventral columns (300x magnification)

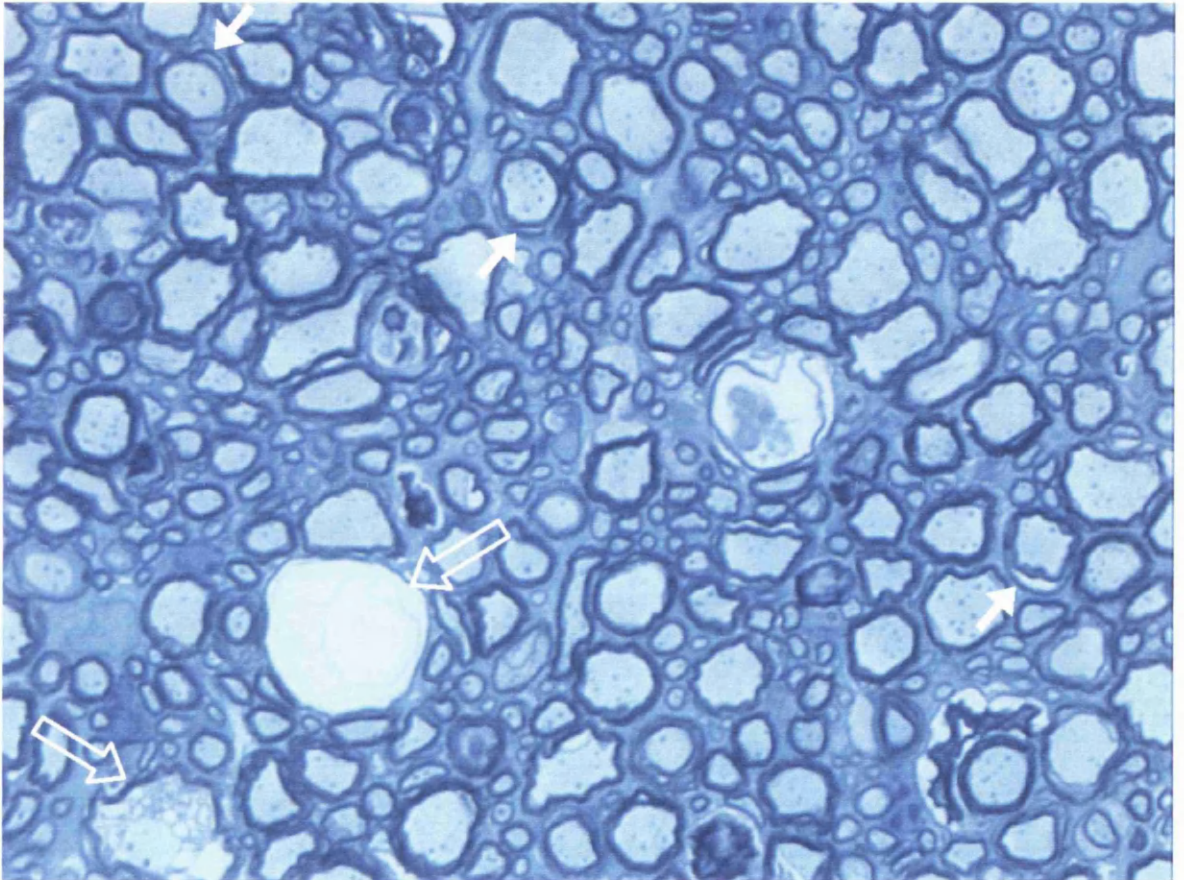


Figure 22 Methylene blue/ azur II stained 1 μ m resin section of ventral columns of spinal cord (C2-3) from a 600 day-old knockout mouse showing vacuolation (open arrows) and splitting (closed arrows) of myelin sheaths (1300x magnification)

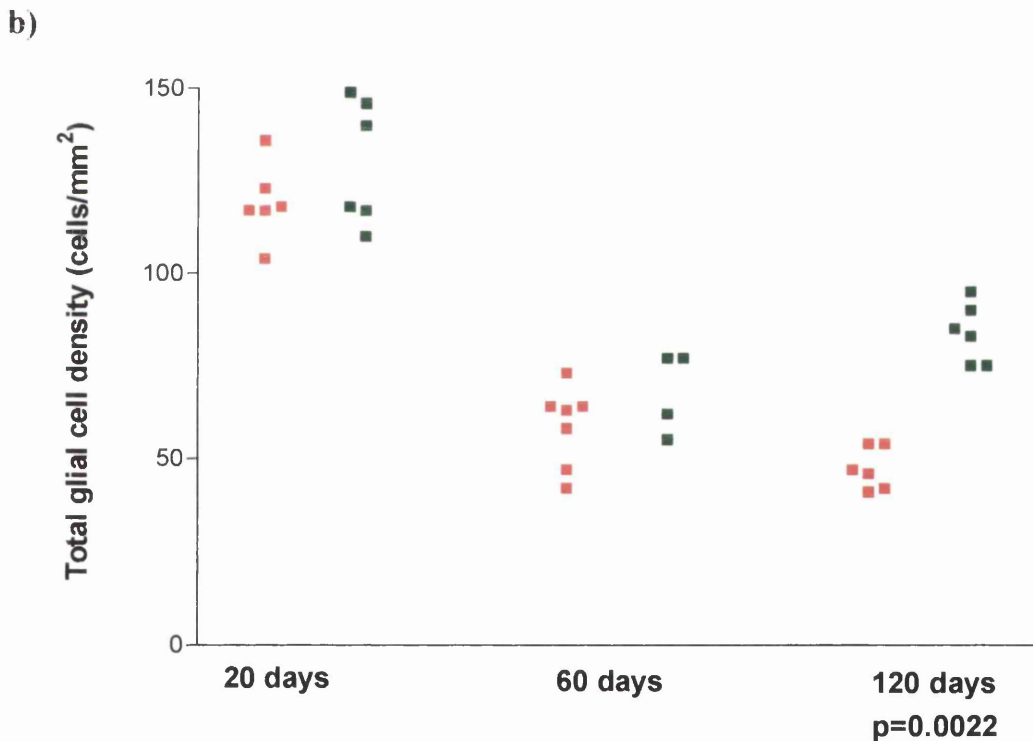
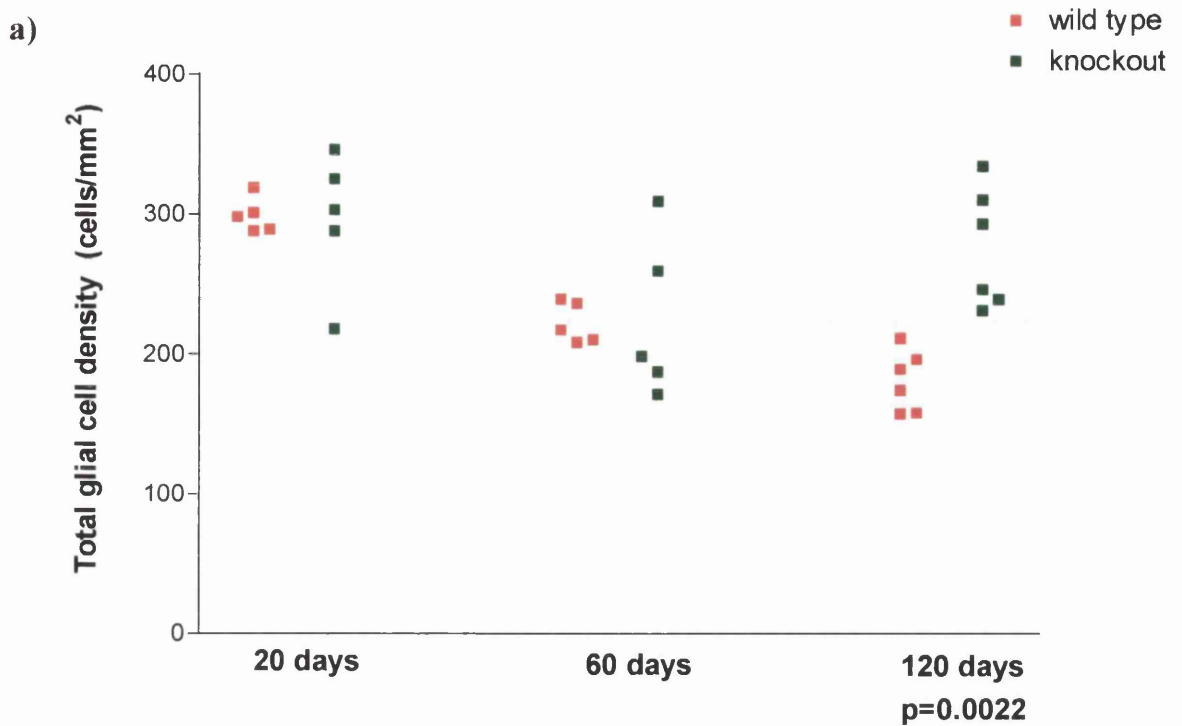


Figure 23 Corrected total cell densities in a) mid optic nerve and b) ventral columns of spinal cord (C2-3) of knockout and wild type mice at 20, 60 and 120 days of age. A significant increase in total corrected cell densities was seen in the knockout mouse at 120 days of age in both areas.

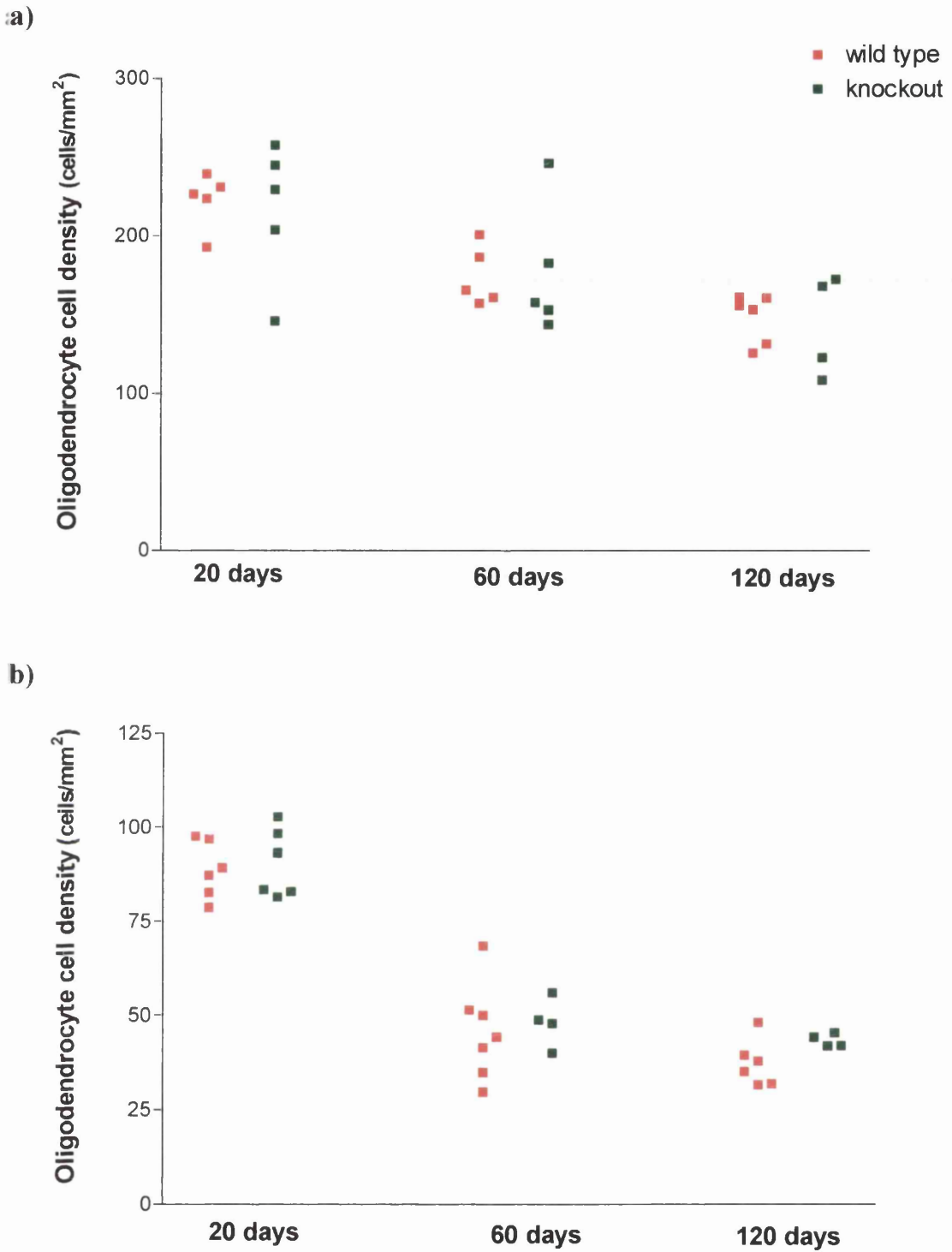


Figure 24A Corrected oligodendrocyte cell densities in a) mid optic nerve and b) ventral columns of spinal cord (C2-3) of knockout and wild type mice at 20, 60 and 120 days of age. No difference in oligodendrocyte numbers was seen at any age between the two groups cont./

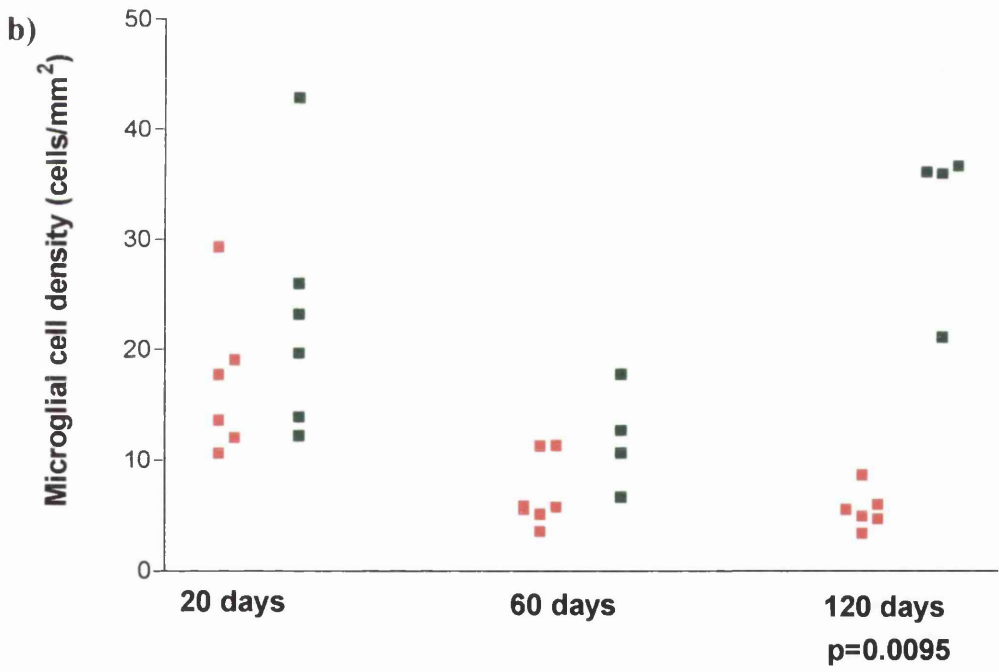
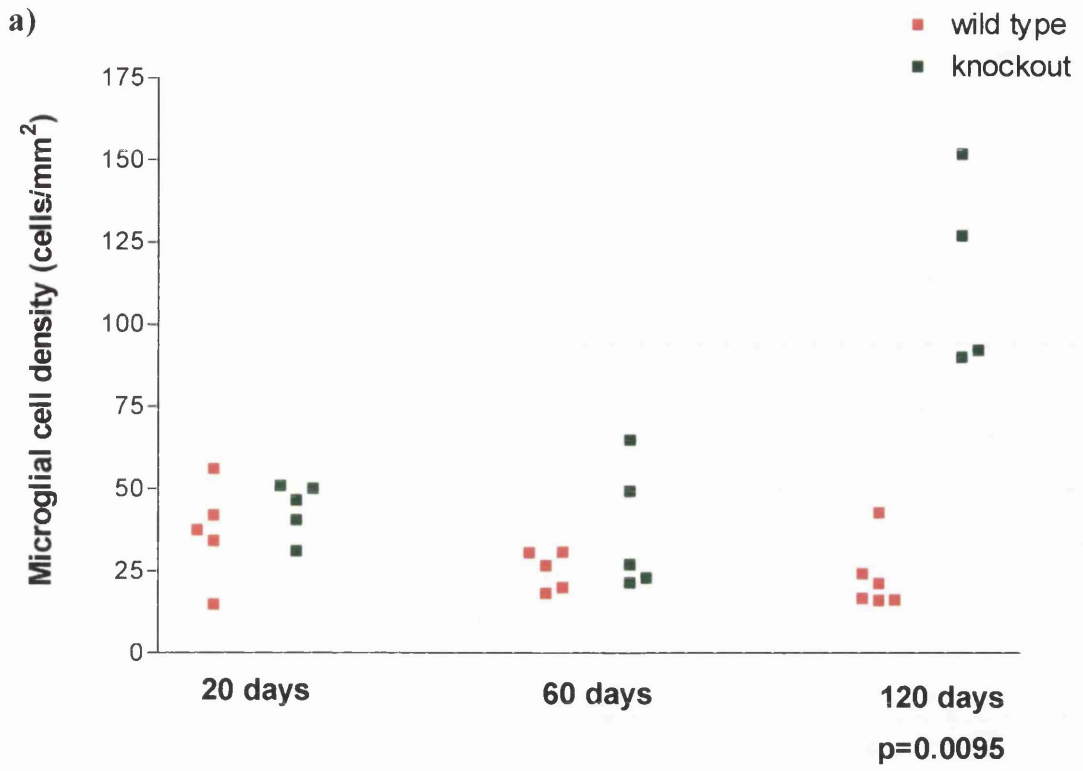


Figure 24B Corrected microglial cell densities in a) mid optic nerve and b) ventral columns of spinal cord (C2-3) of knockout and wild type mice at 20, 60 and 120 days of age. A microgliosis could be shown statistically in both areas in 120 day old knockout mice.

3.4.3.3.3 Confirmation of glial cell morphometry

3.4.3.3.3.1 *In situ* hybridisation

In situ hybridisation using anti-sense *Mog*-riboprobes confirmed that knockout and wild type animals had equivalent numbers of oligodendrocytes in the cervical cord at 20 days of age (Figure 25, page 100).

3.4.3.3.3.2 Immunostaining

CAII immunostaining showed that oligodendrocyte numbers were maintained in knockout mice (Figure 26, page 101) and F4/80 immunostaining demonstrated that a microgliosis developed most prominently in regions containing small diameter fibres (Figure 27, page 102). Although astrocyte cell numbers were normal in these animals, a moderate increase in GFAP staining suggested a degree of astrocyte hypertrophy (Figure 28, page 103).

3.4.3.4 Axonal changes and fibre degeneration

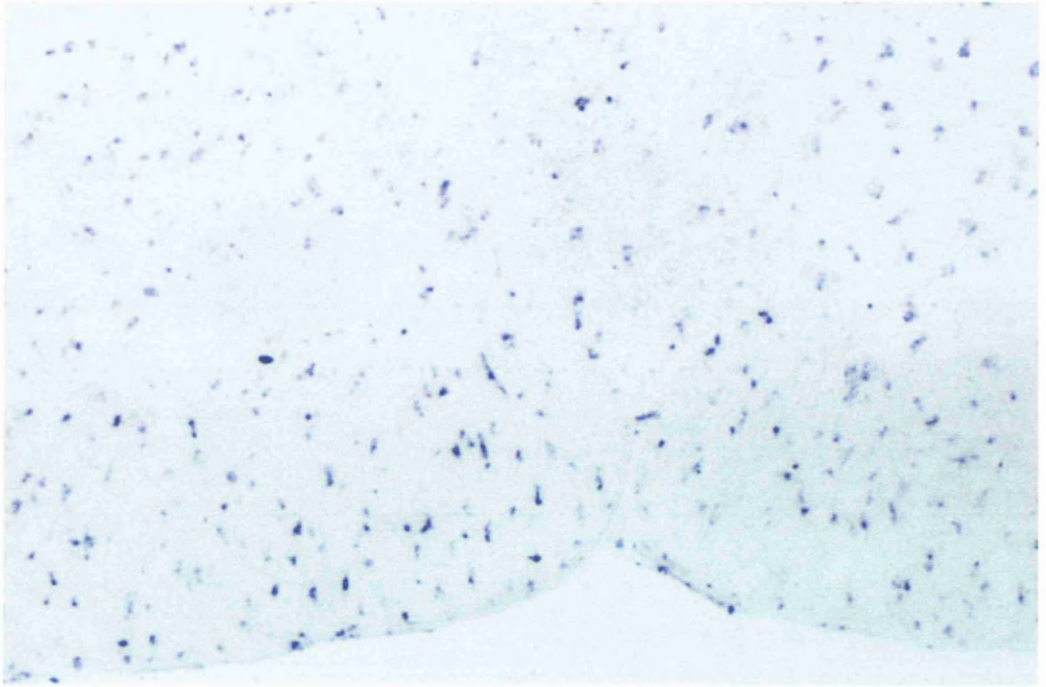
3.4.3.4.1 Ultrastructural features

Swollen axons contained increased numbers of organelles and could be divided into two populations (Figure 29, page 104 and Figure 30, page 105). In younger animals, swellings contained large numbers of dense bodies and mitochondria that appeared to develop at the distal paranode initially. This opinion was based on longitudinal sections of optic nerve in which the majority of axons have their cell bodies in the retina and the term 'distal' reflects the location of the paranode relative to the perikaryon. In older animals, larger swellings contained predominantly neurofilaments located in internodal regions. Degenerate fibres generally had amorphous centres surrounded by degenerating myelin sheaths. Occasionally remnants of axoplasmic organelles could be seen that resembled dense bodies (Figure 31, page 106). No active phagocytosis of myelin debris was seen on either light or electron microscopy.

3.4.3.4.2 The lamina cribrosa

To establish if the axonal changes were isolated to myelinated internodes, sections of the optic nerve in the region of the lamina cribrosa were examined. This region is unusual in the CNS as it is devoid of oligodendrocytes and contains only unmyelinated axons. This allows *in vivo* examination of axons in an oligodendrocyte-deprived environment. As the axons pass from the retinal ganglion cells through this region and into the optic nerve, they acquire myelin sheaths.

a)



b)

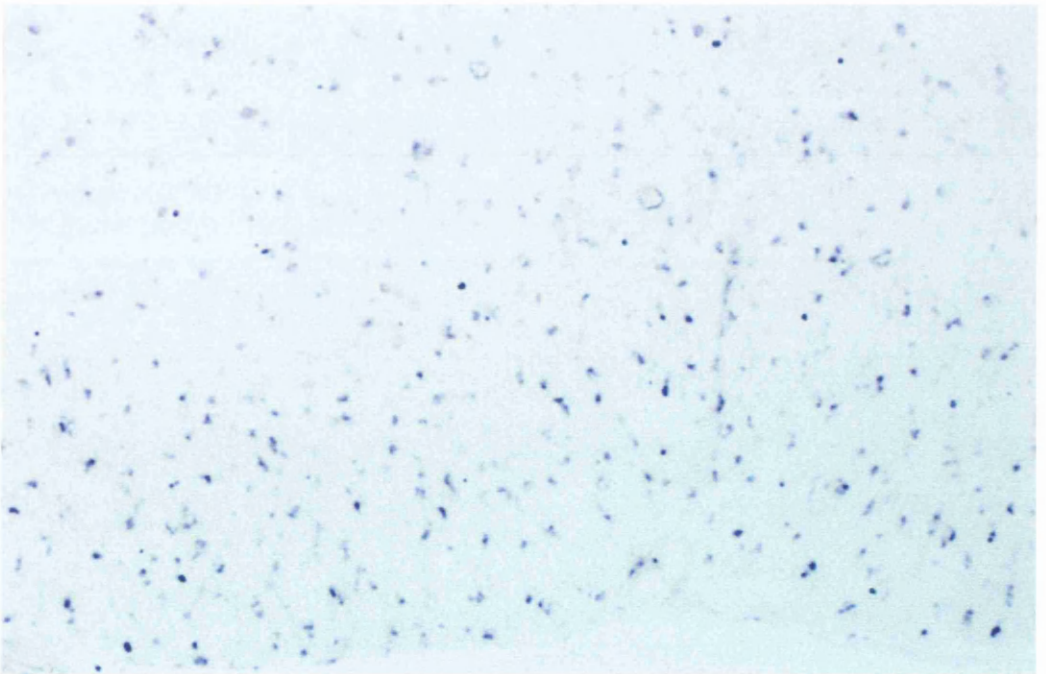
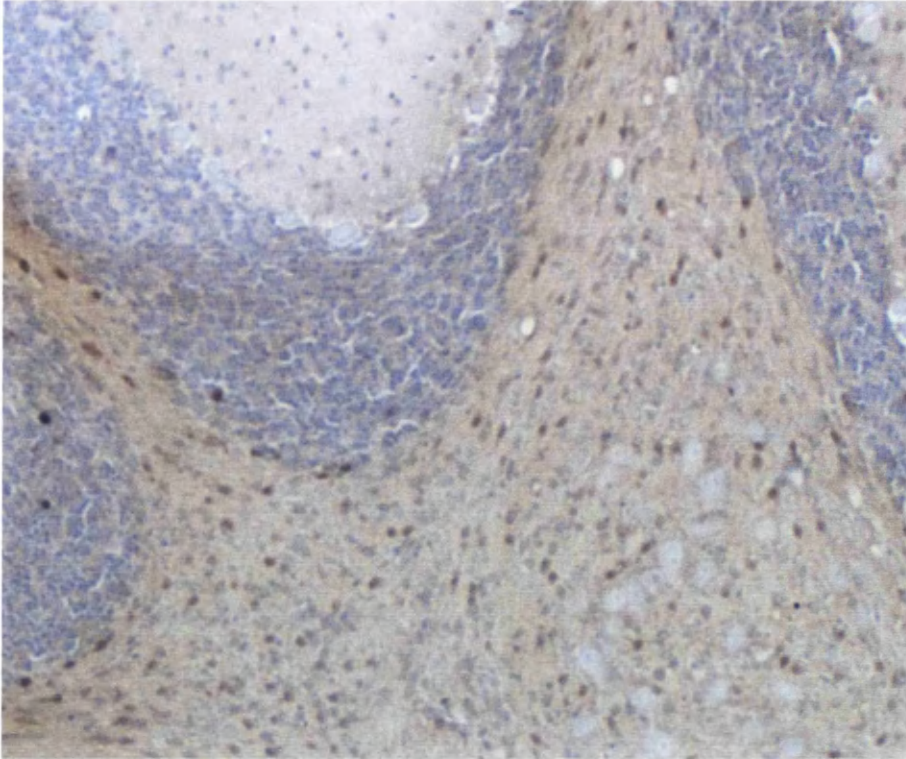


Figure 25 *In situ* hybridisation using digoxigenin-labelled anti-sense *Mog* riboprobes on cryostat sections (15 μ m) of ventral columns of spinal cord (C2-3) from a) wild type and b) knockout mice at 20 days of age. Oligodendrocyte cell densities were equivalent in knockout and wild type mice. (140x magnification)

a)



b)

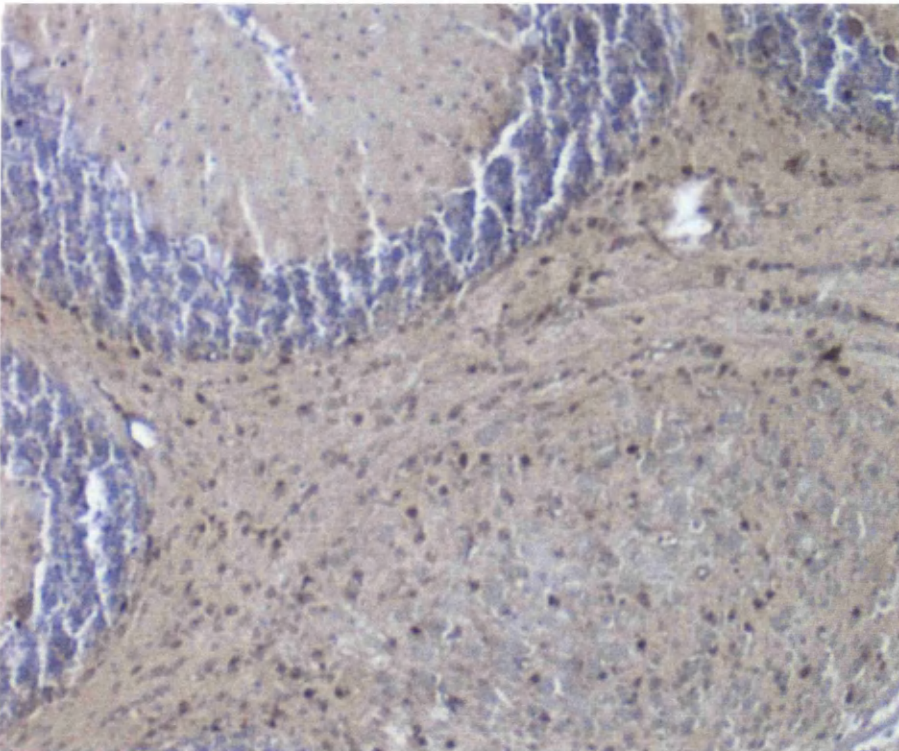


Figure 26 Carbonic anhydrase II immunostaining of oligodendrocyte cell bodies in the cerebellum of 20 day-old wild type (a) and knockout (b) mice. Carbonic anhydrase II positive oligodendrocyte numbers were equivalent between the two mice (270x magnification; haematoxylin counterstain)

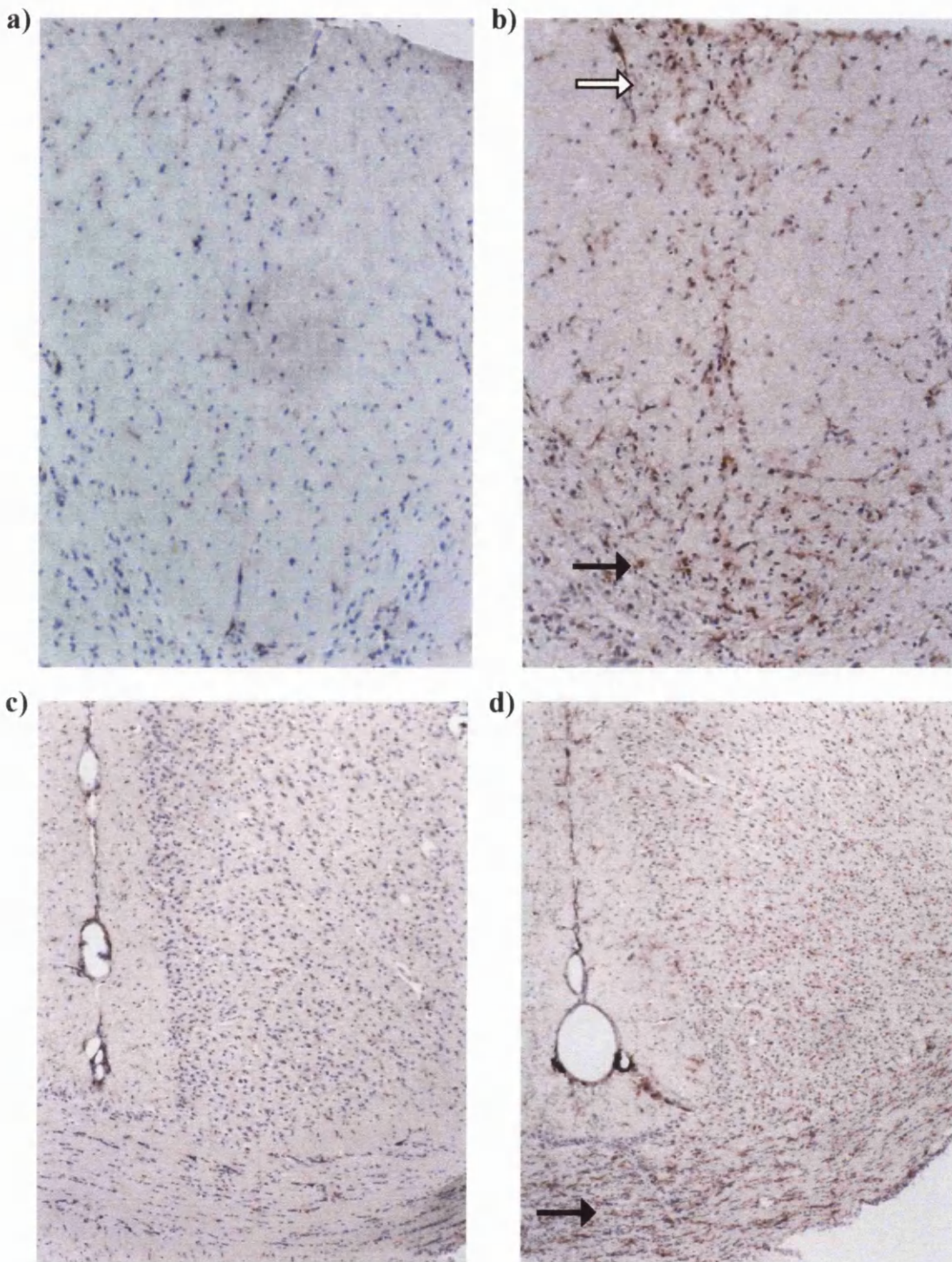


Figure 27 Dorsal columns of cervical spinal cord (a and b; 148x magnification) and corpus callosum and cingulate cortex (c and d; 85x magnification) from aged wild type (a and c) and knockout (b and d) mice immunostained with F4/80. Increased immunostaining was most prominent in the corticospinal tracts (open arrow; b) and fasciculus gracilis (closed arrow; b) in the spinal cord and in the corpus callosum (closed arrow; d) in the knockout mice. A general increase in nuclei indicating a microgliosis was also evident in the knockout mouse.

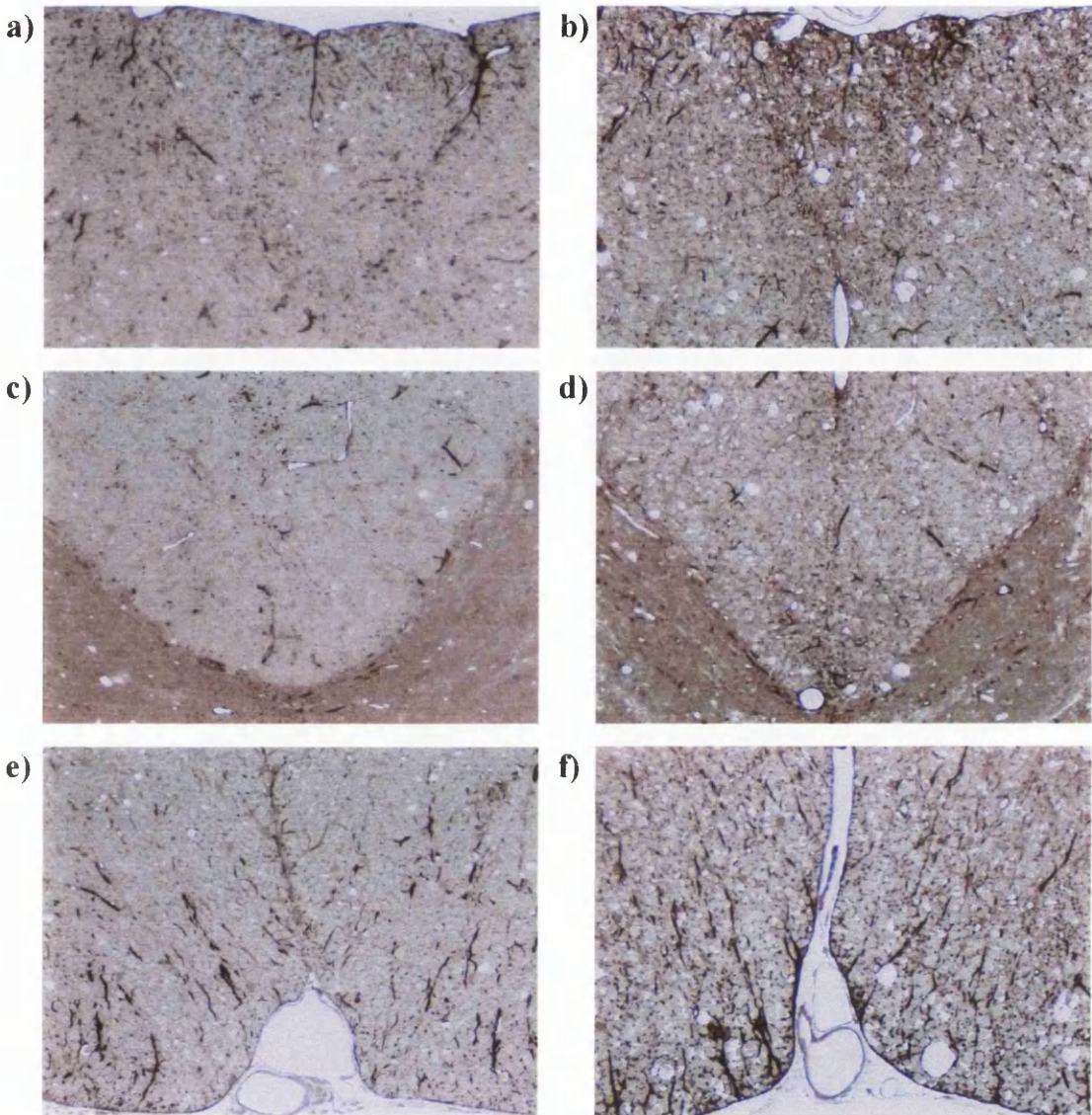


Figure 28 GFAP-immunostained 1 μ m resin sections from wild type (a, c, e) and knockout (b, d, f) mice at ~600 days of age. A slight increase in staining in the fasciculus gracilis (a, b) and corticospinal tracts (c, d) in knockout mice is partly masked by myelin vacuolation. A moderate increase in immunostaining is apparent in the ventral columns of spinal cord (C2-3) in knockout mice (e, f) (145x magnification)

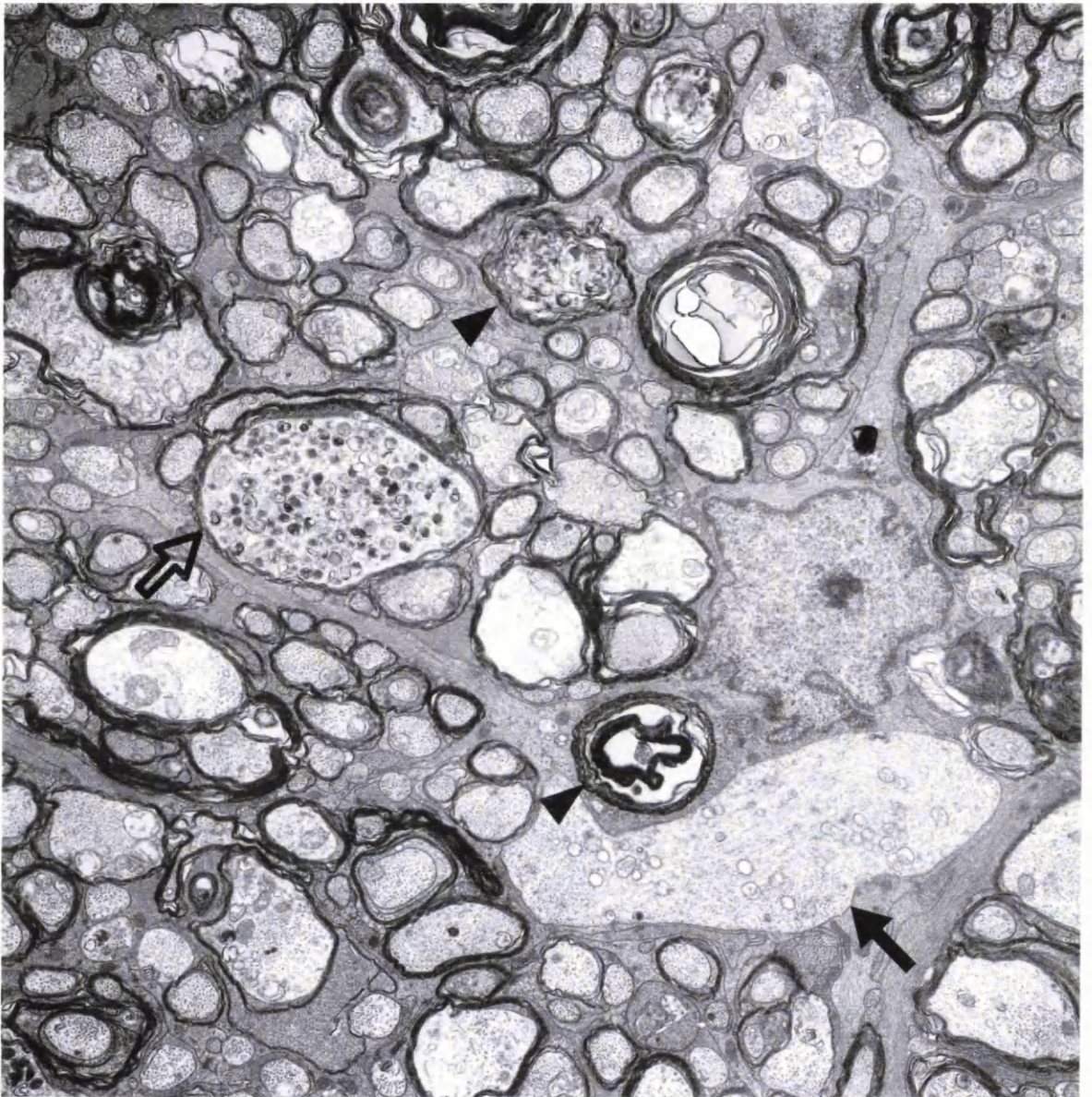
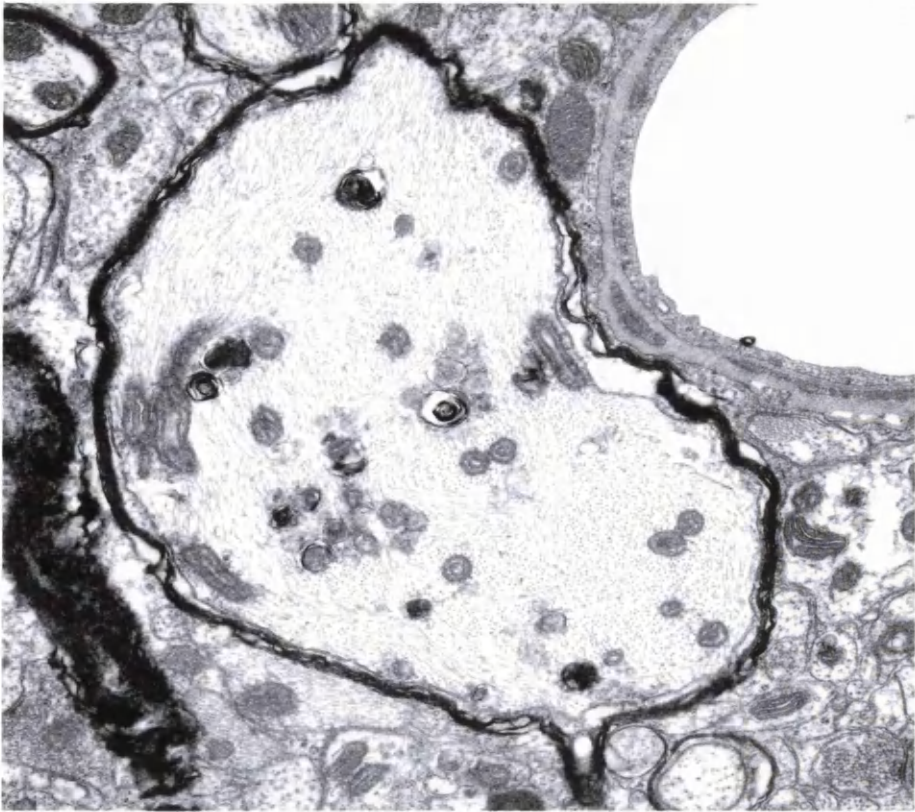


Figure 29 Electron micrograph showing axonal lesions in the optic nerve of a 360 day-old knockout mouse. Axonal pathology included swollen axons containing dense bodies (open arrow) and neurofilaments (closed arrow) and degenerating fibres and their remnants (arrow heads) (8000x magnification)

a)



b)

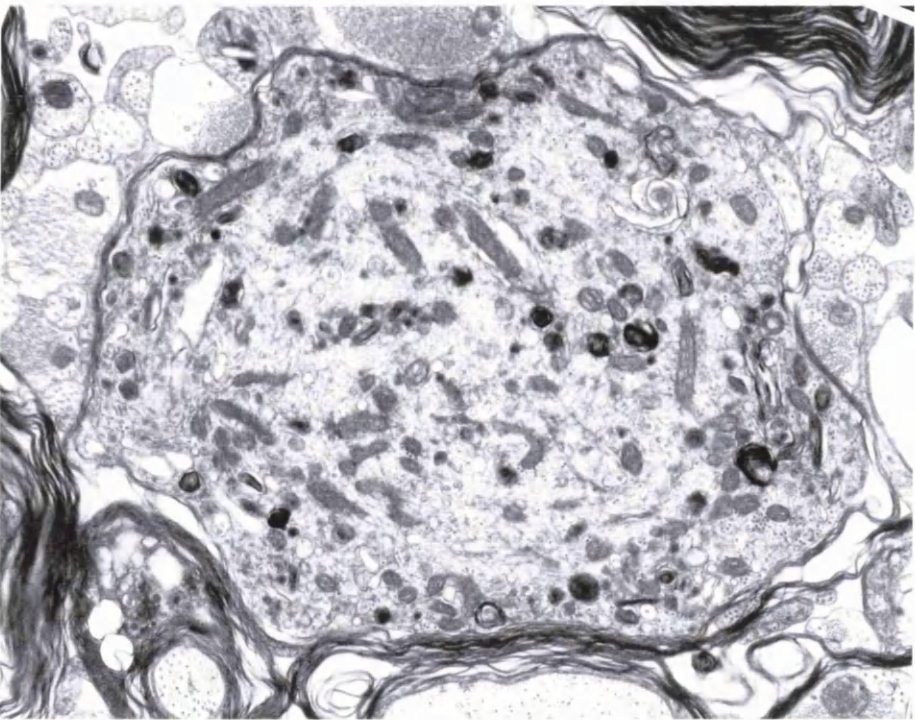


Figure 30 Axonal swellings in knockout mice (20,000x magnification)

a) Myelinated swollen axon containing predominantly neurofilaments and some membrane bound organelles (360 days of age; ventral columns of thoracic cord)

b) Swollen axon containing mitochondria, dense bodies and cytoskeletal elements; an attenuated myelin sheath surrounds this swollen axon (160 days of age; mid optic nerve)

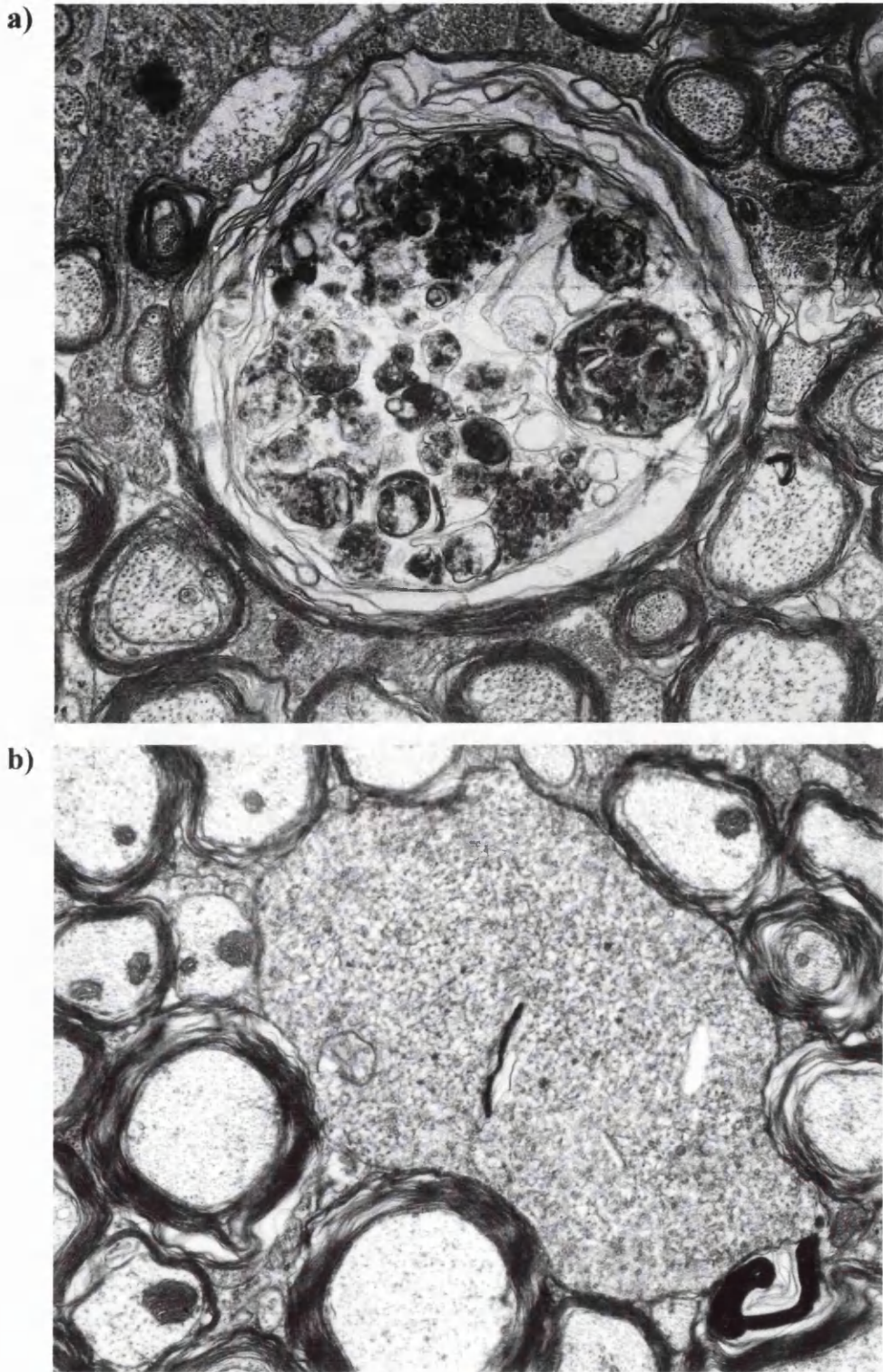


Figure 31 Electron micrographs of degenerate and dystrophic axons in knockout mice (20,000x magnification)

a) Degenerating myelinated fibre containing remnants of membrane bound organelles (160 days of age; mid optic nerve)

b) Myelinated dystrophic axon containing accumulations of smooth axoplasmic reticulum (540 days of age; ventral columns spinal cord)

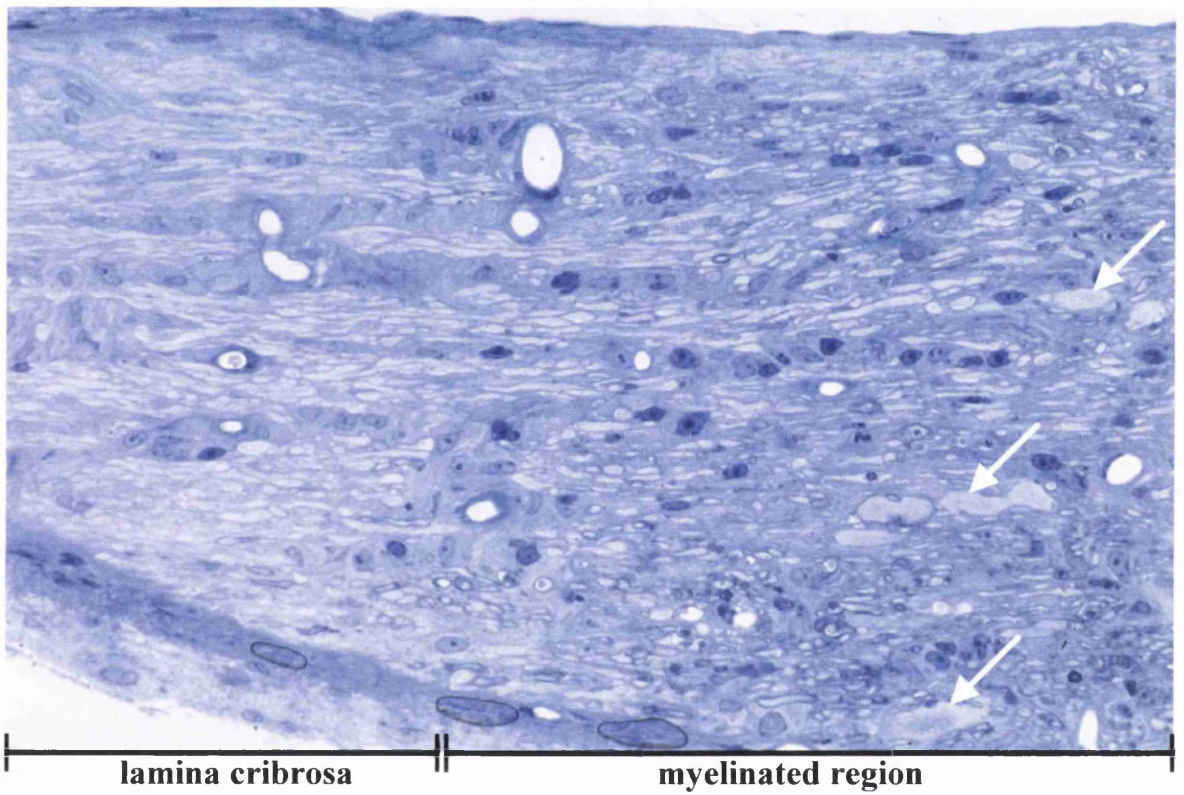


Figure 32 Methylene blue/ azur II stained longitudinal section from the lamina cribrosa of a 600 day-old knockout mouse showing axonal changes in myelinated regions (arrow) (450x magnification)

The majority of axonal swellings were seen in the myelinated region (Figure 32, page 107) although occasional swollen axons crossed the transition zone between the myelinated region and the unmyelinated lamina cribrosa. As these swellings were associated with at least the first myelinated heminode of the axon, they probably arose in the myelinated region and extended into the unmyelinated axon.

3.4.3.5 Myelination and myelin structure

3.4.3.5.1 Myelin ultrastructure and periodicity

Myelin sheaths from knockout mice were poorly compacted and had abnormal periodicity (Figure 33, page 109). Although the major dense line formed normally, the intraperiod lines were disrupted. In some areas the intraperiod lines diverged and separated, in others they condensed to form a single electron-dense structure. Occasional stretches of normal periodicity were seen interspersed between poorly compacted sections of myelin. The myelin sheath showed no other ultrastructural abnormalities. The periaxonal space, inner cytoplasmic tongue and nod of Ranvier were normal. The oligodendrocyte cell body had normal ultrastructural features with no swelling of the rough endoplasmic reticulum or Golgi apparatus.

3.4.3.5.2 Myelination status

The percentages of myelinated and non-myelinated (ensheathed and unmyelinated) axons were calculated from optic nerve and ventral columns of spinal cord (C2-3) in 20, 60 and 120 day-old mice (Figure 34, page 110 and Figure 35, page 111). The knockout mice had a higher percentage of non-myelinated fibres than wild type controls. This was statistically significant at all ages in the optic nerve ($P=0.0286$ at 20 and 60 days; $P=0.0159$ at 120 days, $n=4$) and at 20 and 60 days of age in the ventral columns of spinal cord ($P=0.0286$, $n=4$). However, the differences in percentage of non-myelinated fibres in the spinal cord were much smaller than in the optic nerve. At all ages, ensheathed fibres were well represented in the knockout optic nerve and spinal cord and accounted for approximately 20% to 30% of the non-myelinated fibres. Direct comparison with the proportions of ensheathed and unmyelinated fibres in wild type mice was impossible because of the low numbers of non-myelinated fibres in controls greater than 20 days of age. At 20 days of age, the proportion of non-myelinated fibres that were ensheathed appeared to be equivalent between the wild type and knockout mice.

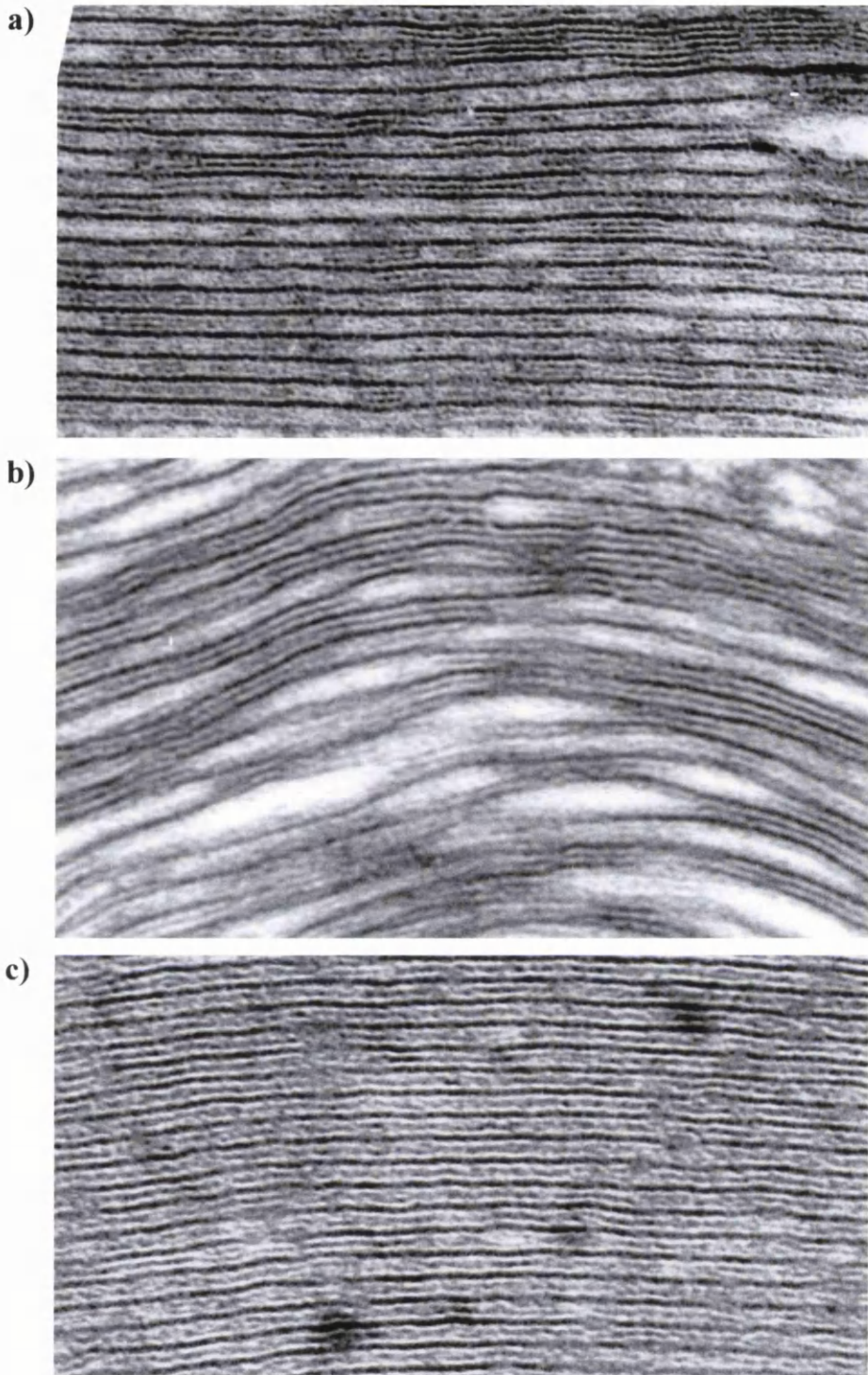
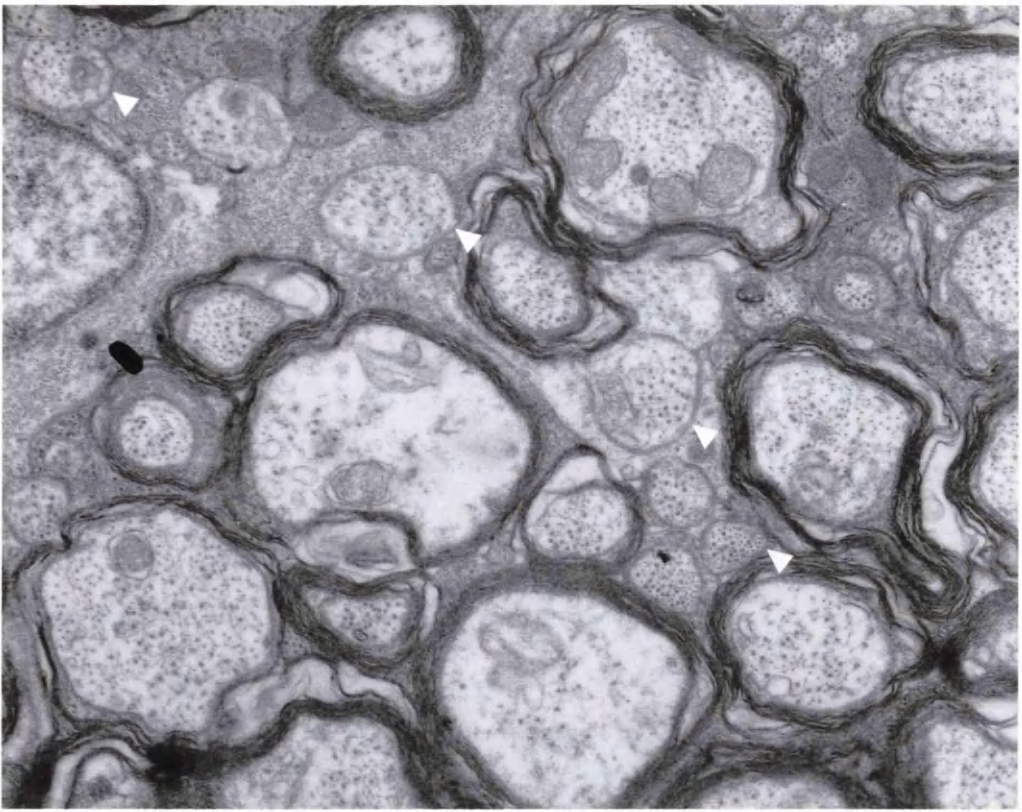


Figure 33 Electron micrograph showing three types of myelin periodicity in knockout mice (120 days of age; mid optic nerve; 300,000x magnification) Myelin demonstrating a) normal periodicity interspersed with lamellae containing condensed intraperiod lines, b) poor compaction with separation at the intraperiod lines, c) condensation of the intraperiod lines

a)



b)

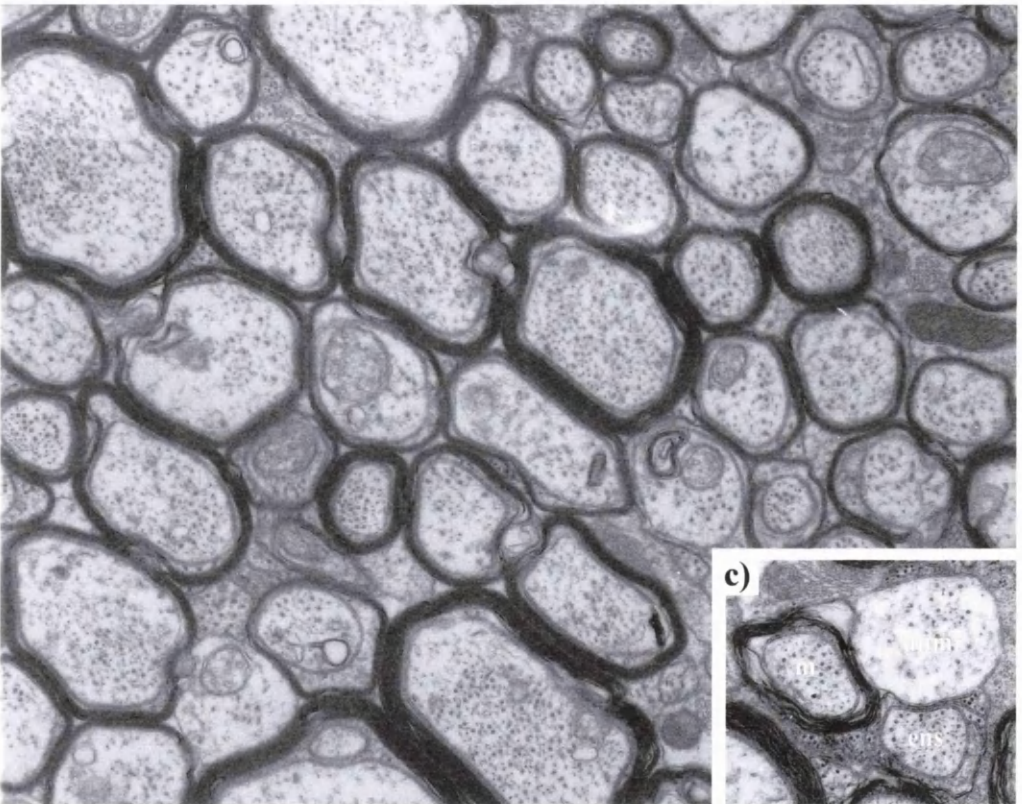


Figure 34 Electron micrographs of optic nerve from knockout and wild type mice at 60 days. A higher percentage of nonmyelinated axons (arrowheads) were found in knockout mice (a) when compared to wild type mice (b). Myelinated (m), ensheathed (ens) and unmyelinated (unm) axons were found in the optic nerve of knockout mice at this age (c) (16,000x magnification)

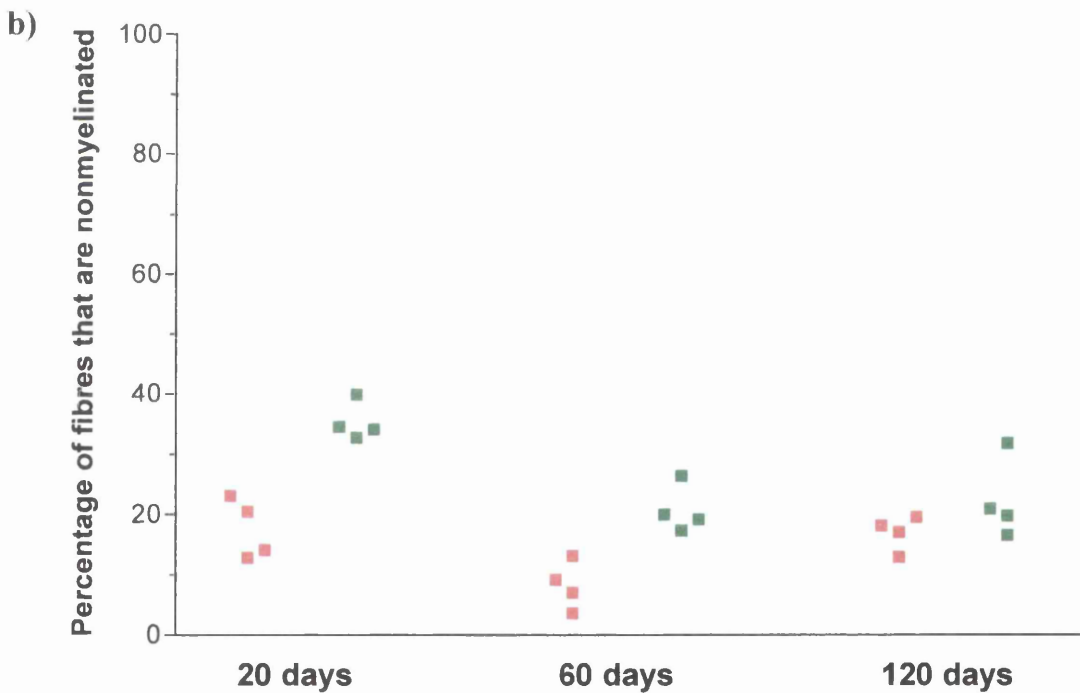
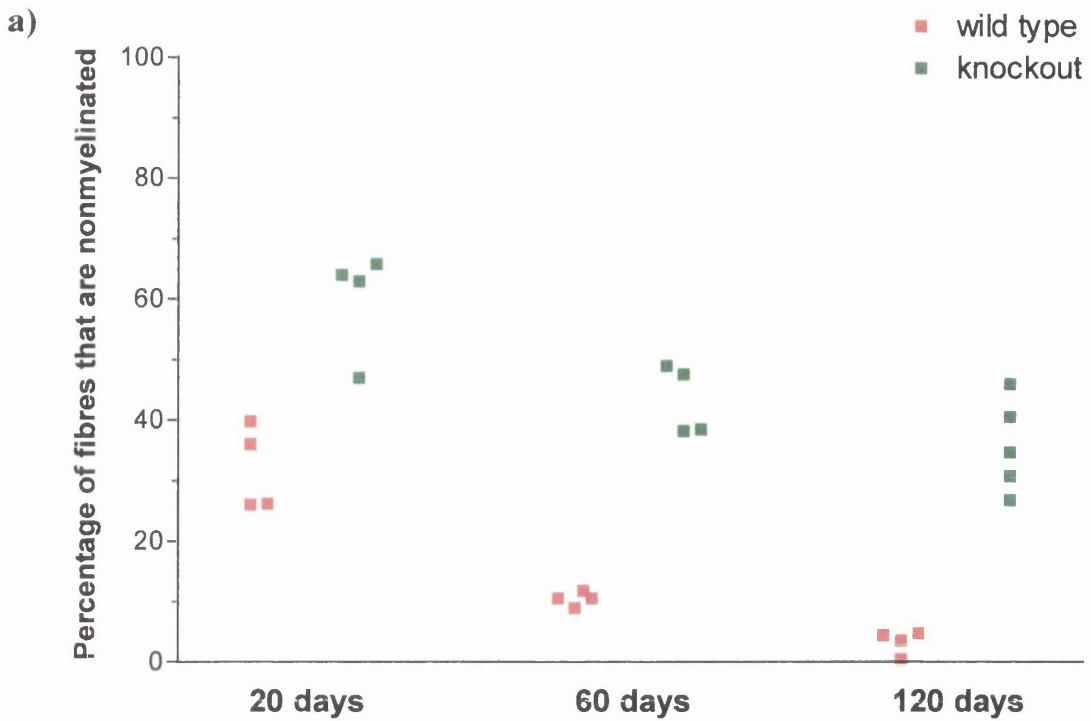


Figure 35 Percentage of non-myelinated (ensheathed and naked) axons in the a) mid optic nerve and b) ventral columns of spinal cord (C2-3) of wild type and knockout mice at 20, 60 and 120 days of age

3.4.3.5.3 Morphometric analysis of axonal diameters

The axon diameters of all fibres, myelinated fibres and non-myelinated (ensheathed and unmyelinated) fibres from the mid optic nerve and ventral columns of spinal cord (C2-3) were compared at 20, 60 and 120 days of age.

In both areas at 20 and 60 days of age, the distributions of combined (myelinated and non-myelinated) axon diameters were comparable between the two groups. When compared to wild type mice, a significant trend towards increased mean axonal diameter was seen in the optic nerve of 120 day-old knockout mice ($P=0.0286$, $n=4$) although this was not reflected in the spinal cord at this age (Figure 36, pages 113 and 114).

In the optic nerve at 20 days of age, the axon diameter frequency distribution for non-myelinated axons was similar in both groups although the knockout mice had a relatively greater proportion of non-myelinated fibres (Figure 37A, page 115). At older ages, the low numbers of non-myelinated fibres in wild type animals made direct comparison between the two groups difficult. In the optic nerve of 60 and 120 day-old knockout mice, the proportion of myelinated fibres less than $0.8\mu\text{m}$ in diameter was lower than in wild type controls. However, the proportions of myelinated fibres greater than $0.8\mu\text{m}$ in diameter were comparable (Figure 37B, page 116).

In the spinal cord, non-myelinated axon diameter distributions showed the relative increase in proportion of non-myelinated fibres in the knockout mice (Figure 38A, page 117). Although the distributions of myelinated fibre diameters were not identical in the spinal cord of knockout and wild type mice, they were very similar (Figure 38B, page 118). At all ages in the knockout spinal cord, the relative number of myelinated fibres less than $1\mu\text{m}$ in diameter was lower than in wild type controls suggesting that a similar trend of reduced numbers of small diameter myelinated fibres as seen in the optic nerve occurred.

In summary, knockout mice developed a full range of axon diameters by 60 days of age although the percentage of fibres that acquired myelin sheaths was reduced. By 120 days of age, the mean axon diameter in the optic nerve of knockout mice was significantly increased compared to controls. In older knockout mice, the proportion of small myelinated axons ($<1\mu\text{m}$ in diameter) in both the optic nerve and spinal cord appeared to be reduced although larger diameter myelinated axons were unaffected.

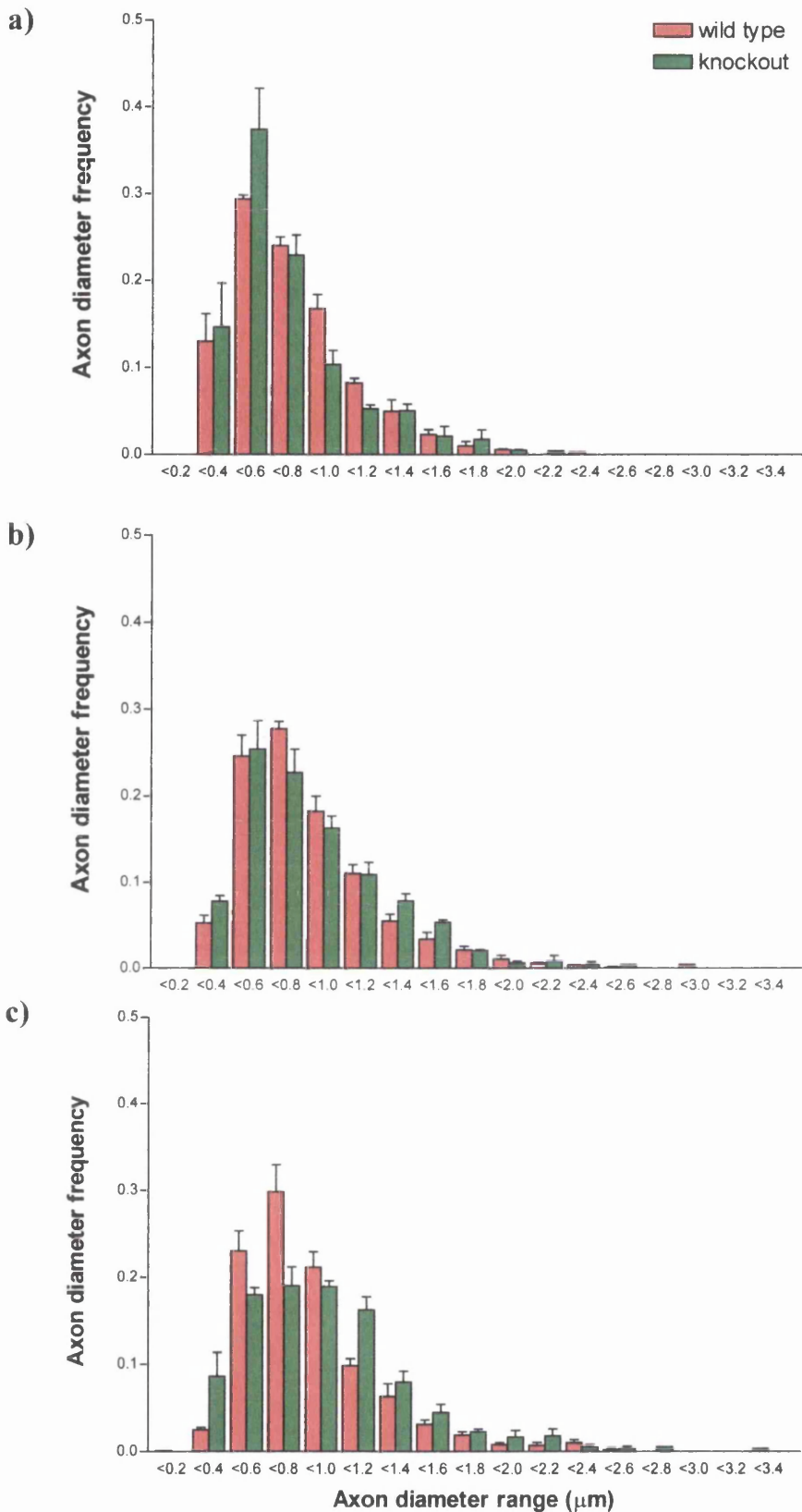


Figure 36A Axon diameter frequency distribution (myelinated and non-myelinated fibres) from mid optic nerve in a) 20, b) 60 and c) 120 day-old knockout and wild type mice (n=4 at each age and genotype; bars=M+SEM)

cont./

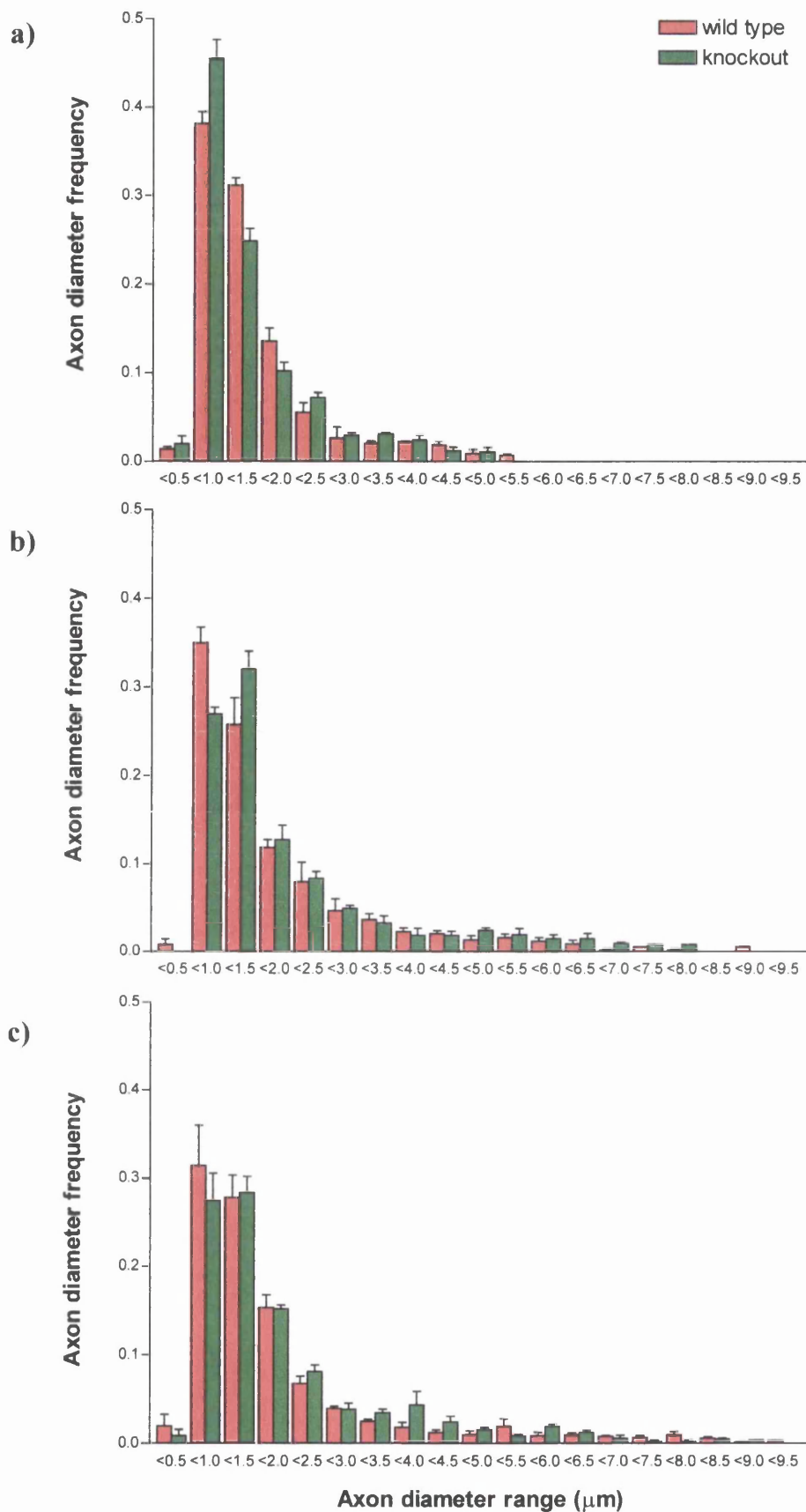


Figure 36B Axon diameter frequency distribution (myelinated and non-myelinated fibres) from ventral columns of spinal cord (C2-3) in a) 20, b) 60 and c) 120 day-old knockout and wild type mice (n=4 at each age and genotype; bars=M+SEM)

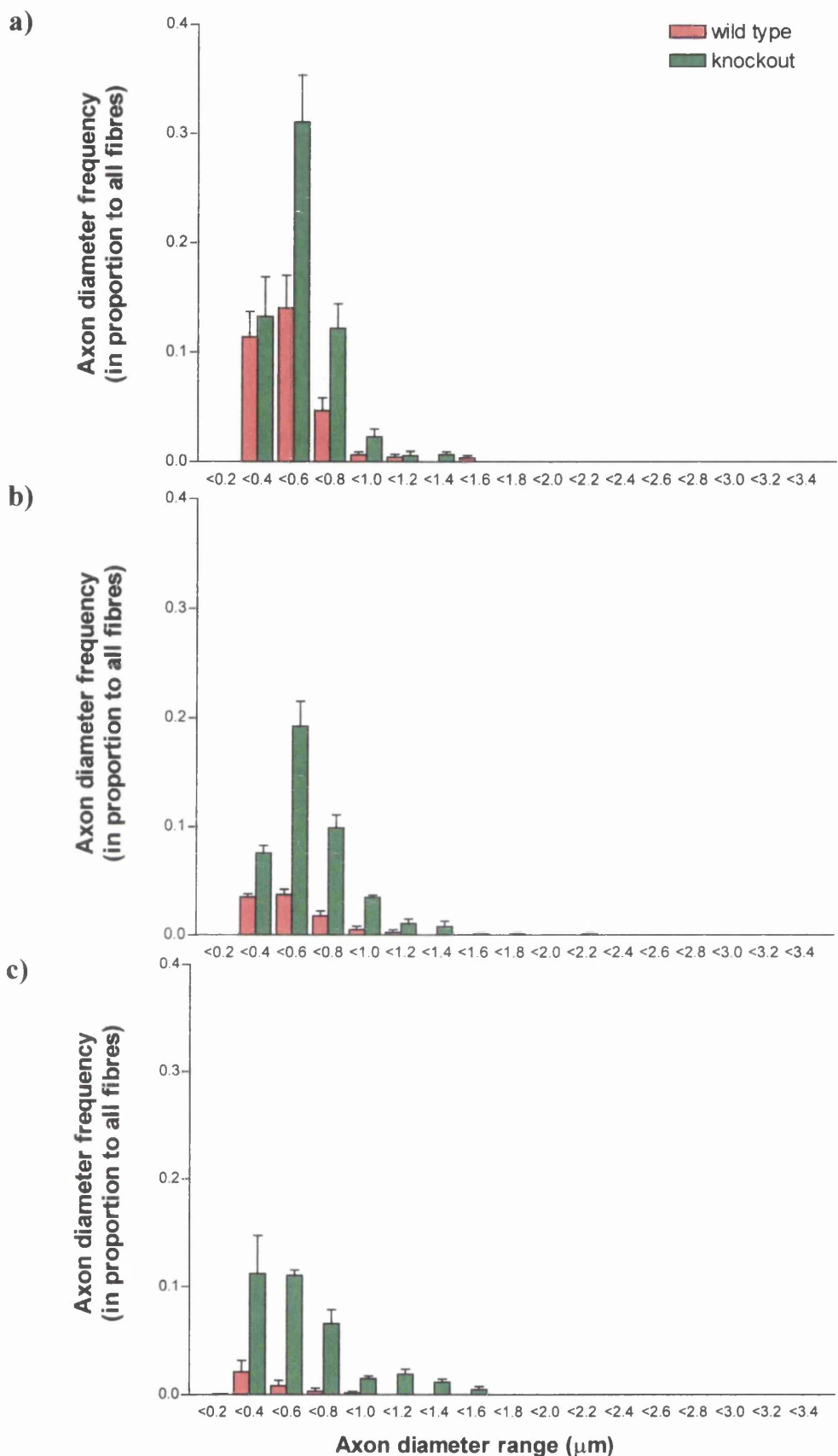


Figure 37A Non-myelinated (naked and ensheathed) axon diameter frequency distribution in proportion to all fibres from mid optic nerve in a) 20, b) 60 and c) 120 day-old knockout and wild type mice (n=4 at each age and genotype; bars=M+SEM)

cont./

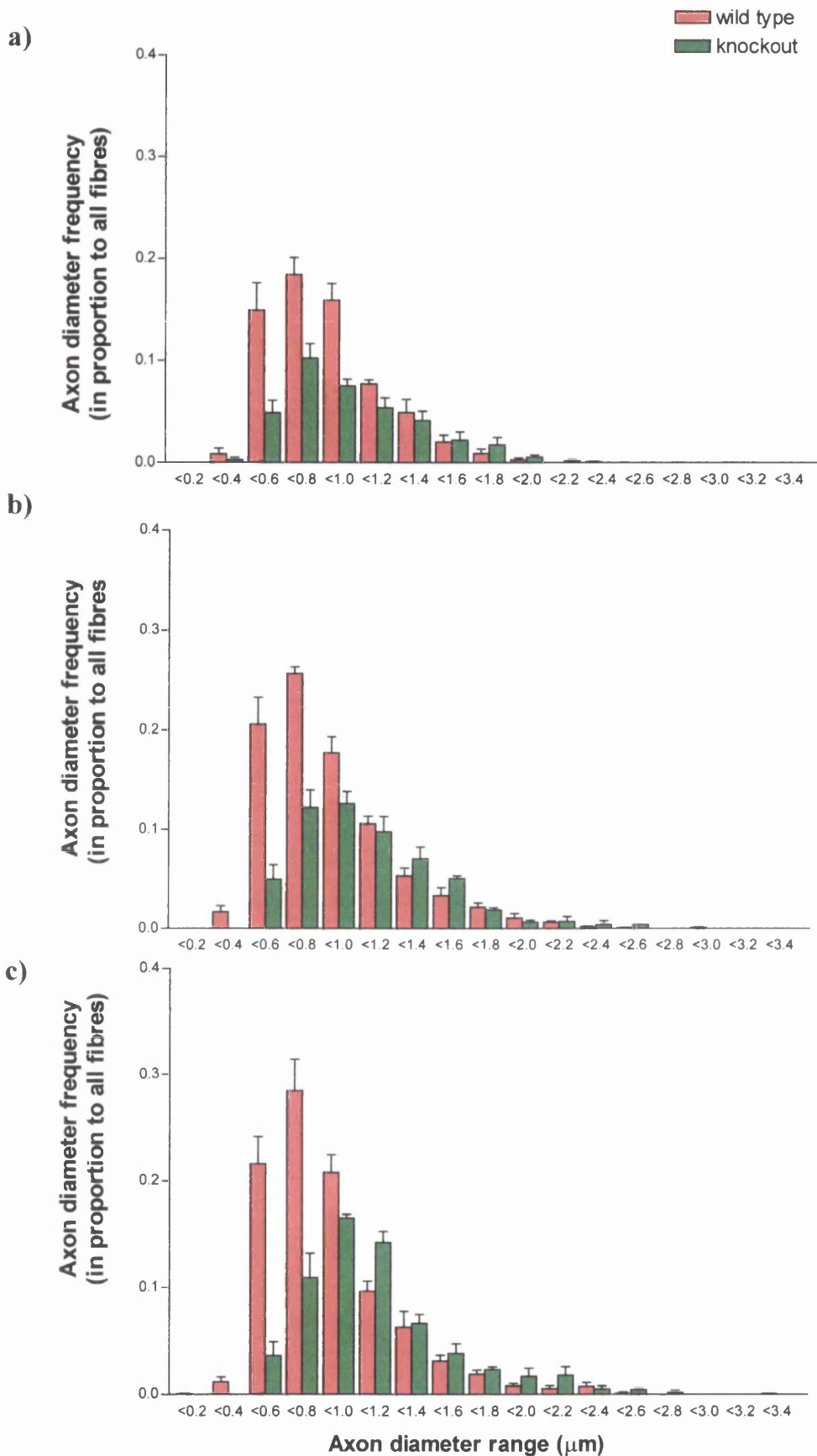


Figure 37B Myelinated axon diameter frequency distribution in proportion to all fibres from mid optic nerve in a) 20, b) 60 and c) 120 day-old knockout and wild type mice (n=4 at each age and genotype; bars=M+SEM)

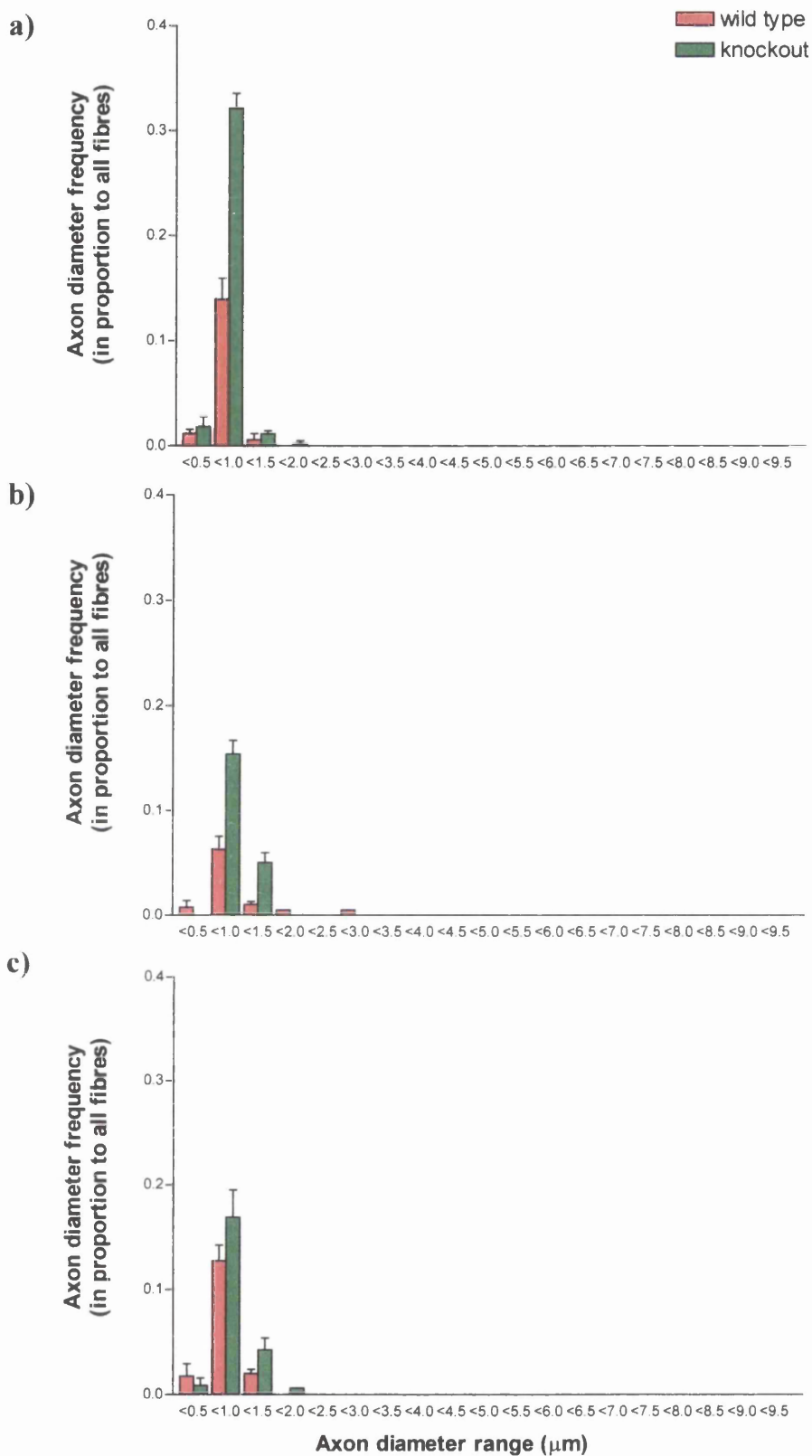


Figure 38A Non-myelinated (naked and ensheathed) axon diameter frequency distribution in proportion to all fibres from ventral columns of spinal cord (C2-3) in a) 20, b) 60 and c) 120 day-old knockout and wild type mice (n=4 at each age and genotype; bars=M+SEM) cont./

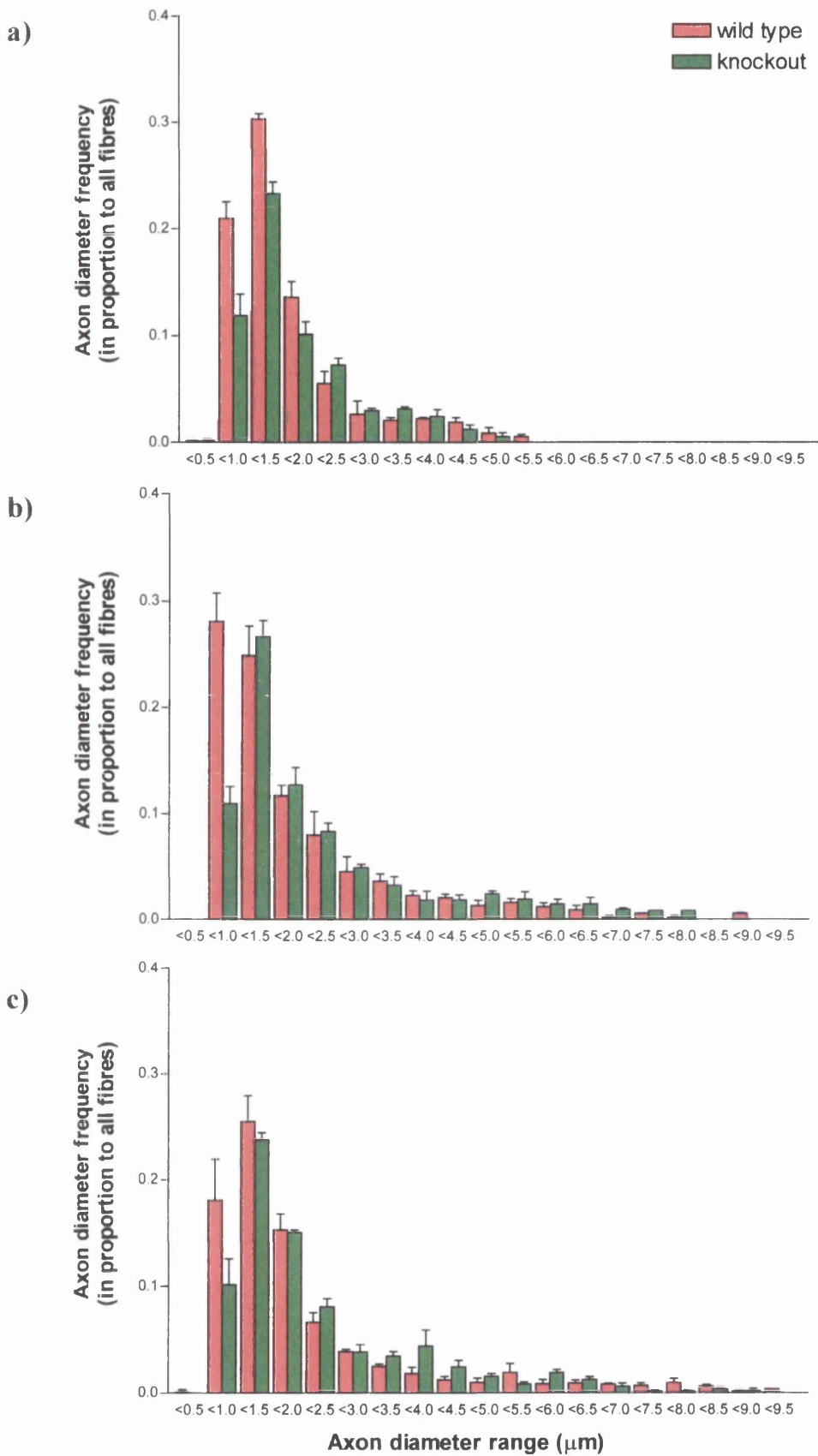


Figure 38B Myelinated axon diameter frequency distribution in proportion to all fibres from ventral columns of spinal cord (C2-3) in a) 20, b) 60 and c) 120 day-old knockout and wild type mice (n=4 at each age and genotype; bars=M+SEM)

3.4.3.5.4 Comparison of fibre densities

The significant increase in mean axonal diameter in the optic nerve of knockout mice at 120 days of age could have represented either a generalised increase in axon diameter or the selective exclusion of small diameter fibres from analysis through neurodegeneration. In order to establish which of these two scenarios occurred, the densities of axons (both myelinated and non-myelinated) were calculated for both groups of mice from the optic nerve at each age.

The relative distributions of axon densities were comparable between wild type and knockout mice at 20 and 60 days of age (Figure 39a, page 120). By 120 days of age, although the distribution of densities of axons greater than 1 μ m in diameter were equivalent, the knockout mice had reduced densities of smaller diameter fibres (Figure 39A, page 120).

To demonstrate that this change represented the loss of small diameter fibres and not the failure of these fibres to develop, relative fibre densities were compared at 60 and 120 days of age for each group (Figure 39B, page 121). Wild type mice showed a slight increase in density of larger diameter fibres over this period but essentially maintained similar density distributions as they aged. Although the knockout mice had a normal distribution of fibre densities at 60 days of age, the densities of fibres less than 1 μ m in diameter was markedly reduced by 120 days of age. At 120 days of age, the distribution of fibres greater than 1 μ m in diameter was similar to that at 60 days of age suggesting that small diameter fibres did develop but were subsequently excluded from the analyses.

The density of axons in the knockout mice was similar to wild type controls at younger ages but dropped as the animals aged. In order to demonstrate this, the total axon densities were compared at 20, 60 and 120 days of age (Figure 39C, page 122)

Taken together, these findings show that the knockout mice developed a full range of axon sizes with normal densities but lost small diameter fibres as they aged. The loss of small diameter fibres coincided with the development of neurodegeneration and probably reflected the exclusion of fibres from morphometric analyses as they develop neurodegenerative changes.

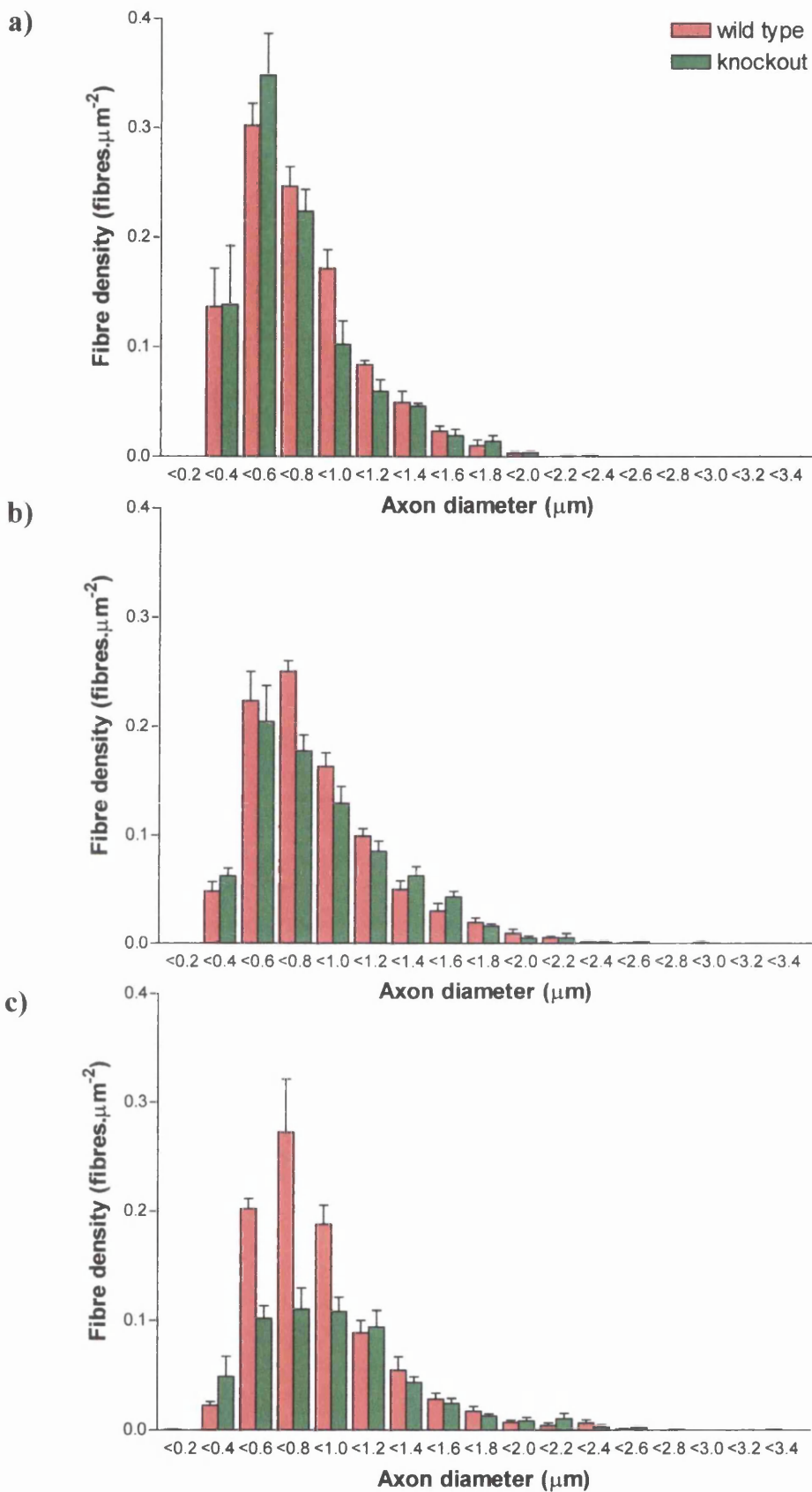


Figure 39A Total fibre densities (myelinated and non-myelinated) from mid optic nerve in a) 20 day, b) 60 day and c) 120 day-old knockout and wild type mice (n=4 at each age and genotype; bars=M+SEM) cont./

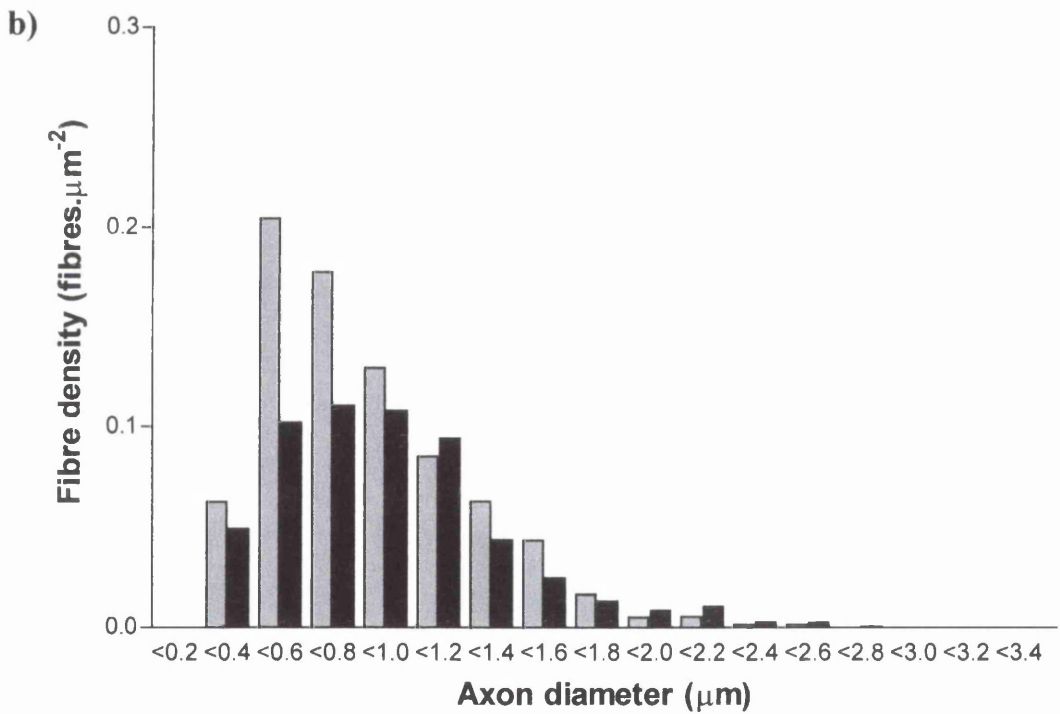
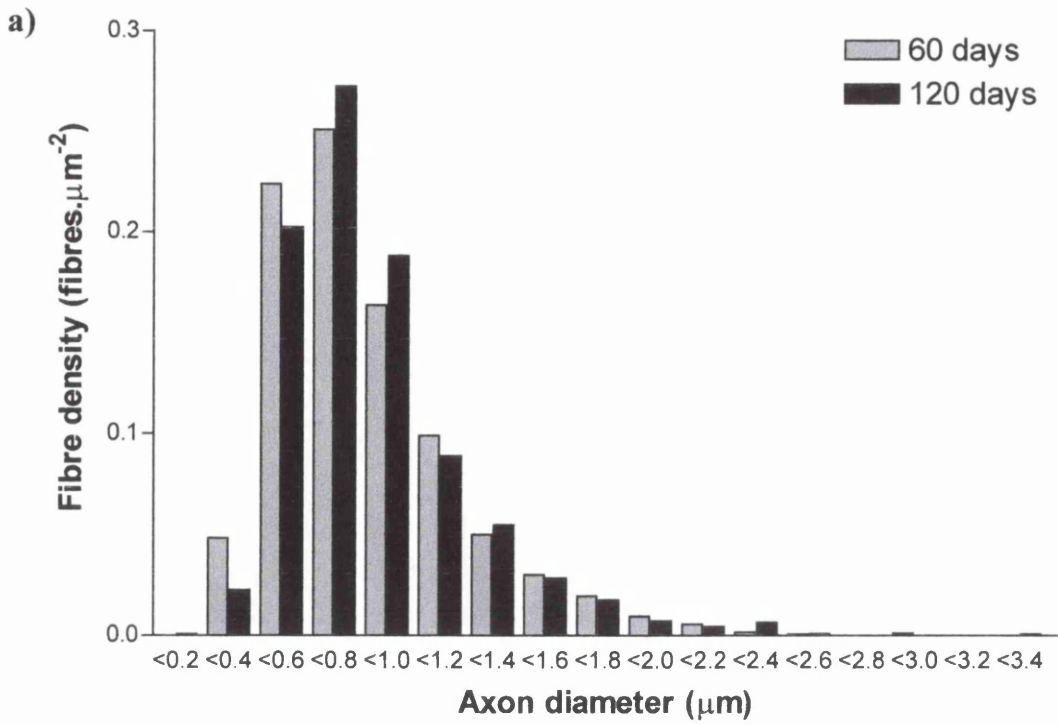


Figure 39B Fibre density distributions from mid optic nerve of a) wild type and b) knockout mice at 60 and 120 days of age (n=4 at each age and genotype)

a) Fibre density distributions in wild type mice were similar at 60 and 120 days of age.

b) An obvious reduction in the density of small diameter fibres (<1µm) in knockout mice was seen by 120 days of age

cont./

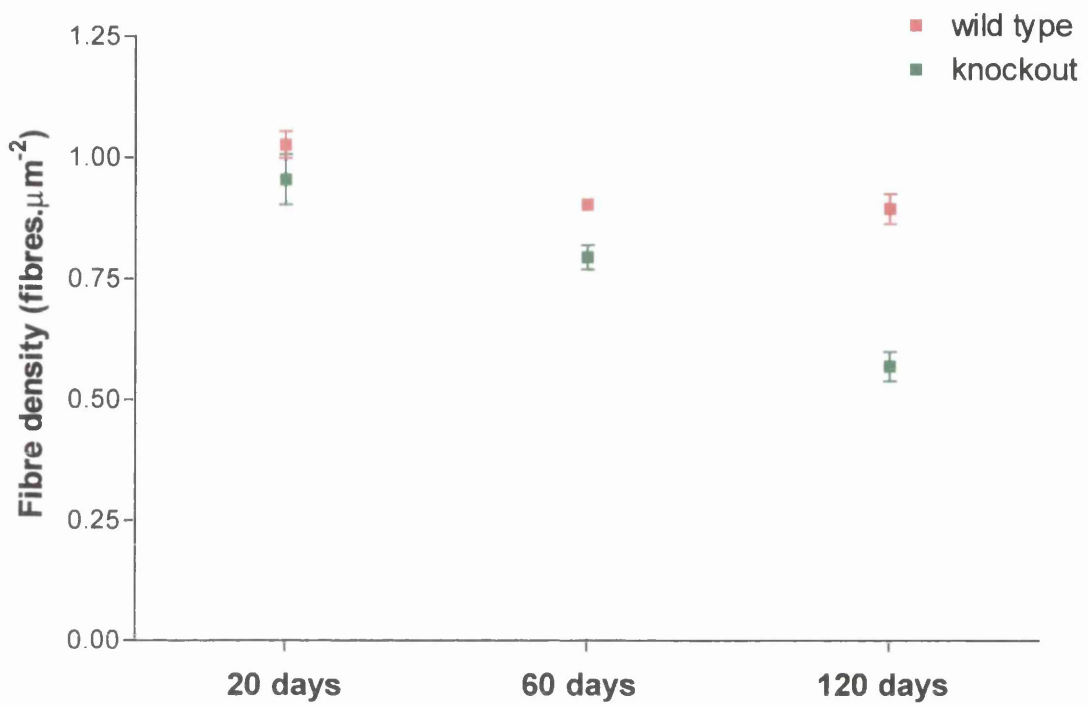


Figure 39C Total fibre densities from mid optic nerve of wild type and knockout mice at 20, 60 and 120 days of age. The two groups of mice had similar fibre densities until 120 days of age when a dramatic reduction in density in knockout mice developed.

(n=4 at each age and genotype; bars=M±SEM)

3.4.4 Survey of the PNS of the *Plp* gene knockout mice

Survey histological examination of the peripheral nervous system of aged knockout mice (greater than 600 days) revealed no abnormalities. Resin sections from the proximal and distal regions of a range of peripheral and cranial nerves showed no evidence of myelin or axonal changes (Figure 40, page 124). Cryosections of a range of skeletal muscles and neuromuscular junctions showed no evidence of changes consistent with neurogenic atrophy or of neuromyopathy.

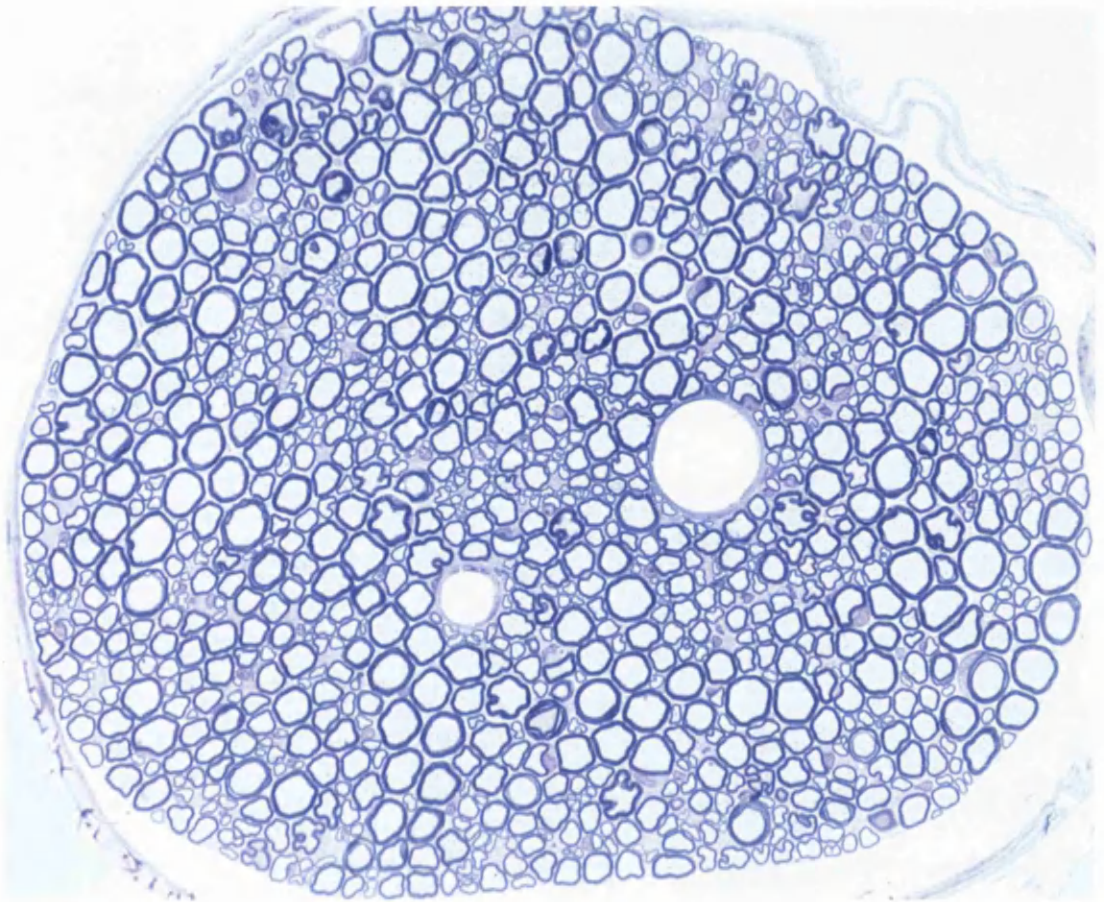


Figure 40 Methylene blue/ azur II stained 1 μ m resin section of sciatic nerve from a 360-day-old knockout mouse showing no evidence of axonal degeneration or demyelination (566x magnification)

3.5 Discussion

Data presented in this chapter demonstrated that the targeting strategy used to create the *Plp^{tmkn1}* allele prevented *Plp* gene expression in hemizygous mice. These mice were capable of elaborating large volumes of myelin and maintaining mature oligodendrocyte numbers into adulthood. Unlike other *Plp* gene mutants, knockout mice remained comparatively normal until they became aged when progressive neurological deficits led to severe debility. From early adulthood (60 days), progressive neurodegenerative changes developed characterised by axonal swelling and fibre degeneration. Coincident with this, a microgliosis developed. Unlike human cases of PMD resulting from *PLP* gene-null alleles, knockout mice had no PNS changes.

The maintenance of mature oligodendrocytes in knockout mice showed that *Plp* gene products are not necessary for the maturation or survival of these cells. It seems unlikely, therefore, that the increased apoptosis and reduced numbers of mature oligodendrocytes seen in the majority of spontaneous *Plp* gene mutants result from the paucity of *Plp* gene products. This study adds weight to the theory that mutated *Plp* gene products lead to oligodendrocyte death through the acquisition of properties that disrupt oligodendrocyte function. In this scenario, maintenance of oligodendrocyte numbers in the *rumpshaker* mouse and *paralytic tremor* rabbit (Gow and Lazzarini, 1996) would reflect the inability of the abnormal *Plp* gene products to disrupt cellular function, not a beneficial effect of continued targeting of DM20 protein to the cell surface. The elaboration of large volumes of myelin and absence of demyelination in the knockout mouse demonstrated that PLP and DM20 proteins are not necessary for the formation or maintenance of central myelin. This contrasts with severe dysmyelination seen in spontaneous *Plp* gene mutants. Dysmyelination in these mutants may result because insufficient oligodendrocytes survive to maturity to form myelin sheaths. An alternative explanation, supported by *in vivo* and *in vitro* studies, is that disrupted PLP/DM20 protein trafficking observed in many of these mutants prevents the elaboration of myelin membranes.

Despite the large volumes of myelin that form in knockout mice, evidence of subtle oligodendrocyte dysfunction does exist. The disrupted periodicity of knockout myelin suggests that PLP and DM20 proteins influence the myelin ultrastructure particularly of the intraperiod line. Abnormalities of the intraperiod lines are reported in most spontaneous *Plp* gene mutants and in the *Plp* gene-null mice described by Boison & Stoffel (1994). The knockout mice described in this thesis had occasional stretches of myelin with normal periodicity interspersed between

abnormal lamellae. More commonly, the intraperiod lines condensed to a single electron dense structure or separated completely. *Plp* gene products, although not essential for the formation of myelin, may stabilise the intraperiod line by acting as struts maintaining both adhesion and spacing between the extracellular leaflets of myelin lamellae. This is supported by transfection and lipid-vesicle studies demonstrating that *Plp* gene products have adhesive properties between the extracellular surfaces of lipid bilayers (Sinoway *et al.*, 1994; Palaniyar *et al.*, 1998). However, the ultrastructural abnormalities of myelin in knockout mice may represent *post mortem* change induced by tissue processing. Striking differences between the periodicity of fresh and fixed myelin demonstrate the potential for processing to alter myelin ultrastructure (Kirschner and Hollingshead, 1980). Karthigasan *et al.* (1996) have demonstrated that *rumpshaker* myelin develops more *post mortem* decompaction than wild type myelin. Although this finding suggests that *rumpshaker* myelin is unstable, it highlights the difficulty in interpreting ultrastructural changes of myelin in mutants.

The failure of a proportion of fibres to myelinate in the knockout mouse provides further evidence of oligodendrocyte dysfunction. Although a wide range of axons sizes remained non-myelinated, the predominance of these changes in the optic nerve compared to the ventral columns of spinal cord suggested that small diameter fibres were preferentially affected. This was supported by the trend in knockout mice towards relatively fewer small-diameter myelinated axons (<0.8µm) despite normal numbers of larger myelinated axons in the same areas. As these trends developed before axonal swellings and degeneration became prominent, it is unlikely that they resulted from selective degeneration of small diameter myelinated axons. On the contrary, the data support selective dysmyelination of some small diameter axons and suggest that this process is not linked to axonal swellings, which are confined to myelinated fibres. These results support a role for the *Plp* gene in the early stages of myelination, perhaps in initial axoglial contact. However, the disruption of normal myelination in knockout mice cannot be linked to a particular stage of axo-oligodendroglial interaction as both ensheathed and unmyelinated axons were well represented. Although the *Plp* gene products cannot be localised to the cell surface before the start of myelin compaction (Schwob *et al.*, 1985), one study suggests that a secreted *Plp* gene product can influence glial development (Yamada *et al.*, 1999). This putative peptide appears to have biological activity at very low concentrations and may be a candidate for influencing axoglial interaction before upregulation of the *Plp* gene (Yamada *et al.*, 1999).

The development of progressive neurological dysfunction in aged knockout mice correlated with increasing axonal swellings and degeneration. Axonal changes have

been implicated in some cases of chronic progressive relapsing multiple sclerosis where reasonable neurological function appears to be maintained until a threshold of axonal pathology is reached (Trapp *et al.*, 1998). Knockout mice presumably have a similar clinical course, remaining normal throughout most of their life but developing neurological dysfunction when axonal changes reach a threshold limit. Axonal swellings also develop in some induced and spontaneous *Plp* gene mutants including the double mutant *shiverer-Plp* gene knockout mouse (Dentinger *et al.*, 1982; Rosenfeld and Friedrich, Jr., 1983; Taraszewska, 1988; Fanarraga *et al.*, 1992; Duncan *et al.*, 1995; Griffiths *et al.*, 1998; Anderson *et al.*, 1998). No swellings developed in *shiverer* controls suggesting that the absence of the *Plp* gene products, not abnormal oligodendrocytes *per se*, led to the development of axonal swellings (Griffiths *et al.*, 1998). The development of axonal changes in a range of deletion, duplication and missense mutations of the *Plp* gene suggests that a common pathogenesis may exist.

The development of axonal changes may arise through either primary neuronal or primary oligodendroglial abnormalities related to the loss of *Plp* gene function. Localisation of *srPlp* and *srDm20* transcripts to some neuronal populations within the adult murine CNS provides the first evidence that the *Plp* gene may have a role in normal neuronal function (Bongarzone *et al.*, 1999). The possibility that this putative role is disrupted resulting in the knockout axonopathy must be considered, however, the data in this thesis does not favour this. Axonal swellings were confined to myelinated regions of the CNS suggesting that their development was dependent on the presence of PLP/DM20-deficient oligodendrocytes. In addition, no evidence of neuronal pathology was found in the neurones of the dorsal root ganglia or the retinal ganglion cell layer, both regions that project axons into the most severely affected white matter tracts. Although this does not prove that a neuronal defect did not cause the knockout axonopathy, it does suggest a more focal axonal problem. The axonal changes in knockout mice eventually affected all white matter regions suggesting that the cellular abnormality leading to these changes was widespread. However, Bongarzone *et al.* (1999) reported that *srPlp* and *srDm20* transcripts were isolated to populations of neurones in the cerebellum, hippocampus and olfactory system predicting a more focal effect. The data presented in this thesis supports a primary oligodendrocyte deficit leading to secondary axonal dysfunction although a primary neuronal defect cannot be categorically excluded. In particular, if *srPlp* and *srDm20* transcripts are identified in wider populations of neurones in the murine CNS, their role in the development of the knockout axonopathy will have to be re-evaluated.

A primary oligodendrocyte defect could lead to the development of axonal changes

if PLP/DM20-deficient oligodendrocytes acquire toxic properties that prove deleterious to the axon. Alternatively, myelinated axons may become dependent on normal PLP/DM20-expressing oligodendrocytes raising the possibility that the *Plp* gene is involved in signal transduction pathways between the mature oligodendrocyte and axon. However, to date, no molecules that interact directly with the PLP or DM20 proteins have been found.

In both the PNS and CNS, the local glial environment can have a profound effect on neuronal structure and function. Studies in the *trembler* mouse demonstrated that Schwann cells can modulate axonal neurofilament phosphorylation and slow axonal transport mechanisms, possibly through a signalling pathway (De Waegh and Brady, 1991; De Waegh *et al.*, 1992). In the CNS, a similar role for the oligodendrocyte in modulating radial axonal growth in a myelin-independent manner has been proposed (Sánchez *et al.*, 1996). Axon ensheathment by the oligodendrocyte process was sufficient to induce local neurofilament accumulation and radial axonal growth possibly through a phosphatase or kinase mediated pathway (Starr *et al.*, 1996; Sánchez *et al.*, 1996). The accumulation of neurofilaments in swollen axons in knockout mice suggests that a similar mechanism could be disrupted. However, the diameters of unaffected axons in the knockout mouse showed normal radial axonal growth to 60 days of age and, subjectively, neurofilament densities were normal. In addition, staining for a range of phosphorylated and non-phosphorylated neurofilament epitopes revealed no abnormalities in knockout axons although occasionally Purkinje cell neurones stained for phosphorylated neurofilaments (Klugmann *et al.*, 1997). Together, these results point towards normal neurofilament structure in the knockout axon and suggest that local phosphatase and kinase systems are not primarily involved in the axonopathy. In the optic nerves of older knockout mice (120 days of age), the trend towards increased mean axonal diameter might indicate a generalised axonal change. However, selective exclusion of small diameter myelinated fibres affected by neurodegeneration, which predominates in this area, could also account for this finding. Similar trends were not identified in optic nerves at 60 days of age, when neurodegenerative changes are mild, nor in ventral columns of spinal cord at 120 days of age, before neurodegeneration could be readily identified in this area. These data support normal radial axonal growth in the knockout mouse with skewing of data through the loss of small diameter axons leading to the changes seen in the optic nerves in older animals.

In transgenic models of motor neurone disease, the accumulation of neurofilament subunits led to reduced slow axonal transport, axonal swelling and degeneration and neuronal death (Côté *et al.*, 1993; Xu *et al.*, 1993a; Xu *et al.*, 1993b; Collard *et al.*,

1995). Some evidence of disrupted fast axonal transport in these mice (Collard *et al.*, 1995) and in motor neurone disease cases (Toyoshima *et al.*, 1998) supports mounting evidence that neurofilaments and microtubules form highly interdependent structures (Julien, 1997; Zhu *et al.*, 1998). Although these studies show the potential for disrupted slow axonal transport to induce axonal changes and secondary fast axonal transport blocks, the balance of data from the knockout mouse suggests a more general disruption of axonal transport. Swellings had changes that were characteristic of both slow (neurofilament) and retrograde-fast (dense body) axonal transport blocks although individual swellings rarely showed accumulation of both neurofilaments and dense bodies. Subjectively, membrane bound organelles accumulated first followed by neurofilaments. These findings suggest that both slow and fast-retrograde axonal transport are equally disrupted, the temporal differences in axonal changes reflecting different transport speeds of organelles. The putative early disruption of these two mechanisms is difficult to reconcile with a single transport defect. It seems more likely that these changes represent secondary responses to an unidentified change in the axoplasmic environment that is related to the loss of *Plp* gene function.

Axonal swellings in transgenic models of neurofilament-related disease developed in proximal regions of large diameter axons (Xu *et al.*, 1993a; Xu *et al.*, 1993b). These axons have the highest rate of neurofilament metabolism and are clear candidates for developing early changes in neurofilament-related disease (Côté *et al.*, 1993; Julien, 1997). In contrast, the knockout axonopathy initially affected small diameter fibre tracts suggesting that the axonal changes were not primarily related to abnormalities of neurofilament metabolism. The spatial and temporal association between swollen and degenerate axons in the knockout mouse suggests that these two processes were linked and appeared to be uniformly distributed throughout the corticospinal tracts and optic nerve, both areas that project axons in a single direction (unquantified data). The development of focal swellings at any point along the length of an axon is more indicative of a focal transport block and suggests that focal axonal function is affected. This provides further support for the knockout axonopathy developing in response to the influence of PLP/DM20-deficient oligodendrocytes rather than a primary neuronal abnormality. To test the hypothesis that the axonal swellings in knockout mice resulted from axonal constriction, axon diameters were assessed. The normal to increased range of inter-nodal axon diameters in knockout mice suggests that constriction of inter-nodal axons did not lead to disruptions of axonal transport or swelling. Microgliosis and astrocyte hypertrophy are commonly associated with axonal degeneration in the CNS (Stoll and Jander, 1999; reviewed by Aldskogius and Kozlova, 1998) and the lack of active demyelination in the knockout mouse suggests that myelin breakdown

and glial responses occur secondary to axonal degeneration.

This study highlights the tract specificity of neurodegenerative changes in knockout mice for small fibre regions and shows that dysmyelination also affects predominantly small diameter axons. Similar tract specificity has been noted in other *Plp* transgenic mice (Anderson *et al.*, 1998). These findings may reflect different responses of subpopulations of axons to oligodendrocyte dysfunction or perturbed function of neuronal subpopulations that express rare *Plp* gene splice variants. Alternatively, they may reflect disrupted *Plp* gene function in subpopulations of oligodendrocytes. Although there are no clear molecular divisions of mature oligodendrocytes, some evidence for functional subpopulations does exist. For example, oligodendrocytes can be separated into those myelinating large numbers of small axons and those myelinating small numbers of large axons (Hildebrand *et al.*, 1993). However, as large diameter axons myelinate in advance of small diameter axons, this may reflect the different temporal recruitment of oligodendrocytes from the same population of premyelinating cells. In fact, the ability of oligodendrocytes from small axon regions to myelinate large diameter axons suggests that functional divisions of premyelinating oligodendrocytes do not exist (Fanarraga *et al.*, 1998). Other divisions are made based on immunocytochemical markers, for example carbonic anhydrase II (Butt *et al.*, 1995), but, again, this may reflect differences in recruitment from a single oligodendrocyte population. It is not within the scope of this study to resolve these issues. However, axons in knockout mice appear to develop normally at least until 20 days of age, as evidenced by normal radial axonal growth. This occurs in the face of oligodendrocyte dysfunction favouring an oligodendrocyte-mediated basis for tract specificity.

At least three *PLP* gene-null mutations have been reported in families suffering from PMD with comparatively mild phenotypes (Raskind *et al.*, 1991; Sistermans *et al.*, 1996; Garbern *et al.*, 1997). The family described by Garbern *et al.* (1997) has a point mutation in the translation initiation codon of exon 1 preventing translation of PLP and DM20 proteins. Although PLP and DM20 proteins are absent from the CNS, the presence of other myelin proteins such as MBP indicates that large volumes of myelin form. *Ante mortem* and *post mortem* examination suggests that these patients myelinate well but subsequently lose myelin. In addition, a segmental demyelinating peripheral neuropathy also develops (Garbern *et al.*, 1997). Although there are similarities between this family and the knockout mouse, the phenotypes do differ with humans developing early onset neurological dysfunction and peripheral neuropathies (Garbern *et al.*, 1997). These contrasting findings are difficult to correlate with similar protein deficits. Early onset neurological

dysfunction may reflect a reduced ability of human cases to compensate for early neurodegenerative changes because of their higher requirements for normal function. Alternatively, such discrepancies may be a function of the absolute greater age of human myelin sheaths; if *Plp/PLP* gene products are required for long-term myelin stability, knockout mice may not survive long enough to show evidence of myelin breakdown. A third alternative is that humans and mice compensate differently for the loss of PLP/DM20 proteins.

The lack of PNS pathology in the knockout mouse suggests that the clinical features related to loss of upper motor neurones causing paresis and disuse muscle atrophy. The discordance of PNS changes between the two species is hard to correlate with the existing data on *Plp* gene expression in the PNS. Garbern *et al.* (1997) are the first workers to demonstrate *Plp* gene products in peripheral myelin lamellae of healthy mammals. The balance of data from other studies suggests that, if present, the *Plp* gene products constitute only a small proportion of the total peripheral myelin proteins and are unlikely to be important structural components (Griffiths *et al.*, 1995). The lack of PNS changes in knockout mice does not support a role for the *Plp* gene in peripheral myelin assembly or maintenance. However, the peripheral neuropathy reported by Garbern *et al.* (1997), which may also affect another *PLP* gene-null PMD family, shared many features with HNPP, a peripheral neuropathy that is exacerbated by nerve compression. The failure to develop PNS changes in knockout mice may reflect the differences in body size and compression stresses on peripheral nerves between mice and humans.

4. *Plp*^{tmkn1} heterozygous mice

4.1 Background

Although female members of PMD families rarely develop phenotypes, clinical abnormalities are occasionally reported (Hodes *et al.*, 1995; Nance *et al.*, 1996; Sivakumar *et al.*, 1999). A proportion of oligodendrocytes in these individuals is predicted to express the mutated allele through the process of X-inactivation as evidenced by mosaic patterns of dysmyelination in heterozygous carriers of the *Plpip*, *Plpip-rsh*, *Plpmd* and *Plpsh* alleles (Rosenfeld and Friedrich, Jr., 1984; Duncan *et al.*, 1987b; Fanarraga *et al.*, 1991; Hodes *et al.*, 1995; Nezu *et al.*, 1996). However, experimental data from *jimpy* heterozygotes demonstrates that the majority of oligodendrocytes in the mature CNS express the wild type allele (Bartlett and Skoff, 1986). Pockets of dysmyelination exist throughout the immature CNS of these mice, particularly affecting the optic nerve (Skoff and Montgomery, 1981; Skoff and Ghandour, 1995) but, as the animals age, hypomyelination in the spinal cord and brain largely resolves leaving a predominantly well myelinated CNS (Bartlett and Skoff, 1986). These results indicate that oligodendrocytes expressing mutant alleles are less likely to elaborate myelin sheaths than their wild type counterparts and suggest that the expression of the mutated *Plp* alleles confers negative properties to oligodendrocytes (Kagawa *et al.*, 1994b; Skoff and Ghandour, 1995). In addition, the studies from the *jimpy* heterozygote (Skoff and Ghandour, 1995), mirrored in studies from other mutants (Fanarraga *et al.*, 1991; Cuddon *et al.*, 1998), demonstrate that the CNS compensates for the reduced number of functional oligodendrocytes possibly explaining why clinical phenotypes are rare. The effects of modifying loci or skewing of X-inactivation, which occurs in a minority of normal cases, may account for the extremes of phenotypes that are seen occasionally in female members of PMD families. Marked variability in neuropathological changes in animals heterozygous for *Plp* gene mutations has been reported even within individuals and may also reflect the random nature of X-inactivation (Duncan *et al.*, 1987b).

4.2 Aims

The heterozygous knockout mouse (*Plp/Plp*^{tmkn1}) offers a unique opportunity to compare the survival and function of PLP/DM20-deficient oligodendrocytes and normal oligodendrocytes side-by-side *in vivo*. In order to establish if isolated

expression of the *Plp^{tmkn1}* allele could induce neurodegeneration in animals also expressing the wild type *Plp* allele, a histological and morphometric analysis of heterozygous knockout mice was undertaken. Immunohistochemistry was used to examine the contribution PLP/DM20-negative oligodendrocytes made to myelination.

4.3 Materials and Methods

4.3.1 Animal breeding

Animals were bred as described in 2.2 *Mouse Breeding* (page 39) and genotypes were confirmed by PCR (see 2.4 *PCR Genotyping*, page 53). During the study, 88 female mice were confirmed to be heterozygous for the *Plp^{tmkn1}* allele.

4.3.2 Histopathology

A histological survey of CNS tissue was performed on 1µm resin sections of spinal cord and optic nerve stained with methylene blue/ azur II (see 2.6.2 *Resin processing and sectioning*, page 59). Tissues were collected from 20, 60, 120, 240, 360 and 540 day-old heterozygous knockout mice and from occasional mice surviving past 540 days of age (n=39; 8 animals were 540 days of age or more).

4.3.3 Immunostaining

Immunohistochemistry was performed on 1µm resin sections from spinal cord (cervical, thoracic and lumbar) and optic nerve as described in 2.9 *Immunohistochemistry* (page 64). Tissue from at least three animals at 10, 20, 120, 240 and 360 days of age and from 6 animals over 540 days of age was examined.

4.3.4 Quantification of axonal changes

Axonal swelling and degeneration in mid optic nerve were assessed by point count analysis as described in 2.8.2 *Quantification of swollen axons and degenerate fibres* (page 62). Hemizygous knockout mice (n=4), heterozygous knockout mice (n=3) and wild type mice (n=3) were compared at 120 days of age.

4.4 Results

4.4.1 Clinical phenotype

Heterozygous knockout mice were indistinguishable from wild type controls until at least 360 days of age. In a proportion of older animals, neurological signs that mirrored those seen in older hemizygous knockout mice developed. Changes included perineal urine staining, poor grip, muscle wastage and paresis that progressed until euthanasia was necessary. The age of onset of the clinical

phenotype was variable even between littermates. Some mice survived to 720 days of age without developing overt signs of neurological dysfunction while others developed signs before 540 days of age.

4.4.2 Histopathology

From 120 days of age, heterozygous knockout mice developed the characteristic neurodegenerative changes seen in PLP/DM20-deficient animals. The changes included axonal swellings, degeneration and microgliosis. These initially affected small diameter fibre tracts but progressed to involve all white matter regions as the mice aged. Most older heterozygous knockout mice had moderate neurodegenerative changes, however, extremes of neurodegeneration were seen occasionally. Some animals had minimal changes at 540 days of age that correlated with normal phenotypes; others developed much more extensive neurodegeneration with early clinical phenotypes (Figure 41, page 136).

4.4.3 Myelin ultrastructure

Poorly compacted myelin sheaths were interspersed between normally compacted sheaths in heterozygous knockout mice (Figure 42, page 137). The distribution of the two populations of myelin sheath appeared to be uniform each being represented throughout the CNS and ensheathing a full range of axon diameters (unquantified data).

4.4.4 Mosaicism of *Plp* gene expression in oligodendrocytes

The myelin sheaths in the CNS of heterozygous knockout mice showed heterogeneity of PLP/DM20 protein expression with the presence of both PLP/DM20-positive and negative sheaths. Some areas appeared to have an evenly distributed mix of PLP/DM20-positive and negative sheaths giving a mosaic pattern of expression (Figure 43, page 138). Other areas had large patches that contained either predominantly PLP/DM20-positive or PLP/DM20-negative sheaths (Figure 43, page 138). The presence of PLP/DM20-deficient myelin was demonstrated by MBP immunoreactivity showing that the lack of PLP/DM20 staining did not indicate a lack of myelin (Figure 44, page 139). Quantification of myelin sheaths suggested that, on average, approximately 67% of sheaths were PLP/DM20-positive (I.R. Griffiths, personal communication), however, variability was seen both within and between individuals. At one extreme, some mice appeared to have predominantly PLP/DM20-positive myelin sheaths and this staining pattern was associated with minimal neurodegenerative changes in older animals (Figure 41, page 136).

4.4.5 Quantification of axonal changes in heterozygous knockout mice

Heterozygous knockout mice developed axonal pathology that was intermediate in degree between that found in hemizygous knockout mice and wild type controls (Figure 45, page 140). Heterozygous knockout mice developed approximately 38% of the volume of swollen axons than hemizygous knockout mice but a disproportionately lower volume of degenerate fibres (approximately 15%).

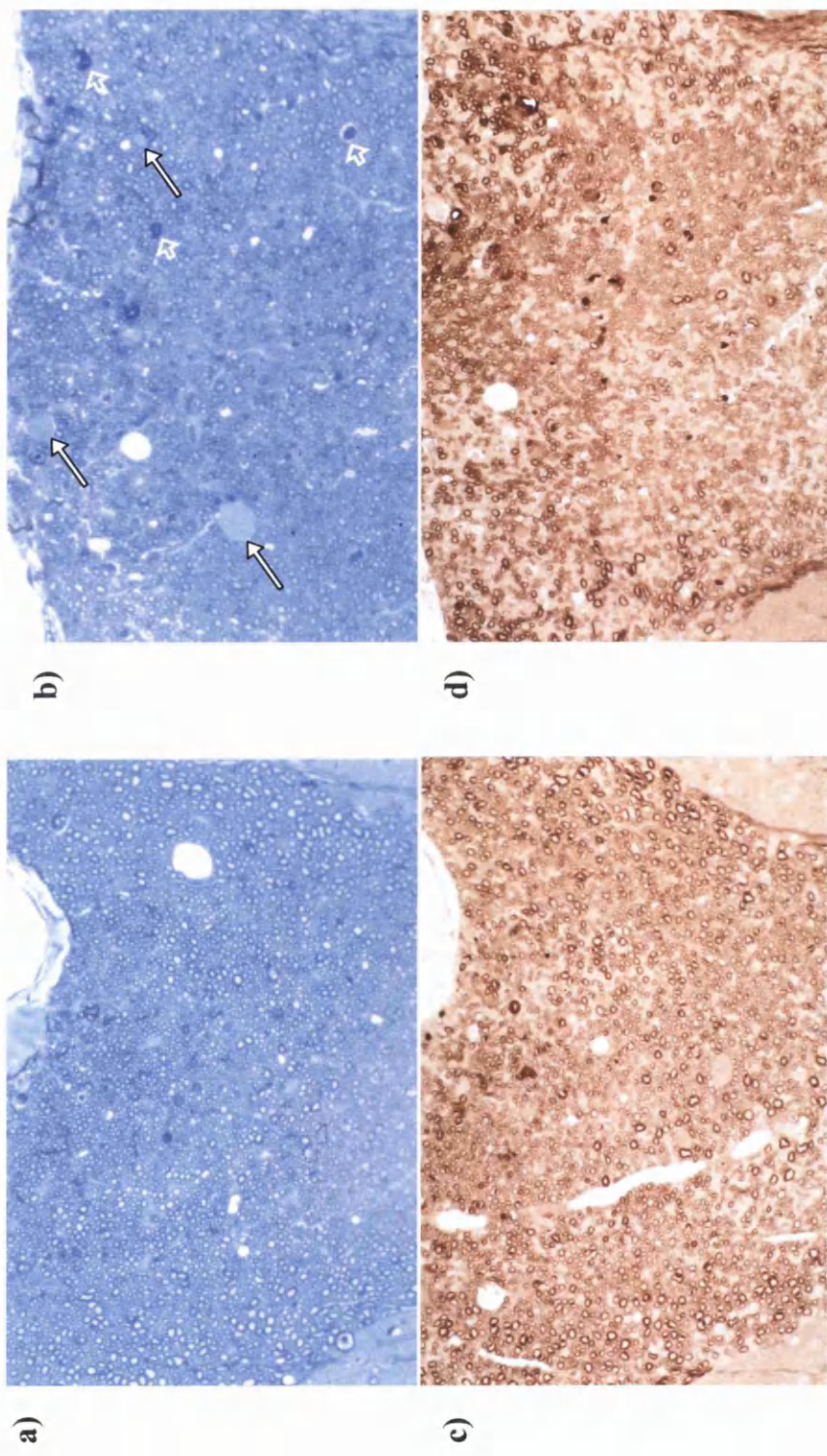


Figure 41 Fasciculus gracilis from mid-thoracic cord of 540-day-old heterozygous knockout mice stained with methylene blue/ azur II (sections a and b) and immunostained using PLP C-terminal antibody (PAP method; sections c and d). One animal (sections a and c) developed minimal neurodegenerative changes and no clinical phenotype that correlated with predominantly PLP/DM20-positive myelin sheaths. The other animal (sections b and d) developed moderate neurodegeneration including swollen axons (closed arrows) and fibre degeneration (open arrows) and a moderate clinical phenotype that correlated with a lower percentage of PLP/DM20-positive myelin sheaths (140x magnification)

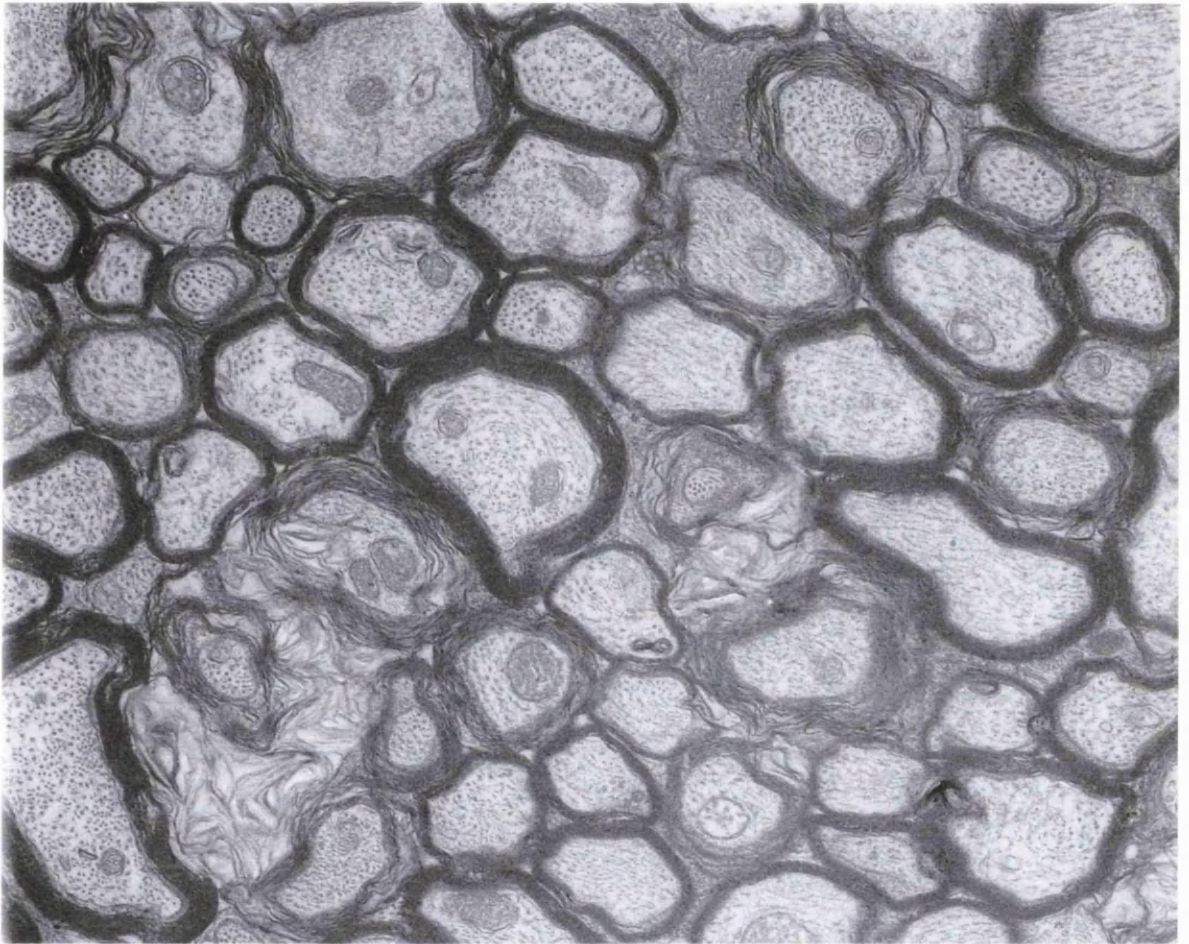
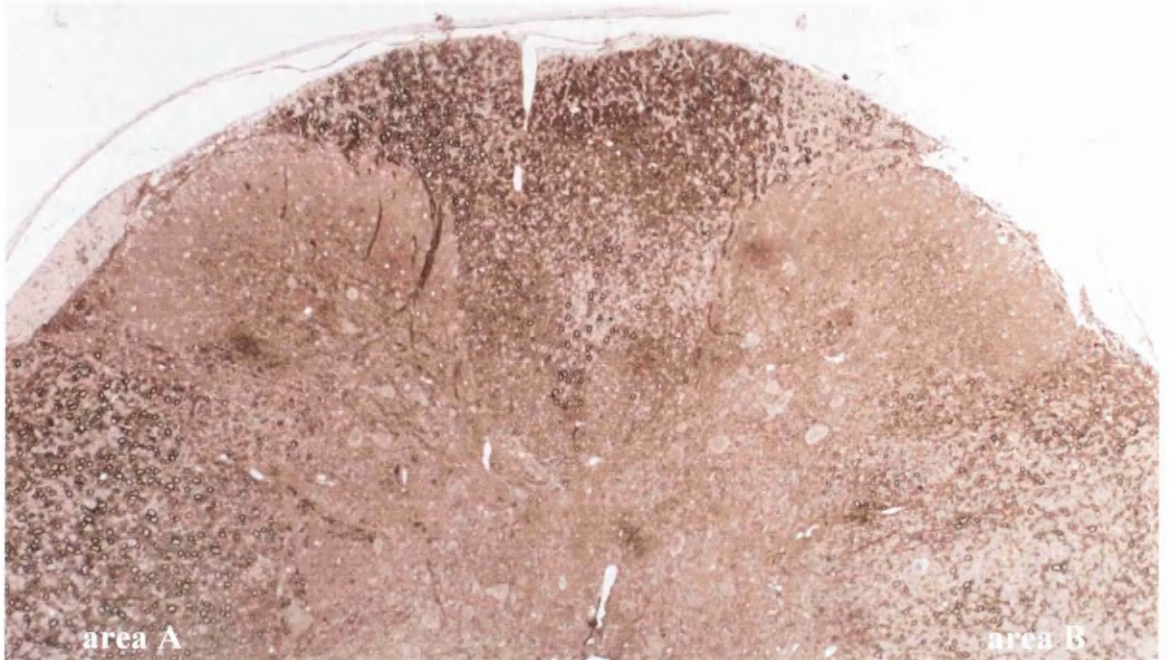
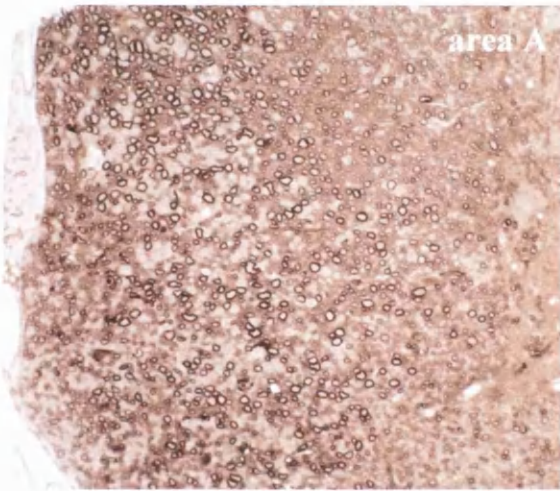


Figure 42 Electron micrograph of optic nerve from a 120 day-old heterozygous knockout mouse (20,000xmagnification)
Both well and poorly compacted myelin sheaths can be seen surrounding axons in this section.

a)



b)



c)

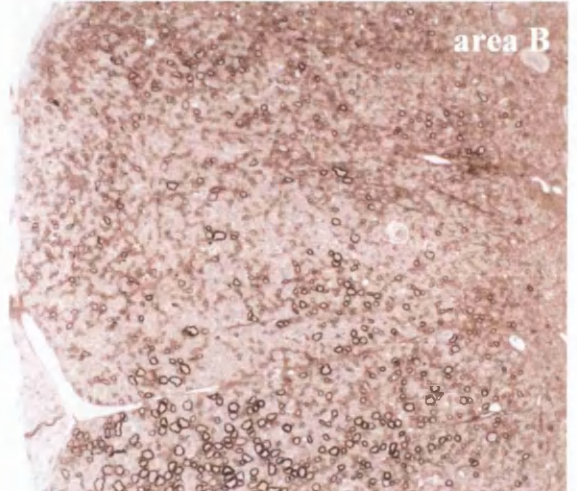
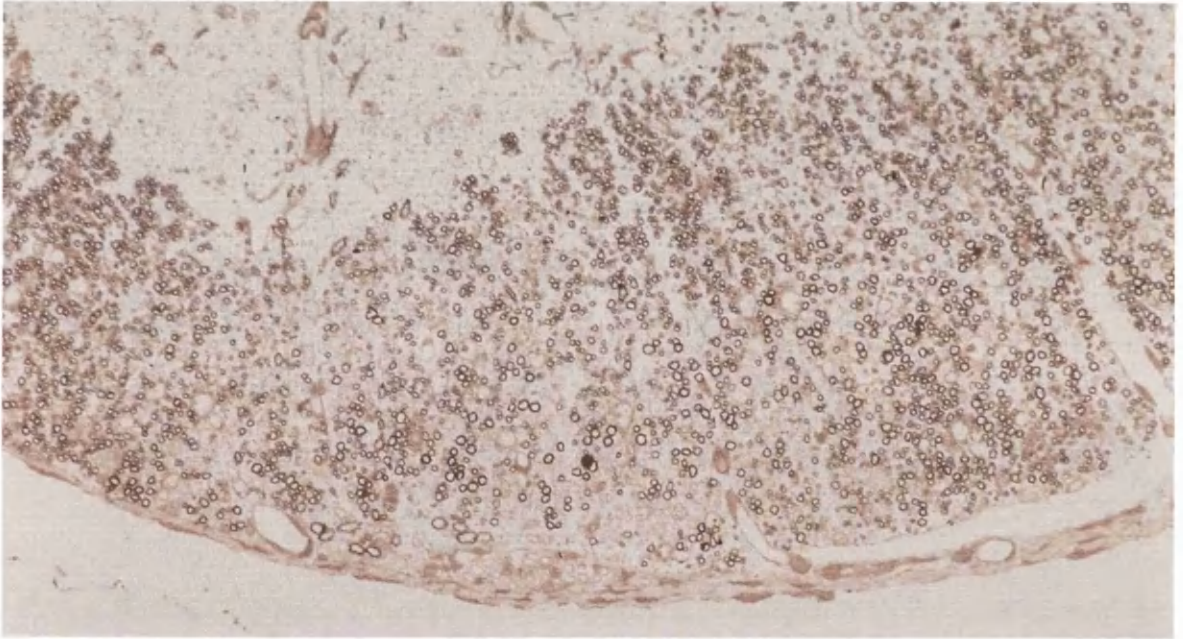


Figure 43 Resin section of dorsal and lateral columns from mid thoracic cord of a 360 day-old heterozygous knockout mouse immunostained with the PLP C-terminal antibody (PAP method)

a) The distribution of PLP/DM20-positive myelin sheaths is variable in this section with both patchy and evenly distributed patterns of immunoreactivity (100x magnification); (b) some areas have evenly distributed positive and negative myelin sheaths; (c) some areas have patches of either positive or negative myelin sheaths (200x magnification)

a)



b)

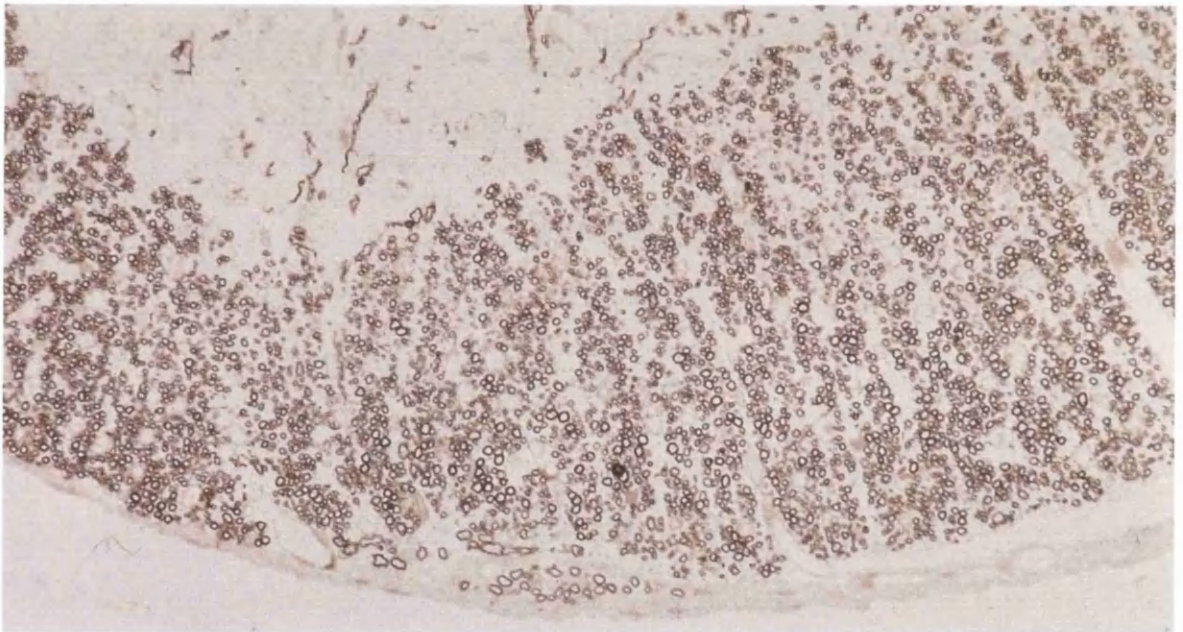


Figure 44 Ventral column of cervical spinal cord (C2-3) from a 20 day-old knockout heterozygous mouse immunostained showing a) PLP/DM20 and b) MBP immunoreactivity (200x magnification)

a) Patchy distribution of PLP/DM20-positive myelin sheaths reflected the variegated expression of the *Plp^{tmkn1}* allele in oligodendrocytes due to random X-inactivation

b) MBP-immunostained serial section demonstrates that PLP/DM20-deficient areas were not devoid of myelin

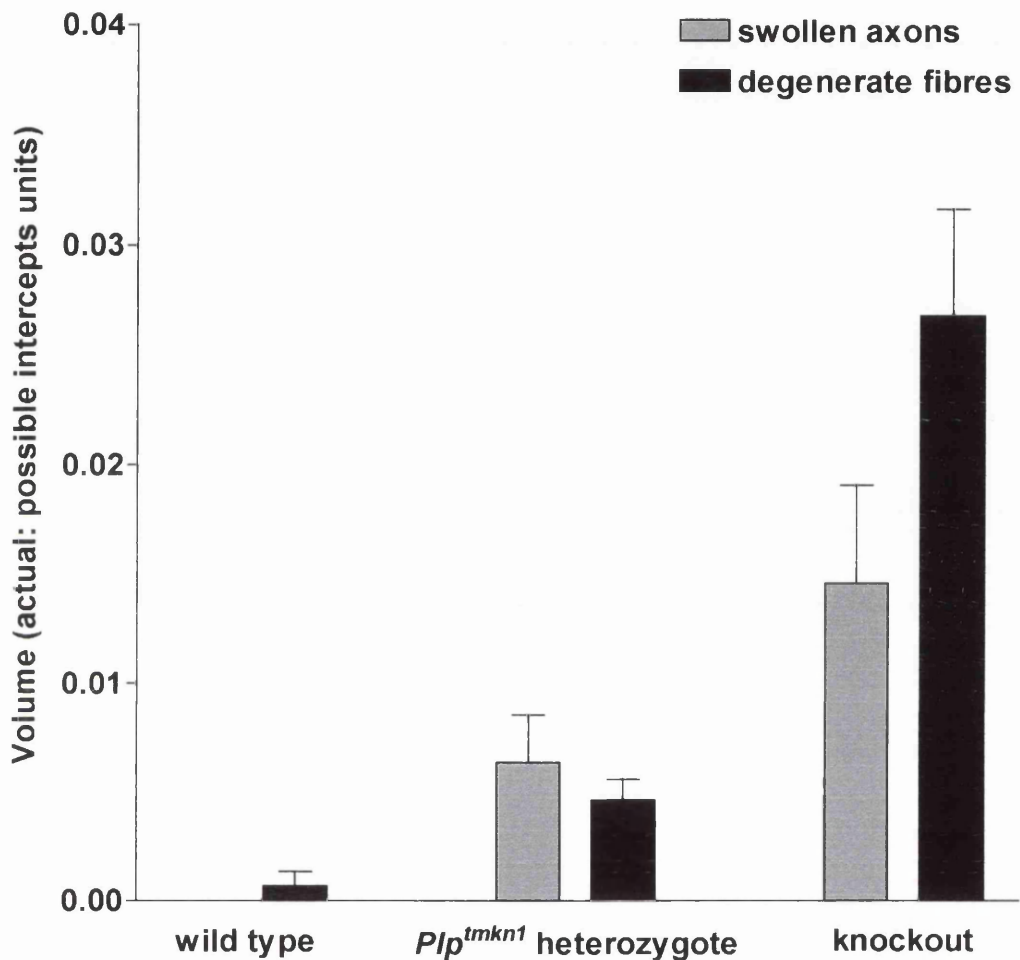


Figure 45 Swollen axon and degenerate fibre volumes assessed by point count analysis of mid optic nerves from 120 day-old wild type, heterozygous knockout and knockout mice. Heterozygous knockout mice showed reduced swollen axon and degenerate fibre volumes when compared to knockout mice. The reduction in degenerate fibre volume was disproportionately large.

4.5 Discussion

Data presented in this chapter demonstrated that mice heterozygous for the *Plp^{tmkn1}* allele developed an intermediate level of neurodegeneration when compared to hemizygous and wild type mice. Heterozygous knockout mice had mosaic patterns of *Plp* gene expression that could be diffuse or patchy and were maintained into adulthood. On average, approximately 67% of myelinated fibres had PLP/DM20-positive myelin sheaths (IR. Griffiths, personal communication) but extremes of *Plp* gene expression were also seen. The variable level of neurodegeneration and clinical phenotypes appeared to correlate broadly with the level of *Plp* gene expression.

The development of axonal swellings in heterozygous knockout mice provides further evidence that interaction with PLP/DM20-deficient oligodendrocytes may disrupt axonal function locally. Adjacent oligodendrocyte processes expressing wild type phenotypes (PLP/DM20-positive) cannot rescue the putative effects of PLP/DM20-deficient oligodendrocytes on axonal function. This suggests that PLP/DM20-deficient oligodendrocyte have either a toxic effect on axonal function or directly influence axonal function locally. However, comparative localisation of axonal changes with PLP/DM20-deficient oligodendrocyte processes has not been performed in this study and the possibility that these changes result from a primary neuronal defect cannot be excluded.

Heterozygous knockout mice developed a degree of axonal swelling that correlated with the proportion of PLP/DM20-deficient myelin sheaths when compared to hemizygous knockout mice (approximately 38%). Indirectly, this suggests that a relationship exists between the percentage of PLP/DM20-deficient oligodendrocyte processes and the severity of axonal swelling. However, the level of axonal degeneration did not follow a similar trend and was less than half the estimated level when compared with hemizygous knockout mice (approximately 15% instead of a predicted 33%). This may indicate that axonal degeneration depends on the cumulative effects of axonal compromise caused by axonal swellings along the length of each axon. In heterozygous knockout mice, the reduced volume of swollen axons may reduce the level of axonal compromise below the threshold for degeneration in the majority of axons. This may explain why some large swollen axons in the aged knockout mouse survive while other axons degenerate.

Although the majority of heterozygous knockout mice had approximately 67% PLP/DM20-positive myelin sheaths, variability was seen both between and within individual animals. The variability in neurodegenerative change and clinical

phenotype appeared to correlate loosely with the level of *Plp* gene expression. In particular, two aged mice (540 and 720 days of age), that had no clinical phenotype and only mild neurodegeneration, had a very low proportion of PLP/DM20-deficient myelin sheaths. The most likely explanation for these extremes of *Plp* gene expression is skewing of X-inactivation that occurs normally in a minority of cases (Belmont, 1996). The reciprocal effect of skewing towards expression of mutated *PLP* alleles in female carriers of PMD may explain the reports of female cases of PMD. Similar correlation of myelin mosaicism and phenotypic severity has been reported in heterozygous females from *shaking pup* colonies that show moderate, resolving clinical signs (Cuddon *et al.*, 1998).

The majority of animals heterozygous for *Plp* gene mutations do not develop clinical disease and show resolving areas of dysmyelination. This probably occurs because oligodendrocytes expressing the mutated allele die or remain inactive and are compensated for by neighbouring oligodendrocytes expressing the wild type allele (Skoff and Ghandour, 1995). Expression of the *Plp^{tmkn1}* allele does not affect oligodendrocyte maturation or survival but does seem to affect axonal function and moderately reduce the ability of mutant oligodendrocytes to elaborate myelin sheaths. In heterozygous knockout mice, oligodendrocytes expressing the *Plp^{tmkn1}* allele are predicted to survive to compete with oligodendrocytes expressing the wild type *Plp* allele. It may be that the survival of a large percentage of oligodendrocytes with mutant phenotypes enables significant neurodegeneration with clinical disease to develop in these mice, a scenario that does not occur in most spontaneous *Plp* gene mutant heterozygotes. A similar mechanism has been proposed to explain clinical disease in female members of a family with a mild form of PMD (Sivakumar *et al.*, 1999).

The distribution of PLP/DM20-negative oligodendrocyte processes in heterozygous knockout mice could be diffuse or patchy and varied both within and between individuals. Patchy areas devoid of *Plp* gene expression may reflect clonal expansion of oligodendrocyte progenitors that express the *Plp^{tmkn1}* allele through clonal inheritance of X-inactivation patterns in heterozygous knockout mice (Duncan *et al.*, 1993; reviewed by Willard, 1995). The patchy pattern mimics areas of dysmyelination seen in heterozygous carriers of spontaneous *Plp* gene mutations where similar distributions of two populations of oligodendrocytes may exist but are more difficult to detect.

5. Transgenic complementation of the *Plp* gene knockout mouse

5.1 Background

Different spatio-temporal expression patterns of PLP and DM20 proteins have led to suggestions that these two isoforms may have different roles in neural development and maintenance (as reviewed in the introduction to this thesis, page 18). The PLP protein has been implicated as an important structural component of compact myelin and the DM20 protein has been implicated in oligodendrocyte development because of its early expression in the embryonic CNS. Some *in vitro* studies suggest that the DM20 protein, which is more lipophilic than PLP (Horvath *et al.*, 1990), may facilitate cellular trafficking of the PLP protein to the cell surface and its subsequent incorporation into myelin presumably through heteromeric interaction (Sinoway *et al.*, 1994; Gow and Lazzarini, 1996; Tomic *et al.*, 1997). These studies show that both isoforms must be expressed in transfected cells before the PLP protein will reach the cell surface. However, other *in vitro* work contradicts these studies showing that PLP protein can reach the cell surface in the absence of DM20 protein (Gow *et al.*, 1994a; Thomson *et al.*, 1997). Clarification of how *in vitro* studies correlate with *in vivo* interactions between these two proteins has been hampered by the inability to directly identify the DM20 protein because it has no unique epitope that is not also present on the PLP protein. As such, although DM20 protein can be localised biochemically to the myelin sheath, it cannot be directly demonstrated in this compartment *in situ* nor can its cellular localisation to other compartments be confirmed. *Plp* gene products do not have cleaved targeting sequences (Milner *et al.*, 1985); however, the amino-terminal has been implicated in targeting these proteins to the cell surface (Colman *et al.*, 1982).

Although transgenic strategies have been developed to study some of these issues, they have been hampered by the inability to study expression of individual components of the *Plp* gene products in the absence of endogenous proteins *in vivo*. The knockout mouse provides a valuable tool for studying the roles of the *Plp* gene isoforms in isolation.

5.2 Aims

This study describes transgenic complementation of the knockout mouse. In order

to confirm that the phenotypic changes described in the knockout mice were attributable directly to the loss of *Plp* gene function, knockout mice were complemented with genomic *Plp* transgenes. Histopathology and morphometric analyses were used to determine if transgenic expression of the *Plp* gene products prevented the neurodegenerative and myelin changes in the knockout mice. To examine the different behaviour of individual isoforms, knockout mice were complemented with *Plp*-cDNA and *Dm20*-cDNA transgenes. To examine the ability of the PLP-LacZ fusion protein to incorporate into the myelin sheath in the absence of endogenous *Plp* gene products, knockout mice were complemented with *Plp-LacZ* fusion transgene (Wight *et al.*, 1993).

5.3 Materials and Methods

5.3.1 Animal breeding and identification

Animals were bred as described in 2.2 *Mouse Breeding* (page 39). Complementation of the knockout mouse with genomic *Plp* transgenes was achieved by crossing with the #66 and #72 lines of mice (Readhead *et al.*, 1994). Complementation of the knockout mouse individually with the PLP and DM20 protein isoforms was achieved by crossing with the *PlpTg1* and *Dm20Tg2* transgenic lines (Nadon *et al.*, 1994) and with the ND3A transgenic line (Mastronardi *et al.*, 1996). The genotypes of these transgenic crosses were confirmed by PCR (see 2.4 *PCR Genotyping*, page 53). The *Plp-LacZ* transgenic mice were maintained as homozygous stock and crossed with homozygous female knockout mice producing male offspring that were hemizygous for both the *Plp-LacZ* transgene and the *Plp^{tmkn1}* allele.

5.3.2 Molecular characterisation of the transgenic complementation models

Plp gene expression in the various mice was compared by semi-quantitative RT-PCR and western analysis at 20 days of age.

5.3.2.1 Tissue collection

Total cellular RNA was extracted from whole brain homogenates as described in 2.3.3 *Extraction of RNA from mouse tissue* (page 47). Protein was extracted from whole brain homogenates and from the myelin fraction of brain as described in 2.13.1 *Extraction of Protein from Tissue* (page 75)

5.3.2.2 Semi-quantitative RT-PCR

To compare transcript levels of the endogenous *Plp* gene and transgenes, semi-quantitative RT-PCR was performed as described in *2.11 Semi-quantitative RT-PCR* (page 71).

5.3.2.3 Western analysis

To compare translation of endogenous *Plp* gene and transgene transcripts, western analysis of protein samples using the anti-PLP C-terminal antibody was performed as described in *2.13 Western Blotting* (page 75).

5.3.3 Histopathology

A histological survey was performed on 1µm resin sections, stained with methylene blue/ azur II, from a range of CNS tissues including spinal cord and optic nerve (see *2.6.2 Resin processing and sectioning*, page 59). Knockout mice complemented with the #66, #72, *PlpTg1* and *Dm20Tg2* transgenes were compared to knockout and wild type controls at 120 days of age. Knockout mice up to 540 days of age complemented with the #72 transgene and up to 240 days of age complemented with the #66 transgene were also examined to establish if transgenic rescue of the knockout phenotype was maintained.

5.3.4 Axonal swelling and degeneration quantification

Point counts were performed on electron micrographs from mid optic nerves as described in *2.8.2 Quantification of swollen axons and degenerate fibres* (page 62). Data from three #72 transgene-complemented knockout mice were compared with data from *4.4.5 Quantification of axonal changes in heterozygous knockout mice* (page 135).

5.3.5 Glial cell quantification

Glial cell quantification was performed on ventral columns of spinal cord (C2-3) and mid optic nerve as described in *2.8.1 Quantification of corrected glial cell densities* (page 61). Data from three #72 transgene-complemented knockout mice were compared with data from *3.4.3.3.1 Corrected total glial cell densities and numbers* (page 88).

5.3.6 Immunostaining

Immunostaining was performed as described in *2.9 Immunohistochemistry* (page 64).

5.4 Results

5.4.1 #66 and #72 transgenic complementation of knockout mice

5.4.1.1 Clinical description

Knockout mice complemented with the #66 transgene (n=9) up to 240 days of age and complemented with the #72 transgene (n=19) up to 540 days of age were examined. Both groups of mice appeared to develop normally showing no evidence of neurological dysfunction. In particular, #72 transgene-complemented knockout mice maintained normal clinical phenotypes at least until 540 days of age (n=5) despite the development of typical knockout phenotypes in transgene-negative littermate controls that were hemizygous for the *Plp^{tmkn1}* allele (n=4).

5.4.1.2 #66 and #72 transgene expression in knockout mice

Transcript (Figure 46, page 147) and western analysis (Figure 47, page 148) showed that #66 and #72 transgenic complementation of knockout mice led to high levels of *Plp* gene expression at both transcript and protein levels.

5.4.1.3 Histological changes

Transgenic complementation with either transgene prevented the development of the neurodegenerative changes characteristic of knockout mice at 120 days of age. The mice developed well myelinated CNS white matter tracts (Figure 48, page 150) with no evidence of axonal swelling, axonal degeneration or microgliosis.

By 18 months of age, occasional swollen axons could be identified in the optic nerve and spinal cord of #72 transgene-complemented knockout mice. However, marked neurodegeneration similar to that seen in the knockout mice did not develop and extensive axonal changes, microgliosis and demyelination that have been reported as late changes in hemizygotes from the #66 and #72 transgenic line (Anderson *et al.*, 1998) were not seen (Figure 49, page 151).

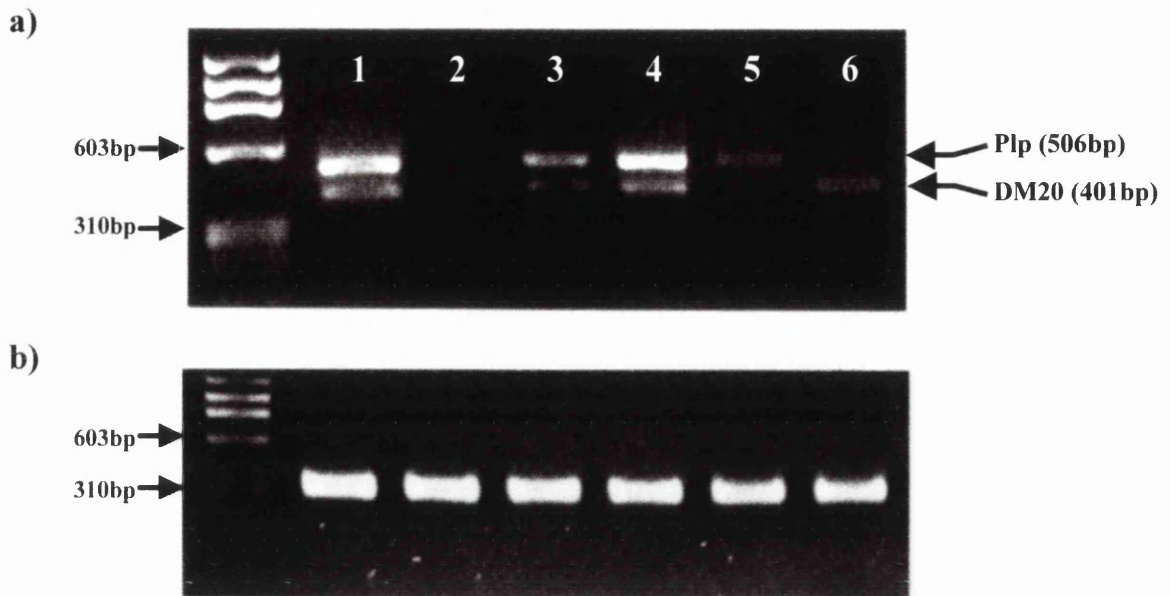


Figure 46 Semi-quantitative RT-PCR analysis of *Plp* gene isoform expression in knockout and transgene-complemented knockout mouse brain at 20 days of age. Lanes 1) wild type, 2) knockout, 3) #66 transgene-complemented knockout, 4) #72 transgene-complemented knockout, 5) *PlpTg1* transgene-complemented knockout, 6) *Dm20Tg2* transgene-complemented knockout, (size marker: DNA/*HaeIII*).

a) On comparison to wild type: no *Plp* or *Dm20* isoform PCR products were detected in the knockout mouse; low (#66) and comparable (#72) *Plp* and *Dm20* PCR products were detected in #66 and #72 transgene-complemented knockout mice; low levels of *Plp* and no *Dm20* isoform PCR products were detected in the *PlpTg1* transgene-complemented knockout mouse; no *Plp* and low levels of *Dm20* PCR products were detected in the *Dm20Tg2* transgene-complemented knockout mouse (30 cycles)

b) RT-PCR using primers designed to detect cyclophylin cDNAs were used to determine equivalency of sample loading and PCR conditions between samples (30 cycles)

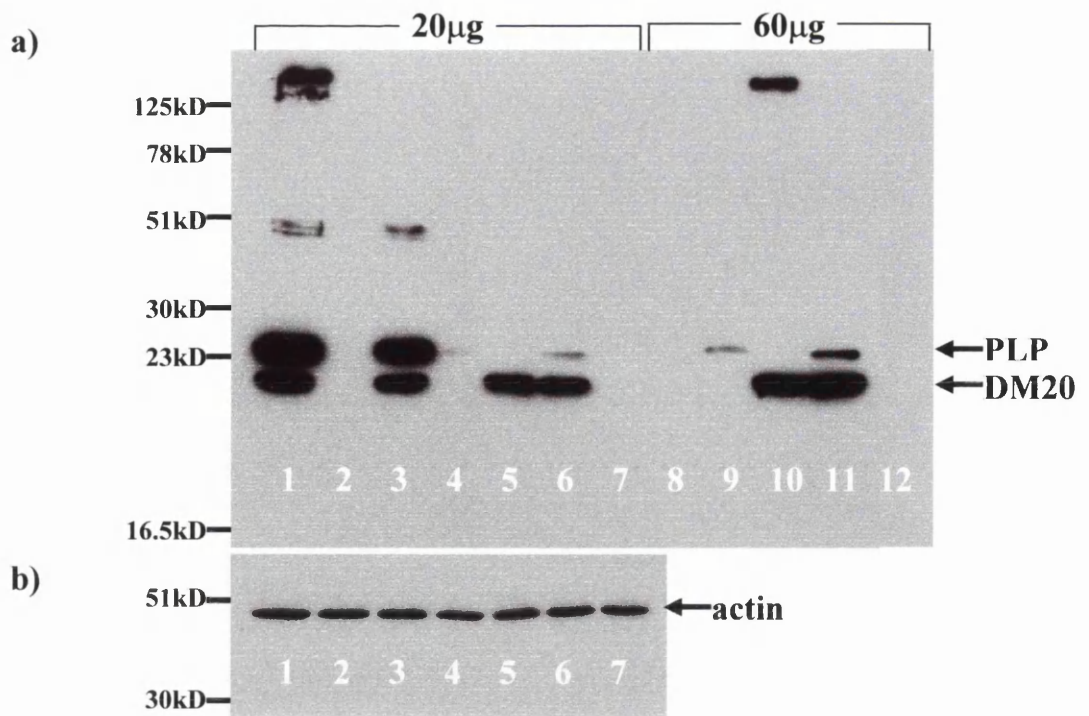


Figure 47 a+b) Western blot of 20 and 60μg aliquots of protein extracted from whole brain of 20 day-old mice.

a) Western blot probed for PLP and DM20 proteins.

Lane 1 - wild type mouse: PLP and DM20 proteins separated in the region of the 23kD marker. Higher molecular weight bands separated below the 51kD marker and above the 125kDa marker and may have represented aggregates of PLP and DM20 proteins.

Lanes 2 and 8 - knockout mouse: no PLP or DM20 protein could be detected in whole brain even at maximal loading (lane 8).

Lane 3 - #72 transgene-complemented knockout mouse: #72 transgenic complementation produced PLP and DM20 protein levels approaching those found in controls (lane 1).

Lanes 4 and 9 - *Plp*Tg1 transgene-complemented knockout mouse: PLP protein was detected but did not approach levels found in controls (lane 1). DM20 protein was not detected even at maximal loading (lane 9).

Lanes 5 and 10 - ND3A transgene-complemented knockout mouse: DM20 protein could be detected in levels approaching those found in controls (lane 1). PLP protein was not detected even at maximal loading (lane 10).

Lanes 6 and 11 - *Plp*Tg1 and ND3A transgenes-complemented knockout mice: Co-expression of *Plp*Tg1 and ND3A transgenes failed to increase PLP protein expression although higher molecular weight bands were seen.

Lanes 7 and 12 - *Dm20*Tg2 transgene-complemented knockout mouse: no DM20 protein could be detected.

b) Western blot probed for actin; lanes 1 to 7 as above: Probing for actin demonstrated that sample loading and detection were equivalent between samples.

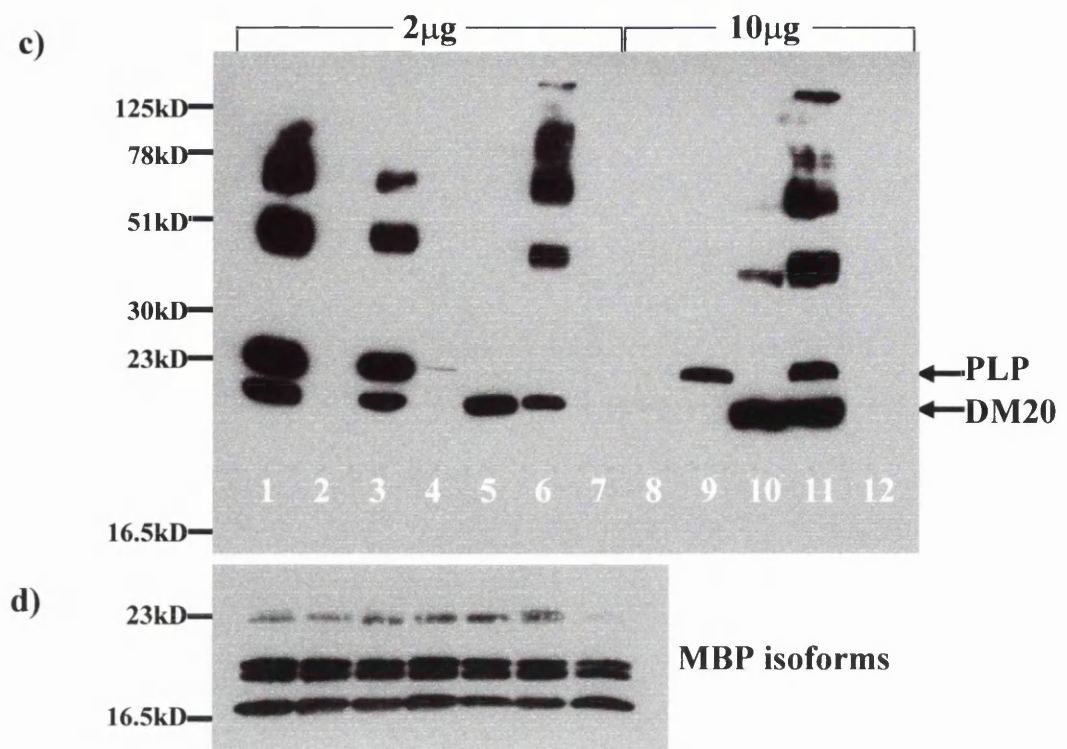


Figure 47 c+d) Western blots of 2 and 10µg aliquots of myelin protein extracts from 20 day-old mouse brain.

a) Western blot probed for PLP and DM20 proteins.

Lane 1 - wild type mouse: PLP and DM20 proteins and higher molecular weight bands are identified in myelin protein extracts.

Lanes 2 and 8 - knockout mouse: no PLP or DM20 protein could be detected in myelin even at maximal loading (lane 8).

Lane 3 - #72 transgene-complemented knockout mouse: PLP and DM20 proteins were present in myelin protein extracts in similar levels to controls (lane 1).

Lanes 4 and 9 - *PlpTg1* transgene-complemented knockout mouse: *PlpTg1* transgene products were identified in myelin extracts indicating that the transgene products enter the myelin sheath. No DM20 protein was detected even at maximal loading (lane 9) and the level of PLP protein was less than in controls (lane 1).

Lanes 5 and 10 - ND3A transgene-complemented knockout mouse: ND3A transgene products were identified in myelin extracts indicating that the transgene products enter the myelin sheath. Even at maximal loading, PLP protein was not detected but high molecular weight bands were identified (lane 10) suggesting that DM20 protein without PLP protein may be able to form aggregates.

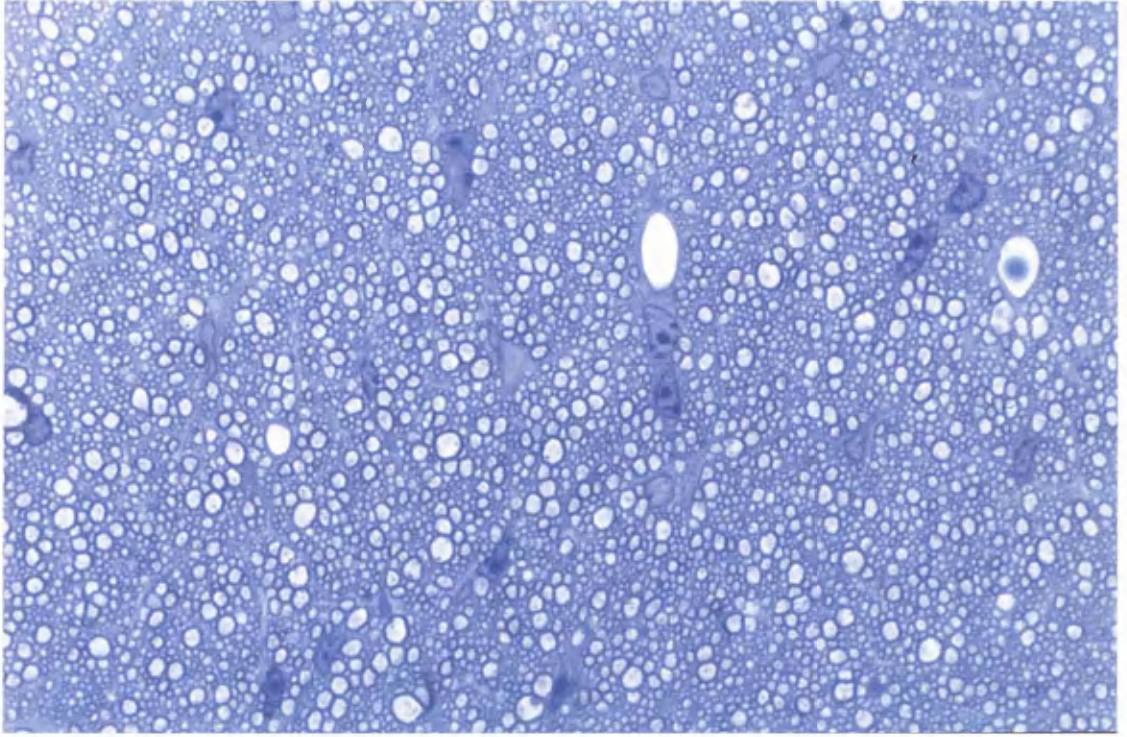
Lanes 6 and 11 - *PlpTg1* and ND3A transgenes-complemented knockout mice: Both transgene products were identified in myelin protein extracts.

Lanes 7 and 12 - *Dm20Tg2* transgene-complemented knockout mouse: no DM20 protein was detected even at maximal loading.

b) Western blot probed for MBP proteins; lanes 1 to 7 as above:

Probing for MBP proteins demonstrated that sample loading and detection were equivalent between samples.

a)



b)

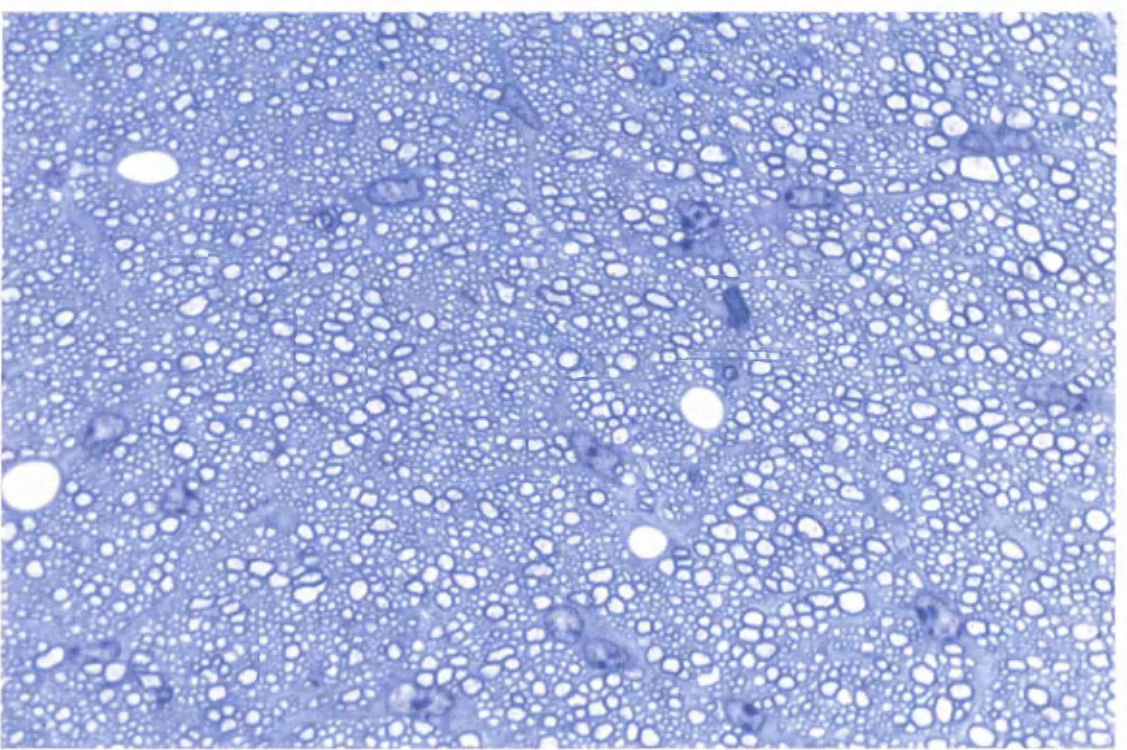


Figure 48 Methylene blue/ azur II stained section of mid optic nerve from 120 day-old knockout mice complemented with a) #72 transgenes and b) #66 transgenes showing no evidence of neurodegeneration or microgliosis (1000x magnification)

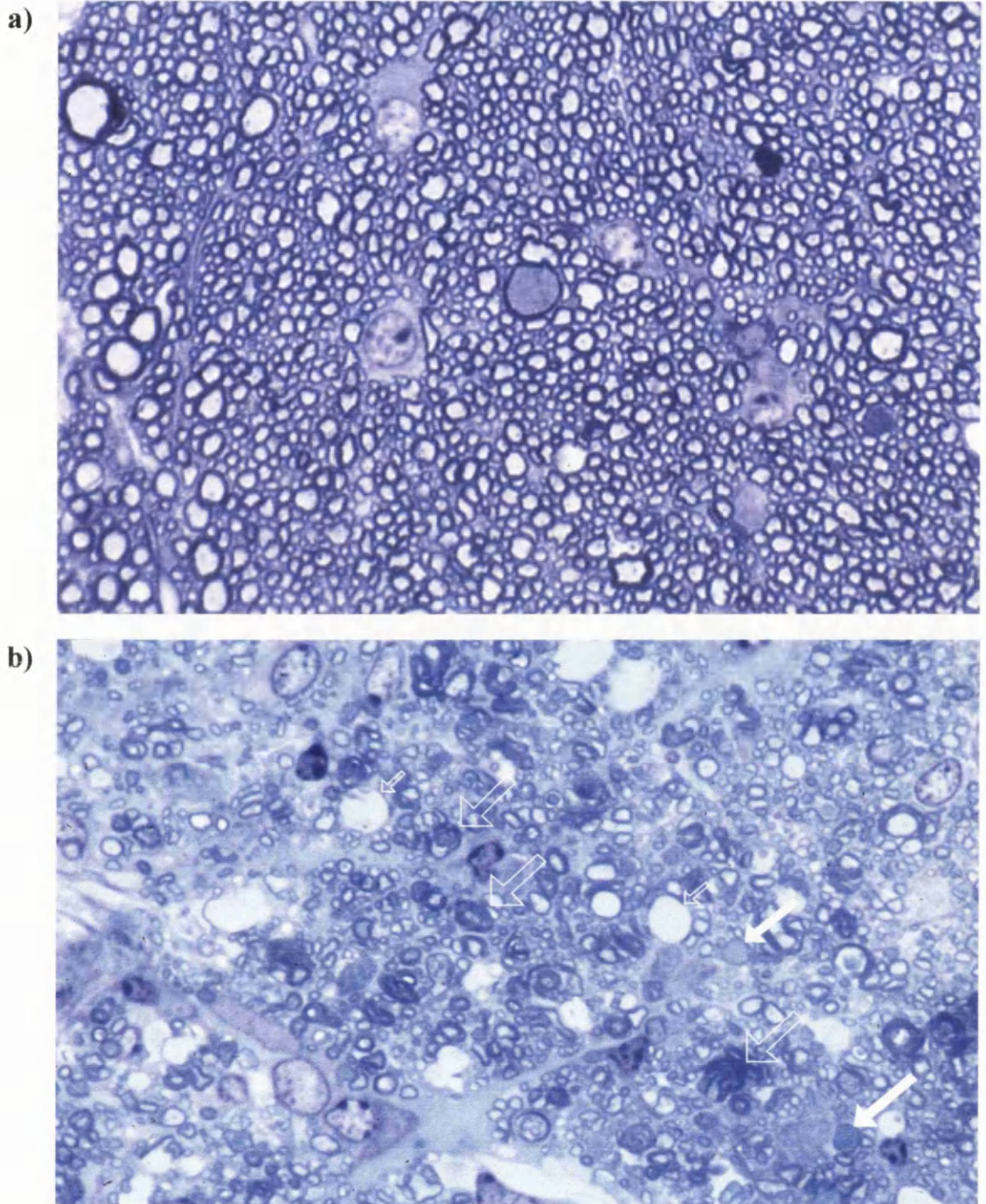


Figure 49 Methylene blue/ azur II stained 1 μ m resin sections of a) dorsal columns of spinal cord (C2-3) from a 540 day-old #72 transgene-complemented knockout mouse and b) mid optic nerve from a 568 day-old hemizygous #72 transgenic mouse (expressing the endogenous *Plp* allele) demonstrating the paucity of axonal swellings (filled arrows) in #72 transgene-complemented knockout mice compared to older animals from the #72 transgenic line. Older #72 hemizygotes also develop redundant myelin sheaths (large open arrows) and myelin vacuolation (small open arrows) (1400x magnification)

5.4.1.4 Immunohistochemistry

Knockout mice complemented with the #66 and #72 transgenes had *Plp* gene products localised to myelin sheaths in the CNS (Figure 50, page 153 and Figure 51a and b, page 154). Although the majority of myelin sheaths in the #72 transgene-complemented knockout mice showed PLP/DM20 immunoreactivity, a proportion did not. This feature was most obvious in the larger diameter fibres of the ventral columns of spinal cord (C2-3) (Figure 51c, page 154) but could be identified throughout the CNS. Despite this finding, the occasional swollen axons in aged #72 transgene-complemented knockout mice could not be localised with PLP/DM20-deficient myelin sheaths (Figure 51d, page 154).

5.4.1.5 Myelin ultrastructure

Ultrastructural examination revealed that the myelin sheaths in #72 transgene-complemented knockout mice showed no decompaction or intraperiod line abnormalities (Figure 52, page 155).

5.4.1.6 Analysis of axonal swelling and degeneration

Point count analysis revealed that the #72 transgene-complemented knockout mice (n=3) had no axonal swellings at 120 days of age. These mice did have occasional degenerate fibres at 120 days of age that were similar in quantity to wild type controls (n=3) and markedly lower than in knockout animals (n=4) (Figure 53, page 156).

5.4.1.7 Glial cell quantification

At 120 days of age, #72 transgene-complemented knockout mice had glial cell densities in the ventral columns of spinal cord (C2-3) and mid optic nerve that were indistinguishable from wild type controls and that were significantly lower than knockout controls ($P=0.0238$) (Figure 54, page 157).

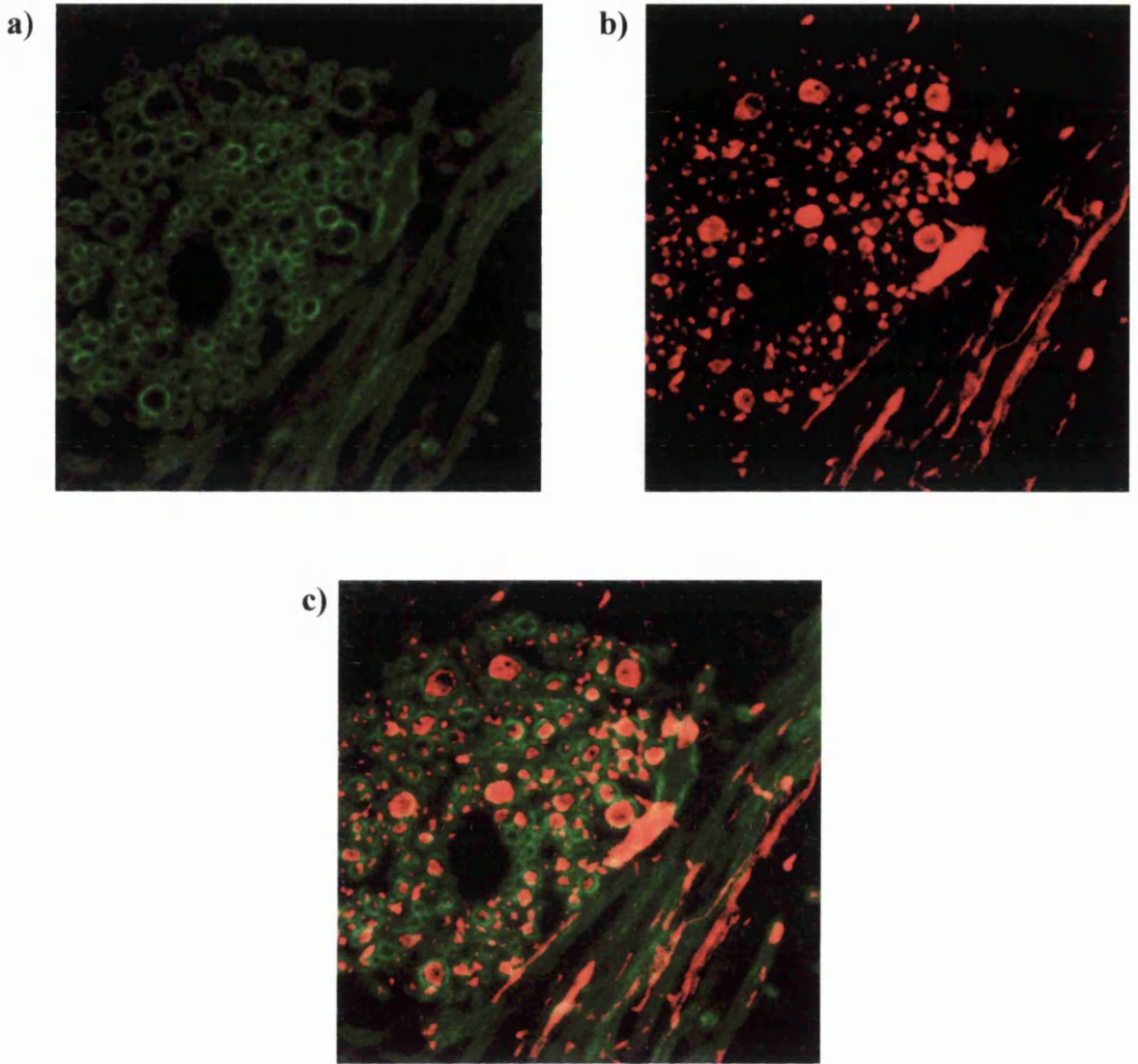


Figure 50 50 μ m vibratome section of cervical cord from 20 day-old #72 transgene-complemented knockout mice showing transgene expression in a cluster of myelinated fibres in the grey matter. The section has been immunostained to show a) PLP/DM20 protein (green) in the myelin sheath, b) phosphorylated neurofilaments (red) in the axon and c) both demonstrating that transgene products localised to the myelin sheath (1300x magnification)

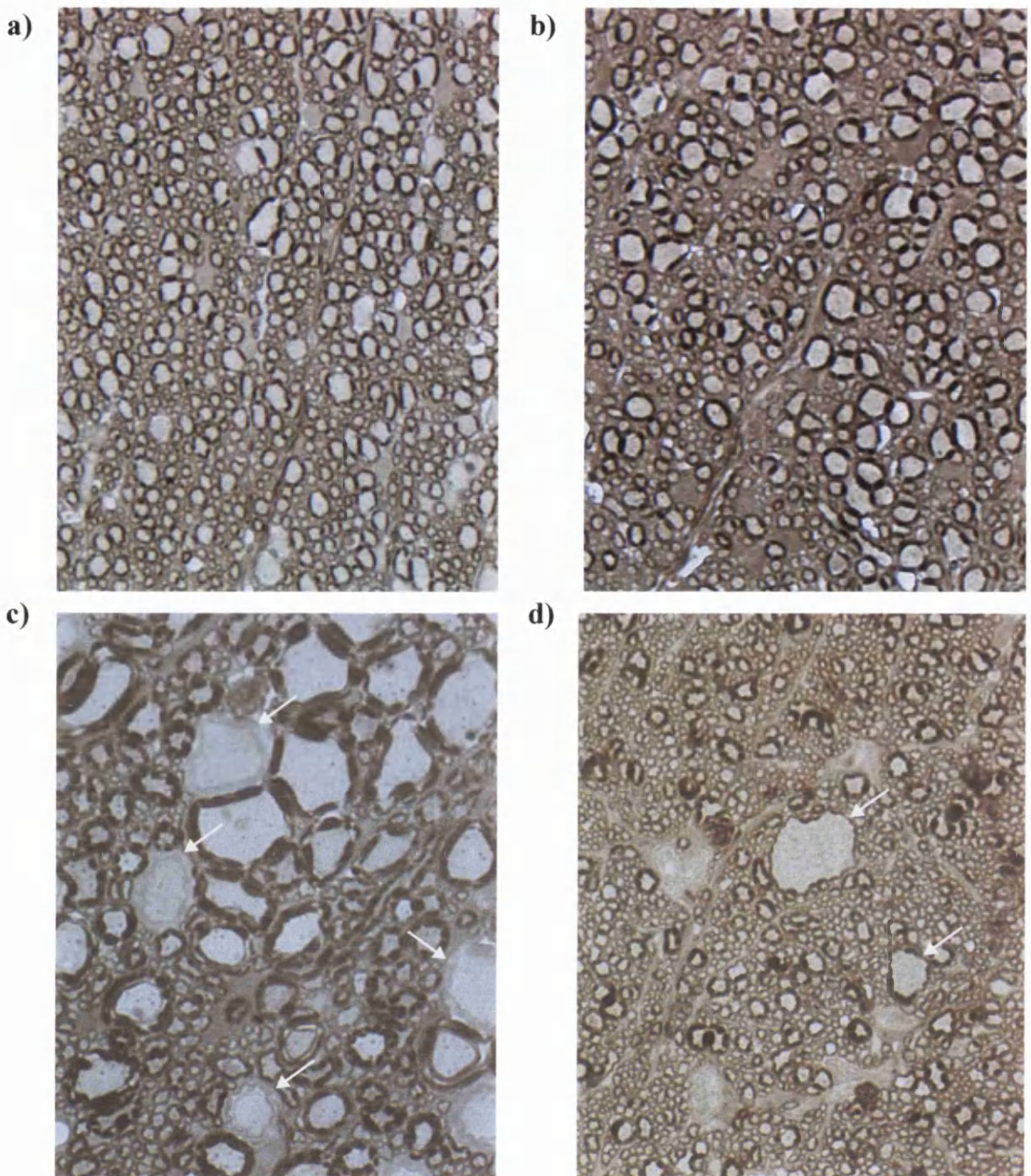


Figure 51 PLP/DM20-positive myelin in 1µm resin sections (PAP method) from #66 and #72 transgene-complemented knockout mice

Ventral columns of spinal cord (C2-3) from 120 day-old knockout mice complemented with a) #72 transgenes and b) #66 transgenes demonstrating transgene products in myelin (615x magnification)

Ventral columns of spinal cord (C2-3) from a 540 day-old #72 transgene-complemented knockout mouse (c) demonstrating several PLP/DM20-negative myelin sheaths (arrows). Mid optic nerve from the same animal (d) showing two swollen axons surrounded by PLP/DM20-positive myelin (arrows) (1067x magnification)

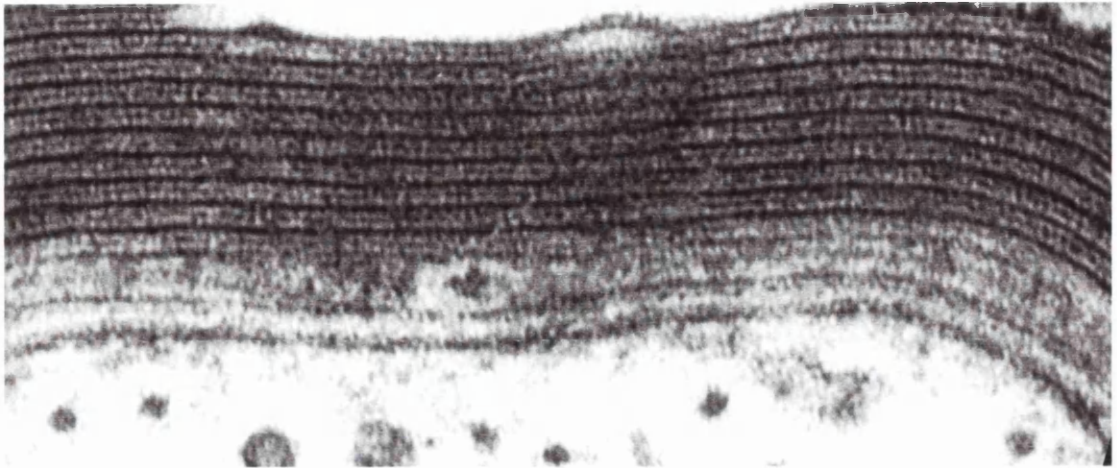


Figure 52 Myelin periodicity in #72 transgene-complemented knockout mice is normal (240,000x magnification)

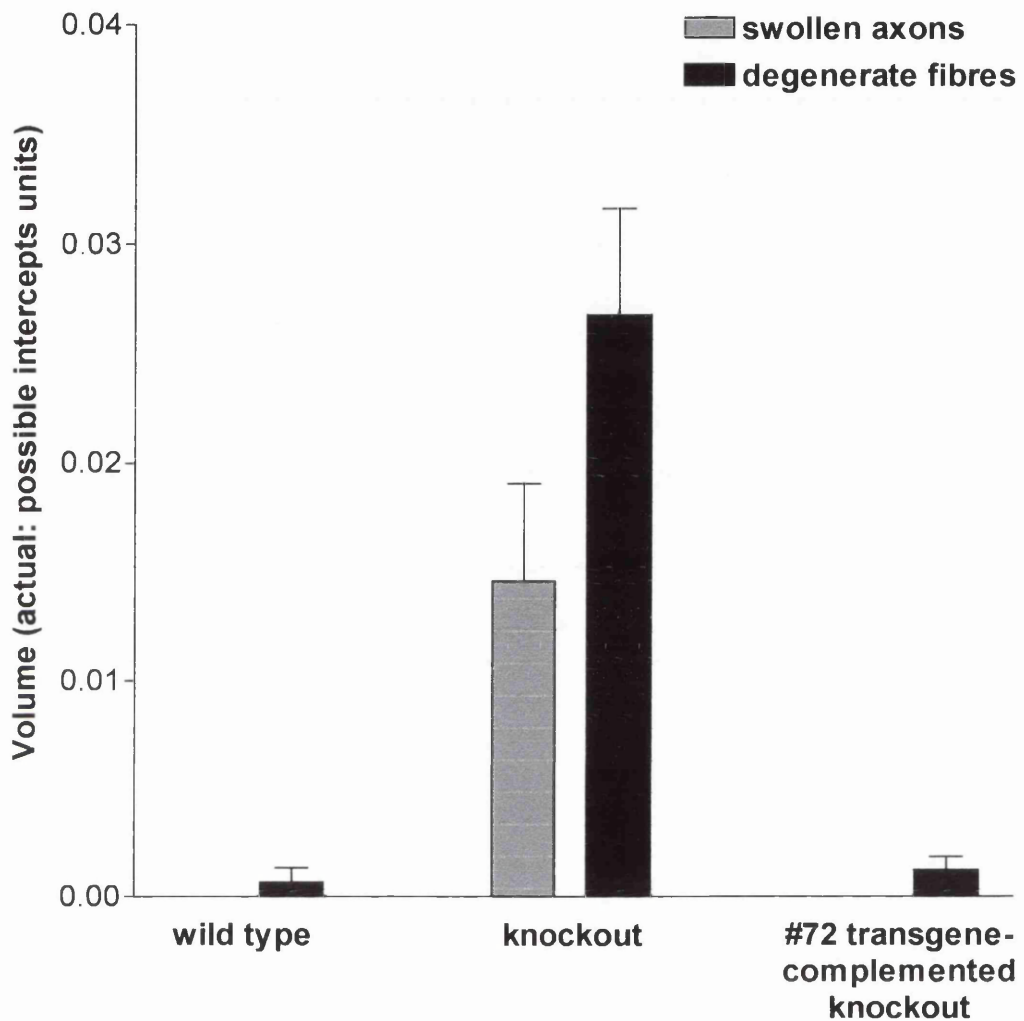


Figure 53 Swollen axon and degenerate fibre volumes assessed by point count analysis of mid optic nerve from 120 day-old wild type, knockout and #72 transgene-complemented knockout mice. #72 transgene-complemented knockout mice were indistinguishable from wild type controls and had no axonal swellings at this age.

- wild type
- knockout
- #72 transgene-complemented

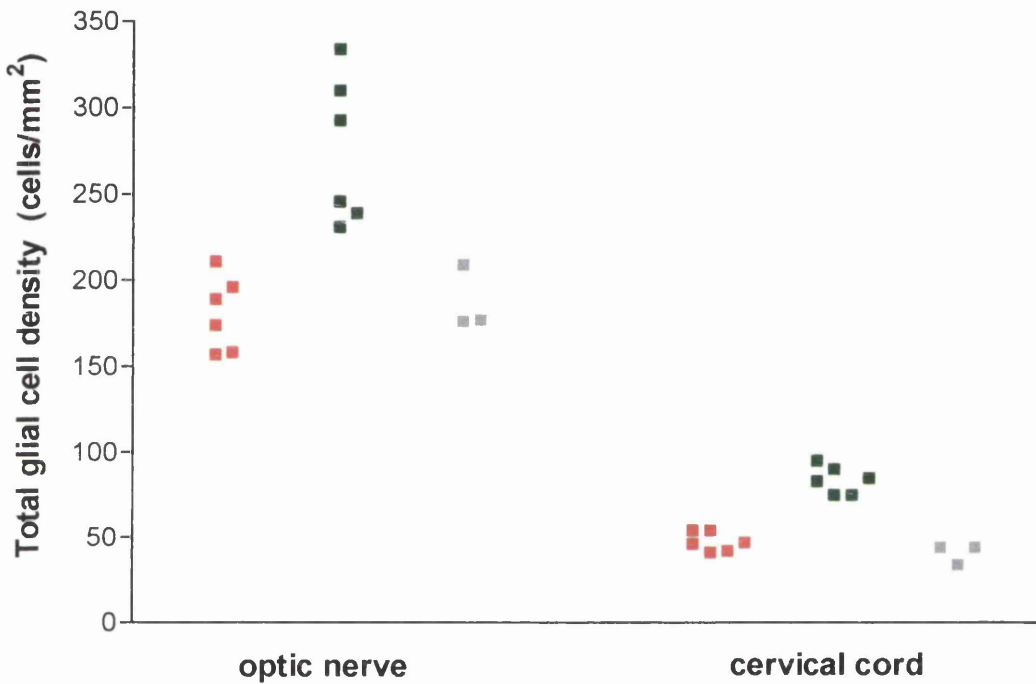


Figure 54 Total corrected cell densities of mid optic nerve and ventral columns of spinal cord (C2-3) from wild type, knockout and #72 transgene-complemented knockout mice at 120 days of age. #72 transgene-complemented knockout mice, unlike knockout mice, did not develop a gliosis and were indistinguishable from wild type controls.

5.4.2 *Plp*-cDNA and *Dm20*-cDNA transgenic complementation of knockout mice

5.4.2.1 Clinical description

PlpTg1 and *Dm20Tg2* transgene-complemented knockout mice developed progressive neurological dysfunction from 12 months of age that was indistinguishable from the knockout phenotype. Early in the course of the investigation, it became apparent that the *Dm20Tg2* transgene-complemented knockout mice did not produce detectable levels of the DM20 protein isoform in central neural tissue (see below). The ND3A transgenic line was obtained from FG. Mastronardi (Department of Biochemistry, University of Toronto) in the hope that this line would produce the DM20 protein in knockout mice. As these mice only became available towards the end of this project, a more detailed description of their clinical features was not possible.

5.4.2.2 *PlpTg1* transgene-complemented knockout mice

5.4.2.2.1 Transgene expression

PlpTg1 transgenic expression in knockout mice produced levels of *Plp*-mRNA considerably lower than in the wild type controls, when compared by semi-quantitative RT-PCR (Figure 46, page 147). PLP protein isoform was detected in the myelin fraction on Western analysis (Figure 47, page 148). The *Dm20* isoform was not expressed at either transcript or protein levels in *PlpTg1* transgene-complemented knockout mice.

5.4.2.2.2 Histological changes

PlpTg1 transgene-complemented knockout mice developed neurodegenerative changes by 120 days of age that were indistinguishable from the pathology in knockout mice (n=5) (Figure 55, page 160).

5.4.2.2.3 Immunohistochemistry

Tissue collected at 20 days of age for cryostat sections and from a range of ages for perfusion fixation was immunostained using both fluorescent and PAP techniques. At 120 days of age, resin sections were immunostained using the PAP technique. At both ages, PLP protein could be identified in myelin sheaths surrounding small diameter axons in the spinal cord (C2-3) and mid optic nerve. Occasional profiles of larger myelin sheaths immunostaining for transgene products were seen but large diameter myelin sheaths in general appeared to be devoid of transgene products

(Figure 56, page 161).

5.4.2.2.4 Myelin ultrastructure

The ultrastructural features of myelin in the CNS of *PlpTg1* transgene-complemented knockout mice were indistinguishable from myelin in knockout controls (Figure 57, page 162). Myelin periodicity ranged from myelin with normal periodicity to myelin with condensation or splitting of the intraperiod lines.

5.4.2.3 *Dm20Tg2* transgene complemented knockout mice

5.4.2.3.1 Transgene expression

RT-PCR indicated that low levels of *Dm20Tg2* transgene transcripts were expressed in *Dm20Tg2* transgene-complemented knockout mice (Figure 46, page 147) and *Plp* isoform transcripts were not detected. However, the DM20 protein isoform could not be detected in the CNS on western analysis at 20 days of age (Figure 47, page 148) or by immunohistochemistry at any age examined (embryonic day 16 and postnatal day 1, 5, 10, 20, 120) (data not shown).

5.4.2.3.2 Histological changes

Dm20Tg2 transgene-complemented knockout mice developed neurodegenerative changes that were indistinguishable from knockout mice by 120 days of age (n=6) (Figure 55, page 160).

5.4.2.4 *PlpTg1/ Dm20Tg2* double transgenic complementation of the knockout mouse

Knockout mice complemented with both the *PlpTg1* and *Dm20Tg2* transgenes developed neurodegenerative changes and progressive clinical phenotypes that were indistinguishable from knockout mice or from the *PlpTg1* transgene-complemented knockout mice (n=10).

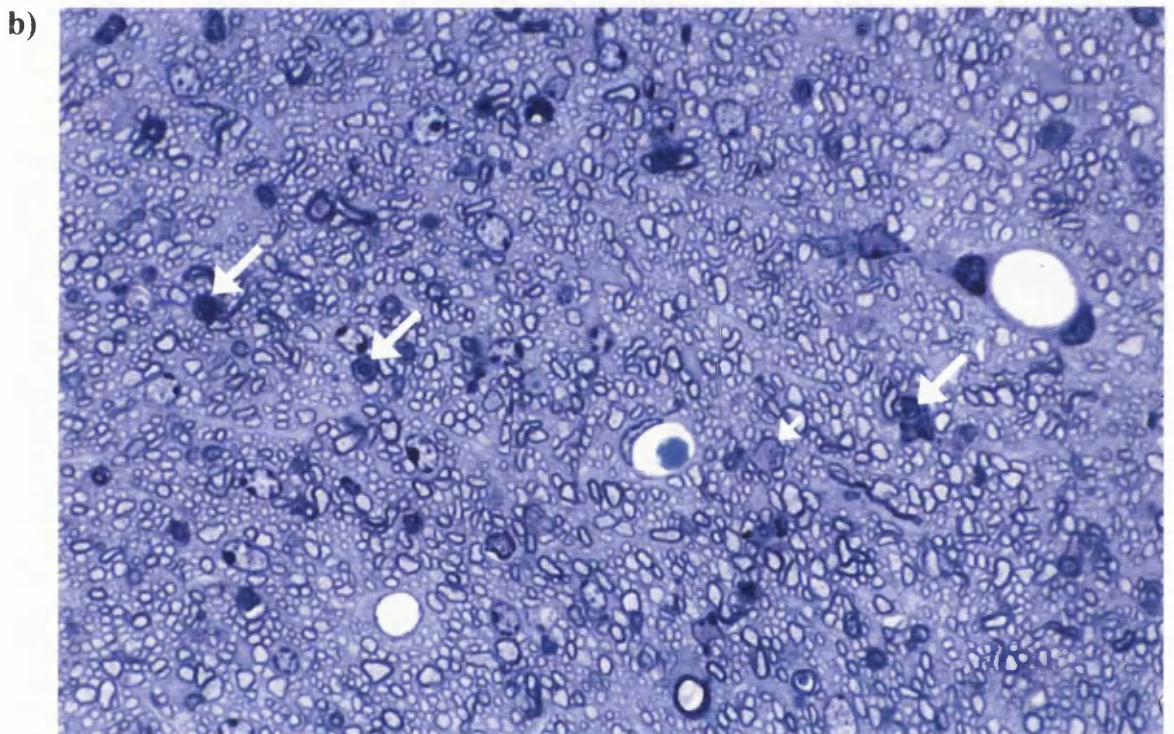
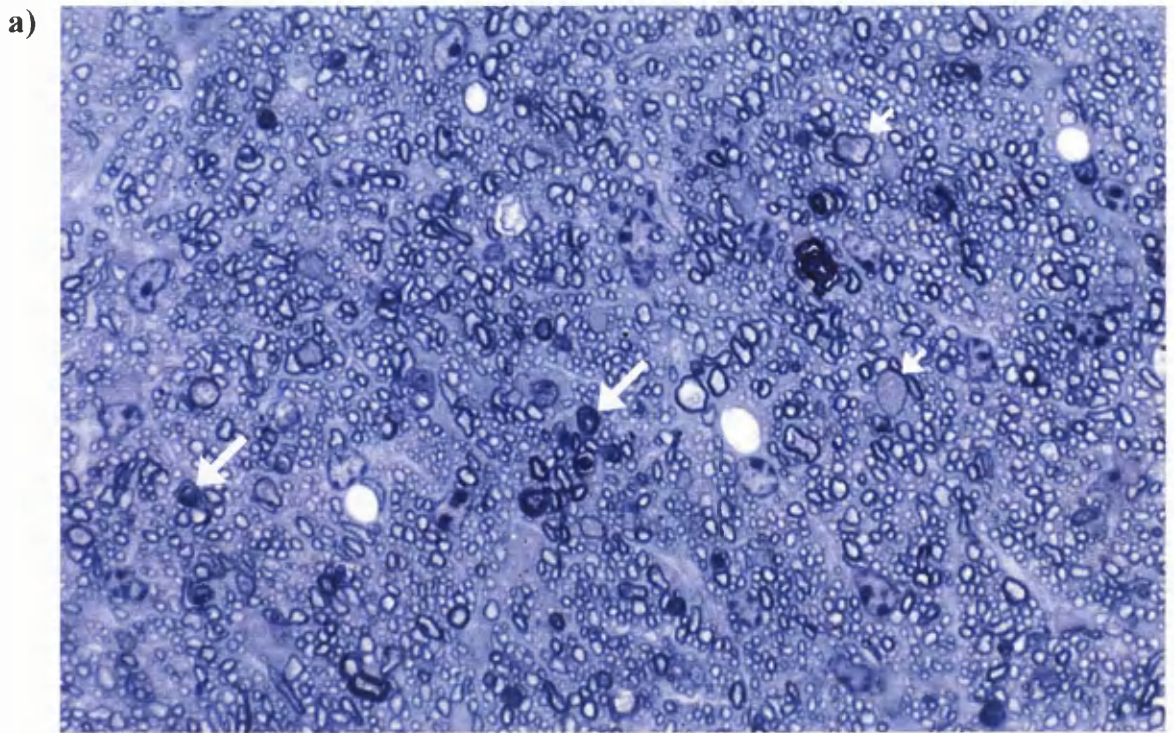


Figure 55 Methylene blue/ azur II stained 1µm resin sections of mid optic nerve from 120 day-old knockout mice complemented with the a) *PlpTg1* transgene and b) *Dm20Tg2* transgene. Both sections show evidence of axonal swelling (small arrows) and axonal degeneration (large arrows) (1000x magnification)

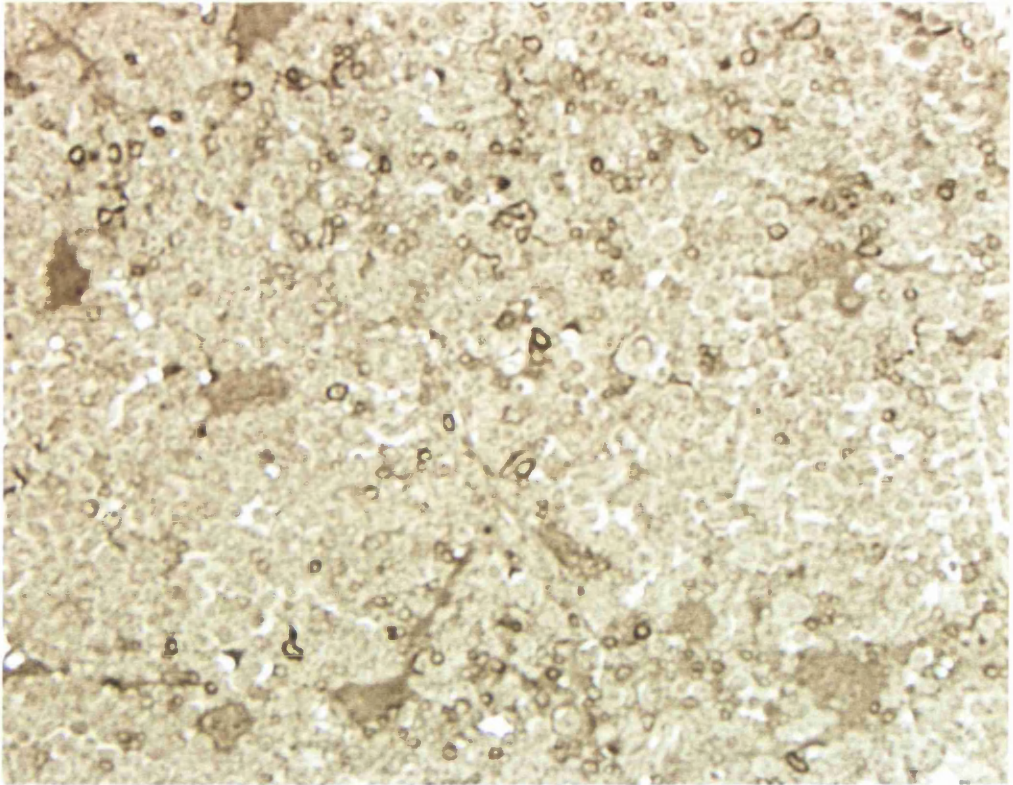
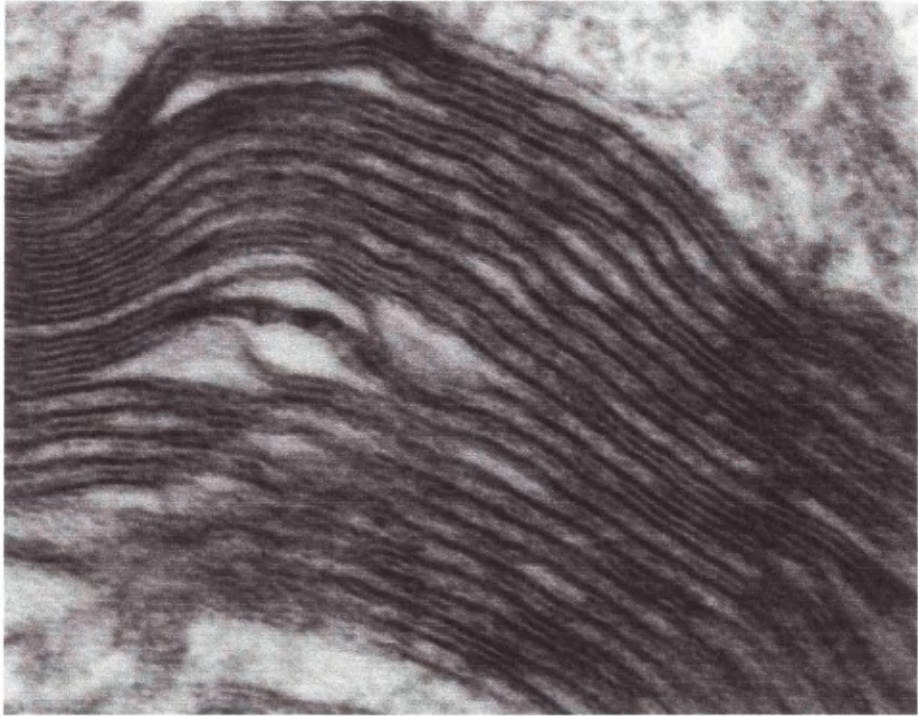


Figure 56 PLP/DM20 immunoreactivity in 1µm resin section of fasciculus gracilis from spinal cord (C2-3) of a *PlpTg1* transgene-complemented knockout mouse at 120 days of age. PLP/DM20-positive myelin sheaths can be seen surrounding some small diameter fibres (1300x magnification)

a)



b)

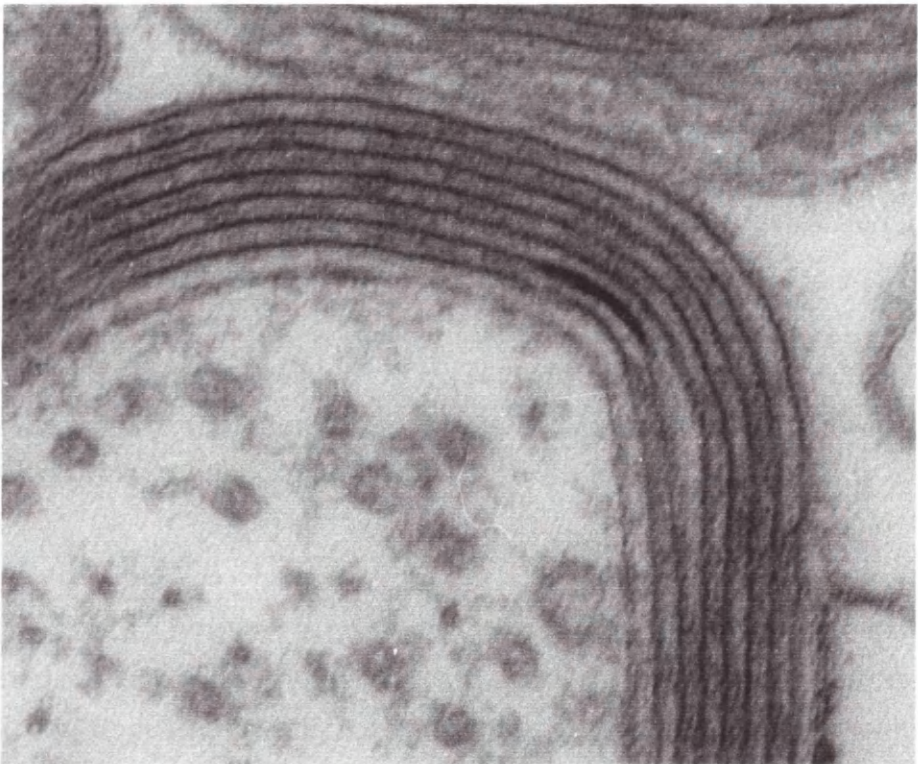


Figure 57 Myelin periodicity in *PlpTg1* transgene-complemented knockout mice (240,000x magnification)

a) *PlpTg1* transgene-complemented knockout mice had myelin lamellae with both condensation and splitting at the intraperiod line although some regions of individual lamellae appeared to have normal periodicity

b) Occasional myelin sheaths were found that were ultrastructurally normal

5.4.2.5 ND3A transgene-complemented knockout mice

5.4.2.5.1 Transgene expression

ND3A transgene-complemented knockout mice produced high levels of DM20 protein but no PLP protein. The transgene products were detected in the myelin fraction on western analysis (Figure 47, page 148).

5.4.2.5.2 Histological changes

ND3A transgene-complemented knockout mice develop neurodegenerative changes by 120 days of age that were indistinguishable from the knockout phenotype (n=4) (Figure 58, page 164).

5.4.2.5.3 Immunohistochemistry

The DM20 protein isoform incorporated into a full range of myelin sheaths by 20 days of age in ND3A transgene-complemented knockout mice (Figure 59, page 165). This was demonstrated by demonstrating PLP/DM20 immunoreactivity using the anti PLP C-terminal antibody and failing to demonstrate PLP protein isoform immunoreactivity using the anti PLP-specific antibody (Figure 59, page 165). By inference, DM20 protein isoform incorporated into a wide range of myelin sheaths within the CNS but no PLP protein isoform was produced.

5.4.2.5.4 Myelin ultrastructure

Myelin from ND3A transgene-complemented knockout mice showed the same range of ultrastructural abnormalities as that from knockout mice (Figure 60, page 166)

5.4.3 *PLP-LacZ* transgenic complementation of knockout mice

Knockout mice expressing the PLP-LacZ fusion protein produced detectable levels of the fusion protein that was expressed in the same spatial expression pattern as the *Plp* gene. In addition, the fusion protein incorporated into the myelin sheath (Figure 61, page 167).

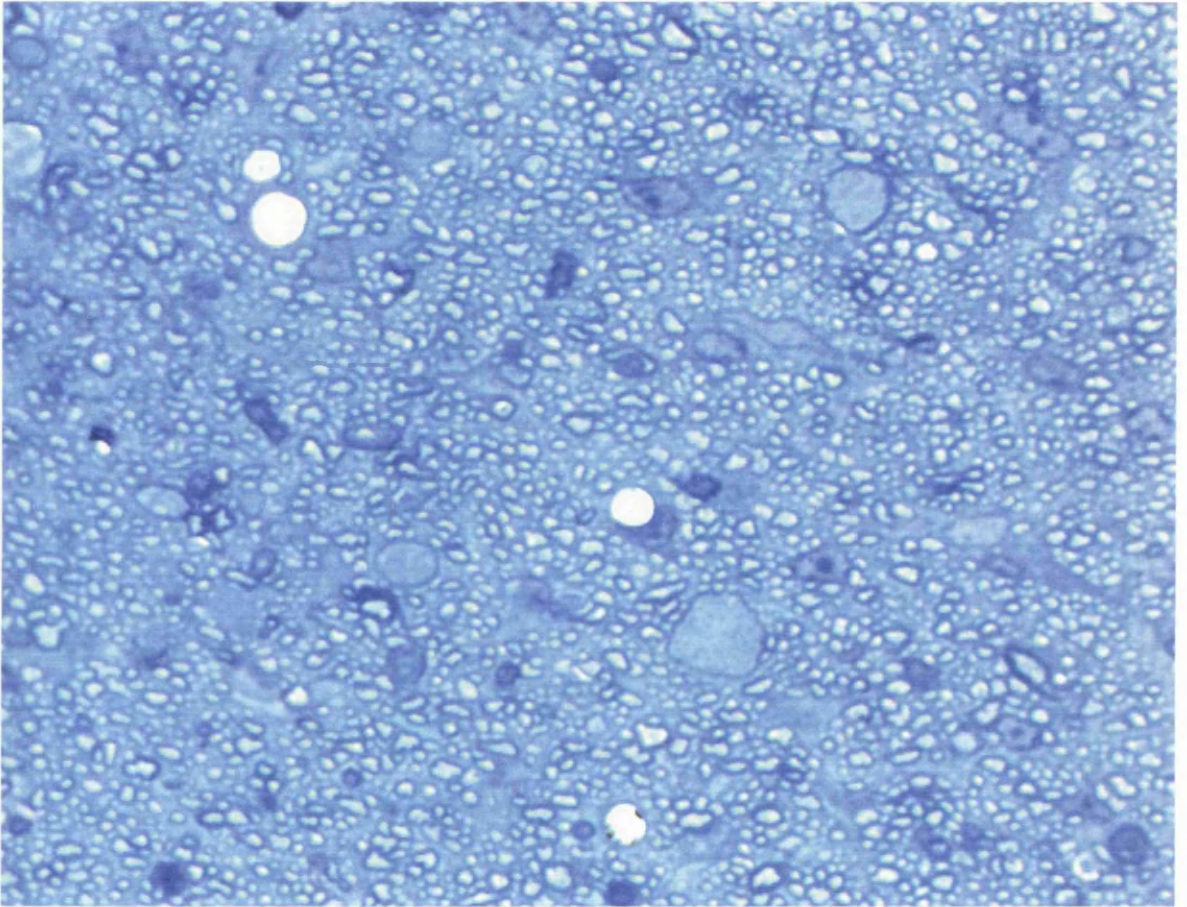


Figure 58 Methylene blue/ azur II stained 1µm resin section of mid optic nerve from a ND3A transgene-complemented knockout mouse at 120 days of age. Swollen axons and a microgliosis were seen by this age indicating that neurodegeneration developed in ND3A transgene-complemented knockout mice (1300x magnification)

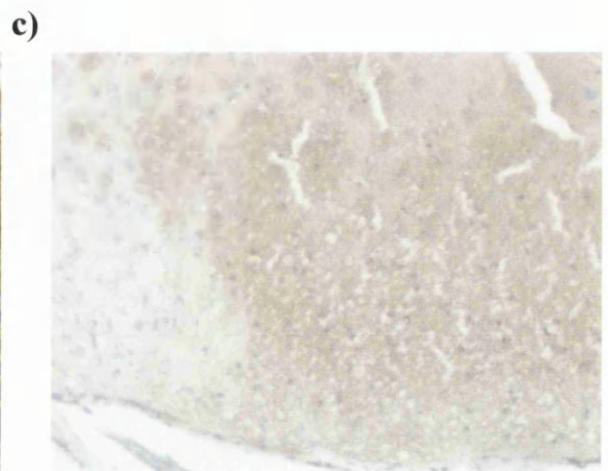
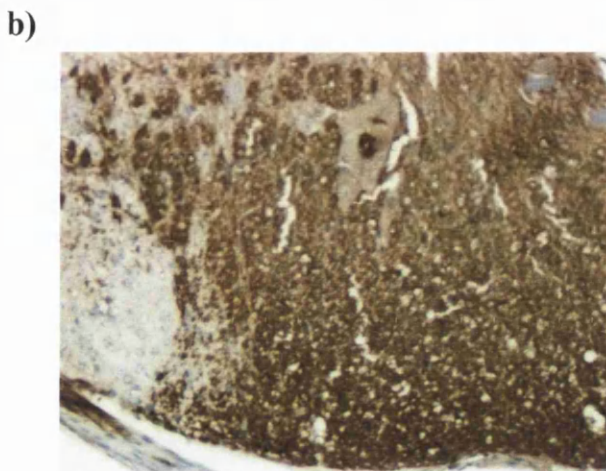
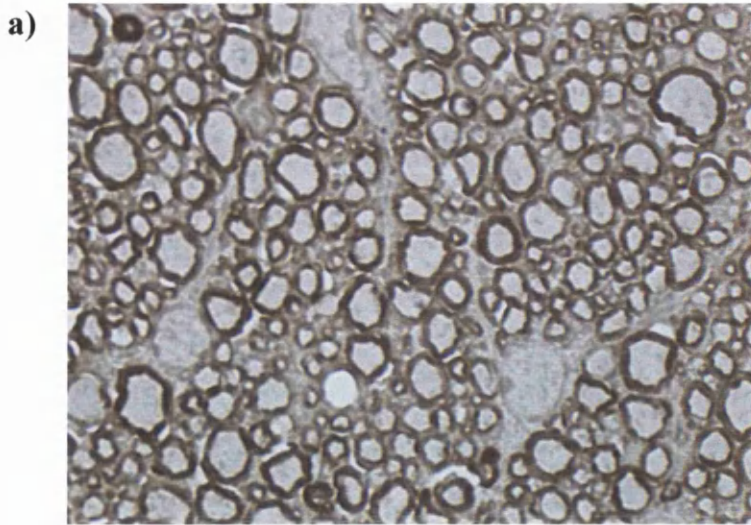


Figure 59 PAP immunostained sections from ND3a transgene complemented knockout mice at 20 days of age

a) 1 μ m resin section showing PLP/DM20-immunoreactivity localised to myelin sheaths of ventral columns of spinal cord (C2-3) (PLP C-terminal antibody) (740x magnification)

Serial 15 μ m paraffin sections showing the lateral columns of spinal cord (C2-3) counterstained with haematoxylin (65x magnification)

b) white matter immunostained using the anti PLP C-terminal antibody

c) no positive staining was seen using the anti PLP isoform-specific antibody
This confirmed that only DM20 protein was produced in ND3A transgene-complemented knockout mice and that it incorporated into a wide range of myelin sheaths.

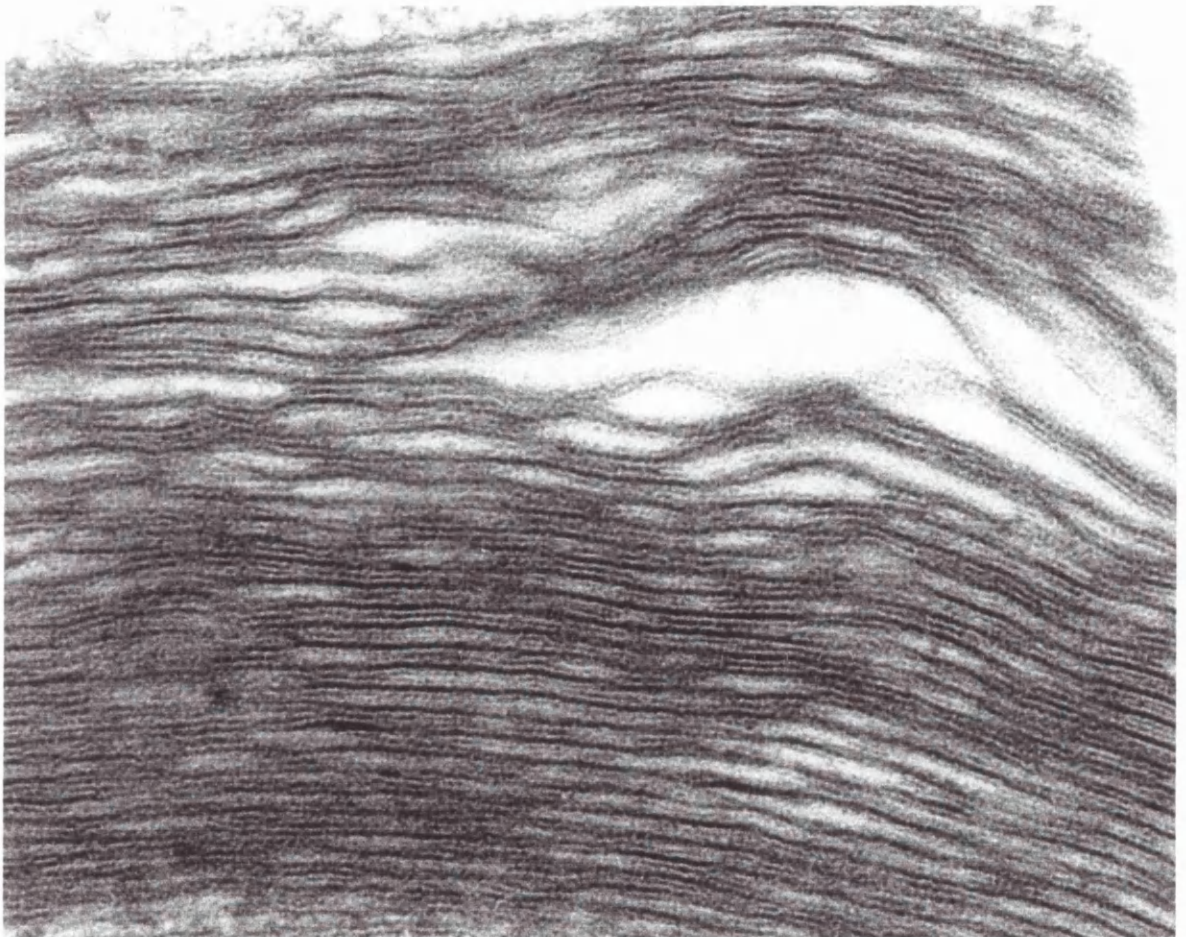


Figure 60 Myelin ultrastructure in ND3A transgene-complemented knockout mice (300,000x magnification)
Myelin was indistinguishable from that in knockout mice showing normal periodicity and both compaction and splitting at the intraperiod line.

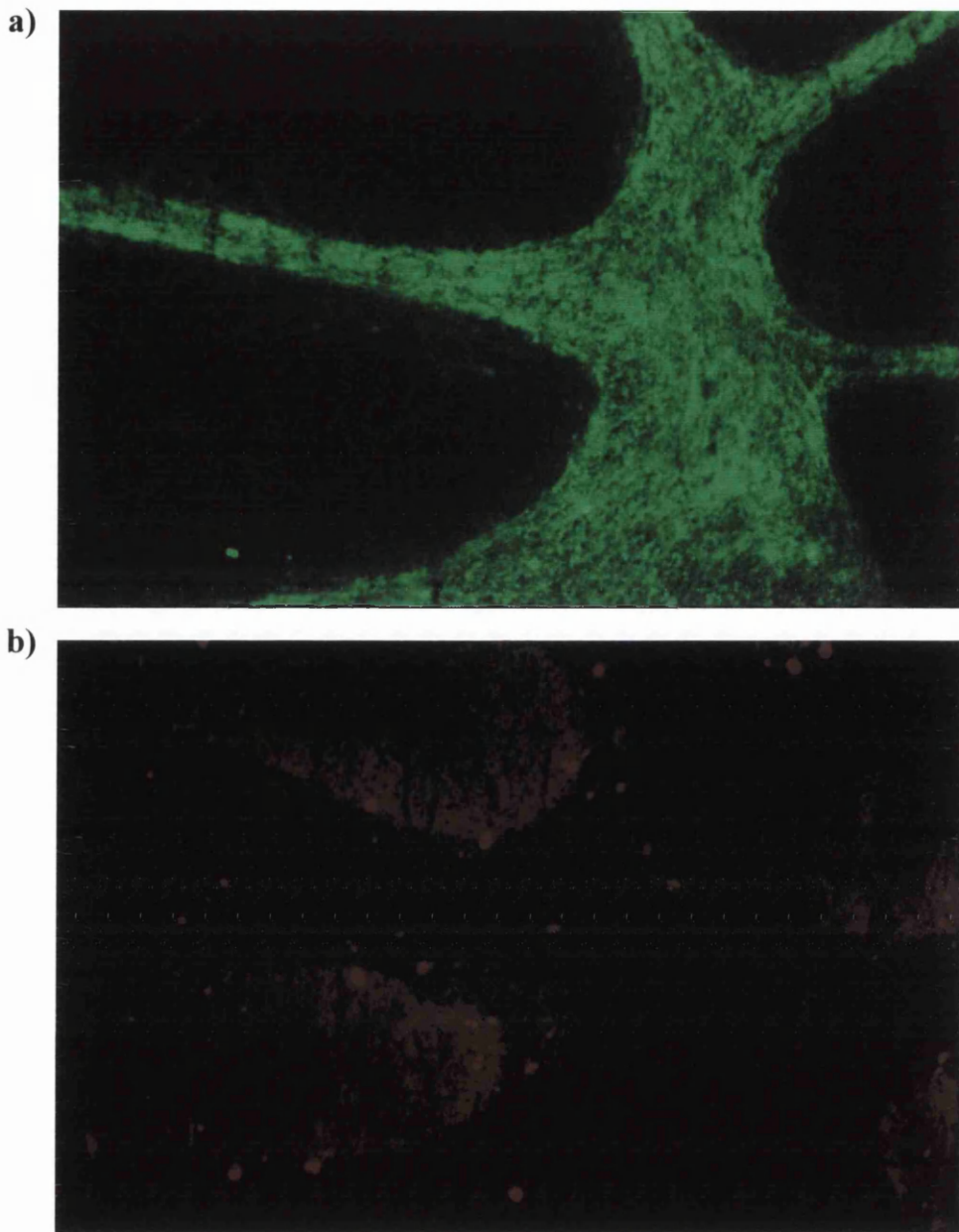


Figure 61 15µm cryosection of sagittal hindbrain from a 20 day-old *PLP-LacZ* transgene-complemented knockout mice (140x magnification)

a) Staining with anti β -galactosidase antibody linked to a FITC-labelled secondary antibody demonstrates high levels of transgene expression throughout myelinated regions of the cerebellum indicating fusion protein incorporation into myelin

b) Immunoreactivity against the PLP/DM20 carboxy terminus cannot be detected demonstrating that the fusion protein incorporates into myelin in the absence of endogenous *Plp* gene products (anti PLP C-terminal antibody detected using a TxR-labelled secondary)

5.5 Discussion

5.5.1 #66 and #72 transgenic complementation of knockout mice

Transcript and protein analysis showed that transgenic complementation using either the #66 or #72 transgene induced high levels of *Plp* gene activity in the knockout mouse approaching the level of endogenous *Plp* gene expression. At 120 days of age, #72 transgenic complementation was shown to prevent the development of axonal and glial changes in knockout mice and #72 transgene-complemented knockout mice produced compacted central myelin sheaths of normal periodicity. These results indicate that the neurodegenerative changes and altered myelin ultrastructure in the knockout mouse are the direct result of loss of *Plp* gene products.

Aged #72 transgene-complemented knockout mice developed occasional axonal swellings similar to those found in knockout mice. These swellings were indistinguishable from swellings found as part of a wider neurodegenerative process in aged hemizygous mice from the #72 transgenic line (Anderson *et al.*, 1998). The swellings in #72 transgene-complemented knockout mice may reflect an incomplete rescue of the knockout phenotype or the partial development of the aged #72 hemizygote phenotype. Alterations of *Plp* gene dosage appear to lead to the development of axonal changes in these lines of mice with both reduced and increased gene dosages causing clinical disease. The severe myelin deficits caused by dysmyelination and demyelination, reported in missense *Plp* gene mutations and over-expressing transgenics, probably result from some mechanism other than gene dosage as they do not develop in the knockout mouse.

Not all myelin sheaths in the CNS of #72 transgene-complemented knockout mice immunostained for *Plp* gene products using a conformation-independent immunohistochemical marker (anti PLP C-terminal antibody). The variable staining of myelin sheaths probably reflects a mosaic pattern of transgene expression within the oligodendrocyte population. Many factors may cause variegated transgenic expression within a population of cells. These include repeat induced gene silencing associated with large transgenic arrays and integration-site dependent influences on the transgenic promoter (reviewed by Sutherland *et al.*, 1997; Garrick *et al.*, 1998; Graubert *et al.*, 1998). Similar stochastic influences on the transgenic promoter probably account for variegated transgenic expression in the #72 transgene-complemented knockout mouse but it is difficult to exclude the possibility that only a proportion of myelin sheaths elaborated by a single oligodendrocyte will incorporate the transgene products. The development of swollen axons in aged #72

transgene-complemented knockout mice may reflect the local influence of PLP/DM20-deficient oligodendrocyte processes on axonal function although a direct association between PLP/DM20-negative myelin sheaths and swollen axons could not be shown.

5.5.2 *Plp*-cDNA and *Dm20*-cDNA transgenic complementation of knockout mice

PlpTg1 transgenic complementation of knockout mice resulted in the incorporation of the PLP protein isoform into central compact myelin. This demonstrates that the PLP protein is capable of appropriate intracellular trafficking, with targeting to and incorporation into the myelin sheath, in the absence of the DM20 protein. Although PLP and DM20 proteins may interact during intracellular processing, as suggested by *in vitro* studies (Gow *et al.*, 1994b; Gow and Lazzarini, 1996), this relationship is not necessary for trafficking of the PLP protein. However, the sparse nature of transgene expression in myelin sheaths of these mice raises the possibility that the DM20 protein isoform may facilitate the intracellular trafficking of PLP protein. A reciprocal role for the PLP isoform in facilitating intracellular trafficking of the DM20 protein is unlikely; *rumpshaker* mice maintain normal DM20 protein trafficking to the cell surface in the presence of low levels of PLP protein (Fanarraga *et al.*, 1992) and the ND3a transgene-complemented knockout mice incorporate DM20 protein into myelin in the absence of the PLP protein isoform.

Expression of the ND3A transgene in knockout mice did not prevent the development of axonal changes or the poor compaction of myelin. As expression of this transgene produced high levels of DM20 protein which incorporated into a wide range of myelin sheaths within the CNS, it is possible to conclude that the DM20 protein isoform cannot rescue the knockout phenotype when expressed in isolation. Similarly, expression of the *PlpTg1* transgene in knockout mice did not prevent the development of axonal changes. This may reflect a requirement for other *Plp* gene isoforms to be expressed in combination with the PLP protein, before neurodegeneration is prevented. However, expression of the *PlpTg1* transgene in knockout mice was poor; low levels of protein were detected by western analysis and only a small proportion of myelin sheaths immunostained for transgene products. Either of these factors may explain the inability of the PLP protein to prevent neurodegeneration in this model which may not reflect the true aetiology of the neurodegenerative changes seen. Similarly, although myelin periodicity was abnormal in *PlpTg1* transgene-complemented knockout mice, poor incorporation of transgene products into individual myelin sheaths makes definitive comments on the ability of the PLP protein to support the structure of the intraperiod line impossible.

Attempts to supplement the knockout phenotype with the *Dm20Tg2* transgene proved to be unsuccessful as no protein could be detected by any method. The expression of DM20 proteins in the absence of PLP protein in embryonic neural tissue (Dickinson *et al.*, 1996), in the PNS (Griffiths *et al.*, 1995) and in ND3A transgene-complemented knockout mice demonstrate that the PLP protein isoform is not required for the appropriate expression of the DM20 protein. The limited expression of the *PlpTg1* transgene in the knockout line demonstrates that the non-coding regions contained within the *Dm20Tg2* transgene can confer a degree of appropriate transgenic regulation. As discussed above (see 5.5.1 #66 and #72 *transgenic complementation of knockout mice*, page 168), several stochastic mechanisms affecting the transgenic promoter may explain the poor levels of expression of both of the *PlpTg1* and *Dm20Tg2* transgenes. Genomic imprinting in transgenic lines has also been widely reported causing variable transgenic repression (reviewed by Chaillet, 1994; Tycko, 1997). This can be dependent on the parental origin of transgenes, their integration sites or the effect of modifying loci from mixed genetic backgrounds. However, the expression of *Dm20Tg2* transgene products in Schwann cells from *jimpy* mice (Anderson *et al.*, 1997) and detection of transcripts in *Dm20Tg2* transgene-complemented knockout mice in this study show that the transgene is transcriptionally competent. Another explanation may be that the transgenic promoter in these two lines of mice promotes expression in the Schwann cell but does not have suitable elements to promote expression in the oligodendrocyte. Alternatively, the promoter may promote expression of the transgenes in a subset of oligodendrocytes or only later during myelination explaining the sparse expression of the *PlpTg1* transgene in small myelin sheaths. A combination of these factors may explain the absence of *Dm20Tg2* transgene products and the low levels of *PlpTg1* transgene products in transgene-complemented knockout mouse.

Although the RT-PCR results support low levels of transgene transcription in both the *PlpTg1* and *Dm20Tg2* transgene complemented knockout mice, this data is semi-quantitative and may not truly reflect the levels of transgene expression. To clarify the level of transgene expression in knockout mice, transcript levels from the various transgenic crosses were compared by northern blot analysis (see 7.12 *Northern blotting*, page 192). However, difficulties in achieving high levels of probe hybridisation prevented accurate assessment of transcript levels even in wild type animals. As the clarification of levels of transgene expression was not a primary goal of the study and due to time and resource constraints, this avenue of research was not pursued.

5.5.3 PLP-LacZ fusion transgene expression in knockout mice

Plp-LacZ transgenic complementation of the knockout mice demonstrated that the PLP-LacZ fusion protein was capable of incorporating into central myelin confirming the original findings of Wight *et al.* (1993). This study adds to these original observations as it shows that the fusion protein incorporates into myelin in the absence of endogenous *Plp* gene products. This excludes the possibility that the fusion protein incorporated into myelin because of interactions between it and the endogenous *Plp* gene products that may have facilitated its intracellular trafficking to and incorporation into central myelin. However, other work in this study does not support the additional conclusions that intron 1 is necessary to ensure the correct spatial expression of the *Plp* gene through repressor activity in non-glial cells (Wight and Dobretsova, 1997). The appropriate expression of DM20 protein in ND3A transgene-complemented knockout mice clearly refute this suggestion as this transgene is appropriately expressed in the absence of intron 1. In fact, this study provides further evidence that the 5' flanking region of the *Plp* gene contains the necessary regulatory elements to direct tissue specific expression of *Plp* gene products. More recent reports from Dobretsova & Wight (1999) suggest that intron 1 contains repressor elements that are regulated through *cis*-acting elements also contained within intron 1. This may explain the contradictory findings between their study and this work as it suggests that, although the *Plp* gene does not require the presence of intron 1 for correct spatial expression, intron 1 may form a complete regulatory subunit that subtly modulates *Plp* gene expression.

6. Final discussion and further work

Data presented in this study has provided valuable insights into the functions of the *Plp* gene. The study aimed to establish if the *Plp* gene had positive roles in myelination and to dissect functional differences between the major isoforms of the *Plp* gene. In addition to clarifying some of these points, the study demonstrated that the *Plp* gene influences normal axonal function and highlighted the complexities of the use of transgenic systems in studying gene function. Differences between the phenotypes of missense *Plp* gene mutants and the knockout mouse suggested that mechanisms other than the loss of functional *Plp* gene products might be involved in the pathogenesis of the severe dysmyelinating disorders. The study also provided strong evidence for genetic redundancy of the murine *Plp* gene in myelin formation and drew comparison with *PLP* gene function in man. The aim of this section is to bring together the phenotypic studies from the transgenic crosses and to suggest future areas of work that may clarify some of the points raised by this thesis.

In summary, expression of the *Plp* gene does not appear to influence oligodendrocyte maturation or survival but does increase the ability of oligodendrocytes to elaborate myelin sheaths. The absence of PLP and DM20 proteins does not prevent the formation of large volumes of central myelin. However, these proteins increase the stability of the intraperiod line although neither is necessary for its formation. Mice deficient in *Plp* gene products develop progressive axonal dysfunction that eventually leads to clinical disease. The axonal pathology is similar to changes seen in other *Plp* gene mutants suggesting that alterations in *Plp* gene dosage affect long-term axonal function and can lead to pathology. Although much of the evidence points towards a focal effect of oligodendrocytes altering local axonal function in the knockout mouse, the possibility that a primary neuronal defect exists cannot be excluded. In particular, the recent identification of minor isoforms of the *Plp* gene (*srPlp* and *srDm20* transcripts) in subsets of neuronal perikarya (Bongarzone *et al.*, 1999) highlights the potential for the *Plp* gene to have a direct role in neuronal function.

Developmental delays (Nadon and Duncan, 1996) and high apoptosis rates (Grinspan *et al.*, 1998) in maturing oligodendrocytes from missense *Plp* gene mutants coupled with early DM20 protein expression in oligodendrocyte progenitors (Lees, 1998) suggest that the *Plp* gene is involved in oligodendrocyte maturation and survival. Although mature oligodendrocyte numbers are maintained in the knockout mouse, a subtle reduction in oligodendrocyte viability could be compensated for by the excess of glial progenitors that are normally seen in the

developing CNS (Barres *et al.*, 1992). In order to fully establish that knockout oligodendrocytes have normal viability, further work looking at survival of immature oligodendrocytes and their progenitors would be necessary. The assessment of apoptosis rates in earlier stages during neural development and myelination of the knockout mouse may clarify these points. An alternative approach could utilise expression of the *Plp-LacZ* transgene in the knockout mouse. A similar transgene construct has been used to study development of early *Dm20* transcript-expressing oligodendrocyte progenitors in the developing murine CNS (Spassky *et al.*, 1998) as the transgene product provides a valuable marker for this cell type. This could be utilised to compare the early development of this subset of oligodendrocytes in the developing CNS of knockout mice, in which these cells cannot be identified conventionally as they do not express *Dm20* transcripts, with control animals.

Mounting evidence supports the ability of oligodendrocytes to influence axonal function in the mature CNS and the knockout mouse may provide an example of disruption of these mechanisms. However, the development of axonal changes cannot be ascribed with confidence to the failure of *Plp* gene expression in the mature oligodendrocytes of these mice until two points have been clarified. Firstly, the possibility that a primary neuronal defect results from the loss of an, as-yet unidentified, role for the *Plp* gene in the neurone must be excluded. Secondly, although knockout oligodendrocytes appear to have comparatively normal phenotypes, the CNS environment in which axonal swellings develop has always been devoid of *Plp* gene products. The possibility that loss of *Plp* gene expression affects neuronal function during development resulting in axonal changes later in life cannot be excluded. The clarification of these points hinges on the ability to induce axonal changes by introducing PLP/DM20-deficient oligodendrocytes to axons that have developed in a normal neural environment. The production of an inducible *Plp* gene knockout allele through, for example, a *Cre-LoxP* recombinase system would provide a model for examining these points *in vivo*. However, this would require a large time and resource commitment, would necessitate a second phenotypic characterisation and would not address the issue of the neuronal or oligodendroglial origin of axonal swellings. More readily accessible *in vivo* approaches exist that can build on the work from the knockout mouse. Intraocular injection of oligodendrocytes is an established technique that has been shown to induce myelination of the retinal neuro-epithelium of the rat (Laeng *et al.*, 1996). This technique would provide a useful starting point from which to study the ability of PLP/DM20-deficient oligodendrocytes to induce axonal changes in wild type animals over a protracted period. Other transplantation techniques in immature animals and dysmyelinated mutants could also be used to induce myelination in

other neural areas such as the spinal cord.

In vitro approaches may provide sophisticated models for establishing the nature of oligodendroglial-axonal interactions that lead to the development of axonal swellings. Initial studies would establish if co-culturing PLP/DM20-deficient neurones and glia induced axonal changes. If an axonal phenotype develops, the effects of altering expression of the *Plp* gene and its isoforms in the neuronal and oligodendroglial populations can be assessed. In addition, the use of conditioned medium may clarify whether a focal oligodendrocyte effect or a secreted product influences axonal function. Although this may provide a valuable model, the major limitations may prove to be the difficulty in inducing *in vitro* myelination and of maintaining cultures for long enough for axonal pathology to develop. Slice cultures may offer a similar *in vitro* approach overcoming some of these problems.

The mechanisms leading to axonal dysfunction must be ascertained in order to establish how the *Plp* gene influences neuronal function. A more detailed morphometric analysis of the cytoskeletal elements may prove beneficial in confirming that knockout axons develop normally. However, pilot immunocytochemical (Griffiths *et al.*, 1998) and electron microscopic investigations show no obvious abnormalities in the majority of axons from knockout mice before axonal swellings and degeneration develop. Similarly, although semi-quantitative western blotting may highlight abnormalities of cytoskeletal metabolism, isolated axonal changes are likely to be masked by the predominance of apparently normal cytoskeletal elements. A more productive approach may be to study axonal function directly. Primary investigations would aim to establish if axonal transport is disrupted and, if so, what mechanisms may be involved. The optic nerve offers an ideal area to examine as it is easily accessible and all axons are orientated in one direction. The introduction of tracer molecules into the retinal ganglion cell layer to study anterograde axonal transport and into the superior colliculus to study retrograde axonal transport are well established techniques (for example Caleo, 1996). *In vitro* approaches may also prove useful for studying individual axoglial interactions but hinge on the ability to identify a neuronal phenotype.

Transgenic complementation demonstrated that the PLP protein can incorporate into myelin in the absence of DM20 protein. In addition, transgenic complementation showed that the DM20 protein expressed in isolation could not prevent the development of neurodegenerative changes or maintain myelin compaction in the knockout mouse. However, the separation of potential roles of PLP and DM20 proteins was hampered by the poor expression of the *PlpTg1* transgene. The failure to prevent myelin ultrastructural abnormalities and neurodegeneration in *PlpTg1*

transgene-complemented knockout mice may have resulted because both PLP and DM20 protein isoforms are necessary to achieve these goals. Alternatively, these findings may reflect the low levels of PLP protein isoform expression in the *PlpTg1* transgene complemented-knockout mouse. Immunohistochemical and morphometric analyses of knockout mice complemented with both the *PlpTg1* and ND3A transgenes would address these issues. Such a study may clarify the influence of the DM20 protein on the trafficking of the PLP protein and may establish how the loss of these two proteins contributes to the development of the knockout phenotype. An alternative hypothesis is that the inability to rescue the knockout phenotype with *PlpTg1* transgenic complementation may relate to the absence of srPLP and srDM20 protein isoforms in the neurones of these mice. The generation of transgene constructs expressing these minor isoforms would be a useful addition to the array of transgenic lines available for modifying the knockout phenotype.

The balance of data from this study suggests that although the expression of the *Plp* gene does not appear to be important in oligodendrocyte maturation and survival, it does improve the ability of oligodendrocytes to elaborate myelin sheaths. This is demonstrated by the selective dysmyelination of small diameter fibres in knockout mice and trend towards the predominance of PLP/DM20-positive myelin sheaths in the heterozygous knockout mouse (I.R. Griffiths, personal communication). The *Plp* gene may have an early role in axo-oligodendroglial interaction, possibly in the initiation of axoglial contact or myelin compaction. The instability of the intraperiod line in knockout mice provides evidence that *Plp* gene products interact at the cell surface and may have adhesive properties. These properties might indicate a role in stabilising initial axoglial contact or in signal transduction pathways. Further morphometric analysis to establish the effect of transgenic complementation on the ability of knockout oligodendrocytes to initiate myelin sheath formation would begin to dissect the roles of the *Plp* gene in this process. The efficacy of the initial stages of axoglial interaction in the knockout mouse might best be addressed using *in vitro* culture systems. If a phenotype can be established, transfection studies could address the role of each isoform in these processes and blocking epitopes using monoclonal antisera may dissect the link between PLP/DM20 structure and function.

Data from this study show that the *Plp* gene has a degree of genetic redundancy in the murine CNS, a phenomenon that is increasingly being recognised in gene knockout studies (reviewed by Nowak *et al.*, 1997; Brookfield, 1997; Gibson and Spring, 1998). Although genetic redundancy may provide some insights into the pathogenesis of *Plp* gene-related disease, it complicates the search for roles that the

Plp gene fulfils in neural development. It is possible, for example, that the *Plp* gene is not vital for myelination but that the role that the *Plp* gene or a closely related member of the same gene family can fulfil in myelination is important. An example of genetic redundancy masking the importance of roles that genes fulfil in myelination is seen with *Mbp* and *P0* gene expression in the PNS. Although MBP protein can be shown to contribute to major dense line formation in the CNS, both P0 and MBP proteins can fulfil this role in the PNS and both must be lost in order to cause PNS major dense line decompaction (Martini *et al.*, 1995). In order to establish if the *Plp* gene has important roles, genes that have the potential to replace those roles must be identified and examined. In the knockout mouse, initial investigations to find candidates for replacing *Plp* gene function, aimed at identifying significant upregulation of members of the *DM* gene family, proved unsuccessful (Klugmann *et al.*, 1997). An alternative approach is to create double gene knockout mice deficient in both *Plp* and *M6a* or *Plp* and *M6b* genes. These mice have been generated but have similar phenotypes to the *Plp* gene knockout mouse suggesting that *M6a* and *M6b* genes do not replace the functions of the *Plp* gene in the murine CNS (I.R. Griffiths, personal communication). Further attempts to identify genes that may replace the roles of the *Plp* gene must be aimed at identifying upregulated genes within the CNS of knockout mice or identifying and screening additional members of the *DM* gene family.

The *Plp* gene knockout mouse has provided a useful model for a subset of PMD disorders and a valuable tool for future investigations into the functions of the isoforms of the *Plp* gene. It has raised relevant questions about the pathogenesis of *Plp* gene-related disease and has highlighted the contribution that axonal changes make in myelin disorders. The differences in onset of disease and PNS changes between knockout mice and humans with functional *PLP* gene null-alleles raises the possibility that the gene may fulfil different roles in the two species. Importantly, the knockout mouse has shown the possibility that the mature oligodendrocyte influences the axon through a *Plp* gene-mediated mechanism. This highlights potential new roles for the *Plp* gene in axoglial interaction.

7. Appendix

7.1 APES-coated slides

APES-coated slides were used for mounting sections for *in situ* hybridisation and immunocytochemistry. Slides were soaked overnight in 5% Decon 90 (Decon Lab Ltd), a detergent, to remove grease, washed in distilled water and oven dried. Once dry, the slides were soaked in 0.25% APES (Sigma) in methylated spirit in a fume hood for 2 minutes. They were rinsed in DEPC-treated water for 2 minutes and oven-dried wrapped in foil. Treated slides were stored at room temperature.

7.2 DEPC-treated water

A 0.1% solution of DEPC was made in distilled water and left for at least 12 hours to inactivate and contaminating RNases. To destroy the DEPC before use, the water was autoclaved at 15lb.in⁻² for 20 minutes and stored sealed at room temperature until use.

7.3 Fixatives

7.3.1 Buffered neutral formaldehyde, 4% (BNF)

For 1 litre of fixative:

100 ml	40% formaldehyde (Merck)
900 ml	tap water
4 g	sodium dihydrogen phosphate
8 g	di-potassium hydrogen phosphate

7.3.2 Karnovsky's modified fixative (paraformaldehyde/ glutaraldehyde 4%/5%)

For 500 ml of fixative:

250 ml	8% paraformaldehyde ¹
100 ml	25% glutaraldehyde
150 ml	0.08M cacodylate buffer ²
250 mg	Calcium chloride

Filter, adjust to pH 7.2 and store at 4°C

¹8% Paraformaldehyde: 20 g paraformaldehyde made up to 250 ml with DW
heat to 65°C
add a few drops of 1M NaOH until solution clears
allow to cool

²0.08M Cacodylate buffer: 17.1224g sodium cacodylate dissolved in 1litre of DW
adjust pH to 7.2

7.3.3 Periodate-lysine-paraformaldehyde

For 1 litre of fixative:

Buffered lysine solution: 13.7g lysine monohydrate in 375ml DW
1.8g sodium hydrogen phosphate in 100ml DW
mix the two solutions to give 475ml buffer, pH7.4

10% Paraformaldehyde: 20g paraformaldehyde made up to 250 ml with DW
heat to 65°C
add a few drops of 1M NaOH until solution clears
allow to cool

The two solutions were stored at 4°C until required (overnight if necessary).
Immediately before use the two solutions were mixed and made up to a final volume of 1 litre using 0.1M phosphate buffer. 2.14g sodium periodate was added and allowed to dissolve.

7.3.4 4% Paraformaldehyde in PBS

For 500 ml of fixative:

500ml of PBS were added to 20g paraformaldehyde, heated to 65°C and cleared by the addition of a few drops of 1M NaOH. The solution was filtered, allowed to cool and the pH was adjusted to 7.2.

7.4 Tissue processing protocols

7.4.1 Paraffin wax processing

Tissues were passed through the following solutions before being blocked in paraffin:

1)	70% methylated spirit/5% phenol	2 hr	room temperature
2)	90% methylated spirit/5% phenol	2 hr	room temperature
3)	methylated spirit	2 hr	room temperature
4)	ethanol/5% phenol	2 hr	room temperature
5)	ethanol/5% phenol	1 hr	room temperature
6)	ethanol/5% phenol	1 hr	room temperature
7)	1% celloidin in methyl benzoate ¹	4 hr	room temperature
8)	xylene	1 hr	room temperature
9)	xylene	1 hr	room temperature
10)	xylene	1 hr	room temperature
11)	paraffin wax	6 hr	60°C
12)	paraffin wax	6 hr	60°C

¹Necoloidine (Merck) solution for microscopy was considered to be 100% celloidin (1ml added per 100ml methyl benzoate).

7.4.2 Resin processing

Tissues were passed through the following solutions before being embedded in resin:

1)	isotonic cacodylate buffer	50 min	4°C
2)	1% OsO ₄ in cacodylate buffer	2 hr	room temperature
3)	isotonic cacodylate buffer ¹	30 min	room temperature
4)	50% ethanol	5 min	4°C
5)	50% ethanol	10 min	4°C
6)	70% ethanol	5 min	4°C
7)	70% ethanol	10 min	4°C
8)	80% ethanol	5 min	4°C
9)	80% ethanol	10 min	4°C
10)	90% ethanol	5 min	4°C
11)	90% ethanol	10 min	4°C
12)	ethanol	20 min	4°C
13)	ethanol	20 min	4°C
14)	propylene oxide	15 min	room temperature
15)	propylene oxide	15 min	room temperature
16)	1:3 resin ² :propylene oxide	13 hr	room temperature
17)	1:2 resin:propylene oxide	6 hr	room temperature
18)	1:2 resin:propylene oxide	18 hr	room temperature
19)	resin	4 hr	30°C

Processed samples were positioned in resin filled silicon moulds and left to polymerise overnight at 60°C.

¹Isotonic cacodylate buffer:

16.05g	sodium cacodylate
3.8g	sodium chloride
0.055g	calcium chloride
0.102g	magnesium chloride

Made up to 1 litre with DW and pH adjusted to 7.2

²Araldite resin:

30g	araldite CY212	(resin)
25.2g	dodecanyl succinic anhydride	(hardener)
1.2ml	2,4,6-tri-dimethylaminomethyl-phenol	(accelerator)
1.0ml	di-butyl phthalate	(plasticiser)

7.5 *In situ* hybridisation solutions and protocols

7.5.1 20x SSC (Sodium chloride/sodium citrate)

This wash contained 3M sodium chloride, 0.3M sodium citrate:

1753g	sodium chloride
882g	sodium citrate

Made up to 10 litres with DW

7.5.2 Prehybridisation washes

Cryosections were kept at 4°C before fixation to prevent activity of endogenous RNases. They were slowly thawed by incubating them in ice-chilled 4% paraformaldehyde that was allowed to heat slowly to room temperature during the first 20 minutes incubation step. The remaining steps and all the steps for paraffin sections were performed at room temperature.

1)	4% paraformaldehyde/ PBS	20 min
2)	PBS	5 min
3)	PBS	5 min
4)	40µg.ml ⁻¹ proteinase K (in 50mM Tris, 5mM EDTA, pH 7.6)	7.5 min
5)	PBS	5 min
6)	4% paraformaldehyde/ PBS	5 min
7 a)	0.1M triethanolamine/ 0.25% acetic anhydride	5 min
b)	refresh by adding more acetic anhydride to a total concentration of 0.5%	5 min
8)	PBS	5 min
9)	0.85% saline	5 min
10)	methylated spirits	5 min
11)	100% ethanol	5 min
12)	100% ethanol	5 min
13)	air dry for at least 2 hours	

7.5.3 Post-hybridisation washes

1)	2x SSC	2.5 hr	50°C
2)	2x SSC/ 50% formamide	1.5 hr	50°C
3)	0.1x SSC	30 min	room temperature
4)	TBS (pH7.5)	15 min	room temperature
5)	10% foetal calf serum in TBS (pH7.5)	45 min	room temperature
6)	1:500 Anti-Digoxigenin-AP Fab fragment in TBS (pH7.5)	1 hr	room temperature
7)	TBS (pH7.5)	5 min	room temperature
8)	TBS (pH7.5)	30 min	room temperature
9)	0.1M Tris/ 0.1M NaCl/ 0.05M MgCl ₂ / pH 9.5	5 min	room temperature
10)	substrate buffer*	5 min -12 hr	room temperature
11)	running water	30 min	room temperature

*see 7.5.4 Alkaline phosphate substrate buffer, page 183

7.5.4 Alkaline phosphate substrate buffer

3.375mg	nitroblue tetrazolium salt in 70% dimethylformamide
1.75mg	5-bromo-4-chloro-3-indolyphosphate, toluidinium salt solution in 100% dimethylformamide
10ml	0.1M Tris, 0.1M NaCl, 0.05M MgCl ₂ , pH 9.5

7.6 Staining protocols

Sections were passed through the following solutions

7.6.1 Dewaxing and hydration of paraffin sections

1)	xylene	2 mins
2)	absolute alcohol	2 mins
3)	methylated spirit	2 mins
4)	water	2 mins
5)	Lugols iodine	1 min
6)	water	1 min
7)	5% sodium thiosulphate	1 min
8)	water	2 mins

7.6.2 Dehydration and clearing of sections

1)	methylated spirits	2 mins
2)	absolute alcohol	2 mins
3)	absolute alcohol	2 mins
4)	histoclear	2 mins
5)	xylene	2 mins

7.6.3 Haematoxylin and eosin

1)	xylene	2 mins
2)	absolute alcohol	2 mins
3)	methyated spirit	2 mins
4)	water	2 mins
5)	Lugols iodine	1 min
6)	water	1 min
7)	5% sodium thiosulphate	1 min
8)	water	2 mins
9)	Mayers haematoxylin*	10 mins
10)	1% acid alcohol	3 dips
11)	water	2 mins
12)	Scots tap water substitute*	1 min
13)	water	2 mins
14)	methyated spirit	10 secs
15)	saturated alcoholic eosin	2 mins
16)	methyated spirit	10 secs
17)	absolute alcohol	2 mins
18)	histoclear	2 mins
19)	xylene	5 mins

* for details see 7.7 Staining solutions

7.6.4 Haematoxylin

1)	running water	2 mins
2)	Mayers haematoxylin *	50 secs
3)	water	wash off excess haematoxylin
4)	Scots tap water substitute *	30 secs

* for details see 7.7 Staining solutions

7.6.5 Staining for electron microscopy

1)	saturated uranyl acetate in 50% ethanol	15 mins
2)	50% ethanol	rinse
3)	50% ethanol	rinse
4)	distilled water	rinse
5)	distilled water	rinse
6)	air dry	
7)	Reynold's lead citrate ¹ (Sodium hydroxide moistened chamber)	10 mins
8)	1M sodium hydroxide	rinse
9)	1M sodium hydroxide	rinse
10)	1M sodium hydroxide	rinse
11)	distilled water	several rinses

¹ **Reynold's lead citrate** (1.2mM lead citrate, 1.8mM sodium citrate, pH 12.0)

1.33g	lead nitrate dissolved in 15ml DW for 1 min vigorous shaking
1.76g	sodium citrate dissolved in 15ml DW for 1 min vigorous shaking

Combine solutions and equilibrate over 30 minutes with occasional shaking. Clear with 1M NaOH and make up to final volume of 50ml with distilled water.

7.7 Staining solutions

7.7.1 Methylene blue/ azur II

1%	methylene blue
1%	azur II
1%	borax

diluted distilled water and filtered before use

7.7.2 Mayers haematoxylin

1g	haematoxylin
10g	potassium alum
0.2g	sodium iodate

in 1 litre of distilled water

bring to boiling point and allow to cool over night then add:

1g	citric acid
50g	chloral hydrate

7.7.3 Scots tap water substitute

3.5g	sodium bicarbonate
20g	magnesium sulphate

in 1 litre of distilled water

7.8 General Buffers

7.8.1 Tris buffered saline

The buffer contained 25mM Tris pH7.4, 136mM NaCl, 2.6mM KCl₂.

3g	Tris base pH7.5
8g	sodium chloride
0.2g	potassium chloride

Dissolved in 800ml of DW, pH adjusted to 7.4 with 1M HCl and volume made up to 1 litre with DW

7.8.2 Phosphate buffered saline (PBS)

The buffer contained

8g	sodium chloride
1.44g	disodium hydrogen phosphate
0.24g	potassium dihydrogen phosphate
0.2g	potassium chloride

Dissolved in 800ml of DW, pH adjusted to 7.4 with 1M HCl and volume made up to 1 litre with DW

7.8.3 0.1M phosphate buffer

The buffer contained

77.4ml	1M disodium hydrogen phosphate
22.6ml	1M potassium dihydrogen phosphate

In 1 litre of DW, pH adjusted to 7.4 with 1M HCl.

7.8.4 Tris-EDTA buffer (TE buffer)

The buffer contained 10mM Tris pH 8.0, 1mM EDTA:

500µl	1M Tris pH 8.0
100µl	0.5M EDTA

Made up to 50ml with SDW

7.8.5 Tris acetate EDTA buffer x10 (TAE buffer)

The buffer contained 40mM Tris acetate, 1mM EDTA:

48.4g	Tris base
11.4ml	glacial acetic acid
20ml	0.5M EDTA

Made up to 1 litre in DW

7.9 Hybaid Recovery™ buffers

All solutions were commercially prepared and supplied with the Hybaid Recovery™ Quick Flow Midi Kit (Hybaid)

7.9.1 Resuspension solution (Hybaid) containing RNase

50mM	Tris-HCl pH8.0
10mM	EDTA
100µg.µl ⁻¹	RNase

stored at 4°C

7.9.2 Cell lysis solution (Hybaid)

200mM	NaOH
1.0%	SDS

7.9.3 Neutralisation solution (Hybaid)

3.2M	potassium acetate/ acetic acid pH5.5
------	--------------------------------------

7.9.4 Equilibration solution (Hybaid)

600mM	NaCl
100mM	sodium acetate/ acetic acid pH5.0
0.15%	Triton X-100

7.9.5 Wash solution (Hybaid)

800mM	NaCl
100mM	sodium acetate/ acetic acid pH5.0

7.10 Gel loading dye x6 (for TAE conditions)

30%	glycerol in SDW
0.25%	bromophenol blue
0.25%	xylene cyanol FF

7.11 Bacteriological media

7.11.1 Luria-Bertani (LB) medium

10g	tryptone (Oxid)
5g	yeast extract (Oxid)
10g	sodium chloride

Made up to 1 litre with DW, pH adjusted to 7.0 using 5N sodium hydroxide and autoclaved for 20 minutes at 15psi and stored at 4°C.

7.11.2 Ampicillin-LB medium

100 $\mu\text{g}\cdot\text{ml}^{-1}$ ampicillin was added to LB medium and stored at 4°C.

7.11.3 Ampicillin-LB agar plates

1.2% ampicillin agar plates were prepared by adding 12g agar (Agar bacteriological, Oxid) to the LB medium solution before autoclaving. The mixture was autoclaved, allowed to cool to ~50°C and 100 $\mu\text{g}\cdot\text{ml}^{-1}$ ampicillin was added. 30ml of the solution were poured into each 90mm petri dish and stored at 4°C. Before use, the plates were incubated at 37°C for 2 hours to reduce the moisture content of the agar and thus maintain well-defined colonies.

7.12 Northern blotting

7.12.1 RNA electrophoresis and transfer to nylon membranes

Denaturing gel electrophoresis was used to separate RNA species for northern blotting. 5µg aliquots of total cellular RNA in 0.1% formaldehyde, 0.5% formamide were heat denatured at 65°C for 15 minutes to destroy secondary RNA structures. This allowed RNA species to be separated on the basis of size on 1.3% agarose gels containing 6.4% formaldehyde. Electrophoresis was performed using a midi-rig (Model H3-SET, Anachem) gel system. The buffer used for electrophoresis and for melting agarose contained 0.02M sodium 3-(N-morpholino) propane-sulphonic acid, 5mM sodium acetate, 1mM EDTA (pH7.0). After electrophoresis, the gels were rinsed several times in DEPC-treated water to remove formaldehyde.

RNA samples were transferred to Hybond-N+ nylon membranes (Amersham) using a SL-8164 capillary blotting unit (Anachem). The nylon membrane was pretreated by saturating in DEPC-treated water and then in 20x SSC. Capillary transfer was performed in 20x SSC over 3 hours. Once completed, the membrane was rinsed in 6x SSC to remove any contaminating agarose and air-dried on 3MM filter paper (Whatman). RNA was covalently bound to the membrane by UV illumination using a XL-1000 (Spectronics Corporation) UV crosslinker.

The membrane was stained with methylene blue to assess RNA transfer and to identify the 28S and 18S ribosomal bands that migrate with 5.1kb and 1.9kb RNA species respectively (Darling and Brickell, 1994). This was achieved by washing at room temperature in 5% acetic acid for 15 minutes with gentle agitation followed by 5% sodium acetate/ 0.04% methylene blue for 10 minutes without agitation. Excess stain was removed by rinsing in DEPC-treated water and the 28S and 18S band positions were marked on the membrane. The membrane was air-dried on 3MM filter paper (Whatman) and stored at 4°C wrapped in polyvinyl chloride film (Saran Wrap, Dow) before hybridisation.

7.12.2 Random-primed DNA probe production

The pC4 plasmid (Nave *et al.*, 1986) was used to generate random-primed DNA probes to detect *Plp* gene transcripts by northern blotting. The pC4 plasmid contains a full-length murine *Plp*-cDNA generated from the 2.4kb population of *Plp* gene transcripts that was released by *Bam*H1 digestion. Probes were generated from 50ng of linearised pDNA denatured by heating to 100°C for 10 minutes and quenched on ice. Random priming using a commercial reaction mix (High Prime,

Boehringer Mannheim) and 50 μ Ci 32 P- α -dCTP (specific activity 37TBq.mM⁻¹: <1000Ci.mM⁻¹) (Amersham) produced radiolabelled oligonucleotides. The reaction mix was incubated at 37°C for 10 minutes and was then quenched by the addition of ethylene-di-amine-tetra-acetate (EDTA) to 0.02M and heating to 65°C for 10 minutes. Labelled probe was separated from unincorporated isotope by column chromatography using Nick Columns (Pharmacia Biotech) following manufacturers' recommendations. The column filtrate was collected in ~100 μ l aliquots which were assessed for radioactivity. Aliquots with the highest activity contained labelled probe and were pooled giving specific activities of 5x10⁸-5x10⁹ cpm. μ g⁻¹. The probe was stored at -20°C until use.

7.12.3 Prehybridisation, hybridisation and washing

Prehybridisation and hybridisation were performed at 65°C in a Micro-4 hybridisation oven with rotisserie (Hybaid) using preheated Rapid-hyb buffer (Amersham). The nylon membrane was saturated with preheated 2x SSC and placed in the hybridisation cylinder. To reduce non-specific binding of probe to the membrane, the membrane was prehybridised in 10ml of Rapid-hyb buffer for 3 hours. Immediately before hybridisation, the probe was denatured by heating to 100°C for 10 minutes and quenched on ice. The probe was mixed with 5 ml of preheated Rapid-hyb buffer and added to the prehybridisation solution to hybridise overnight. Unbound probe was removed from the membrane by washing in two low stringency washes (2x SSC/ 0.1%SDS) followed by two high stringency washes (0.1x SSC/ 0.1%SDS). Each wash was performed on a shaking platform at 65°C and lasted 30 minutes. Between washes, the background activity of the membrane was estimated using a Geiger counter to prevent excessive washing and removal of hybridised probe. After washing, the filter was dried on 3MM filter paper (Whatman), sealed in a double polythene bag and used for autoradiography.

7.12.4 Autoradiography

Two Cronex 10S radiographic films (DuPont) were exposed to the filter in a lightproof cassette at -70°C and developed using a Cronex-130 (DuPont) automatic processor. One film was developed after 24 hours to assess probe strength and the second film was developed up to 7 days later.

8. Abbreviations

International System of Units (SI) notation and other units accepted for use with SI notations have been used throughout this thesis and are not listed.

APES	3-aminopropyltriethoxy-silane
BNF	buffered neutral paraformaldehyde
bp	base pair
C2-3	second to third cervical spinal cord segments
CAII	carbonic anhydrase II
CD2	CD2 antigen (p50), sheep red blood cell receptor
CD44	CD44 antigen (homing function and Indian blood group system)
cDNA	complimentary deoxyribonucleic acid
CMT1A	Charcot-Marie-Tooth disease type 1A
CNP	2',3',cyclic nucleotide 3'-phosphodiesterase
CNS	central nervous system
cpm	counts per minute
DAB	3,4,3',4',-tetraminobiphenyl hydrochloride
DAPI	4',6-diamidino-2-phenylindole
dCTP	2'-deoxy-cytidine-5'-triphosphate
DEPC	diethyl pyrocarbonate
DM20	26.5kDa protein isoform encoded by <i>Plp</i> gene
DNA	deoxyribonucleic acid
DNase	deoxyribonuclease
dNTP	deoxynucleoside triphosphate
DTT	dithiothreitol
DW	distilled, deionised water
EAAT2	excitatory amino acid transporter 2
EDTA	ethylene-di-amine-tetra-acetate
EGTA	ethyleneglycol-bis (β -aminoethylether)- N,N'-tetraacetic acid
F1	first filial generation
FITC	fluorescein isothiocyanate
gDNA	genomic deoxyribonucleic acid
GFAP	glial fibrillary acidic protein
<i>golli-mbp</i> gene	gene of oligodendrocyte lineage

H & E	haematoxylin and eosin
HNPP	hereditary neuropathy with liability to pressure palsies
HSV	herpes simplex virus
Il-15	interleukin-15
kb	kilobase
kDa	kiloDalton
L1CAM	L1 cell adhesion molecule
LacZ	beta-galactosidase
LAMP2	lysosome -associated membrane protein 2
LB	Luria-Bertani
MAG	myelin-associated glycoprotein
MBP	myelin basic protein
MOBP	myelin-associated oligodendrocytic basic protein
MOG	myelin/oligodendrocyte glycoprotein
MOPS	3-(N-morpholino) propane-sulphonic acid
MOSP	myelin oligodendrocyte specific protein
M_r	relative molecular weight
mRNA	messenger ribonucleic acid
<i>neo</i>	<i>neomycin resistance</i>
NGS	normal goat serum
NTP	nucleoside triphosphate
OMIM	Online Mendelian Inheritance in Man entry
OMpg	oligodendrocyte-myelin glycoprotein
OSP	oligodendrocyte specific protein
P0	myelin protein zero
PAP	peroxidase-anti-peroxidase
PBS	phosphate buffered saline
PCR	polymerase chain reaction
PDGFR α	platelet derived growth factor α receptor
pDNA	plasmid deoxyribonucleic acid
PLP	proteolipid protein (30kDa protein isoform encoded by <i>Plp</i> gene)
P-L-P	periodate-lysine-paraformaldehyde
<i>PLP</i> gene	<i>proteolipid protein</i> (human gene)
<i>Plp</i> gene	<i>proteolipid protein</i> (non-human gene)
<i>Plp/PLP</i> gene	<i>proteolipid protein</i> (collectively human and non-human genes)

<i>Plpjp</i>	<i>jimpy</i>
<i>Plpjp-4j</i>	<i>jimpy-4j</i>
<i>Plpjp-msd</i>	<i>myelin synthesis deficient</i>
<i>Plpmd</i>	<i>myelin deficient</i>
<i>Plppt</i>	<i>paralytic tremor</i>
<i>Plpsh</i>	<i>shaking pup</i>
<i>Plptmkn1</i>	targeted mutation of the <i>Plp</i> gene (Klugmann <i>et al.</i> 1997)
PMD	Pelizaeus-Merzbacher disease
PMP22	peripheral myelin protein 22
PNS	peripheral nervous system
RNA	ribonucleic acid
RNase	ribonuclease
rpm	revolutions per minute
RT-PCR	reverse transcription polymerase chain reaction
SDS	sodium dodecyl sulphate
SDS-PAGE	sodium dodecyl sulphate polyacrylamide gel electrophoresis
SDW	sterile distilled water
sec	second
SPG2	Spastic Paraplegia Type 2
srDM20	soma-restricted DM20 protein isoform
srPLP	soma-restricted PLP protein isoform
<i>Sry</i> gene	<i>sex-determining region of the Y chromosome</i> gene
SSC	sodium chloride/sodium citrate buffer
ssDNA	single stranded deoxyribonucleic acid
ssRNA	single stranded ribonucleic acid
TAE	tris acetate ethylene-di-amine-tetra-acetate buffer
<i>Taq</i>	<i>thermophilus aquaticus</i>
TBq	terabecquerel
TBS	tris buffered saline
TE	tris ethylene-di-amine-tetra-acetate buffer
TEMED	N,N,N,N',tetramethylethylenediamine
<i>tk</i>	<i>thymidine kinase</i>
TLCK	N α -p-tosyl-L-lysine chloro-methyl ketone
tRNA	transfer ribonucleic acid
TXR	Texas red

U	unit
UTP	uridine-5'-triphosphate
UTR	untranslated region
UV	ultraviolet

9. Reference List

- Agrawal,H.C. and Agrawal,D. (1991) Proteolipid protein and DM-20 are synthesized by Schwann cells, present in myelin membrane, but they are not fatty acylated. *Neurochemical Research*. **16**, 855-858.
- Aldskogius,H. and Kozlova,E.N. (1998) Central neuron-glia and glial-glia interactions following axon injury. *Progress in Neurobiology*. **55**, (1)1-26.
- Anderson,T.J. Effects of increased dosage of the *Plp* gene: a study in transgenic mice University of Glasgow; 1997;
- Anderson,T.J., Montague,P., Nadon,N.L., Nave,K.-A. and Griffiths,I.R. (1997) Modification of Schwann cell phenotype with *Plp* transgenes: evidence that the PLP and DM20 isoproteins are targeted to different cellular domains. *Journal of Neuroscience Research*. **50**, 13-22.
- Anderson,T.J., Schneider,A., Barrie,J.A., Klugmann,M., McCulloch,M.C., Kirkham,D., Kyriakides,E., Nave,K.-A. and Griffiths,I.R. (1998) Late-onset neurodegeneration in mice with increased dosage of the proteolipid protein gene. *Journal of Comparative Neurology*. **394**, 506-519.
- Aruga,J., Okano,H. and Mikoshiba,K. (1991) Identification of the new isoforms of mouse myelin basic protein: the existence of exon 5a. *Journal of Neurochemistry*. **56**, 1222-1226.
- Austyn,J.M. and Gordon,S. (1981) F4/80: a monoclonal antibody directed specifically against the mouse macrophage. *Eur.J.Immunol.* **11**, 805-815.
- Barres,B.A. (1997) Neuron-Glia Interactions. *Molecular and Cellular Approaches to Neural Development*. Cowan,W.M., Jessell,T.M. and Zipursky,S.L., editors: Oxford University Press, New York, pp. 26-63.
- Barres,B.A., Hart,I.K., Coles,H.S.R., Burne,J.F., Voyvodic,J.T., Richardson,W.D. and Raff,M.C. (1992) Cell death and control of cell survival in the oligodendrocyte lineage. *Cell*. **70**, 31-46.
- Barres,B.A., Jacobson,M.D., Schmid,R., Sendtner,M. and Raff,M.C. (1993) Does oligodendrocyte survival depend on axons. *Current Biology*. **3**, 489-497.
- Barrese,N., Mak,B., Fisher,L. and Moscarello,M.A. (1998) Mechanism of

- demyelination in DM20 transgenic mice involves increased fatty acylation. *Journal of Neuroscience Research*. **53**, (2)143-152.
- Bartlett,W.P. and Skoff,R.P. (1986) Expression of the jimpy gene in the spinal cords of heterozygous female mice. I. An early myelin deficit followed by compensation. *Journal of Neuroscience*. **6**, 2802-2812.
- Belmont,J.W. (1996) Genetic control of X inactivation and processes leading to X-inactivation skewing. *American Journal of Human Genetics*. **58**, 1101-1108.
- Bhat,S. and Pfeiffer,S.E. (1986) Stimulation of oligodendrocytes by extracts from astrocyte-enriched cultures. *Journal of Neuroscience Research*. **15**, 19-27.
- Bignami,A., Eng,L.F. and Uyeda,C.T. (1972) Localization of the glial fibrillary acidic protein in astrocytes by immunofluorescence. *Brain Research*. **43**, 429-435.
- Billings-Gagliardi,S., Kirschner,D.A., Nadon,N.L., DiBenedetto,L.M., Karthigasan,J., Lane,P., Pearsall,G.B. and Wolf,M.K. (1995) Jimpy 4J: A new X-linked mouse mutation producing severe CNS hypomyelination. *Developmental Neuroscience*. **17**, 300-310.
- Bizzozero,O.A. and Lees,M.B. (1999) Fatty acid composition of myelin proteolipid protein during vertebrate evolution. *Neurochemical Research*. **24**, (2)269-274.
- Boison,D., Büssow,H., D'Urso,D., Müller,H.-W. and Stoffel,W. (1995) Adhesive properties of proteolipid protein are responsible for the compaction of CNS myelin sheaths. *Journal of Neuroscience*. **15**, 5502-5513.
- Boison,D. and Stoffel,W. (1989) Myelin-deficient rat: a point mutation in exon III (A->C, Thr75->Pro) of the myelin proteolipid protein causes dysmyelination and oligodendrocyte death. *EMBO J*. **8**, 3295-3302.
- Boison,D. and Stoffel,W. (1994) Disruption of the compacted myelin sheath of axons of the central nervous system in proteolipid protein-deficient mice. *Proceedings of the National Academy of Sciences USA*. **91**, 11709-11713.
- Bongarzone,E.R., Campagnoni,C.W., Kampf,K., Jacobs,E., Handley,V.W., Schonmann,V. and Campagnoni,A.T. (1999) Identification of a new exon in the myelin proteolipid protein gene encoding novel protein isoforms that are restricted to the somata of oligodendrocytes and neurons. *Journal of*

Neuroscience. **19**, 8349-8357.

- Bonneau,D., Rozet,J.-M., Bulteau,C., Berthier,M., Mettey,R., Gil,R., Munnich,A. and Le Merrer,M. (1993) X-linked spastic paraplegia (SPG2): clinical heterogeneity at a single locus. *Journal of Medical Genetics*. **30**, 381-384.
- Brookfield,J.F. (1997) Genetic redundancy. *Adv.Genet.* **36**, 137-155.
- Butt,A.M., Ibrahim,M., Ruge,F.M. and Berry,M. (1995) Biochemical subtypes of oligodendrocyte in the anterior medullary velum of the rat as revealed by the monoclonal antibody Rip. *Glia*. **14**, 185-197.
- Caleo,M. (1996) Different rates of horseradish peroxidase transport in the optic nerve of neonatal and adult rats. *Neuroscience*. **72**, 725-730.
- Cambi,F. and Kamholz,J. (1994) Transcriptional regulation of the rat PLP promoter in primary cultures of oligodendrocytes. *Neurochemical Research*. **19**, 1055-1060.
- Cambi,F., Tang,X.M., Cordray,P., Fain,P.R., Keppen,L.D. and Barker,D.F. (1996) Refined genetic mapping and proteolipid protein mutation analysis in X-linked pure hereditary spastic paraplegia. *Neurology*. **46**, 1112-1117.
- Cameron-Curry,P. and Le Douarin,N.M. (1995) Oligodendrocyte precursors originate from both the dorsal and the ventral parts of the spinal cord. *Neuron*. **15**, 1299-1310.
- Campagnoni,C.W., Garbay,B., Micevych,P., Pribyl,T., Kampf,K., Handley,V.W. and Campagnoni,A.T. (1992) DM20 mRNA splice product of the myelin proteolipid protein gene is expressed in the murine heart. *Journal of Neuroscience Research*. **33**, 148-155.
- Canoll,P.D., Kraemer,R., Teng,K.K., Marchionni,M.A. and Salzer,J.L. (1999) GGF/neuregulin induces a phenotypic reversion of oligodendrocytes. *Molecular and Cellular Neuroscience*. **13**, (2)79-94.
- Canoll,P.D., Musacchio,J.M., Hardy,R., Reynolds,R., Marchionni,M.A. and Salzer,J.L. (1996) GGF/neuregulin is a neuronal signal that promotes the proliferation and survival and inhibits the differentiation of oligodendrocyte progenitors. *Neuron*. **17**, 229-243.
- Capecchi,M.R. (1994) Targeted gene replacement. *Scientific American*. 52-59.

- Chaillet,J.R. (1994) Genomic imprinting: lessons from mouse transgenes. *Mutat.Res.* **307**, (2)441-449.
- Chandross,K.J., Cohen,R.I., Paras,P., Jr., Gravel,M., Braun,P.E. and Hudson,L.D. (1999) Identification and characterization of early glial progenitors using a transgenic selection strategy. *Journal of Neuroscience.* **19**, (2)759-774.
- Chomczynski,P. and Sacchi,N. (1987) Single-step method of RNA isolation by acid guanidinium-thiocyanate-phenol-chloroform extraction. *Annals of Biochemistry.* **162**, 156-159.
- Clarke,P.G.H. (1992) How inaccurate is the Abercrombie correction factor for cell counts? *Trends in Neurosciences.* **15**, 211-212.
- Coggeshall,R.E. (1992) A consideration of neural counting methods. *Trends in Neurosciences.* **15**, 9-12.
- Colello,R.J., Pott,U. and Schwab,M.E. (1994) The role of oligodendrocytes and myelin on axon maturation in the developing rat retinofugal pathway. *Journal of Neuroscience.* **14**, 2594-2605.
- Collard,J.-F., Côté,F. and Julien,J.-P. (1995) Defective axonal transport in a transgenic mouse model of amyotrophic lateral sclerosis. *Nature.* **375**, 61-64.
- Colman,D.R., Kreibich,G., Frey,A.B. and Sabatini,D.D. (1982) Synthesis and incorporation of myelin polypeptides into CNS myelin. *Journal of Cell Biology.* **95**, 598-608.
- Cook,J.L., Irias-Donaghey,S. and Deininger,P.L. (1992) Regulation of rodent myelin proteolipid protein gene expression. *Neuroscience Letters.* **137**, 56-60.
- Côté,F., Collard,J.-F. and Julien,J.-P. (1993) Progressive neuronopathy in transgenic mice expressing the human neurofilament heavy gene: A mouse model of amyotrophic lateral sclerosis. *Cell.* **73**, 35-46.
- Crawley,J.N. (1996) Unusual behavioral phenotypes of inbred mouse strains - Commentary. *Trends in Neurosciences.* **19**, 181-182.
- Cuddon,P.A., Lipsitz,D. and Duncan,I.D. (1998) Myelin mosaicism and brain plasticity in heterozygous females of a canine X-linked trait. *Annals of Neurology.* **44**, (5)771-779.

- D'Urso,D., Brophy,P.J., Staugaitis,S.M., Gillespie,C.S., Frey,A.B., Stempak,J.G. and Colman,D.R. (1990) Protein zero of peripheral nerve myelin: biosynthesis, membrane insertion and evidence for homotypic interaction. *Neuron*. **2**, 449-460.
- Danielson,P.E., Forss-Petter,S., Brow,M.A., Calavetta,L., Douglass,J., Milner,R.J. and Sutcliffe,J.G. (1988) p1B15: a cDNA clone of the rat mRNA encoding cyclophilin. *DNA*. **7**, 261-267.
- Darling,D.C., Brickell,P.M. (1994) Electrophoresis of RNA and northern blotting. *Nucleic acid blotting: the basics*. Darling,D.C. and Bricknell,P.M., editors: IRL Press, Oxford, pp. 45-60.
- Daubas,P., Pham-Dinh,D. and Dautigny,A. (1994) Structure and polymorphism of the mouse myelin/oligodendrocyte glycoprotein gene. *Genomics*. **23**, 36-41.
- De Stefano,N., Matthews,P.M., Fu,L.Q., Narayanan,S., Stanley,J., Francis,G.S., Antel,J.P. and Arnold,D.L. (1998) Axonal damage correlates with disability in patients with relapsing-remitting multiple sclerosis - Results of a longitudinal magnetic resonance spectroscopy study. *Brain*. **121**, (8)1469-1477.
- De Waegh,S.M. and Brady,S.T. (1991) Local control of axonal properties by Schwann cells: Neurofilaments and axonal transport in homologous and heterologous nerve grafts. *Journal of Neuroscience Research*. **30**, 201-212.
- De Waegh,S.M., Lee,V.M.Y. and Brady,S.T. (1992) Local modulation of neurofilament phosphorylation, axonal caliber, and slow axonal transport by myelinating Schwann cells. *Cell*. **68**, 451-463.
- Dentinger,M.P., Barron,K.D. and Csiza,C.K. (1982) Ultrastructure of the central nervous system in a myelin deficient rat. *Journal of Neurocytology*. **11**, 671-691.
- Diaz,R.S., Monreal,J. and Lucas,M. (1990) Calcium movements mediated by proteolipid protein and nucleotides in liposomes prepared with the endogenous lipids from white matter. *Journal of Neurochemistry*. **55**, 1304-1309.
- Dickinson,P.J. Developmental expression of the proteolipid protein gene in the nervous system 1995; 83 p.
- Dickinson,P.J., Fanarraga,M.L., Griffiths,I.R., Barrie,J.A., Kyriakides,E. and

- Montague,P. (1996) Oligodendrocyte progenitors in the embryonic spinal cord express DM-20. *Neuropathology and Applied Neurobiology*. **22**, 188-198.
- Diehl,H.-J., Schaich,M., Budzinski,R.-M. and Stoffel,W. (1986) Individual exons encode the integral membrane domains of human proteolipid protein. *Proceedings of the National Academy of Sciences USA*. **83**, 9807-9811.
- Dobretsova,A. and Wight,P.A. (1999) Antisilencing: Myelin proteolipid protein gene expression in oligodendrocytes is regulated via derepression. *Journal of Neurochemistry*. **72**, (6)2227-2237.
- Duncan,I.D. (1995) Inherited disorders of myelination of the central nervous system. *Neuroglia*. Kettenmann,H. and Ransom,B.R., editors: Oxford University Press, Oxford, pp. 843-858.
- Duncan,I.D., Hammang,J.P. and Jackson,K.F. (1987b) Myelin mosaicism in female heterozygotes of canine shaking pup and myelin-deficient rat mutants. *Brain Research*. **402**, 168-172.
- Duncan,I.D., Hammang,J.P. and Trapp,B.D. (1987a) Abnormal compact myelin in the myelin-deficient rat: absence of proteolipid protein correlates with a defect in the intraperiod line. *Proceedings of the National Academy of Sciences USA*. **84**, 6287-6291.
- Duncan,I.D., Jackson,K.F., Hammang,J.P., Marren,D. and Hoffman,R. (1993) Development of myelin mosaicism in the optic nerve of heterozygotes of the X-linked myelin-deficient (*md*) rat mutant. *Developmental Biology*. **157**, 334-347.
- Duncan,I.D., Nadon,N.L., Hoffman,R.L., Lunn,K.F., Csiza,C. and Wells,M.R. (1995) Oligodendrocyte survival and function in the long-lived strain of the myelin deficient rat. *Journal of Neurocytology*. **24**, 745-762.
- Dyer,C.A. (1993) Novel oligodendrocyte transmembrane signaling systems: Investigations utilizing antibodies as ligands. *Molecular Neurobiology*. **7**, 1-22.
- Dyer,C.A., Hickey,W.F. and Geisert,E.E., Jr. (1991) Myelin/oligodendrocyte-specific protein: A novel surface membrane protein that associates with microtubules. *Journal of Neuroscience Research*. **28**, 607-613.
- Espinosa de los Monteros,A. and Vellis,J. (1990) Oligodendrocyte differentiation:

Developmental and functional subpopulations. *NATO ASI Series*. **43**, 33-45.

- Fanarraga, M.L., Griffiths, I.R., McCulloch, M.C., Barrie, J.A., Cattanach, B.M., Brophy, P.J. and Kennedy, P.G.E. (1991) Rumpshaker: an X-linked mutation affecting CNS myelination. A study of the female heterozygote. *Neuropathology and Applied Neurobiology*. **17**, 289-297.
- Fanarraga, M.L., Griffiths, I.R., McCulloch, M.C., Barrie, J.A., Kennedy, P.G.E. and Brophy, P.J. (1992) Rumpshaker: an X-linked mutation causing hypomyelination. Developmental differences in myelination and glial cells between the optic nerve and spinal cord. *Glia*. **5**, 161-170.
- Fanarraga, M.L., Griffiths, I.R., Zhao, M. and Duncan, I.D. (1998) Oligodendrocytes are not inherently programmed to myelinate a specific size of axon. *Journal of Comparative Neurology*. **399**, 94-100.
- Fanarraga, M.L., Sommer, I., Griffiths, I.R., Montague, P., Groome, N.P., Nave, K.-A., Schneider, A., Brophy, P.J. and Kennedy, P.G.E. (1993) Oligodendrocyte development and differentiation in the rumpshaker mutation. *Glia*. **9**, 146-156.
- Ferra, F.de., Engh, H., Hudson, L., Kamholz, J., Puckett, C., Molineaux, S. and Lazzarini, R.A. (1985) Alternative splicing accounts for the four forms of myelin basic protein. *Cell*. **43**, 721-727.
- Filbin, M.T. and Tennekoon, G.I. (1991) The role of complex carbohydrates in adhesion of the myelin protein, P₀. *Neuron*. **7**, 845-855.
- Filbin, M.T., Walsh, F.S., Trapp, B.D., Pizzey, J.A. and Tennekoon, G.I. (1990) Role of P₀ protein as a homophilic adhesion molecule. *Nature*. **344**, 871-872.
- Friedrich, V.L., Jr., Koniecki, D.L. and Massa, P.T. (1980) Neuronal abnormalities in the cerebellum of quaking and shiverer mice. *Neurological Mutations Affecting Myelination*. Baumann, N., editor: Elsevier, Amsterdam, pp. 141-146.
- Fruttiger, M., Montag, D., Schachner, M. and Martini, R. (1995) Crucial role for the myelin-associated glycoprotein in the maintenance of axon-myelin integrity. *Eur.J.Neurosci*. **7**, 511-515.
- Fujita, N., Kemper, A., Dupree, J., Nakayasu, H., Bartsch, U., Schachner, M., Maeda, N., Suzuki, K. and Popko, B. (1998) The cytoplasmic domain of the large myelin-associated glycoprotein isoform is needed for proper CNS but

- not peripheral nervous system myelination. *Journal of Neuroscience*. **18**, (6)1970-1978.
- Fujiwara,K. (1994) Mouse hepatitis virus. *Virus infections of rodents and langomorphs*. Osterhaus,A.D.M.E., editor: Elsevier Science BV, Amsterdam, pp. 249-257.
- Gabriel,J.M., Erne,B., Pareyson,D., Sghirlanzoni,A., Taroni,F. and Steck,A.J. (1997) Gene dosage effects in hereditary peripheral neuropathy - Expression of peripheral myelin protein 22 in Charcot-Marie-Tooth disease type 1A and hereditary neuropathy with liability to pressure palsies nerve biopsies. *Neurology*. **49**, (6)1635-1640.
- Garbern,J.Y. (2000) Point and Other Small Mutations of *PLP*. *Pelizaeus-Merzbacher disease (PMD) Web page*. Wayne State University, Detroit, MI. World Wide Web URL: <http://www.med.wayne.edu/Neurology/plp.html>
- Garbern,J.Y., Cambi,F., Tang,X.M., Sima,A.A.F., Vallat,J.M., Bosch,E.P., Lewis,R., Shy,M., Sohi,J., Kraft,G., *et al.* (1997) Proteolipid protein is necessary in peripheral as well as central myelin. *Neuron*. **19**, (1)205-218.
- Gardinier,M.V., Macklin,W.B., Diniak,A.J. and Deininger,P.L. (1986) Characterization of myelin proteolipid mRNAs in normal and jimpy mice. *Molecular and Cellular Biology*. **6**, 3755-3762.
- Garrick,D., Fiering,S., Martin,D.I. and Whitelaw,E. (1998) Repeat-induced gene silencing in mammals [see comments]. *Nat.Genet*. **18**, (1)56-59.
- Gencic,S., Abuelo,D., Ambler,M. and Hudson,L.D. (1989) Pelizaeus-Merzbacher disease: An X-linked neurologic disorder of myelin metabolism with a novel mutation in the gene encoding proteolipid protein. *American Journal of Human Genetics*. **45**, 435-442.
- Gencic,S. and Hudson,L.D. (1990) Conservative amino acid substitution in the myelin proteolipid protein of jimpy^{msd} mice. *Journal of Neuroscience*. **10**, 117-124.
- Gerlai,R. (1996) Gene-targeting studies of mammalian behavior: Is it the mutation or the background genotype. *Trends in Neurosciences*. **19**, 177-181.
- Gibson,T.J. and Spring,J. (1998) Genetic redundancy in vertebrates: polyploidy and persistence of genes encoding multidomain proteins. *Trends Genet*. **14**,

(2)46-50.

- Gout,O., de Santo,R., Arnheiter,H., *et al.* (1991) A transgenic tag for tracking transplanted glial cells. [Abstract] *Society for Neuroscience Abstracts*. **17**, 157.9.
- Gow,A., Friedrich,V.L., Jr. and Lazzarini,R.A. (1994a) Intracellular transport and sorting of the oligodendrocyte transmembrane proteolipid protein. *Journal of Neuroscience Research*. **37**, 563-573.
- Gow,A., Friedrich,V.L., Jr. and Lazzarini,R.A. (1994b) Many naturally occurring mutations of myelin proteolipid protein impair its intracellular transport. *Journal of Neuroscience Research*. **37**, 574-583.
- Gow,A. and Lazzarini,R.A. (1996) A cellular mechanism governing the severity of Pelizaeus- Merzbacher disease. *Nature Genetics*. **13**, 422-428.
- Gow,A., Southwood,C.M. and Lazzarini,R.A. (1998) Disrupted proteolipid protein trafficking results in oligodendrocyte apoptosis in an animal model of Pelizaeus-Merzbacher disease. *Journal of Cell Biology*. **140**, (4)925-934.
- Graubert,T.A., Hug,B.A., Wesselschmidt,R., Hsieh,C.L., Ryan,T.M., Townes,T.M. and Ley,T.J. (1998) Stochastic, stage-specific mechanisms account for the variegation of a human globin transgene. *Nucleic Acids Res*. **26**, (12)2849-2858.
- Griffiths,I.R., Dickinson,P. and Montague,P. (1995) Expression of the proteolipid protein gene in glial cells of the post-natal peripheral nervous system of rodents. *Neuropathology and Applied Neurobiology*. **21**, 97-110.
- Griffiths,I.R., Klugmann,M., Anderson,T.J., Yool,D., Thomson,C.E., Schwab,M.H., Schneider,A., Zimmermann,F., McCulloch,M.C., Nadon,N.L., *et al.* (1998) Axonal swellings and degeneration in mice lacking the major proteolipid of myelin . *Science*. **280**, 1610-1613.
- Griffiths,I.R., Scott,I., McCulloch,M.C., Barrie,J.A., McPhilemy,K. and Cattanach,B.M. (1990) Rumpshaker mouse: a new X-linked mutation affecting myelination: evidence for a defect in PLP expression. *Journal of Neurocytology*. **19**, 273-283.
- Grinspan,J.B., Coulalaglou,M., Beesley,J.S., Carpio,D.F. and Scherer,S.S. (1998) Maturation-dependent apoptotic cell death of oligodendrocytes in myelin-

deficient rats. *Journal of Neuroscience Research*. **54**, (5)623-634.

- Hall, A., Giese, N.A. and Richardson, W.D. (1996) Spinal cord oligodendrocytes develop from ventrally derived progenitor cells that express PDGF alpha-receptors. *Development*. **122**, (12)4085-4094.
- Hanemann, C.O. and Müller, H.W. (1998) Pathogenesis of Charcot-Marie-Tooth IA (CMTIA) neuropathy. *Trends in Neurosciences*. **21**, (7)282-286.
- Hardy, R.J. and Friedrich, V.L., Jr. (1996) Oligodendrocyte progenitors are generated throughout the embryonic mouse brain, but differentiate in restricted foci. *Development*. **122**, 2059-2069.
- Hartman, B.K., Agrawal, H.C., Agrawal, D. and Kalmbach, S. (1982) Development and maturation of central nervous system myelin: comparison of immunohistochemical localization of proteolipid protein and basic protein in myelin and oligodendrocytes. *Proceedings of the National Academy of Sciences USA*. **79**, 4217-4220.
- Hedreen, J.C. (1998) What was wrong with the Abercrombie and empirical cell counting methods? A review. *Anatomical Record*. **250**, (3)373-380.
- Hildebrand, C., Remahl, S., Persson, H. and Bjartmar, C. (1993) Myelinated nerve fibres in the CNS. *Progress in Neurobiology*. **40**, 319-384.
- Hirokawa, N. (1993) Axonal transport and the cytoskeleton. *Current Opinion in Neurobiology*. **3**, 724-731.
- Hodes, M.E., Blank, C.A., Pratt, V.M., Morales, J., Napier, J. and Dlouhy, S.R. (1997) Nonsense mutation in exon 3 of the proteolipid protein gene (PLP) in a family with an unusual form of Pelizaeus-Merzbacher disease. *American Journal of Medical Genetics*. **69**, (2)121-125.
- Hodes, M.E., DeMyer, W.E., Pratt, V.M., Edwards, M.K. and Dlouhy, S.R. (1995) Girl with signs of Pelizaeus-Merzbacher disease heterozygous for a mutation in exon 2 of the proteolipid protein gene. *American Journal of Medical Genetics*. **55**, 397-401.
- Hodes, M.E. and Dlouhy, S.R. (1996) The proteolipid protein gene: double, double, ... and trouble. *American Journal of Human Genetics*. **59**, 12-15.
- Hodes, M.E., Pratt, V.M. and Dlouhy, S.R. (1993) Genetics of Pelizaeus-Merzbacher

disease. *Developmental Neuroscience*. **15**, 383-394.

- Horvath,L.I., Brophy,P.J. and Marsh,D. (1990) Influence of polar residue deletions on lipid-protein interactions with the myelin proteolipid protein. Spin-label ESR studies with DM-20/lipid recombinants. *Biochemistry*. **29**, 2635-2638.
- Hudson,L.D., Berndt,J., Puckett,C., Kozak,C.A. and Lazzarini,R.A. (1987) Aberrant splicing of proteolipid protein and mRNA in the dysmyelinating jimpy mutant mouse. *Proceedings of the National Academy of Sciences USA*. **84**, 1454-1458.
- Hudson,L.D., Nadon,N.L. (1992) Amino acid substitutions in proteolipid protein that cause dysmyelination. *Myelin: Biology and Chemistry*. Martenson,R.E., editor: CRC Press, Boca Raton, pp. 677-702.
- Hudson,L.D., Puckett,C., Berndt,J., Chan,J. and Gencic,S. (1989) Mutation of the proteolipid protein gene PLP in a human X chromosome-linked myelin disorder. *Proceedings of the National Academy of Sciences USA*. **86**, 8128-8131.
- Hummler,E., Cole,T.J., Blendy,J.A., Ganss,R., Aguzzi,A., Schmid,W., Beermann,F. and Schutz,G. (1994) Targeted mutation of the CREB gene: compensation within the CREB/ATF family of transcription factors. *Proc.Natl.Acad.Sci.U.S.A.* **91**, (12)5647-5651.
- Inoue,K., Osaka,H., Imaizumi,K., Nezu,A., Takanashi,J., Arii,J., Murayama,K., Ono,J., Kikawa,Y., Mito,T., *et al.* (1999) Proteolipid protein gene duplications causing Pelizaeus-Merzbacher disease: Molecular mechanism and phenotypic manifestations. *Annals of Neurology*. **45**, (5)624-632.
- Inoue,K., Osaka,H., Kawanishi,C., Sugiyama,N., Ishii,M., Sugita,K., Yamada,Y. and Kosaka,K. (1997) Mutations in the proteolipid protein gene in Japanese families with Pelizaeus-Merzbacher disease. *Neurology*. **48**, (1)283-285.
- Inoue,Y., Kagawa,T., Matsumura,Y., Ikenaka,K. and Mikoshiba,K. (1996) Cell death of oligodendrocytes or demyelination induced by overexpression of proteolipid protein depending on expressed gene dosage. *Neuroscience Research*. **25**, 161-172.
- Isenmann,S., Wahl,C., Krajewski,S., Reed,J.C. and Bähr,M. (1997) Up-regulation of Bax protein in degenerating retinal ganglion cells precedes apoptotic cell death after optic nerve lesion in the rat. *European Journal of Neuroscience*.

- Janz,R. and Stoffel,W. (1993) Characterization of a brain-specific Sp 1-like activity interacting with an unusual binding site within the myelin proteolipid protein promoter. *Biological Chemistry Hoppe-Seyler*. **374**, 507-517.
- Johnson,R.S., Roder,J.C. and Riordan,J.R. (1995) Over-expression of the DM-20 myelin proteolipid causes central nervous system demyelination in transgenic mice. *Journal of Neurochemistry*. **64**, 967-976.
- Julien,J.P. (1997) Neurofilaments and motor neuron disease. *Trends in Cell Biology*. **7**, (6)243-249.
- Kagawa,T., Ikenaka,K., Inoue,Y., Kuriyama,S., Tsujii,T., Nakao,J., Nakajima,K., Aruga,J., Okano,H. and Mikoshiba,K. (1994a) Glial cell degeneration and hypomyelination caused by overexpression of myelin proteolipid protein gene. *Neuron*. **13**, 427-442.
- Kagawa,T., Nakao,J., Yamada,M., Shimizu,K., Hayakawa,T., Mikoshiba,K. and Ikenaka,K. (1994b) Fate of jimpy-type oligodendrocytes in jimpy heterozygote. *Journal of Neurochemistry*. **62**, 1887-1893.
- Kamholz,J., Sessa,M., Scherer,S., Vogelbacker,H., Mokuno,K., Baron,P., Wrabetz,L., Shy,M. and Pleasure,D. (1992) Structure and expression of proteolipid protein in the peripheral nervous system. *Journal of Neuroscience Research*. **31**, 231-244.
- Kanfer,J., Parenty,M., Goujet-Zalc,C., Monge,M., Bernier,L., Campagnoni,A.T., Dautigny,A. and Zalc,B. (1989) Developmental expression of myelin proteolipid, basic protein and 2', 3'-cyclic nucleotide 3'-phosphodiesterase transcripts in different rat brain regions. *Journal of Molecular Neuroscience*. **1**, 39-46.
- Kaplan,M.R., Meyer-Franke,A., Lamber,S., Bennett,V., Duncan,I.D., Levinson,S.R. and Barres,B.A. (1997) Induction of sodium channel clustering by oligodendrocytes. *Nature*. **386**, (6626)724-728.
- Karthigasan,J., Evans,E.L., Vouyiouklis,D.A., Inouye,H., Borenshteyn,N., Ramamurthy,G.V. and Kirschner,D.A. (1996) Effects of rumpshaker mutation on CNS myelin composition and structure. *Journal of Neurochemistry*. **66**, 338-345.
- Katsuki,M., Sato,M., Kimura,M., Yokoyama,M., Kobayashi,K. and Nomura,T.

- (1988) Conversion of normal behavior to shiverer by myelin basic protein antisense cDNA in transgenic mice. *Science*. **241**, 593-595.
- Kimura,M., Sato,M., Akatsuka,A., Saito,S., Ando,K., Yokoyama,M. and Katsuki,M. (1998) Overexpression of a minor component of myelin basic protein isoform (17.2 kDa) can restore myelinogenesis in transgenic *shiverer* mice. *Brain Research*. **785**, (2)245-252.
- King,H. Phenotypic and genetic analysis of the hindshaker mutation University of Glasgow; 1998;
- Kirschner,D.A. and Hollingshead,C.J. (1980) Processing for electron microscopy alters membrane structure and packing in myelin. *Journal of Ultrastructural Research*. **73**, 211-232.
- Kitagawa,K., Sinoway,M.P., Yang,C., Gould,R.M. and Colman,D.R. (1993) A proteolipid protein gene family: Expression in sharks and rays and possible evolution from an ancestral gene encoding a pore-forming polypeptide. *Neuron*. **11**, 433-448.
- Klugmann,M., Schwab,M.H., Pühlhofer,A., Schneider,A., Zimmermann,F., Griffiths,I.R. and Nave,K.-A. (1997) Assembly of CNS myelin in the absence of proteolipid protein. *Neuron*. **18**, 59-70.
- Knapp,P.E. (1996) Proteolipid protein: Is it more than just a structural component of myelin. *Developmental Neuroscience*. **18**, 297-308.
- Knapp,P.E., Benjamins,J.A. and Skoff,R.P. (1996) Epigenetic factors up-regulate expression of myelin proteins in the dysmyelinating jimpy mutant mouse. *Journal of Neurobiology*. **29**, 138-150.
- Koeppen,A.H., Csiza,C.K., Willey,A.M., Ronne,M., Barron,K.D., Dearborn,R.E. and Hurwitz,C.G. (1992) Myelin deficiency in female rats due to a mutation in the PLP gene. *Journal of the Neurological Sciences*. **107**, 78-86.
- Kurihara,T., Sakuma,M. and Gojobori,T. (1997) Molecular evolution of myelin proteolipid protein. *Biochemical and Biophysical Research Communications*. **237**, (3)559-561.
- Kühn,R. and Schwenk,F. (1998) Advances in gene targeting methods. *Current Opinion in Immunology*. **9**, 183-188.
- Lachapelle,F., Lapie,P., Campagnoni,A.T. and Gumpel,M. (1991)

- Oligodendrocytes of the jimpy phenotype can be partially restored by environmental factors in vivo. *Journal of Neuroscience Research*. **29**, 235-243.
- Laeng,P., Molthagen,M., Yu,E.G.X. and Bartsch,U. (1996) Transplantation of oligodendrocyte progenitor cells into the rat retina: Extensive myelination of retinal ganglion cell axons. *Glia*. **18**, 200-210.
- Laezza,C., Wolff,J. and Bifulco,M. (1997) Identification of a 48-kDa prenylated protein that associates with microtubules as 2',3'-cyclic nucleotide 3'-phosphodiesterase in FRTL-5 cells. *FEBS Letters*. **413**, (2)260-264.
- Lathe,R. (1996) Mice, gene targeting and behaviour: more than just genetic background. *Trends in Neurosciences*. **19**, 183-186.
- Lees,M.B. (1998) A history of proteolipids: A personal memoir. *Neurochemical Research*. **23**, (3)261-271.
- Lemke,G. (1988) Unwrapping the genes of myelin. *Neuron*. **1**, 535-543.
- Lepage,P., Helynck,G., Chu,J.-Y., Luu,B., Sorokine,O., Trifilieff,E. and Van Dorsselaer,A. (1986) Purification and characterization of minor brain proteolipids: use of fast atom bombardment-mass spectrometry for peptide sequencing. *Biochimie*. **68**, 669-686.
- Linington,C., Webb,M. and Woodhams,P.L. (1984) A novel myelin-associated glycoprotein defined by a mouse monoclonal antibody. *Journal of Neuroimmunology*. **6**, 387-396.
- Lipsitz,D., Goetz,B.D. and Duncan,I.D. (1998) Apoptotic glial cell death and kinetics in the spinal cord of the myelin-deficient rat. *Journal of Neuroscience Research*. **51**, (4)497-507.
- Lipton,H.L., Rozhon,E.J. and Bandyopadhyay,P. (1994) Picornavirus infections. *Virus infections of rodents and langomorphs*. Osterhaus,A.D.M.E., editor: Elsevier Science BV, Amsterdam, pp. 373-385.
- Macklin,W.B., Campagnoni,A.T., Deininger,P.L. and Gardinier,M.V. (1987) Structure and expression of the mouse proteolipid protein gene. *Journal of Neuroscience Research*. **18**, 383-394.
- Martini,R., Mohajeri,M.H., Kasper,S., Giese,K.P. and Schachner,M. (1995) Mice doubly deficient in the genes for P0 and myelin basic protein show that both

- proteins contribute to the formation of the major dense line in peripheral nerve myelin. *Journal of Neuroscience*. **15**, 4488-4495.
- Mastronardi,F.G., Ackerley,C.A., Arsenault,L., Roots,B.I. and Moscarello,M.A. (1993) Demyelination in a transgenic mouse: A model for multiple sclerosis. *Journal of Neuroscience Research*. **36**, 315-324.
- Mastronardi,F.G., Ackerley,C.A., Roots,B.I. and Moscarello,M.A. (1996) Loss of myelin basic protein cationicity in DM20 transgenic mice is dosage dependent. *Journal of Neuroscience Research*. **44**, 301-307.
- Mattei,M.G., Alliel,P.M., Dautigny,A., Passage,E., Pham-Dinh,D., Mattei,J.F. and Jolles,P. (1986) The gene encoding for the major brain proteolipid (PLP) maps on the q-22 band of the human X chromosome. *Human Genetics*. **72**, 352-353.
- McLaurin,J., Ackerley,C.A. and Moscarello,M.A. (1993) Localization of basic proteins in human myelin. *Journal of Neuroscience Research*. **35**, 618-628.
- McMorris,F.A. and McKinnon,R.D. (1996) Regulation of oligodendrocyte development and CNS myelination by growth factors: Prospects for therapy of demyelinating disease. *Brain Pathology*. **6**, 313-329.
- McPhilemy,K., Mitchell,L.S., Griffiths,I.R., Morrison,S., Deary,A.W., Sommer,I. and Kennedy,P.G.E. (1990) Effect of optic nerve transection upon myelin protein gene expression by oligodendrocytes: evidence for axonal influences on gene expression. *Journal of Neurocytology*. **19**, 494-503.
- Meyer,T., Munch,C., Knappenberger,B., Liebau,S., Volkel,H. and Ludolph,A.C. (1998) Alternative splicing of the glutamate transporter EAAT2 (GLT-1). *Neurosci.Lett*. **241**, (1)68-70.
- Mikol,D.D., Rongnoparut,P., Allwardt,B.A., Marton,L.S. and Stefansson,K. (1993) The oligodendrocyte-myelin glycoprotein of mouse: Primary structure and gene structure. *Genomics*. **17**, 604-610.
- Milner,R.J., Lai,C., Nave,K.-A., Lenoir,D., Ogata,J. and Sutcliffe,J.G. (1985) Nucleotide sequence of two mRNAs for rat brain myelin proteolipid protein. *Cell*. **42**, 931-939.
- Mimault,C., Giraud,G., Courtois,V., Cailloux,F., Boire,J.Y., Dastugue,B., Boespflug-Tanguy,O. and Clin Eur Network Brain Dysmyelinating (1999) Proteolipoprotein gene analysis in 82 patients with sporadic Pelizaeus-

- Merzbacher disease: Duplications, the major cause of the disease, originate more frequently in male germ cells, but point mutations do not. *American Journal of Human Genetics*. **65**, (2)360-369.
- Montague,P., Barrie,J.A., Thomson,C.E., Kirkham,D., McCallion,A.S., Davies,R.W., Kennedy,P.G.E. and Griffiths,I.R. (1998) Cytoskeletal and nuclear localization of MOBP polypeptides. *European Journal of Neuroscience*. **10**, 1321-1328.
- Montague,P., Dickinson,P.J., McCallion,A.S., Stewart,G.J., Savioz,A., Davies,R.W., Kennedy,P.G.E. and Griffiths,I.R. (1997) Developmental expression of the murine *Mobp* gene. *Journal of Neuroscience Research*. **49**, (2)133-143.
- Montague,P., Griffiths,I.R. (1997) Molecular biology of the glia: components of myelin-PLP and minor myelin proteins. *Molecular Biology of Multiple Sclerosis*. Russell,W.C., editor: J.Wiley & Sons, Chichester, pp. 55-69.
- Montgomery,D.L. (1994) Astrocytes: form, functions, and roles in disease. *Vet Pathol*. **31**, (2)145-167.
- Nadon,N.L., Arnheiter,H., Chang,S., *et al.* (1989) Expression of the human proteolipid protein gene in transgenic mice. [Abstract] *Journal of Cellular Biochemistry*. **130**, 181.
- Nadon,N.L., Arnheiter,H. and Hudson,L.D. (1994) A combination of PLP and DM20 transgenes promotes partial myelination in the jimpy mouse. *Journal of Neurochemistry*. **63**, 822-833.
- Nadon,N.L. and Duncan,I.D. (1995) Gene expression and oligodendrocyte development in the myelin deficient rat. *Journal of Neuroscience Research*. **41**, 96-104.
- Nadon,N.L. and Duncan,I.D. (1996) Molecular analysis of glial cell development in the canine 'shaking pup' mutant. *Developmental Neuroscience*. **18**, 174-184.
- Nadon,N.L., Duncan,I.D. and Hudson,L.D. (1990) A point mutation in the proteolipid protein gene of the "shaking pup" interrupts oligodendrocyte development. *Development*. **110**, 529-537.
- Nance,M.A., Boyadjiev,S., Pratt,V.M., Taylor,S., Hodes,M.E. and Dlouhy,S.R. (1996) Adult-onset neurodegenerative disorder due to proteolipid protein gene mutation in the mother of a man with Pelizaeus- Merzbacher disease. *Neurology*. **47**, 1333-1335.
- Nave,K.-A., Bloom,F.E. and Milner,R.J. (1987b) A single nucleotide difference in

- the gene for myelin proteolipid protein defines the *jimpy* mutation in mouse. *Journal of Neurochemistry*. **49**, 1873-1877.
- Nave,K.-A., Lai,C., Bloom,F.E. and Milner,R.J. (1986) Jimpy mutant mouse: A 74-base deletion in the mRNA for myelin proteolipid protein and evidence for a primary defect in RNA splicing. *Proceedings of the National Academy of Sciences USA*. **83**, 9264-9268.
- Nave,K.-A., Lai,C., Bloom,F.E. and Milner,R.J. (1987a) Splice site selection in the proteolipid protein (PLP) gene transcript and primary structure of the DM-20 protein of central nervous system myelin. *Proceedings of the National Academy of Sciences USA*. **84**, 5665-5669.
- Nave,K.-A. and Lemke,G. (1991) Induction of the myelin proteolipid protein (PLP) gene in C6 glioblastoma cells: Functional analysis of the PLP promoter. *Journal of Neuroscience*. **11**, 3060-3069.
- Newman,S., Kitamura,K. and Campagnoni,A.T. (1987) Identification of a cDNA coding for a fifth form of myelin basic protein. *Proceedings of the National Academy of Sciences USA*. **84**, 886-890.
- Nezu,A., Kimura,S., Uehara,S., Osaka,H., Kobayashi,T., Haraguchi,M., Inoue,K. and Kawanishi,C. (1996) Pelizaeus-Merzbacher-like disease: Female case report. *Brain and Development*. **18**, 114-118.
- Noll,E. and Miller,R.H. (1993) Oligodendrocyte precursors originate at the ventral ventricular zone dorsal to the ventral midline region in the embryonic rat spinal cord. *Development*. **118**, 563-573.
- Norton,W.T., Cammer,W. (1984) Isolation and characterization of myelin. *Myelin*. Morell,P., editor: Plenum Press, New York and London, pp. 147-196.
- Nowak,M.A., Boerlijst,M.C., Cooke,J. and Smith,J.M. (1997) Evolution of genetic redundancy. *Nature*. **388**, (6638)167-171.
- Nussbaum,J.L. and Mandel,P. (1973) Brain proteolipids in neurologically mutant mice. *Brain Research*. **61**, 295-310.
- Online Mendelian Inheritance in Man, OMIM (TM). Johns Hopkins University, Baltimore, MD. MIM Number **102540** (1999) World Wide Web URL: <http://www.ncbi.nlm.nih.gov/omim/>
- Online Mendelian Inheritance in Man, OMIM (TM). Johns Hopkins University,

- Baltimore, MD. MIM Number **102610** (1998) World Wide Web URL: <http://www.ncbi.nlm.nih.gov/omim/>
- Online Mendelian Inheritance in Man, OMIM (TM). Johns Hopkins University, Baltimore, MD. MIM Number **312080** (1999) World Wide Web URL: <http://www.ncbi.nlm.nih.gov/omim/>
- Online Mendelian Inheritance in Man, OMIM (TM). Johns Hopkins University, Baltimore, MD. MIM Number **312920** (1998) World Wide Web URL: <http://www.ncbi.nlm.nih.gov/omim/>
- Ono,K., Bansal,R., Payne,J., Rutishauser,U. and Miller,R.H. (1995) Early development and dispersal of oligodendrocyte precursors in the embryonic chick spinal cord. *Development*. **121**, 1743-1754.
- Osaka,H., Inoue,K., Kawanishi,C., *et al.* (1996) Proteolipid protein gene analysis in Pelizaeus-Merzbacher disease. [Abstract] *American Journal of Human Genetics*. **10**, A276.
- Palaniyar,N., Semotok,J.L., Wood,D.D., Moscarello,M.A. and Harauz,G. (1998) Human proteolipid protein (PLP) mediates winding and adhesion of phospholipid membranes but prevents their fusion. *Biochimica et Biophysica Acta: Bio-Membranes*. **1415**, (1)85-100.
- Pearsall,G.B., Nadon,N.L., Wolf,M.K. and Billings-Gagliardi,S. (1997) Jimpy-4J mouse has a missense mutation in exon 2 of the *Plp* gene. *Developmental Neuroscience*. **19**, (4)337-341.
- Perry,V.H., Hume,D.A. and Gordon,S. (1985) Immunohistochemical localization of macrophages and microglia in the adult and developing mouse brain. *Neuroscience*. **15**, 313-326.
- Plück,A. (1996) Conditional mutagenesis in mice: the cre/loxP recombination system. *Int.J.Exp.Path.* **77**, 269-278.
- Popko,B., Puckett,C., Lai,E., Shine,H.D., Readhead,C., Hunt,S.W.1., Sidman,R.L. and Hood,L. (1987) Myelin deficient mice: expression of myelin basic protein and generation of mice with varying levels of myelin. *Cell*. **48**, 713-721.
- Popot,J.-L., Dinh,D.P. and Dautigny,A. (1991) Major myelin proteolipid: The 4- α -helix topology. *Journal of Membrane Biology*. **120**, 233-246.

- Pribyl,T.M., Campagnoni,C., Kampf,K., Handley,V.W. and Campagnoni,A.T. (1996) The major myelin protein genes are expressed in the human thymus. *Journal of Neuroscience Research*. **45**, 812-819.
- Pribyl,T.M., Campagnoni,C.W., Kampf,K., Kashima,T., Handley,V.W., McMahon,J. and Campagnoni,A.T. (1993) The human myelin basic protein gene is included within a 179-kilobase transcription unit: Expression in the immune and central nervous systems. *Proceedings of the National Academy of Sciences USA*. **90**, 10695-10699.
- Prinz,M., Hanisch,U.K., Kettenmann,H. and Kirchhoff,F. (1998) Alternative splicing of mouse IL-15 is due to the use of an internal splice site in exon 5. *Brain Res.Mol.Brain Res*. **63**, (1)155-162.
- Privat,A., Jacque,C., Bourre,J.M., Dupouey,P. and Baumann,N. (1979) Absence of the major dense line in myelin of the mutant mouse shiverer. *Neuroscience Letters*. **12**, 107-112.
- Quarles,R.H., Colman,D.R., Salzer,J.L. and Trapp,B.D. (1992) Myelin-associated glycoprotein:structure-function relationships and involvement in neurological diseases. *Myelin: biology and chemistry*. Martenson,R.E., editor: CRC Press Inc., Boca Ranton, pp. 413-448.
- Raff,M.C., Mirsky,R., Fields,K.L., Lisak,R.P., Dorfman,S.H., Silberberg,D.H., Gregson,N.A., Liebowitz,S. and Kennedy,M.C. (1978) Galactocerebroside is a specific marker for oligodendrocytes in culture. *Nature*. **274**, 813-816.
- Raine,C.S. (1984) Morphology of myelin and myelination. *Myelin*. Morell,P., editor: Plenum Press, New York, pp. 1-50.
- Ransom,B.R., Yamate,C.L., Black,J.A. and Waxman,S.G. (1985) Rat optic nerve: disruption of gliogenesis with 5-azacytidine during early postnatal development. *Brain Research*. **337**, 41-49.
- Raskind,W.H., Williams,C.A., Hudson,L.D. and Bird,T.D. (1991) Complete deletion of the proteolipid protein gene (PLP) in a family with X-linked Pelizaeus-Merzbacher disease. *American Journal of Human Genetics*. **49**, 1355-1360.
- Readhead,C., Popko,B., Takahashi,N., Shine,H.D., Saavedra,R.A., Sidman,R.L. and Hood,L. (1987) Expression of a myelin basic protein gene in transgenic shiverer mice: correction of the dysmyelinating phenotype. *Cell*. **48**, 703-712.

- Readhead,C., Schneider,A., Griffiths,I.R. and Nave,K.-A. (1994) Premature arrest of myelin formation in transgenic mice with increased proteolipid protein gene dosage. *Neuron*. **12**, 583-595.
- Remahl,S. and Hildebrand,C. (1990) Relation between axons and oligodendroglial cells during initial myelination. I. The glial unit. *Journal of Neurocytology*. **19**, 313-328.
- Rosen,C.L., Bunge,R.P., Ard,M.D. and Wood,P.M. (1989) Type 1 astrocytes inhibit myelination by adult rat oligodendrocytes *in vitro*. *Journal of Neuroscience*. **9**, 3371-3379.
- Rosenbluth,J., Stoffel,W. and Schiff,R. (1996) Myelin structure in proteolipid protein (PLP)-null mouse spinal cord. *Journal of Comparative Neurology*. **371**, 336-344.
- Rosenfeld,J. and Friedrich,V.L., Jr. (1983) Axonal swellings in jimpy mice: does lack of myelin cause neuronal abnormalities? *Neuroscience*. **10**, 959-966.
- Rosenfeld,J. and Friedrich,V.L., Jr. (1984) Hypomyelination and recovery of the myelin deficit in heterozygous jimpy mice. *International Journal of Developmental Neuroscience*. **2**, 21-32.
- Roth,H.J., Kronquist,K., Pretorius,P.J., Crandall,B.F. and Campagnoni,A.T. (1986) Isolation and characterization of a cDNA coding for a novel human 17.3K myelin basic protein (MBP) variant. *Journal of Neuroscience Research*. **16**, 227-238.
- Roussel,G., Neskovic,N.M., Trifilieff,E., Artault,J.-C. and Nussbaum,J.L. (1987) Arrest of proteolipid transport through the Golgi apparatus in jimpy brain. *Journal of Neurocytology*. **16**, 195-204.
- Salvati,S., Sanchez,M., Campeggi,L.M., Suchanek,G., Breitschop,H. and Lassmann,H. (1996) Accelerated myelinogenesis by dietary lipids in rat brain. *Journal of Neurochemistry*. **67**, 1744-1750.
- Saugier-Veber,P., Munnich,A., Bonneau,D., Rozet,J.-M., Le Merrer,M., Gil,R. and Boespflug-Tanguy,O. (1994) X-linked spastic paraplegia and Pelizaeus-Merzbacher disease are allelic disorders at the proteolipid protein locus. *Nature Genetics*. **6**, 257-262.
- Sánchez,I., Hassinger,L., Paskevich,P.A., Shine,H.D. and Nixon,R.A. (1996) Oligodendroglia regulate the regional expansion of axon caliber and local

- accumulation of neurofilaments during development independently of myelin formation. *Journal of Neuroscience*. **16**, 5095-5105.
- Schindler,P., Luu,B., Sorokine,O., Trifilieff,E. and Van Dorsselaer,A. (1990) Developmental study of proteolipids in bovine brain: a novel proteolipid and DM-20 appear before proteolipid protein (PLP) during myelination. *Journal of Neurochemistry*. **55**, 2079-2085.
- Schliess,F. and Stoffel,W. (1991) Evolution of the myelin integral membrane proteins of the central nervous system. *Biological Chemistry Hoppe-Seyler*. **372**, 865-874.
- Schneider,A., Griffiths,I.R., Readhead,C. and Nave,K.-A. (1995) Dominant-negative action of the *jimpy* mutation in mice complemented with an autosomal transgene for myelin proteolipid protein. *Proceedings of the National Academy of Sciences USA*. **92**, 4447-4451.
- Schneider,A., Montague,P., Griffiths,I.R., Fanarraga,M.L., Kennedy,P.G.E., Brophy,P.J. and Nave,K.-A. (1992) Uncoupling of hypomyelination and glial cell death by a mutation in the proteolipid protein gene. *Nature*. **358**, 758-761.
- Schwab,M.E. and Schnell,L. (1989) Region-specific appearance of myelin constituents in the developing rat spinal cord. *Journal of Neurocytology*. **18**, 161-169.
- Schwob,V.S., Clark,H.B., Agrawal,D. and Agrawal,H.C. (1985) Electron microscopic immunocytochemical localization of myelin proteolipid protein and myelin basic protein to oligodendrocytes in rat brain during myelination. *Journal of Neurochemistry*. **45**, 559-571.
- Screaton,G.R., Bell,M.V., Jackson,D.G., Cornelis,F.B., Gerth,U. and Bell,J.I. (1992) Genomic structure of DNA encoding the lymphocyte homing receptor CD44 reveals at least 12 alternatively spliced exons. *Proc.Natl.Acad.Sci.U.S.A.* **89**, (24)12160-12164.
- Seitelberger,F. (1995) Neuropathology and genetics of Pelizaeus-Merzbacher disease. *Brain Pathology*. **5**, 267-273.
- Sinoway,M.P., Kitagawa,K., Timsit,S., Hashim,G.A. and Colman,D.R. (1994) Proteolipid protein interactions in transfectants: Implications for myelin assembly. *Journal of Neuroscience Research*. **37**, 551-562.

- Sisternans,E.A., De Coo,R.F., De Wijs,I.J. and Van Oost,B.A. (1998) Duplication of the proteolipid protein gene is the major cause of Pelizaeus-Merzbacher disease. *Neurology*. **50**, (6)1749-1754.
- Sisternans,E.A., De Wijs,I.J., De Coo,R.F.M., Smit,L.M.E., Menko,F.H. and Van Oost,B.A. (1996) A (G-to-A) mutation in the initiation codon of the proteolipid protein gene causing a relatively mild form of Pelizaeus-Merzbacher disease in a Dutch family. *Human Genetics*. **97**, 337-339.
- Sivakumar,K., Sambuughin,N., Selenge,B., Nagle,J.W., Baasanjav,D., Hudson,L.D. and Goldfarb,L.G. (1999) Novel exon 3B proteolipid protein gene mutation causing late-onset spastic paraplegia type 2 with variable penetrance in female family members. *Annals of Neurology*. **45**, (5)680-683.
- Skoff,R.P. (1995) Programmed cell death in the dysmyelinating mutants. *Brain Pathology*. **5**, 283-288.
- Skoff,R.P. and Ghandour,M.S. (1995) Oligodendrocytes in female carriers of the jimpy gene make more myelin than normal oligodendrocytes. *Journal of Comparative Neurology*. **355**, 124-133.
- Skoff,R.P. and Montgomery,I.N. (1981) Expression of mosaicism in females heterozygous for jimpy. *Brain Research*. **212**, 175-181.
- Solly,S.K., Thomas,J.L., Monge,M., Demerens,C., Lubetzki,C., Gardinier,M.V., Matthieu,J.M. and Zalc,B. (1996) Myelin/oligodendrocyte glycoprotein (MOG) expression is associated with myelin deposition. *Glia*. **18**, 39-48.
- Sorg,B.A., Smith,M.M. and Campagnoni,A.T. (1987) Developmental expression of the myelin proteolipid protein and basic protein mRNA in normal and dysmyelinating mutant mice. *Journal of Neurochemistry*. **49**, 1146-1154.
- Spassky,N., Goujet-Zalc,C., Parmantier,E., Olivier,C., Martinez,S., Ivanova,A., Ikenaka,K., Macklin,W., Cerruti,I., Zalc,B., *et al.* (1998) Multiple restricted origin of oligodendrocytes. *Journal of Neuroscience*. **18**, (20)8331-8343.
- Starr,R., Attema,B., DeVries,G.H. and Monteiro,M.J. (1996) Neurofilament phosphorylation is modulated by myelination. *Journal of Neuroscience Research*. **44**, 328-337.
- Stoll,G. and Jander,S. (1999) The role of microglia and macrophages in the pathophysiology of the CNS. *Prog.Neurobiol.* **58**, (3)233-247.

- Sturrock,R.R. (1983b) Problems of glial identification and quantification in the ageing central nervous system. *Brain Ageing: Neuropathology and Neuropharmacology*. Cervos-Navarro,J. and Sarkander,H.-I., editors: Raven Press, New York, pp. 179-209.
- Sturrock RR. Cervos-Navarr J and Sarkander IH, editors.Problems of glial identification and quantification in the ageing central nervous system. New York: Raven press; 1983a; 179p.
- Sutherland,H.G., Martin,D.I. and Whitelaw,E. (1997) A globin enhancer acts by increasing the proportion of erythrocytes expressing a linked transgene. *Mol.Cell Biol.* **17**, (3)1607-1614.
- Taraszevska,A. (1988) Ultrastructure of axons in disturbed CNS myelination in *pt* rabbit. *Neuropat.Pol.* **26**, (3)387-402.
- Tetzloff,S.U. and Bizzozero,O.A. (1993) Proteolipid protein from the peripheral nervous system also contains covalently bound fatty acids. *Biochemical and Biophysical Research Communications.* **193**, 1304-1310.
- Thomson,C.E., Montague,P., Jung,M., Nave,K.-A., Griffiths,I.R. and Nave,K.A. (1997) Phenotypic severity of murine *Plp* mutants reflects *in vivo* and *in vitro* variations in transport of PLP isoproteins. *Glia.* **20**, 322-332.
- Timsit,S., Martinez,S., Allinquant,B., Peyron,F., Puelles,L. and Zalc,B. (1995) Oligodendrocytes originate in a restricted zone of the embryonic ventral neural tube defined by DM-20 mRNA expression. *Journal of Neuroscience.* **15**, 1012-1024.
- Timsit,S.G., Bally-Cuif,L., Colman,D.R. and Zalc,B. (1992) DM-20 mRNA is expressed during the embryonic development of the nervous system of the mouse. *Journal of Neurochemistry.* **58**, 1172-1175.
- Tosic,M., Dolivo,M., Domanska-Janik,K. and Matthieu,J.-M. (1994) Paralytic tremor (*pt*): A new allele of the proteolipid protein gene in rabbits. *Journal of Neurochemistry.* **63**, 2210-2216.
- Tosic,M., Gow,A., Dolivo,M., Domanska-Janik,K., Lazzarini,R.A. and Matthieu,J.M. (1996) Proteolipid/DM-20 proteins bearing the paralytic tremor mutation in peripheral nerves and transfected Cos-7 cells. *Neurochemical Research.* **21**, 423-430.
- Tosic,M., Matthey,B., Gow,A., Lazzarini,R.A. and Matthieu,J.M. (1997)

- Intracellular transport of the DM-20 bearing shaking pup (*shp*) mutation and its possible phenotypic consequences. *Journal of Neuroscience Research*. **50**, (5)844-852.
- Toyoshima,I., Sugawara,M., Kato,K., Wada,C., Hirota,K., Hasegawa,K., Kowa,H., Sheetz,M.P. and Masamune,O. (1998) Kinesin and cytoplasmic dynein in spinal spheroids with motor neuron disease. *Journal of the Neurological Sciences*. **159**, (1)38-44.
- Trapp,B.D., Bernier,L., Andrews,B. and Colman,D.R. (1988) Cellular and subcellular distribution of 2',3'-cyclic nucleotide 3'-phosphodiesterase and its mRNA in the rat central nervous system. *Journal of Neurochemistry*. **51**, 859-868.
- Trapp,B.D., Nishiyama,A., Cheng,D. and Macklin,E. (1997) Differentiation and death of premyelinating oligodendrocytes in developing rodent brain. *Journal of Cell Biology*. **137**, (2)459-468.
- Trapp,B.D., Peterson,J., Ransohoff,R.M., Rudick,R., Mörk,S. and Bö,L. (1998) Axonal transection in the lesions of multiple sclerosis. *New England Journal of Medicine*. **338**, (5)278-285.
- Trapp,B.D. and Quarles,R.H. (1984) Immunocytochemical localization of the myelin-associated glycoprotein. Fact or artifact? *Journal of Neuroimmunology*. **6**, 231-249.
- Trofatter,J.A., Dlouhy,S.R., DeMyer,W., Conneally,P.J. and Hodes,M.E. (1989) Pelizaeus-Merzbacher disease: tight linkage to proteolipid protein gene exon variant. *Proceedings of the National Academy of Sciences USA*. **86**, 9427-9430.
- Tycko,B. (1997) DNA methylation in genomic imprinting [see comments]. *Mutat.Res.* **386**, (2)131-140.
- Vela,J.M., Dalmau,I., González,B. and Castellano,B. (1996) The microglial reaction in spinal cords of jimpy mice is related to apoptotic oligodendrocytes. *Brain Research*. **712**, 134-142.
- Verity,A.N. and Campagnoni,A.T. (1988) Regional expression of myelin protein genes in the developing mouse brain: in situ hybridization studies. *Journal of Neuroscience Research*. **21**, 238-248.
- Warf,B.C., Fok-Seang,J. and Miller,R.H. (1991) Evidence for the ventral origin of

- oligodendrocyte precursors in the rat spinal cord. *Journal of Neuroscience*. **11**, 2477-2488.
- Weimbs,T. and Stoffel,W. (1992) Proteolipid protein (PLP) of CNS myelin: Positions of free, disulfide-bonded, and fatty acid thioester-linked cysteine residues and implications for the membrane topology of PLP. *Biochemistry*. **31**, 12289-12296.
- Wight,P.A. and Dobretsova,A. (1997) The first intron of the myelin proteolipid protein gene confers cell type-specific expression by a transcriptional repression mechanism in non-expressing cell types. *Gene*. **201**, (1-2)111-117.
- Wight,P.A., Duchala,C.S., Readhead,C. and Macklin,W.B. (1993) A myelin proteolipid protein-LacZ fusion protein is developmentally regulated and targeted to the myelin membrane in transgenic mice. *Journal of Cell Biology*. **123**, 443-454.
- Willard,H.F. (1995) The sex chromosomes and X inactivation. *The metabolic and inherited basis of inherited disease*. Scriver,C.R., Beaudet,A.L. and Sly,W.S., editors: McGraw-Hill, New York, pp. 719-737.
- Willard,H.F. and Riordan,J.R. (1985) Assignment of the gene for myelin proteolipid protein to the X chromosome: implications for X-linked myelin disorders. *Science*. **230**, 940-942.
- Williams,M.A. (1977) Stereological techniques. *Practical Methods in Electron Microscopy. Vol. 6. Quantitative Methods in Biology*. Glauert,A.M., editor: North Holland, Amsterdam, pp. 5-84.
- Woodward,K., Kendall,E., Vetrie,D. and Malcolm,S. (1998) Pelizaeus-Merzbacher disease: Identification of Xq22 proteolipid-protein duplications and characterization of breakpoints by interphase FISH. *American Journal of Human Genetics*. **63**, (1)207-217.
- Wrabetz,L., Taveggia,C., Feltri,M.L., Quattrini,A., Awatramani,R., Scherer,S.S., Messing,A. and Kamholz,J. (1998) A minimal human MBP promoter *lacZ* transgene is appropriately regulated in developing brain and after optic enucleation, but not in shiverer mutant mice. *Journal of Neurobiology*. **34**, (1)10-26.
- Xu,Z., Cork,L.C., Griffin,J.W. and Cleveland,D.W. (1993b) Increased expression of neurofilament subunit NF-L produces morphological alterations that

- resemble the pathology of human motor neuron disease. *Cell*. **73**, 23-33.
- Xu,Z., Cork,L.C., Griffin,J.W. and Cleveland,D.W. (1993a) Involvement of neurofilaments in motor neuron disease. *Journal of Cell Science*. **106 Suppl. 17**, 101-108.
- Yamada,M., Ivanova,A., Yamaguchi,Y., Lees,M.B. and Ikenaka,K. (1999) Proteolipid protein gene product can be secreted and exhibit biological activity during early development. *Journal of Neuroscience*. **19**, (6)2143-2151.
- Yamamoto,Y., Mizuno,R., Nishimura,T., Ogawa,Y., Yoshikawa,H., Fujimura,H., Adachi,E., Kishimoto,T., Yanagihara,T. and Sakoda,S. (1994) Cloning and expression of myelin-associated oligodendrocytic basic protein. A novel basic protein constituting the central nervous system myelin. *Journal of Biological Chemistry*. **269**, 31725-31730.
- Yamamoto,Y., Yoshikawa,H., Nagano,S., Kondoh,G., Sadahiro,S., Gotow,T., Yanagihara,T. and Sakoda,S. (1999) Myelin-associated oligodendrocytic basic protein is essential for normal arrangement of the radial component in central nervous system myelin. *European Journal of Neuroscience*. **11**, (3)847-855.
- Yan,Y., Lagenaur,C. and Narayanan,V. (1993) Molecular cloning of M6: Identification of a PLP/DM20 gene family. *Neuron*. **11**, 423-431.
- Yoshida,M. and Colman,D.R. (1996) Parallel evolution and coexpression of the proteolipid proteins and protein zero in vertebrate myelin. *Neuron*. **16**, 1115-1126.
- Yoshihara,Y., Oka,S., Ikeda,J. and Mori,K. (1991) Immunoglobulin superfamily molecules in the nervous system. *Neuroscience Research*. **10**, 83-105.
- Zhu,Q.Z., Lindenbaum,M., Levavasseur,F., Jacomy,H. and Julien,J.P. (1998) Disruption of the NF-H gene increases axonal microtubule content and velocity of neurofilament transport: Relief of axonopathy resulting from the toxin β,β' -iminodipropionitrile. *Journal of Cell Biology*. **143**, (1)183-193.